UNIVERSIDAD NACIONAL DE COLOMBIA

SEDE MANIZALES

PRACTICAL APPLICATION OF THERMODYNAMICS IN THE OPTIMAL SYNTHESIS OF CHEMICAL AND BIOTECHNOLOGICAL PROCESSES

Héctor Alexánder Forero Hernández

Practical Application of Thermodynamics in the Optimal Synthesis of Chemical and Biotechnological Processes

Héctor Alexánder Forero Hernández

Thesis submitted in partial fulfillment of the requirements for the degree of:

Master of Science in Engineering - Chemical Engineering

Advisor:

Ph.D., M.Sc, Chemical Engineer Carlos Ariel Cardona Alzate

Research line:

Chemical and Biotechnological Processes Engineering

Research group:

Chemical, Catalytic and Biotechnological Processes

Universidad Nacional de Colombia sede Manizales

Instituto de Biotecnología y Agroindustria, Facultad de Ingeniería y Arquitectura, Departamento de

Ingeniería Química

Manizales, Colombia

2015

Aplicación de la Termodinámica en la Síntesis Óptima de Procesos Químicos y Biotecnológicos

Héctor Alexánder Forero Hernández

Tesis presentada como requisito parcial para optar al título de:

Magister en Ingeniería Química

Director:

Ph.D., M.Sc, Ingeniero Químico Carlos Ariel Cardona Alzate

Línea de investigación:

Ingeniería de Procesos Químicos y Biotecnológicos.

Grupo de investigación:

Procesos Químicos, Catalíticos y Biotecnológicos.

Universidad Nacional de Colombia sede Manizales

Instituto de Biotecnología y Agroindustria, Facultad de Ingeniería y Arquitectura, Departamento de

Ingeniería Química.

Manizales, Colombia.

2015

"The mountains have rules. They are harsh rules, but they are there, and if you keep to them you are safe. A mountain is not like men. A mountain is sincere. The weapons to conquer it exist inside you, inside your soul".

Walter Bonatti.

Acknowledgements

My first and most sincere appreciation goes to my supervisor Professor Carlos Ariel Cardona Alzate. He showed me kindness and patience throughout my enrolment in the Masters programme at the National University of Colombia at Manizales. He also gave me helpful advice and comments at every stage, and supported me every time I needed it. I really appreciated his constant encouragement to complete this thesis and his devoted supervision.

I would also like to thank to Professor Yuri Andrianovich Pisarenko and Doctor Anastasiya Valereevna Frolkova from Moscow Institute of Fine Chemical Technology (Russia). Their emphasis on methodology made me rethink my theoretical and empirical researches. They taught me about strict and scientific attitude needed for academic research, whilst their insight, criticism, and intellectual rigor and academic enthusiasm influenced me profoundly.

Thanks to the National University of Colombia, to the Faculty of Engineering and Architecture, to the Research and Extension Office and to the Administrative Department of Science, Technology, and Innovation -Colciencias - for financial support during my studies.

I wish to express my gratitude to the academic staff in the Chemical Engineering Department and the Research Group in Chemical, Catalytic and Biotechnological processes for their helpful discussions and supportive feedback during the research process. Thanks also to the 'Wise Guys', my friends and colleagues who made this study period happy and memorable.

Finally, I would like to express my deepest love to my parents, Héctor and Luz Marina, and my sisters, Natalia and Tatiana, for their full support and understanding.

And thanks to the Sun, the one that shines on everyone.

Abstract

In most chemical engineering design problems it is required a complex set of research steps so as to establish the operating conditions in which the process reaches the highest conversion, yield and productivity. However, these steps are tedious, complex and can lead to mistakes. To differ from this, the coupled application of the thermodynamics and the graph-theory appears can be considered as an alternative to design chemical and biotechnological processes. So, in that way, this master's thesis presents a strategy to synthetize, to design and to evaluate conventional and non-conventional process schemes using Process Engineering techniques from a complete set of different configurations that corresponds to maximal yield of a target product to find good initial estimates to perform calculations and rigorous simulations. A theoretical evaluation was followed to corroborate different possibilities in operation conditions provided for the models for both types of approaches. This kind of evaluation was therefore particularly useful for assessing feasibility of chemical production systems and moreover it provided a realistic measure of the potential for improving the efficiency of the overall process.

Keywords: Thermodynamics. Reactive distillation. Graph-theory. Mathematical modelling. Phase equilibria. Distillation.

Resumen

Actualmente, para solucionar el problema de diseño de procesos para la industria química, se requiere de un complejo conjunto de pasos de investigación con el fin de establecer las condiciones de operación en las cuales el proceso alcanza los mejores valores de conversión, rendimiento y productividad, los cuales resultan ser muy costosos y tediosos. La finalidad de este proyecto de investigación es sintetizar, diseñar y evaluar esquemas convencionales de procesos químicos y biotecnológicos usando Ingeniería de Procesos junto a técnicas de modelamiento matemático basadas en la termodinámica. Para el desarrollo de este objetivo principal, la metodología propuesta se fundamenta en la aplicación teórica de la termodinámica y como herramienta fundamentales en la cualificación y cuantificación del comportamiento de diversos sistemas (mezclas), proporcionando a su vez criterios y directrices para el adecuado modelamiento y posterior evaluación de esquemas de procesos más eficientes desde un punto de vista técnico y energético.

Palabras clave: Termodinámica. Destilación reactiva. Teoría de Grafos. Modelado matemático. Equilibrio de fases. Destilación.

Content

List of figures

List of tables

List of Publications

Research papers

Restrepo, J. B., **Forero, H. A**, Cardona, C. A. 2014. The Analysis of Chemical Engineering Process Plants and their Models Represented by Networks. *Chemical Engineering Science*, Elsevier. Status: Pre-accepted. Third revision in progress.

Participation in events

Aristizabal, V., **Forero, H. A,** Cardona, C.A. Energy costs vs. quality of jet biofuels from biomass.. In: United States. 2014. Event: Biomass Conference and Expo.

Aristizabal, V., **Forero, H. A,** Cardona, C. A. Sustainable production of jet biofuels in tropical countries. In: United States. 2014. Event: 36th Symposium on Biotechnology for Fuels and Chemicals.

Forero, H. A, Moncada, J., Cardona, C. A. Optimal design of separation trains for biofuel production. In: Czech Republic. 2014. Evento: 21st International Congress of Chemical and Process Engineering CHISA.

Dávila, J. A., **Forero, H. A,** Cardona, C. A. Techno-economic assessment of the supercritical extraction of antioxidant compounds and fatty acids from Avocado (*Persea americana*). In: Czech Republic. 2014. Evento: 21st International Congress of Chemical and Process Engineering CHISA.

Forero, H. A, Moncada, J., Cardona, C. A. Importance of optimal design of downstream processing in biorefineries. In: Spain. 2014. Event: 10th International Conference on Renewable Resources and Biorefineries.

Forero, H. A, Cardona, C. A. Comparación de modelos termodinámicos en el análisis topológico de mezclas. In: Colombia. 2014. Event: XXVII Congreso Interamericano y Colombiano de Ingeniería Química.

Forero, H. A, Cardona, C. A. Aplicación de la termodinámica en la síntesis óptima de procesos químicos. In: Colombia. 2014. Event: XXVII Congreso Interamericano y Colombiano de Ingeniería Química.

Forero, H. A, Pisarenko, Yu. A., Cardona, C. A. Petlyuk and DWC distillation columns: Separation possibilities assessment. In: United States. 2014. Event: AIChE Annual Meeting.

Forero, H. A, Hernández, V., Cardona, C. A. Use of graph theory for designing efficient biorefineries. In: United States. 2014. Event: AIChE Annual Meeting.

Forero, H. A, Camelo, A. F., Pisarenko, Yu. A., Cardona, C. A. Use of thermodinamic topological analysis for designing the amyl acetate process. In: United States. 2014. Event: AIChE Annual Meeting.

Forero, H. A, Aristizabal, V., Gómez, A., Cardona, C. A. Thermodynamic analysis of a lignocellulose-based furfural biorefinery. In: United States. 2014. Event: AIChE Annual Meeting.

Books

Toro, L. A., **Forero, H. A.,** Cardona, C. A. Modelamiento y simulación en Ingeniería Química. Ed: Universidad Nacional de Colombia. Status: Pending of publication.

Software

Toro, L. A., **Forero, H. A.,** Cardona, C. A. Ecuación de Estado de Beattie – Bridgeman. In: Colombia. Code developed in: Matlab R2009a.

Toro, L. A., **Forero, H. A.,** Cardona, C. A. BLATER: Solución numérica al problema de Blasius. In: Colombia. Code developed in: Matlab R2009a.

Toro, L. A., **Forero, H. A.,** Cardona, C. A. REDO: Solución de Sistemas de Ecuaciones Diferenciales. In: Colombia. Code developed in: Matlab R2009a.

Toro, L. A., **Forero, H. A.,** Cardona, C. A. SISTAN: Solución de sistemas de ecuaciones diferenciales lineales no homogéneos con coeficientes constantes. In: Colombia. Code developed in: Matlab R2009a.

Toro, L. A., **Forero, H. A.,** Cardona, C. A. PETA: Evaluación de la pirolisis de etano. In: Colombia. Code developed in: Matlab R2009a.

Toro, L. A., **Forero, H. A.,** Cardona, C. A. R-RUK: Solución de un reactor con control de temperatura. Code developed in: Matlab R2009a.

Toro, L. A., **Forero, H. A.,** Cardona, C. A. RT-RUK: Solución de un reactor sin control de temperatura. Code developed in: Matlab R2009a.

Toro, L. A., **Forero, H. A.,** Cardona, C. A. ALETA: Solución al problema de las aletas en transferencia de calor. Code developed in: Matlab R2009a.

Toro, L. A., **Forero, H. A.,** Cardona, C. A. COL-ALETA: Solución al problema de las aletas en transferencia de calor. Code developed in: Matlab R2009a.

Toro, L. A., **Forero, H. A.,** Cardona, C. A. BLAVEL. Code developed in: Matlab R2009a.

Participation of this Thesis in Research Projects

Bioenergy and Food Security Rapid Appraisal. In cooperation with the Food and Agriculture Organization of the United Nations (FAO) in Rome through the National University of Colombia at Manizales. Position: Software developer.

Evaluación termodinámica de procesos de transformación de lignocelulósicos. The Administrative Department of Science, Technology, and Innovation -*Colciencias*- in cooperation with the the National University of Colombia at Manizales. Position: Researcher.

Introduction

The concept of "clean technology" is becoming more interesting now that new environmentally friendly laws are being introduced relative to control the energy consumption in the chemical industry and the pollutants produced by its activity. Even though big efforts have been made to adequate chemical technology for the purpose of addressing eco-efficiency, there are still lots of processes and operating units which have to be optimized in order to enhance the overall yields or further improve the quality of the products at a lower cost and lower energy expenditure.

Nearly every chemical process has a section in the flowsheet where the separation of a multicomponent mixture into products is performed. For each of the resulting separation schemes, more than one separation method could be possible. Moreover, as more than one separation task will normally be needed, the best arrangement of separation tasks must be set up. Then, for each of the selected separation methods in a separation system, an appropriate and reliable set of operating conditions must be established [1].

In the case of separation units, as highlighted for several authors [2-4], they are a massive consumer of energy. Therefore, chemical engineers are necessary to search for a novel and alternate methods for more energy efficient separations. Generally, process design is founded on a heuristic, physical or mathematical programming methodology [5]. By joining them it is possible to take advantage of their benefits while overcoming their weaknesses. This is possible to be done by reviewing them and classifying fields of improvement or synthesizing new structures. However, nowadays non-conventional separations are either very expensive or not well understood to be applied. They can, though, be the most promising methods for addressing those concerns. Hence, improving our understanding of design of non-conventional separation tasks appears to be the most realistic alternative. In order to achieve this objective, a design tool is necessary to allow an engineer easily

and innovatively create any arrangement and not be limited by any prearranged notions close to optimal structures [6].

A very important subject in chemical engineering calculations is the selection of a proper physical property method that will precisely define the phase equilibrium of the chemical system. Missing or insufficient physical properties can weaken the precision of a model or even prevent one from executing the simulation. Consequently, finding good values for insufficient or missing physical property parameters is decisive to an effective simulation. However, this depends strongly upon selecting accurate estimation methods [7]. In this sense, selecting the correct thermodynamic model for a specific system of components is very significant to an engineer, as a design is only as good as the model used. Even at the theoretical design phase of a distillation scheme, it is required a model that suitably describes the system so that initial decisions can be made as for column sequencing and arranging [8]. The results of calculation models are highly affected by the particular assumptions made in the plant model and by the model parameters [9].

The present thesis presents an integrated background where two techniques for synthesis and design of chemical process flowsheets and separation tasks were combined so as to each technique serves as a shortcut to provide basic information required to find a solution for a design problem. The techniques are: thermodynamic based approach and structural optimization based approach. Both methods are taken as initial estimates for the calculation of the final optimal flowsheet. The methodology includes the development of representation, different ways to assess process alternatives and an approach to examine all the feasible alternatives. The major challenge to apply this method, though, involves the fact that feasible solutions are very reliant on the design problem being addressed. The approaches applied two design methods with simulation and property calculation based on experimental procedures so that near-optimal flowsheets can be evaluated, tested (via simulation) and analyzed.

Thesis Hypothesis

It is possible to apply a methodology which relates the physicochemical behavior of the compounds and the influence they have in the determination of the optimal operating conditions of chemical and biochemical processes, using a process engineering approach based on the topological thermodynamics and the graph-theory.

Thesis Objectives

General Objective

To apply a methodology that allows synthesizing more sustainable chemical processes through optimal conceptual designs.

Specific Objectives

- To apply the topological thermodynamics to generate separation and reaction schemes for selected conventional and non-conventional chemical processes.
- To develop a short-cut method in order to obtain a set of initial possibilities on the main process variables to find near-optimal process schemes.
- To compare several different generated schemes and to determine which ones have technical and economic advantages over the conventional schemes.
- To compare conventional design methods of chemical process with the approaches provided by the topological thermodynamics and the graph-theory.

1. Simultaneous reaction – separation processes

Overview

Through the years, the meaning of *simultaneous reaction-separation process* has been subject to discussion. Some authors have given particular importance to the reactor naming them as "multifunctional reactors" [10, 11]. Others have placed more relevance to the separation system, not only in the specific case of separation improved by reactions [12], but also for the case of the synthesis of products of commercial interest [13]. This latter type of definition is more accurate for a simultaneous reaction-separation process regardless of the goal that is being pursued (to produce or to separate a product) and could be summarized as follows: a process where simultaneously and coupled chemical transformation and separation of a reacting mixture take place in the same apparatus in order to selectively remove a desired product. Thus, *simultaneous process* does not simply mean the occurrence of processing and separation of a mixture in a single apparatus, but the joint implementation of the processes with a certain synergy. From the above it is possible to conclude, that a simultaneous process is not just the sum of its components.

By overlaying the reacting and separating properties of the components, it is possible to overcome the thermodynamic restrictions and limitations that would exist if both processes were carried out independently, e.g. equilibrium conversion in a reaction and separation selectivity. The degree of elimination of these restrictions defines areas in which the simultaneous process will have clear advantages over the conditional ways of performing a chemical transformation. As is widely known, rectification or fractional distillation is the most important technique for separating mixtures into their pure components; hence, this is one of the reasons enhanced distillation processes such as reactive distillation is becoming more studied and used in industry [13].

1.1. The topological thermodynamics as a tool for designing simultaneous reaction - separation processes

The design and study of technologies to fulfill the objective of reducing pollution and energy consumption for obtaining chemical products must be based on the description of the phenomena involved in the processes, i.e. the theory and models that adequately explain them. As a result, it is possible to set predictive mechanisms to achieve some previous established conditions of the process such as quality, energy advantages over other alternatives, etc. Typically, at this stage the operating conditions and certain static parameters are determined. All this information is then used in rigorous simulation, where the main objective is to obtain an optimized technological scheme. The next stage includes a corroborating laboratory results level, which will be replicated on a different scale of productivity such as the pilot plant. The above design strategy represents the global trend in Chemical Process Engineering.

In the specific case of separation operations, they usually require the maximum rate of energy consumption in a process. Furthermore, their efficiency in the separation of multicomponent mixtures is largely dependent on the level of contamination of the entire process. Due to its high productivity, fractional distillation or rectification is the separation operation most used in the work. Many modifications have been made to distillation looking to increase efficiency and minimize energy consumption during separation of mixtures: Integrated Petlyuk columns, azeotropic distillation, extractive distillation, reactive distillation, etc.

For separating multicomponent mixtures, the theory has provided a wealth of information and methods for analyzing the problem. Basis of phase equilibrium and thermodynamic modeling, theory of distribution coefficients and relative volatilities, the McCabe - Thiele and Savarit - Ponchon methods for binary mixtures, the properties and predictive methods of azeotropy, efficiencies of mass transfer units, equilibrium and no equilibrium models with their respective MESH equation, and calculation algorithms, are just some of the most significant advances in the theory of distillation. However, the rigorous methods of calculation and experimentation prevailed over preliminary theoretical analysis.

Only the appearance of a new theory showed notorious benefits of its application as short cut method for design distillation systems. This theory was called in different ways: differential, geometric, graph - analytic or holistic distillation theory. It is based on the graphic study of integral trajectories distillation under condition of infinite or finite reflux. It is applicable to mixtures of any

number of components, but its graphic representation is restricted to only mixtures of three, four and even five components. This is not a limitation considering that the most difficult multicomponent mixture to separate does not exceed five components.

The origin of the theory of differential distillation dates back to 1901 when Schreinemakers proposed the distillation trajectories in ternary systems [14]. At that time, these developments were not well received by the academic community, which led to a lack of continuity of jobs in that area. Then, during the Second World War, when the technical results were needed as quickly as possible, preference was given to the calculation methods based on rigorous distillation models [13]. Thereafter, thanks to the rapid development of programming languages, mathematical algorithms for the solution of differential equations involved in the models received more attention from the academic community. Only in the 60s the results of Schreinemakers were resumed, appearing then studies that provided a theory about the distillation paths based on thermodynamics of physical and chemical equilibrium. It was investigated by authors like Storonkin and Morachevsky in 1956 [15], Swietoslawsky in 1959 [16], Prigogine in 1960 [17], De Groot in 1964 [18], Zharov between 1960-1975 and Serafimov between 1967-1975 [13], Vogelpohl in 1964 [19, 20], Petlyuk between 1960-1977 [21-23], among others. The response of the academic community was swift and emerged several schools that tried to assimilate the general theory of distillation: Doherty and Perkins between 1978-2000 [13], Stichlmair between 1980-1999 [13], Espinosa between 1987-2000 [24, 25] and so forth. Nowadays, this theory is used as a short-cut method for distillation systems and its purpose is to save time and large amounts of money in simulations and experiments. Serafimov et.al (1967-2002) directed their focus towards distillation schemes with total efficiency, i.e. under infinite reflux and number of stages [13]. The behavior of the trajectories of the distillation process to such conditions is commonly called Thermodynamic-Topological Analysis. This analysis has been used worldwide with great success for the separation of multicomponent mixtures. For over three decades it has been also applied for simultaneous reaction-separation processes (analysis of the process statics) by Pisarenko [13].

A Thermodynamic-Topological Analysis allows synthesizing more appropriate technological schemes for distillation systems. The information required to perform this analysis is minimal: boiling point of pure components and azeotropes, molar composition, quality of the components to be separated, solubility or liquid-liquid equilibria if present [26].

The key feature of simultaneous reaction - separation processes is the possibility of increase the reaction rate and delay the generation of undesired products (or even completely excludes it). This

happens due to a constant-concentration of the reactants through mass exchange in the reaction zone allowing the existence of the process in the kinetic region [27].

The improvement of the chemical reaction conversion enables the process not only to overcome the thermodynamic constraints (e.g. extents of reaction higher than the equilibrium under given conditions), but also to reduce the residence time of the reactants per cycle decreasing then the existence of parallel reactions due to a low concentration of products. On the other hand, the increase in the selectivity is related to the fact that high reaction rates (and consequently high conversion) can be achieved under "soft" conditions, for example, at lower temperatures. Therefore, it is possible to consider reactive distillation as a *clean technology* because its application provides the process advantages such as simplicity of the technological scheme and energetic optimization due to the heat generated by the reaction which might be used to boil the mixture inside the column.

A reactive distillation set-up is convenient to be applied to the following cases:

 a. Processes carried out in liquid phase: the heat of reaction can be employed to partially evaporate the reaction mixture during its separation.
 b. Reversible reactions limited by chemical equilibrium: improvement in the conversion compared with the equilibrium value because a selective exchange of substances from the reaction zone is achieved. Example: Production of methyl acetate [28].
 c. Selective removal of products: it promotes the reduction of undesired parallel reactions which increases the selectivity of the process. Example: Production of Diisopropyl ether [29].
 d. Separation of products with complex azeotropy: reactive distillation increases the driving force of the separation process because the azeotropes disappear while one of the components is consumed by the chemical reaction in certain sections of the tower. Example: Separation of lactic acid from fermented broth [30].
 e. Irreversible reactions: these reactions are characterized by a huge decrease in the reaction rate once the reaction is complete. Example: Production of acetates by esterification of acetic anhydride.

As the inefficiencies in conventional processes have become apparent, companies have successfully implemented reactive distillation in oxidation, alkylation, carboxylation and decarboxylation, epoxidation, production of spirits, esterification, hydrolysis, condensation and polymerization, isomerization, hydration and dehydration, thermal decomposition among other

processes where this technique has a positive influence. Figure 1.1 presents the proposed framework for checking whether a reactive distillation process is economically and technically attractive.

Check RD technical constraints
- Type of main reactions
- Stoichiometry of reactions
- Kinetics and equilibrium
- Vapor-liquid equilibrium data
- Enthalpy of reaction

Number of products < 2 — No / Yes

Last step of main reaction is reversible — No / Yes

Check temperature $|T_D - T_{R\,min}| \leq 120$ — No / Yes

e.g. DMD synthesis, phenol resin liquefication

Check critical properties $(T_{R\,min} < T_C)$ and $(P_O < P_C)$ — No / Yes

Is equilibrium constant acceptable? $K_{EQ} \geq 0.01$ — No / Yes

Check kinetics of main reaction $k_F \geq \pm 20\% \, k_R$ — No / Yes

Side reactions present? — No / Yes

$|T_S - T_{R\,min}| > |T_D - T_{R\,min}|$ — No / Yes

e.g. methyl acetate hydrolysis reaction

Check relative volatility $\alpha \geq 1.1$ — No / Yes

Is relative volatility (α) temperature dependent? — No / Yes

$T_{R\,main} \ll T_{V\,reactant}$ — No / Yes

Conventional process or other hybrid process is recommended

Check if reactive distillation is economically attractive

Are inerts present? — No / Yes

High equilibrium constant $K_{EQ} \geq 1$ — No / Yes

Check heat of reaction
Endothermic $\Delta Hr > 0$ Exothermic $\Delta Hr < 0$

$\Delta H_{vap} > \Delta H_R$ — No / Yes

$|T_D - T_{R\,min}| \leq 50$ — No / Yes

e.g. toluene disproportionation process

Production rate higher than 0.5-1 kton/year — Yes / No

Gross profit margin > 15% — No / Yes

e.g. fatty acids esterification, methyl acetate synthesis

Reactive distillation is technically possible and economically attractive. Proceed with process synthesis, design and optimization.

Reactive distillation is technically possible, but not economically attractive

KF	Forward reaction rate
KR	Reverse reaction rate
KEQ	Equilibrium constant
PO	Pressure of RD column
PC	Critical pressure
TR_main	Main reaction temperature
TV_reactant	Vaporization temperature
TC	Critical temperature
TS	Side reaction temperature
TD	Distillation temperature
α	Relative volatility
ΔHvap	Enthalpy of vaporization
ΔHR	Enthalpy of reaction

Figure 1-1: Framework for checking if reactive distillation is an attractive option or not.

1.2. Applications of the topological thermodynamics

The Thermodynamic-Topological Analysis can be applied in:

1. Conventional distillation.

By describing the phase equilibrium in a multicomponent system (through curves of constant boiling or trajectories of the distillation process for example), it is possible to identify the difficulties of separating a mixture. All this can be seen graphically in a triangle, tetrahedron or pentatope whose vertices represent the components of the mixture, the edges the binary mixtures and the faces the ternary mixtures. As is known, most of the mixtures of interest to the chemical industry are composed by three, four or five components, thus, it is always possible in each case to solve two concerns: the chances of obtaining pure components or fractions required in the distillate and bottoms; and defining a priori the most convenient technological scheme to achieve the required separation. It is important to note that one of the advantages of an algorithm based on thermodynamic-topological techniques is the ability to extend the method to mixtures of any number of components. The only problem in these cases is that, for example a mixture of 15 components will be impossible to observe graphically the characterization of the mixture and the results obtained.

2. Distillation trains with pressure swing.

The study of how pressure affects the composition of an azeotrope in a binary mixture and how to propose the best separation scheme for it is not a very complicated task. When the mixture is of three or four component, the difficulty arises in knowing how the distillation boundaries (also known as thermodynamic separatrixes) were affected and then deciding between several possible technological schemes in order to find the most appropriate.

3. Azeotropic distillation.

In the case of using a third component that forms an azeotrope with one or both starting components to achieve a structure of the phase diagram that allows the easy removal of initial flavorful, the main problem is the choice of solvent. In this case the solvent should be chosen according to the new structure of the phase diagram and its ability to achieve a separation of the pure components.

4. *Extractive distillation.*

If the solvent of the above case does not create azeotropes, but modifies the relative volatility of the mixture to be separated, its choice should be based on the study of relative volatility curves, in order to establish which of these is amending more intensely this volatility and requiring minimal amount added. Thermodynamic topological analysis allows the study of isovolatility and also provides an evaluation of the results of the extractive effect in the synthesis of the technological scheme.

5. *Reactive Distillation.*

One of the main challenges of performing the chemical reaction and distillation in the same equipment is to understand how a phenomenon affects the other. It is necessary to understand how the restrictions imposed by the reaction in chemical equilibrium can be overcome by the separation and how the reaction can improve the separation of the resulting reaction mixtures. In this sense, the thermodynamic-topological analysis allows the graphical study of the trajectories (approximate) in a reactive distillation process and how they are located in the area before and after the chemical equilibrium. The most important result is to know the possibility of achieving steady states with high conversion which are feasible to implement. With this information it is then possible to synthesize the basic flow chart of the process for further optimization through rigorous simulation.

6. *Distillation with pervaporation.*

By adding a selective membrane to the distillation scheme, the concentration fields are redistributed. This means that the thermodynamic constraints of the phase diagram for the distillation regions generate extra specific separation capabilities to the process. By hybridizing the membrane process can be achieved that some restricted concentrations to a single region overcome the distillation boundaries being then located in the desired region. To accomplish these goals through graphical analysis techniques, thermodynamic-topological analysis constitutes an effective tool for selecting the most appropriate technological scheme.

7. *Reactive Extraction.*

The extraction may be characterized at a static level by using tie lines X_1-X_2, which are defined by mathematical modeling or by experiments. By having a region of complete miscibility and another region of complete immiscibility, it is then possible to graphically overlay the chemical equilibrium in order to calculate the values of chemical affinity to be achieved at

steady state. However, it is possible to solve both liquid-liquid and chemical equilibrium simultaneously if the reaction rates are very fast.

From the abovementioned fields of application of the Thermodynamic-Topological Analysis is inferred that the primary objective of this study is the synthesis of technological schemes that achieve a desired purity in the distillation columns with minimum energy consumption.

1.3. Reactive Distillation

In comparison with conventional distillation, reactive distillation settles conditions on reaction conversion and product composition. Therefore, degrees of freedom in such a kind of process must be fixed to fulfill these conditions at the same time an objective function, for instance, energy consumption or the total annual operating cost is optimized. The above-mentioned degrees of freedom should cover specifications such as temperature, pressure, location of reactant feed flows, number of reactive stages, number of stripping and rectifying stages, holdup of the reactive stages, reboiler duty and reflux ratio [13]. In distillation, the basic operating conditions to be specified are the composition of heavy key and light key components in the distillate and in the bottom respectively. The retention has a relative low influence on the modeling of a steady-state distillation column; it is important on when modelled as a dynamic system. The column diameter can be calculated from the vapor load equation, after determining the vapor flows necessary to reach the chosen separation. Nevertheless, the retention is essential in reactive distillation as the speeds of reaction are highly dependent on the liquid retention and the quantity of existing catalyst on every stage. Hence, to design a reactive distillation it is necessary to follow an iterative method because the liquid retention has to be established before the entire process can be calculated. This indicates that stage retention is supposed and the column is calculated to reach the chosen product compositions and conversion. Thus, the column diameter is estimated along with the necessary amount of liquid on the reactive stages matching a supposed retention.

Reactive distillation is particularly important in processes where the phase equilibrium and chemical coincide. The reaction and separation occur in the same region of the distillation equipment, or in other words, a set of initial reactants are transformed having then a separation of the desired products and recover of the remaining reactants. Furthermore, as both processes happen simultaneously in the same apparatus, there must exist an appropriate coincidence between the temperatures and pressures necessary to carry out the reaction and separation as presented by

Figure 1.2 [31, 32]. Consequently, the simultaneous process is not possible when there is no an important correspondence of the operating settings to perform the reaction and separation.
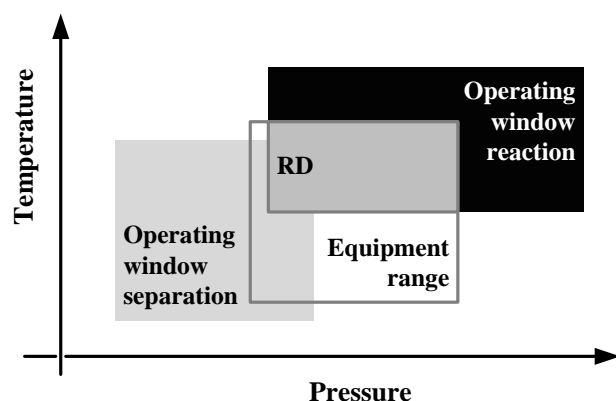
Figure 1-2: Overlying of operating conditions for reaction, separation, and apparatus.

An insignificant amount of industrial uses of reactive distillation have been applied for various decades, but nowadays, despite the comprehension and studies to describe the phenomena, its industrial application remains impractical [33]. Today, the most installed reactive distillation process in the industry is the methyl tert-butyl ether (MTBE) production process, which is an oxygenate for gasoline. Some esters are manufactured by reactive distillation too being ethyl tert-butyl ether (ETBE), tert-amyl methyl ether (TAME) or fatty acid methyl esters (FAME) some examples [34, 35]. Table 1.1 presents the most important applications of reactive distillation to date:

Table 1-1: Main industrial applications of reactive distillation

Reaction type	Catalyst / Internals
Alkylation	
Alkyl benzene from ethylene/propylene and benzene	Zeolite beta, molecular sieves
Amination	
Amines from ammonia and alcohols	H_2 and hydrogenation catalyst
Carbonylation	
Acetic acid from CO and methanol/dimethyl ether	Homogeneous
Condensation	
Diacetone alcohol from acetone	Heterogeneous
Bisphenol-A from phenol and acetone	N/A
Trioxane from formaldehyde	Strong acid catalyst, zeolite ZSM-5

Table 1-1 (cont.): Main industrial applications of reactive distillation

Esterification	
Methyl acetate from methanol and acetic acid	H_2SO_4, Dowex 50, Amberlyst-15
Ethyl acetate from ethanol and acetic acid	N/A
2-Methylpropyl acetate from 2-methyl propanol and acid	Katapak-S
Butyl acetate from butanol and acetic acid	Cation-exchange resin
Fatty acid methyl esters from fatty acids and methanol	H_2SO_4, Amberlyst-15, Metal oxides
Fatty acid alkyl esters from fatty acids and alkyl alcohols	H_2SO_4, Amberlyst-15, metal oxides
Cyclohexyl carboxylate from cyclohexene and acids	Ion-exchange resin bags
Etherification	
MTBE from isobutene and methanol	Amberlyst-15
ETBE from isobutene and ethanol	Amberlyst-15/pellets, structured
TAME from isoamylene and methanol	Ion-exchange resin
DIPE from isopropanol and propylene	ZSM 12, Amberlyst-36, zeolite
Hydration/dehydration	
Mono ethylene glycol from ethylene oxide and water	Homogeneous
Hydrogenation/dehydrogenation	
Cyclohexane from benzene	Alumina-supported Ni catalyst
MIBK from benzene	Cation-exchange resin with Pd/Ni
Hydrolysis	
Acetic acid and methanol from methyl acetate and water	Ion-exchange resin bags
Acrylamide from acrylonitrile	Cation exchanger, copper oxide
Isomerization	
Iso-paraffins from n-paraffins	Chlorinated alumina and H_2
Nitration	
4-Nitrochlorobenzene from chlorobenzene and nitric acid	Azeotropic removal of water
Transesterification	
Ethyl acetate from ethanol and butyl acetate	Homogeneous
Diethyl carbonate from ethanol and dimethyl carbonate	Heterogeneous
Vinyl acetate from vinyl stearate and acetic acid	N/A
Unclassified reactions	
Monosilane from trichlorosilane	Heterogeneous
Methanol from syngas	$Cu/Zn/Al_2O_3$ and inert solvent
DEA from monoethanolamine and ethylene oxide	N/A

For several years it was supposed that reaction and distillation can be integrated into an improved column with different conditions or supplementary external volume. Nevertheless, a reactive distillation column is only suitable in reactions that are fast enough so as to achieve better yields inside an established residence time. The design of a reactive distillation process should be focused on to find operating conditions fulfilling these two conditions: enough residence time and the vital investment.

Reactive distillation processes are distributed into homogeneous catalyzed or autocatalyzed, and heterogeneous catalyzed by a compact catalyst. The reaction rate with respect to autocatalytic reactions can be modified only by the temperature or pressure of the reactive distillation apparatus. The use of homogeneous catalysis lets the speed of reaction to be modified by a change in the amount of catalyst used and, consequently, the performance of the kinetics can be improved over a varied sort of operating conditions in the reactive distillation column. While homogeneous catalysis is likely adjustable to a variation in the operating conditions, it involves high-priced separation procedures to recover the catalyst. Instead, heterogeneous catalysis needs a different arrangement inside the column, consequently adding a limit in the amount and concentration of catalyst that can be used.

Figure 1.3 shows the basic notions to select equipment for process requiring either homogeneous or heterogeneous catalysis [36]. Regarding heterogeneous catalysis it is necessary to include in the equipment an additional volume to hold the catalyst.
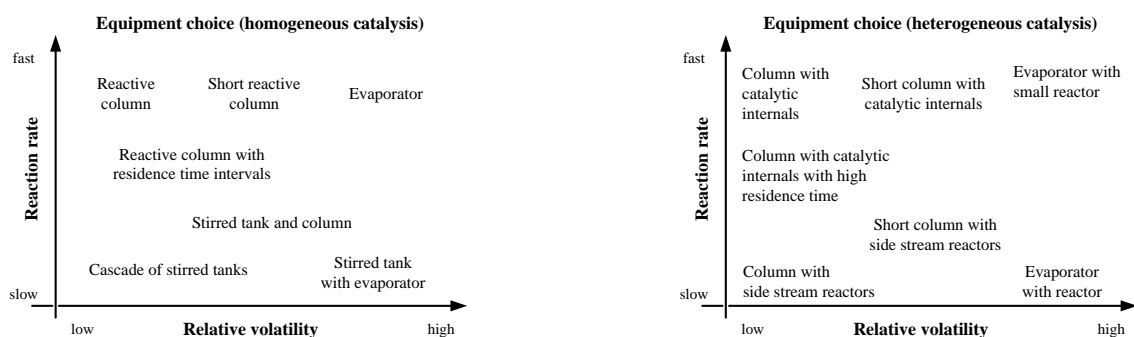
Figure 1-3: Equipment choice for homogeneous (a) and heterogeneous (b) catalysis.

1.4. Reactive Distillation – Modelling and Design

The selective exchange between the reaction and separation zone enables to reach higher conversions at the equilibrium when temperature, pressure and initial composition are given. Therefore, a method is required to estimate the effects of the selective mass exchange in the separation process which are usually dependent on the physical properties of the components [37]. An example illustrating how a chemical reaction in one of the existing phases influences the intensity of mass exchange between them is shown in Figure 1.4a. The presence of the chemical reaction in the liquid phase leads to decrease the concentration of *B* in this phase and consequently to increase the driving force of mass transfer of substances from the vapor to the liquid. In Figure 1.4b is shown the case where the existence of a chemical reaction in a multicomponent liquid mixture allows to move the composition of the mixture to be separated distillation from a region to another, which greatly increases the chances of separation of the mixture.
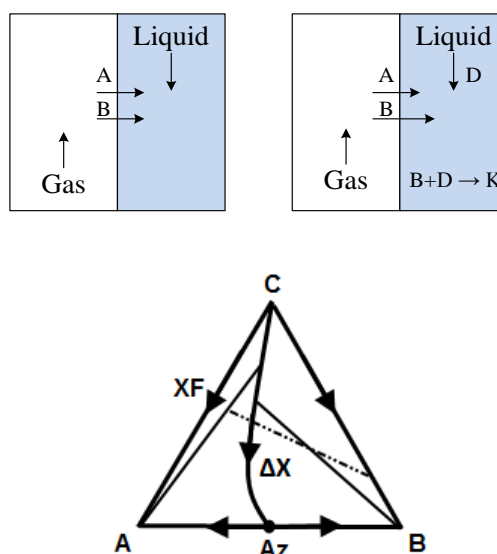
Figure 1-4: Intensification of mass exchange a) Influence of the reaction on mass transfer intensity b) Shift of mixture composition to another distillation region.

Thus, for example, in the case of the reactive distillation, the reaction allows to pass a region where the reagent *A* is the component that is obtained as a bottom product W_1 to a region where the product *C* is obtained as bottom. This is based on the principle of redistribution of concentration fields [13]. However, it is necessary to consider that some of these studied factors (volume of reaction zone, reaction enthalpy and flows structure) affect the simultaneous process -reactive distillation- in an ambiguous way and in each case the design requires additional analysis through simulation and experimental measures. Therefore, advanced mathematical methods are also needed

to solve the complex models that describe reactive distillation. However, it is critical to perform a theoretical analysis in order to obtain optimal alternatives for its practical understanding.

1.5.   Basic concepts

Initial mixture

This mixture corresponds to a hypothetic mixture of all streams that feed the reactive distillation column. The composition of an initial mixture is expressed by the following equation [26]:

$$X_i^F = \frac{1}{F}\sum_{j=1}^{n} F_j X_i^{F_j} \tag{0.1}$$

Pseudoinitial mixture

It is composed by a hypothetic mixture of every product flows. The pseudoinitial mixture composition is defined by :

$$X_i^* = \frac{1}{F^*}\left(PX_i^P + WX_i^W + \sum_{j=1}^{n} U_j X_i^{U_j} \right) \tag{0.2}$$

The pseudoinitial mixture composition is related to the stoichiometry of reaction and is placed on linear fields which can be called chemical interaction fields. The way compositions are disposed, and thus the steady states, is clearly governed by the pseudoinitial mixture composition when the process is carried out at ∞/∞ regime (especially in direct and indirect separation). Hence, the pseudoinitial mixture composition is treated as a steady state as well [26].

Chemical interaction field

It can be calculated by the following equation:

$$X^* = \left[1 - \sum_{\rho=1}^{m} v_\rho \xi_\rho \right] X^F + \sum_{\rho=1}^{m} \Omega_\rho \xi_\rho \tag{0.3}$$

The dimension of the *chemical interaction field* corresponds to the amount of linearly independent reactions. Its arrangement in the concentration simplex is fixed by the composition of the initial mixture and the reaction stoichiometry [26].

Distillation region

A distillation region is the area in the concentration simplex where under formulated distillate condition exist only one distillate or only one bottom. In the concentration simplex these fields are characterized by a group of distillation lines forming a bouquet. In each distillation region a

residue curve map consists of one stable and one unstable node. The mass balance lines overall through the vertices and azeotropes restrict the regions where obtaining a desired product composition is possible. The line or plane which separates a distillation region is called *first degree separatrix*; these lines or planes are the extension of the thermodynamic limit (azeotrope) of zero dimension to a dimension greater than one.

Can be described as the space of the concentration simplex filled with a group of distillation paths (see Figure 1-5). The distillation limits in the concentration simplex state the distillation regions [38].
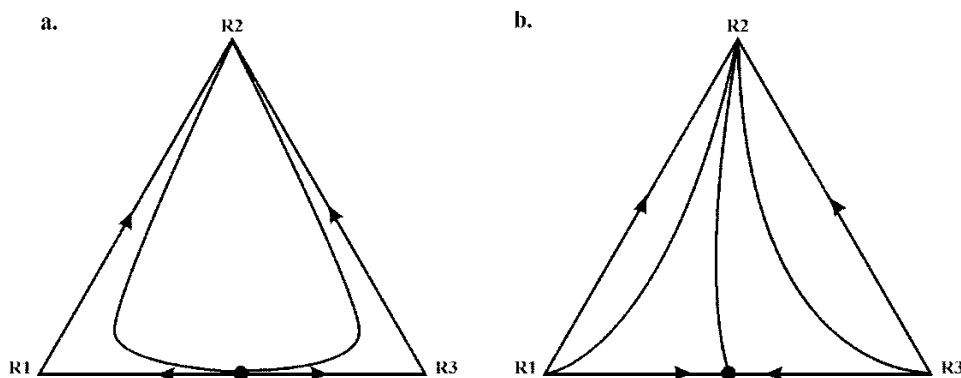
Figure 1-5: Distillation regions a) one region; b) two regions.

Distillation subregion

Distillation subregions are those sections of the distillation chart that qualitatively differ from the quality of any product, without considering the method of separation proposed, i.e. formulated distillate or bottom. The line or plane that separates the distillation subregions is called *second order separatrix.*

It is the subdivision of all initial mixtures that correspond to a qualitatively identical product flow composition once a separation method - direct or indirect – is given. So, in the case for the left and right distillation subregions (see Figure 1-6), the distillate composition for indirect separation belongs to one-dimensional distillation region *R*(*Az* and *AzR*, respectively. In the case shown in Figure 1-6c the bottom compositions *R,* and *R3* belong to different continuous distillation regions. It is necessary to point that for every separation method there is an indicated set of distillation subregions (see Figure 1.6) [38].
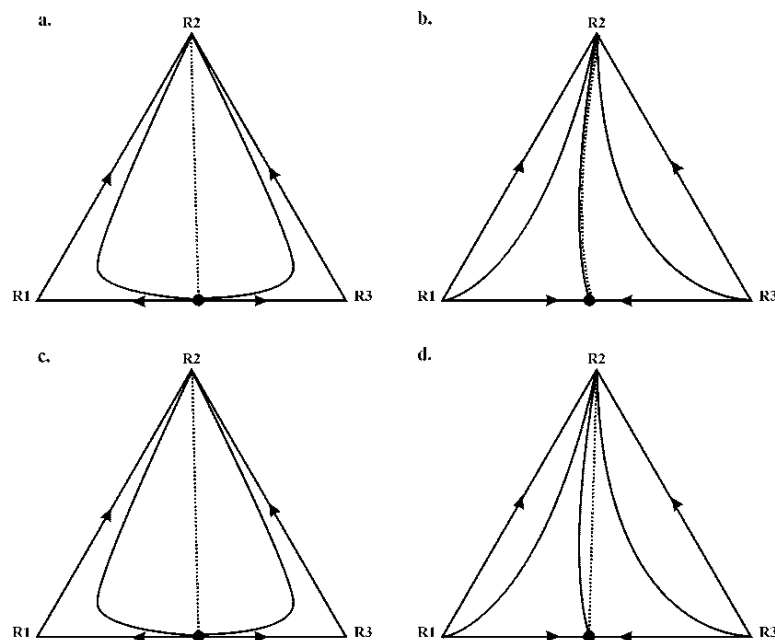
Figure 1-6: Distillation regions a, b) direct separation; c,d) indirect separation.

To complete this method it is necessary to construct the reactive distillation path which can be computed without considering the productivity of the reaction. The reactive distillation path is an important element in the analysis of the process statics since it allows the estimation of the composition profile. This profile leads to an evaluation of the chances to reach good reaction productivity. For a process operating under ∞/∞ regime neither the location of the feed stream nor the way the reaction zone is disposed have an effect on the path. The path depends only on the composition of the mixture that is actually separated in the reactive distillation column (i.e. pseudoinitial mixture). Then, the composition of the pseudoinitial mixture is set by the composition of the initial mixture and the extent of every reaction.

The method to construct a reactive distillation path was suggested by Serafimov and Pisarenko [39]. If the method is applied for a direct separation, it follows these steps:

1. The mass balance line is calculated by two points in the phase equilibrium diagram: the fixed low boiling fixed point and the point of separated mixture (pseudoinitial mixture) composition X^*.
2. The intersection between the mass balance line and the distillation region boundaries defines a conjugated bottom X^W (product flow).

3. From the bottom product composition X^W a tie-line is drew along the borders of distillation region boundaries in a downward course to the boiling point until a stable node is reached. Indeed, this tie-line represents the path reactive distillation follows.

Chemical interaction field

The chemical equilibrium manifold is an array of liquid phase compositions for which the rate of all chemical reactions involved is equal to zero. This surface splits the concentration simplex for every reaction into zones of both forward and reverse direction. The dimension of the chemical equilibrium manifold is established by the Gibbs' phase rule.

1.6.   Analysis of the process statics

As pointed by Kiva et al, reacting systems are generally characterized by a significant deviation from the ideal behavior, which is expressed in complex azeotropies and limited solubility of the present substances in the system. Consequently, the process is limited by the separation that is also restricted by the structure of phase equilibrium [38].

The general principles to perform an initial analysis of the process statics for a continuous reactive distillation are studied in [13]. The main objective of performing this analysis is the right use of theory in the synthesis of optimal structures and technological systems with a deep scientific basis. The analysis of the process statics is used in the conceptual design of many industrial processes, especially during the construction of flowsheets from linked unit models and the allocation of key products in the output currents. Through this approach, it is possible to replace experimental studies in a laboratory or pilot plants by computational procedures using appropriate mathematical models. At the same time, modeling of reactive distillation is complicated by the non-ideality present in reacting systems because their properties vary significantly while the concentration of both reactants and products changes. The design and development of a simultaneous reaction-separation process is much more complex than a conventional distillation, as it is required to solve some additional problems: to choose an appropriate catalyst (homogeneous, heterogeneous), to define a place for its location inside the tower and to use energy of the chemical interaction for heating purposes. There is an increasing role of advanced mathematical methods for modeling non-conventional separation processes. These are important in defining optimal conditions for performing the process whose condition has multiparametric nature [40, 41].

The *analysis of the process statics* is defined as a short-cut method and a fundamental tool for studying the possibility of perform a simultaneous reaction-separation process. It allows the

selection of the so-called limiting steady states, which represent the points where maximum conversion and selectivity in a reactive distillation can be achieved. Furthermore, this analysis gives engineers criteria to propose the corresponding technological scheme based on the principles of process intensification. This analysis is useful since it comes before mathematical and experimental modeling that would represent a large investment of time and capital to design of a distillation processes.

The *analysis of the process statics* uses certain ideas of reactive distillation processes, assuming that: reactions in chemical equilibrium are considered and the reactive distillation column operates under ∞/∞ regime (maximum efficiency, infinite number of stages and reflux) [39]. This analysis is performed in order to obtain the product compositions of each scheme included within the limits of the distillation region; this may help to predict the constraints of the system, the potential separation schemes and exclude the operations in which these limitations do not break. In conclusion, for such schemes the analysis of the process statics affects the behavior of the operating line (representation of the distribution of compositions in all sections of the column, rectification, stripping and reaction) of the respective pseudo steady state. Once this line is specified for a pseudo concentration, the chemical force needed to carry out the process is evaluated in order to predict the extent of a pseudo steady state and to determine its capacity to become a limiting steady state in practice [26].

Among the features of the method the following can be noted:

    (a) The method requires few initial data: model parameters of phase and chemical equilibrium and reaction stoichiometry.

    (b) The method is applicable to mixtures with a number of components and chemical reactions.

    (c) The method is appropriate to highly non-ideal mixtures, including azeotropic mixtures and blends with limited solubility.

    (d) The method can easily be formalized as algorithm.

    (e) The method allows the selection of the feasible limiting steady states.

    (f) The method reduces computational time and simplifies the use of large-scale experiments.

    (g) The method has been successfully tested in the design of many industrial processes.

In the structure of the model used for the analysis of the process statics analysis in reactive distillation operating under ∞/∞ regime (at maximum efficiency) the parameters to be stablished

are the product flow ratio (P / W) and the volume of the reaction zone and its location. It is feasible to change in some limits the extents of reaction by varying the volume of equivalent reaction zones and their distribution inside the column. Subsequently, it is possible also to take into account the extents of reaction as independent operating parameters. As a final result, the procedure used will provide a complete set of steady states with the corresponding operating parameters, allowing engineers to analyze and synthesize the corresponding technological scheme.

Steps to analyze and design a reactive distillation processes

The general methodology proposed to analyze and design a reactive distillation based on thermodynamics insights is shown the following scheme [26, 30]:

1. *Compatibility study between reacting and separating components*
    Reaction must be carried in liquid phase. Temperature and pressure for the reaction must satisfy the specification of activity of the catalyst employed. Handling of reagents (solvents, inert, catalysts), safety, etc.

2. *Analysis of the influence of separation on the reaction*
    Thermodynamic topological techniques are used to find the most favored distillation regions by the extent of reaction and selective removal of components.

3. *Thermodynamic topological analysis (analysis of the process statics)*
    Possibilities and restrictions with respect to the separation by distillation are identified in the reacting system in order to find the limiting trajectories where high conversion and practical feasibility can be achieved.

4. *Mathematical modeling*

5. *Verification of mathematical model*

6. *Simulation*
    A simplified flow diagram gives the location of the feed tray and reaction zone so as to have maximum selectivity, high conversion and thus maximum yield and purity of the products with the minimum energy consumption.

7. *Physical Experimentation*
    It should be as low as possible and only to verify theoretically obtained results.

8. *Dynamics (evaluation of the process through time)*
    It depends on if there are multiple steady states (presence or absence) and their stability. Control and automation.

9. *Comparison of reactive distillation schemes with other reaction - separation schemes*

Use of short-cut methods in order to find costs and energy balances.

10. Pilot plant
11. Installation in the industry.

2. Graph-Theory applied to Process Synthesis

Overview

Flowsheet generation, i.e., process synthesis, is the conceptualization step of designing any process [13]. It organizes the process so that it is optimal or at least near optimal in terms of one or more criteria that may be economic, environmental, and/or societal. Flowsheeting or network synthesis of an entire process is the macroscale synthesis or design activity for which the two major classes of methods corresponding to heuristic and algorithmic or mathematical-programming methods are available; this is also the case for mesoscale synthesis involving networking of a group of processing equipment or unit operations so that they collectively perform a specific processing function, and microscale synthesis involving the assembling of a single piece of processing equipment or unit operation like the approach presented by the reactive distillation case. The improvement of the heuristic as well as algorithmic methods is attributable to substantial work carried out during the last three decades [13], methods that were used in the development of this thesis.

Heuristics or rules of thumb are established on the basis of past experience and existing knowledge or databases. Usually, the procedure for implementing heuristic methods is relatively straightforward; only moderate computational effort is required. Consequently, globally or near globally optimal solutions are frequently unobtainable through the heuristic methods alone. One of the most prominent algorithmic methods, namely, the conventional mixed-integer programming (MIP) method, attempts to handle with these complexities by transforming an optimal network synthesis problem by manually interconnecting the processing units exhaustively to create a super-structure containing all possible substructures (networks), and solving the resultant optimization problem with a mathematical – programming solver and a simulation engine [42, 43].

Obviously, robust decision-making tools and very efficient computational procedures are needed to overcome the combinatorial complexities of process-network synthesis. A significant progress has been made in recent years toward achieving such a goal by the introduction of a novel class of graphs, called process graphs or P-graphs, and by the parallel establishment of a set of axioms and development of a group of combinatorially complex algorithms [44]. The core of the P- graph method for process synthesis lies in the capability the method has to define not only the optimal flowsheet but also the near-optimal flowsheets in ranked order.

2.1. P-graph Approach

The basis of the combinatorial or graph-theoretic method to generate optimal or near-optimal schemes include an innovative way to represent a chemical process as process graphs (P-graphs); a group of rules describing the fundamental characteristics of process flowsheets; and a set of rigorous algorithms that can be coded on a programming engine developed by Fan et al [45].

P-graphs

As pointed by Fan et al "a P-graph is a directed bipartite graph, i.e., digraph; it comprises two types of vertices or nodes" [44]. As shown in Figure 2.1, there are two types of vertices: the first one with circles representing the raw materials (*m*) and the second one with horizontal bars representing the operating units necessary to carry out the process (*o*). The lines with a symbol specifying the path of the flow of a material stream connect vertexes of material flows or operating units. Therefore, a P-graph is described as the resulting graph (*m*, *o*) of the combination between the vertices correspondent to the materials and the operating units. Figure 2.2 presents ordinary and P-graph schemes of a reactor and a distillation column. It must also be said that while P-graphs are able of exclusively represent different flowsheets arrangements in process synthesis, ordinary digraphs lack such capability [44].
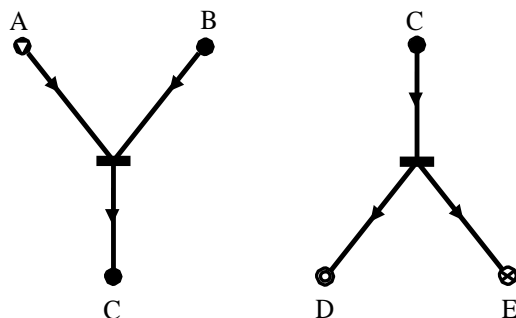
Figure 2-1: P-graph representation of a reactor and a distillation column.

In Figure 2.1 *A* is the raw material, *B* and *C* are intermediate materials, *D* is the desired product and *E* is an undesired byproduct.

Conventional P-graph
Reactor

Conventional P-graph
Distillation column
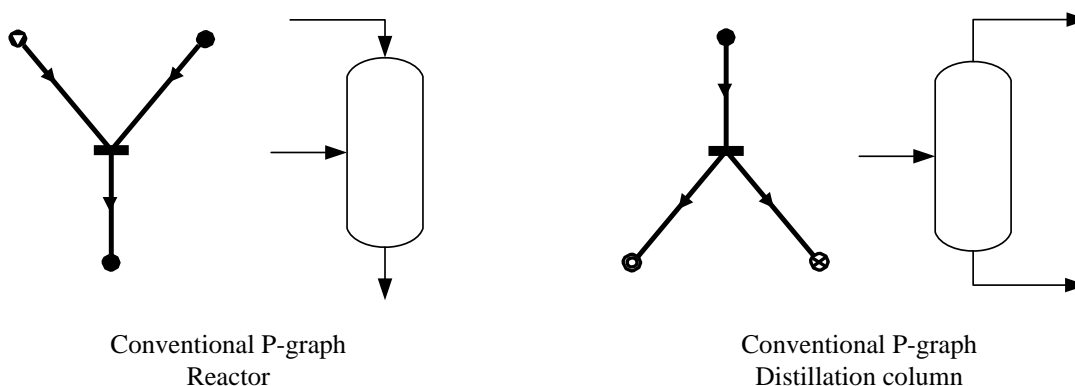
Figure 2-2: Reactor and distillation column represented as p-graphs.

Axioms

A set of axioms were developed by Fan et al to formulate the above concepts into a mathematically rigorous theory. These axioms are presented in their original statements [46]:

> "*P-graph (m, o) represents a combinatorially feasible process network, i.e., flowsheet, leading from the starting raw materials to the final products, if it satisfies Axioms (S1) through (S5) are given below (34-43):*
>
> *(S1) Every final product is represented in the graph: it suggests that every product is produced by at least one of the operating units of the flowsheet.*
>
> *(S2) A material vertex has no input if and only if it represents a raw material: a material is not produced by any operating unit of the system if and only if this material is a raw material.*
>
> *(S3) Only operating units defined in the synthesis problem are considered: only the plausible operating units of the problem are taken into account in the synthesis.*
>
> *(S4) Every operating unit has at least one path leading to a material vertex representing a final product: any operating unit of the system has a series of connections eventually leading to the operating unit generating at least one of the products.*
>
> *(S5) If a material vertex belongs to the graph, it must be an input to or output from at least one operating unit vertex in the graph*".

When each axiom is stand-alone applied they become impractical, however, when the 5 axioms are applied together they operate as a mesh to reduce all combinatorially unachievable or unacceptable flowsheets, which are regularly incorporated in the complete flowsheet.

Algorithms

The axioms lead the creation of proficient algorithms needed to perform the design of an achievable set of flowsheets. These procedures are algorithm MSG (Maximal Structure Generation) to generate the maximal scheme covering all the possible flowsheets, and hence, is the superstructure with minimal difficulty (*34-36*); algorithm SSG (Solution Structure Generation) to generate a whole set of combinatorially possible solution flowsheets that are contained in the maximal flowsheet (*35, 36*); and algorithm ABB (Accelerated Branch and Bound) to generate the improved a small amount of possible flowsheets using a branch-and-bound method, ordered according to an objective function right from the maximal structure (*37, 40*).

However, no attempt was made in the current work to provide rigorous mathematical discussion of the algorithms which are detailed in the references cited (*34-43*).

Algorithm MSG (Maximal Structure Generation)

The maximal structure of a chemical process in a design problem contains all the combinatorially possible flowsheets that are able to reach a set of products from the indicated raw materials having the optimal flowsheet contained in these possible arrangements. The application of this algorithm comprises four stages [44]:

1. The design problem is fixed by entering a set *M* of all the possible materials to be considered, a set *P* of the products to be obtained, a set *R* of the raw materials to be processed, and a set *O* of all possible operating units. The set *M* includes not only the intermediate materials linked with the operating units in set *O* but also the final products in set *P* and the raw materials in set *R*.
2. An initial structure of the flowsheet is made by joining all the shared material nodes.
3. The operating units and materials that are not included in the maximal structure are rejected, step by step and beginning from the raw-material finale, of the previously entered flowsheet by evaluating the nodes in a material vertex with those in the following operating-unit vertex to determine that none of the nodes violates an axiom. The removal of one node frequently leads to the rejection of other nodes connected to it.

4. The nodes are connected starting from the final-product end, of the residual entered flowsheet by evaluating if some of the connected nodes do not fulfill the conditions stablished by the axioms. Certainly, many of the nodes continue connected in the entered flowsheet generated in the second stage, However, some of the possible connections in the initial flowsheet can be removed in the third stage; they have to be reestablished in this final stage.

Algorithm SSG (Solution Structure Generation)

The maximal structure generated contains all the combinatorially possible solutions or combinatorially possible flowsheets that are able to reach a set of products from the indicated raw materials having. These flowsheets range from the simplest to the most complex, or complete, which is represented by the maximal structure itself. Obviously, the optimal structure in terms of an objective function, often the cost, is contained within the maximal structure; nevertheless, the simplest is not necessarily the optimal.

Algorithm SSG (solution structure generation) renders it possible to generate all the solution structures. It gives rise to the computational procedure for generating the solution structures. Particularly, algorithm SSG exposes all the possible flowsheets of the process to be designed. This algorithm has been established on the basis of a mathematical tool, called decision mapping (DM) which is also based on heuristic considerations [44, 47].

With the maximum structure generated by algorithm MSG and the decision mapping on the P-graph defined, it is possible to describe step by step a procedure for implementing the algorithm. This procedure allows the generation of an entire set containing the achievable flowsheets that can produce every desired product with all or some of the specified materials and operating units.

Algorithm ABB

Algorithm SSG generates with speed all the structures representing the combinatorially possible flowsheets from the maximal structure. Moreover, these flowsheets are deemed feasible if they can be optimized in terms of the profit or any other appropriate objective function. Consequently, they can be ranked according to the magnitude of the objective function.

When the number of solution structures generated by algorithm SSG is exceedingly large, their optimization can be indeed time consuming. In practice, only a fixed number of the optimal and near-optimal solution structures should be of interest to the designer, thereby

eliminating the need to generate all other solution structures. This can be accomplished with algorithm ABB (accelerated branch and bound); moreover, this algorithm ranks automatically the resultant network structures, i.e., feasible flowsheets. As its name implies, this algorithm resorts to the notion of branch and bound even though it differs substantially from the majority, if not all, of the conventional branch-and-bound methods.

Basic branch and bound.

Human activities often involve "yes-or-no" or "include- or-exclude" decisions that are discrete in nature. This is particularly the case in synthesizing any engineering systems; chemical-process systems are no exception. Moreover, for quantification, such discrete decisions are expressed as integer variables in general and binary variables in particular when the value of 0 or 1 is assumed. This gives rise to integer programming (IP) and mixed integer programming (MIP) when the performance equations, or the models, of the components, e.g., operating units in the case of process-network synthesis, are functions of one or more continuous variables [42, 47].

3. Methods

Overview

Regarding the solution methods, there are basically two approaches studied in this work: the first one is an integrated approach for the production of methyl acetate by reactive distillation based on two short-cut methods and the second one is a multi-level approach based on the graph-theory for the separation of the mixture resulting from the ABE fermentation [13].

The methodology includes an efficient analysis of an extensive variety of thermodynamic properties of the components to be generated and separated, description of appropriate processing methods (which takes advantages of the dissimilarities in the properties inherent in every component) and identification of methods to solve these tasks (solution of the problem using different techniques). The employment of the interactions between thermodynamic properties and process engineering principles, the physical viability restrictions for two design problems were analyzed and the equivalent process flowsheets were also determined. It was proved that since any optimal process must fulfill the thermodynamic and physical boundaries, the resulting optimal flowsheet must be inside a range established by the used methodology [36, 41].

The other analysis provided in this work highlights parts of complex systems. Unfortunately, the analysis of the process statics to design reactive distillation systems is both difficult to produce and difficult to interpret. To tackle the first problem, this work describes how information can be obtained from conventional mass balances in order to design a reactive distillation column using additional data obtained from experimental measures. To face the second problem, the work introduces a general calculation that makes an interpretation of the analysis of the process statics practically more meaningful by means of a short-cut method [26].

The applied methodology is hierarchical and involves two stages. The first stage deals with the study of the interactions between thermodynamic properties of the components to be generated and separated and their corresponding processing techniques. The second stages deals with the methods to process these systems. At the end of the second stage, a tentative flowsheet is generated including all the possible combinations that fulfill the previously defined restrictions for the process. Two additional stages were also used using a graph-theoretic based approach methodology. Stages three and four deal with the calculation of the optimal flowsheets considering operating and economic criteria. In this way, the thermodynamic based method generated information on processing alternatives, which was employed to create a maximal flowsheet and an initial estimative to the optimization problem.

Then, so as to overcome the requirement to evaluate all feasible flowsheets before identifying the optimal one, different rules to select the results are used. These rules, also known as heuristics, allow the engineer finding several satisfactory solutions of the design problem. The heuristic methods are in fact conventional and well established, having as a basis the knowledge of the designer of the physical and chemical phenomena linked to the operating units. This method gives no reliability of optimality.

3.1.   Analysis of the process statics for systems with located reaction zone

This method was used to find the best arrangement to calculate a distillation column, providing a set of alternatives to be qualitatively calculated. In systems where appropriate operating conditions are set to locate the reaction in a section of the column, it is possible for the compounds inside the column to be stable (both reactants and products), providing then the possibility of removing pure substances from a reacting mixture due to the effect of the simultaneous reaction-separation process.

The strategy of analysis includes [48, 49]:

a) *Determination of the conditions to carry out the process.* Before starting the design process it is essential to determine the optimal preconditions for the process such as temperature, pressure, and concentration of reactants, catalyst phase and feeding phase.

b) *Reaction zone location.* If the catalyst is solid, the reaction zone must be located over a so-called bed on the stage. If there is not catalyst or if it is liquid, the reaction zone can be located by setting specific areas inside the column where the concentration of reactants is

high. For instance, if the catalyst is a liquid with a boiling point between the boiling points of the products, the conditions can be chose in order to have the reaction located in the central part of the column. The approaches for locating the reaction zone must be specially measured for each specific case.

c) *Creation of the distillation chart and definition of the distillation regions and subregions.*
   To perform this analysis it is necessary to develop a representative phase diagram of the information acquired in previous steps (boiling and azeotropic points) and then set up its distillation regions and subregions.

d) *Improvement of the location of the distillation limits.*
   Usually, the compositions of the pseudoinitial mixtures to be separated in a reactive distillation are part of different distillation regions. Hence, the group of product-flow compositions and the value of the operating specification *P/W* rely on the position of distillation limits. They can be located accurately applying a phase equilibrium diagram.

e) *Construction of the chemical equilibrium line (surface)*
   The chemical equilibrium is the line (or plane) in which for all compositions contained in such space the chemical transformation rate equals to zero. These lines or planes break the concentration simplex in two regions; one of them represents the section where the forward reaction is favored while in the other section the reverse reaction occurs. To perform this calculation it is needed to simultaneously solve Equations (2.4 and 2.5) assuming that the reactions are carried out in liquid phase. These equations relate the thermodynamic properties of the system such as: temperature, pressure and the initial compositions.

$$K_i = \prod_{i=1}^{c} (\gamma_i * X_i)^{\upsilon_i} \qquad (0.4)$$

$$\sum_{i=1}^{c} X_i = 1 \qquad (0.5)$$

f) *Arrangement of the feed compositions and calculation of their chemical interaction field.*
   The concept of chemical interaction line (or surface) for reacting multicomponent systems was introduced by Barbosa et al [50, 51]. This line (or surface) determines the statics of the chemical component. Its dimension is represented by the number of independent chemical reactions and its construction and location in the concentration simplex is determined by the composition of the initial mixture and the stoichiometry of the reactions. The different values contained therein represent the amount of moles formed as a result of the chemical conversion; its magnitude is determined by the capacity of the reaction zone. This can be varied by modifying the corresponding parameters of the reaction system. To plot the reaction lines it is necessary to find the reaction pole (Π) by using the Equation 2.6. A

reaction pole represents the starting point coordinate of the extent of reaction vectors in the concentration simplex. By its calculation it is possible to identify the reaction direction and progression. Once this point is set, lines from the maximum conversion point to another coordinate within the reaction plane are drawn, defining different paths or lines of advance.

$$L_1 = L_2 * \frac{Np}{Nr - Np}$$

(0.6)

g) *Check of limiting steady states from the P/W = f(x*) dependence.*

Before starting the search, $P/W = f(x^*)$ curves are divided into sections, each being equivalent to the product flow compositions in one distillation subregion. The point where the $P/W = f(X)$ curves pass from one subregion to another are simply identified. At this position, the product composition leaves the lower dimension distillation region located at the limit of the major distillation region. Then, for each of the sections, the steady-state point is found at its precise limit and its resultant value of P/W. Those steady states are described by the highest conversions in specified distillation subregions, therefore, being then the limiting steady states. Once the pseudoinitial composition x^* and the process operating specification *P/W* are determined for each steady state, the amount and compositions of product flows can be found. Then, the steady state points for arbitrarily chosen initial compositions for both direct and indirect separation are linked to sets characterized by lines in the concentration simplex.

h) *Feasibility of the predicted steady states is checked.*

At first, reactive distillation paths must be drawn. Abovementioned were shown approaches for tracing such trajectories [78, 79]. Then, for the steady states with analogous trajectories, it is necessary to determine if the separation and chemical reaction will secure their reaching. Separation guarantees the steady state, only when the next conditions are fulfilled:

1. It must be a path in contact with the mass balance line, whose place is ruled by the compositions of the projected product flows.
2. The path must be present in the entire concentration simplex; it means that for every component of the mixture, there must be a segment of the path where the concentration of the component is higher than zero.

To evaluate how the chemical reaction guarantees the achievement of the steady states, the study is shortened to verify the probability of their and eventual productivity. It is also required to determine if there is a section of the path, with finite length, located in the

region where the forward reaction rules the process. Due to this analysis, it is possible to select the practical limiting steady states.

i) *Selection of alternatives to the process*

It is required to define the rate and compositions of product flows to be removed, tentative position of the reaction zone and the location of feed point for chosen steady states.

j) *Synthesis of the process flow diagram*

A schematic design strategy is presented in Figure 2-2.

```
┌─────────────────────────────────┐
│  Study of compatibility of the  │
│  reaction and separation        │
│  components.                     │
└─────────────────────────────────┘
               │
┌─────────────────────────────────┐
│  Analysis of the influence of   │
│  the separation component on     │
│  the reaction.                   │
└─────────────────────────────────┘
               │
┌─────────────────────────────────┐      ┌──────────────────────────────────────┐
│  Thermodynamic topological      │─────▶│  This analysis allows the selection of │
│  analysis (statics analysis).    │      │  optimal operating conditions from a   │
└─────────────────────────────────┘      │  complete set of different             │
               │                          │  configurations that corresponds to    │
                                          │  maximal yield of a target product.    │
                                          └──────────────────────────────────────┘
┌─────────────────────────────────┐
│  Mathematic modeling and        │
│  corroboration.                  │
└─────────────────────────────────┘
               │
┌─────────────────────────────────┐
│  Simulation of a simplified     │
│  diagram                         │
└─────────────────────────────────┘
               │
┌─────────────────────────────────┐
│  Dynamics (performance in time) │
│  and comparison between the      │
│  schemes                         │
└─────────────────────────────────┘
               │
┌─────────────────────────────────┐
│  Pilot plant and launching in   │
│  industry                        │
└─────────────────────────────────┘
```

Figure 3-1: General scheme for analyzing and designing a reactive distillation process.

To perform a thermodynamic topological analysis it is necessary to describe the system including a minimum amount of initial information, and then the process follows the next sequence:
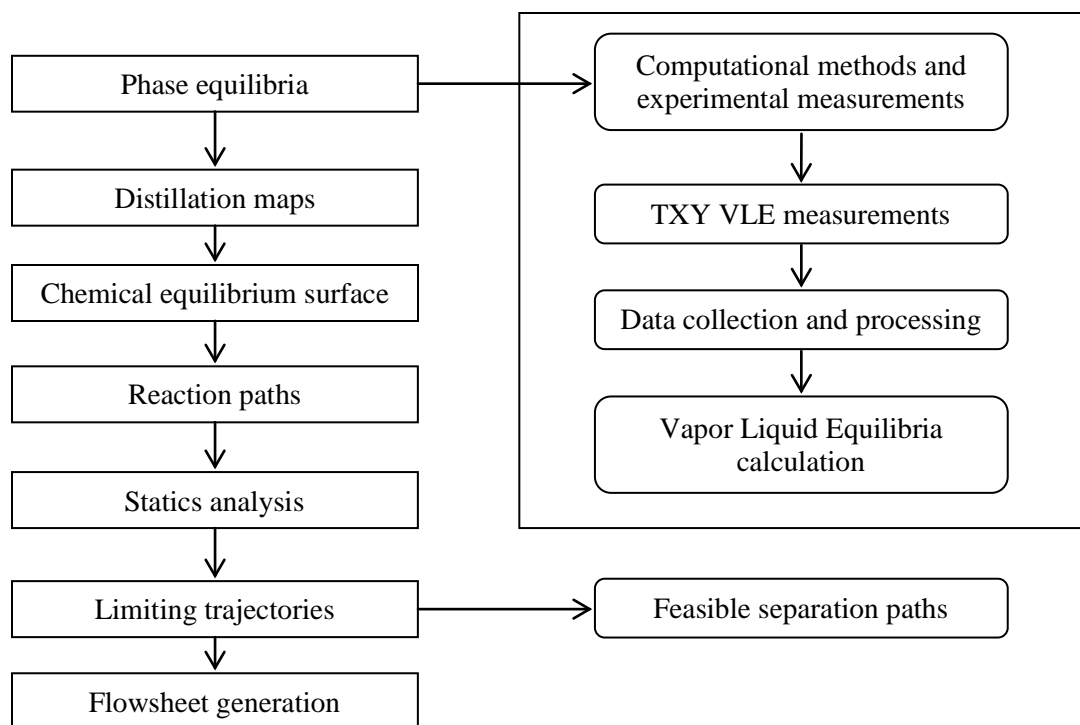
Figure 3-2: Steps to perform a thermodynamic topological analysis.

3.2.   Rigorous calculation of the reactive distillation column

For the design of the distillation sequences was used a shortcut design methodology (Wang - Henke) to obtain the specifications for a distillation column and to perform a comparison between the models used. Results show remarkable differences in structure, energy consumption, behavior and performance of the sequences. In the development of this work two methods were used for solving the steady state model of the reactive distillation column. The first method is an extension of the method of Wang - Henke to conventional distillation columns, called bubble point method, which was extended to reactive distillation columns by Suzuki, Yagi, Komatsu and Hirata [52, 53]. The complete mathematic model is presented in Annex C (Chapter 9).

The extension of the method developed by Wang - Henke has the advantage that is easy to solve by programming, since the method organizes the equations in a tridiagonal matrix, which is much easier to solve. The disadvantage of this method is that in many cases does not reach the desired convergence. Since the extension of the method of Wang - Henke fails in some cases; it must be used another method to achieve the desired convergence while solving the system. The second method used is based on the Newton – Raphson algorithm, where all the equations are solved simultaneously. It is worth noting that although both methods require initial values of the variables

to start the calculations, the extension of the Wang - Henke method only needs values of temperature and vapor flows, i.e. *2n* variables must be assumed, while in the calculation of the Newton - Raphson are need initial values for all the variables, i.e. $n(3 + 2c)$ variables, which makes the method of Newton - Raphson much more sensitive to the choice of the initial values.

In general, the solving process starts with the Wang – Henke method, although it cannot reach a desired convergence, it would provide a good starting point for further calculations by the Newton – Raphson method.

In the simulation of each of the cases for the reactive distillation of methyl acetate was followed a special methodology in order to achieve convergence. In general, the system of equations becomes unstable when the reaction rates are high. To achieve convergence in each of the cases studied, the simulation started with a very low reaction rate, for example at reaction rates where conversion is around 1%. Once the desired convergence for this reaction rate is reached, the simulation starts to increase the reaction rate gradually until reaching a high conversion percentage, being very careful.

Several methods were studied to get the system to the desired convergence, for example, use of thermodynamic homotopy (to introduce the fugacity coefficient), variation of the step size in the Newton - Raphson method. There were tested several initialization schemes Wang cycle - Henke, using then the variation in the reaction rate from a small value to the desired conversion. This procedure is known as kinetic homotopy.

In the model applied in this work the following assumptions were taken into account:

− The vapor hold-up in the stages is negligible compared to the liquid hold-up. This assumption is acceptable because in conventional systems the pressure is moderate and the density of the liquid is much higher than the density of the vapor.
− The liquid retained on the plate is perfectly mixed, i.e., the liquid flow leaving a stage has the same concentration of the liquid on the stage.
− The vapor phase and the liquid phase leaving each plate are in phase equilibrium.
− The reaction occurs only in the liquid phase and is represented by a kinetic equation.
− The pressure drop through the distillation column is negligible, that is, the pressure in the column is uniform.

A schematic design strategy is presented in Figure 3.3, Figure 3.4 and Figure 3.5.

START

Specify:

[Fi], [zi,j], [Ti,j], [Uj],

[Wj],[Qj], n, Li, Ui, Vi, P

Calculate initial values:

[Tj], [xi,j], [yi,j], [Vj], [Lj]

$k = 0$

$k = k+1$

Calculate the Jacobian matrix

$J\left(\vec{X}^{k-1}\right)$

Calculate the vector of functions

$\vec{F}\left(\vec{X}^{k-1}\right)$

Solve via Gauss-Jordan elimination

$J\left(\vec{X}^{k-1}\right)\cdot\Delta\vec{X}^{k} = -\vec{F}\left(\vec{X}^{k-1}\right)$

Calculate

$\vec{X}^{k} = \vec{X}^{k-1} + \Delta\vec{X}^{k}$

1

F   Feed flow
z   Feed composition
x   Liquid composition
y   Vapor composition
T   Temperature
P   Pressure
Q   Heat duty
L   Liquid flow rate
V   Vapor flow rate

1

Calculate the Euclidean norm of the discrepancy functions

$$\left\|\vec{F}\left(\vec{X}^{k}\right)\right\| = \sqrt{\sum_{t}\left(f_{t}\left(\vec{X}^{k}\right)\right)^{2}}$$

Yes $\left\|\vec{F}\left(\vec{X}^{k}\right)\right\| < \left\|\vec{F}\left(\vec{X}^{k-1}\right)\right\|$ Not

Calculate

S_{k}

Calculate

$\vec{X}^{k} = \vec{X}^{k-1} + S_{k}\Delta\vec{X}^{k}$

Calculate the Euclidean norm of the discrepancy functions

$$\left\|\vec{F}\left(\vec{X}^{k}\right)\right\| = \sqrt{\sum_{t}\left(f_{t}\left(\vec{X}^{k}\right)\right)^{2}}$$

Not $\sqrt{\sum_{t}\left(f_{t}\left(\vec{X}^{k}\right)\right)^{2}} \leq \lambda$ Yes

Calculate

Q_{1} and Q_{c}

END

Figure 3-3: Wang – Henke and Newton – Raphson algorithm applied to design of reactive distillation columns.
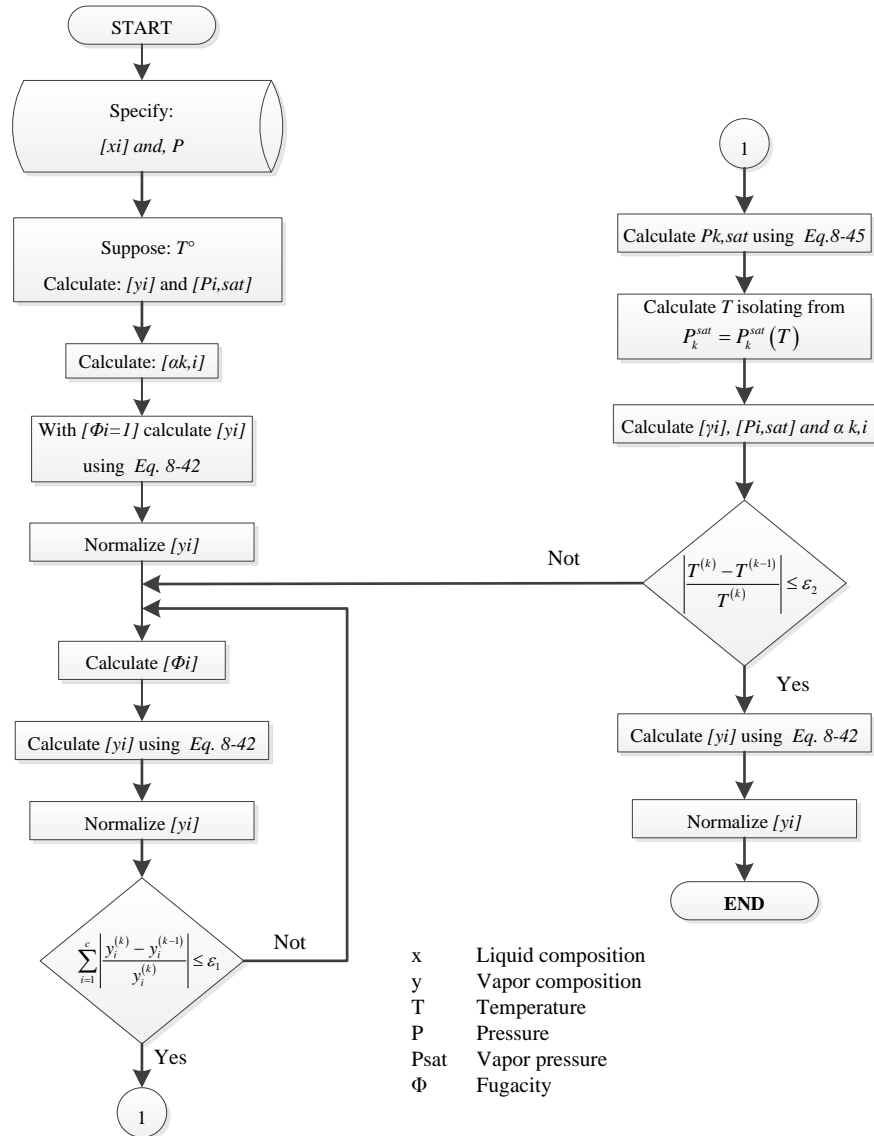
Figure 3-4: Bubble point calculation.

3.3. Implementation of P-graphs algorithms

As mentioned in Chapter 2, these algorithms resorts to the fundamental notion of branch and bound. The method does not exploit the structural features of the process system. This is magnified when the model is based on the conventional super-structure containing all possible networks, the majority of which tends to be combinatorially infeasible and thus redundant for any sizeable process. In contrast, these algorithms judiciously exploits the structural features of the process to be synthesized, which manifest themselves in the maximal structure consisting of only combinatorially feasible networks, or flowsheets. Totally unlike the conventional super-structure, the maximal structure does not contain any redundant networks and can be algorithmically

constructed efficiently. Moreover, branching involved in constructing the maximal structure is executed at an operating unit or a material or materials uniquely associated with it as they exist in the maximal structure. Thus, the sizing of any operating unit with a certain throughput can be carried independent of the execution of synthesis; naturally, the continuous variables in the governing equations of the operating unit are involved in this sizing. The procedure is initiated at the final, or desired, product and proceeds upward through the maximal structure towards the raw materials. Nevertheless, unlike the implementation of these algorithms, not all these solution structures that are only combinatorially feasible need be to separately optimized in implementing algorithm branch and bound [44].

The mathematical-programming problem consists of the constraints and the cost function. For the process networks system problems, the constraints comprise the mass balances, the amounts of products to be manufactured to meet the demand, and the availability of raw materials. The mass balances must be satisfied by all the intermediate materials in such a way that the amount of each material produced is greater than or equal to the amount consumed. The intermediate materials must be produced and also consumed. The cost function represents the cost of the network, i.e., the plant of the process synthesized, which is regarded as being equal to the total sum of the investment cost (capital cost), operating costs of the operating units, and prices of the raw materials. Here, the cost of any operating unit is simply considered to be in the form, $a + bx$, where x is the size or capacity of the operating unit; a, the fixed charge, or cost; and b, the proportional constant representing the cost of the operating unit of unit size. The fixed and proportional costs are equal to the sum of the fixed and proportional parts of both the capital and operating costs over the payout period, respectively. Thus:

$$\text{Operating cost} = a_{operating} + b_{operating}\,x$$

$$\text{Capital cost} = a_{capital} + b_{capital}\,x$$

$$\text{Annualized capital cost} = \frac{a_{capital}}{\text{Payout period}} + \frac{b_{capital}}{\text{Payout period}}\,x$$

$$= a_{operating} + b_{operating}\,x + \frac{a_{capital}}{\text{Payout period}} + \frac{b_{capital}}{\text{Payout period}}\,x$$

$$= \left(a_{operating} + \frac{a_{capital}}{\text{Payout period}} \right) + \left(b_{operating} + \frac{b_{capital}}{\text{Payout period}} \right) x$$

$$= a + bx$$

Naturally, the sizing and costing of operating units can be explicitly carried out independent of each other for any given feed rate to the system. The overall cost of the system can be simply

computed as the sum of the annualized costs of individual units included in the flowsheet. These costs are obtained by simulating all the structures using the commercial software Aspen Plus.

The next concept maps show the strategy to be followed in order to represent the downstream processing as a process graph and to find optimal flowsheets [45, 46].
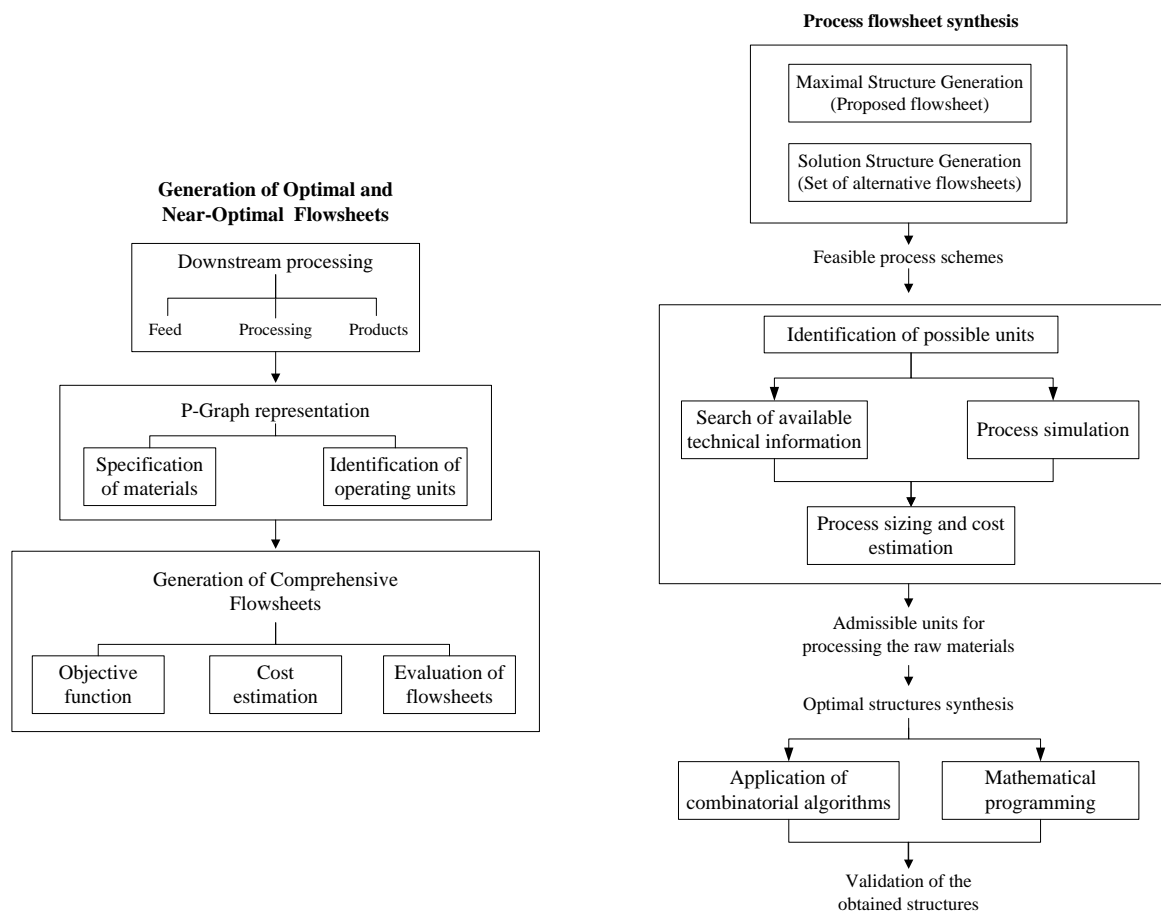
Figure 3-5: Main steps for the synthesis of a process through combinatorial algorithms.

3.4. Methods used in the experimental set-up

In this work, six binary systems (methanol + acetic acid, methanol + methyl acetate, methanol + water, methyl acetate + acetic acid and water + acetic acid) were studied experimentally. These systems are important in the design of reactive distillation processes, especially in the esterification of acetic acid with alcohols like methanol to obtain methyl acetate. Additionally, the binary interaction parameter of the second virial coefficient (k_{12}) and the non-random two liquid (*NRTL*) model parameters (α_{12} and α_{21}) were calculated for these nine binary systems at subatmospherical pressure (580 mmHg). Experimental data were correctly correlated using Peng–Robinson equation

of state (EOS) coupled with the Wong–Sandler mixing rules. The principal goal is to fit binary model parameters, and to extend from there on the calculation to multicomponent reactive systems [9, 54].

Apparatus and procedure

For the experimental determination of phase equilibrium, a recirculation still modified by Cardona has been used [55]. This equipment is also utilized to study phase equilibrium in systems with chemical reaction, and it is shown in Figure 3.6. In this apparatus the fed sample is constantly recycled by means of a system type Cottrell (system that consists of a tube with an electrical resistance that vaporizes the mixture). This tube is connected to another one of smaller diameter which allows an intense recirculation in whole system to assure that the phases are in contact. After the first operation hour, samples are extracted every 15 minutes until reaching the stabilization of the system in study (approximately 2 hours). Temperatures were measured by digital thermometers with ±0.05°C. At the beginning of the every run, the pressure was measured with barometer CASIO. Only when the pressure was of 580mmHg (normal pressure in Manizales, 2167m above sea level) the experiment was carried out. The samples of liquid and vapor obtained were analyzed together by means of refractive index.
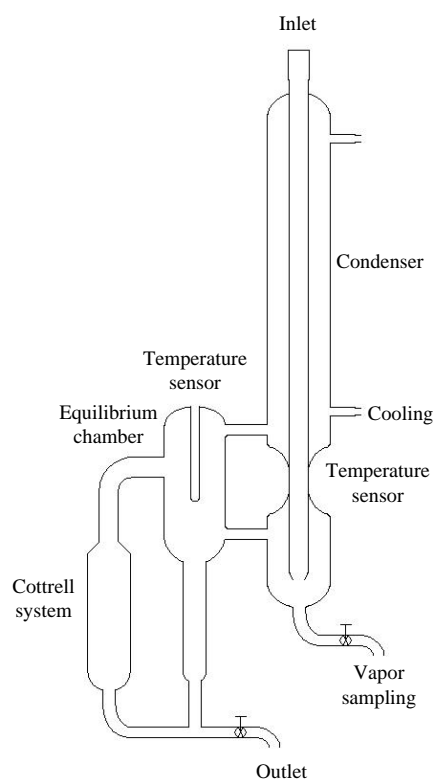
Figure 3-6: Basic scheme of the recirculation still.

Chemicals

Acetic acid (GR grade, +99%), methanol (GR grade, +99%), and ethyl acetate (GR grade, +99%) were purchased from Riedel-de Haen. Methyl acetate (GR grade, +99%) was purchased from Merck, and the deionized water (electric resistance, 18.2Ω/cm) was generated by a Millipore distilled water generator.

Objective functions for model fitting

In order to develop a correlation for certain thermodynamic property, all the parameters that influence this property must be determined and then study the influence of each of these parameters on the property under consideration, using literature data available for this purpose. In the case of Vapor-Liquid equilibrium data, where pressure P, temperature T, liquid x_i and vapor y_i molar fractions are given, also the deviation between the experimental and predicted activity coefficients or excess Gibbs energies can be used to fit the required binary parameters [8, 56].

Furthermore, the parameters can be determined by a simultaneous fit to different properties to cover properly the composition and temperature dependence of the activity coefficients. In order to determine the optimal parameters for the Vapor-Liquid equilibrium model, three objective functions that require bubble point temperature calculation from an additional iterative process were analyzed. The objective functions involve additional iterative procedures for calculating their optimal values and are explicit models because the adjusted variables are calculated from a bubble point pressure calculation algorithm. The studied objective function are [54]:

$$f_1 = \sum_{i=1}^{np} \sum_{j=1}^{nc} \left(\frac{x_{i,j}^{\exp} - x_{i,j}^{calc}}{x_{i,j}^{\exp}} \right)^2$$

$$f_2 = \sum_{i=1}^{np} \sum_{j=1}^{nc} \left(\frac{y_{i,j}^{\exp} - y_{i,j}^{calc}}{y_{i,j}^{\exp}} \right)^2$$

$$f_3 = \sum_{i=1}^{np} \left(\frac{T_i^{\exp} - T_i^{calc}}{T_i^{\exp}} \right)^2 + \sum_{i=1}^{np} \sum_{j=1}^{nc} \left(\frac{x_{i,j}^{\exp} - x_{i,j}^{calc}}{x_{i,j}^{\exp}} \right)^2 + \sum_{i=1}^{np} \sum_{j=1}^{nc} \left(\frac{y_{i,j}^{\exp} - y_{i,j}^{calc}}{y_{i,j}^{\exp}} \right)^2$$

As it is observed in the third objective function, this relation is a complement of functions two previous equations. However, this does not assure that the binary parameters obtained by these three functions will be identical. Although these objective functions have very similar computing times, the vapor–liquid equilibrium calculations using their optimal parameters will give a major

precision represented in the pressure or the vapor phase composition (or both), but this depends of the objective function form.

The parameters were estimated using the Levenberg-Marquardt minimization algorithm for each mixture with the objective functions above presented. The optimal NRTL model parameters ($\alpha12$ and $\alpha21$) and the second virial coefficient interaction parameter ($k12$) are reported for the reactive mixture in the next chapter material. The deviations between experimental data and calculated values with Peng-Robinson Equation of State and the Wong–Sandler mixing rules were established through the relative percentage deviations in the bubble point temperature:

$$\Delta T = \sum_{j=1}^{N_p} \frac{\left|T_{\exp+x/y} - T_{cal+x/y}\right|}{T_{\exp+x/y}} \left(\frac{100}{N_p}\right)$$

The absolute mean deviation in the molar fraction in the vapor and liquid phase are as follows:

$$\Delta y = \sum_{j=1}^{N_p} \left|y_{\exp} - y_{cal}\right| \left(\frac{1}{N_p}\right)$$

$$\Delta x = \sum_{j=1}^{N_p} \left|x_{\exp} - x_{cal}\right| \left(\frac{1}{N_p}\right)$$

They are also reported in the following chapter. The optimal parameters found i were used to predict the phase equilibrium of the considered mixtures in the reactive system.

4. Results – Reactive distillation

4.1.   Characterization of the system

Production of Methyl Acetate by reactive distillation

The system studied was the production of methyl acetate by the reaction of methanol with acetic acid. This system has limitations that make it an excellent candidate for its production by reactive distillation. First, the chemical equilibrium does not favor the formation of methyl acetate, so that a large excess of methanol or acetic acid is needed to obtain high conversions of the limit reactant. Second, the existence of azeotropes adds an extra difficulty to separate the components involved in the reaction, which requires in the traditional process one or more additional separation steps increasing then the production costs [28, 57].

Methyl acetate is a solvent used in the industry as a coating for plastics or as a solvent for paints, cosmetics or fragrances. The production of high-purity methyl acetate by chemical reaction between methanol and acetic acid is difficult due to the limitations of chemical equilibrium and the formation of two minimum boiling point azeotropes (methyl acetate - methanol and methyl acetate – water). The first problem causes difficulties in the reaction as low conversions are achieved and the second difficulty complicates the operation due to the presence of azeotropes, needing then the use of additional separation operations to the distillation, such as liquid-liquid extraction.

Conventional processes for producing methyl acetate use multiple reactors in which a large excess of one of the reactants is used to achieve high conversions. Some others use a series of vacuum and atmospheric columns to change the composition of the azeotrope composed by methyl acetate and water. Refined methyl acetate is separated from unreacted reactants, which are recycled to the reaction. Other schemes use a series of distillation columns at atmospheric pressure and a column with an extracting agent such as ethylene glycol monomethyl ether, which acts as an agent to break the azeotrope between the methyl acetate and methanol.

In Figure 4.1 the conventional process for producing methyl acetate is presented, this process uses a reaction unit and nine separation columns. In Figure 4.2 the production process using reactive distillation is presented. The comparison between these two processes clearly shows one of the best advantages of reactive distillation which is the savings in the cost of capital.
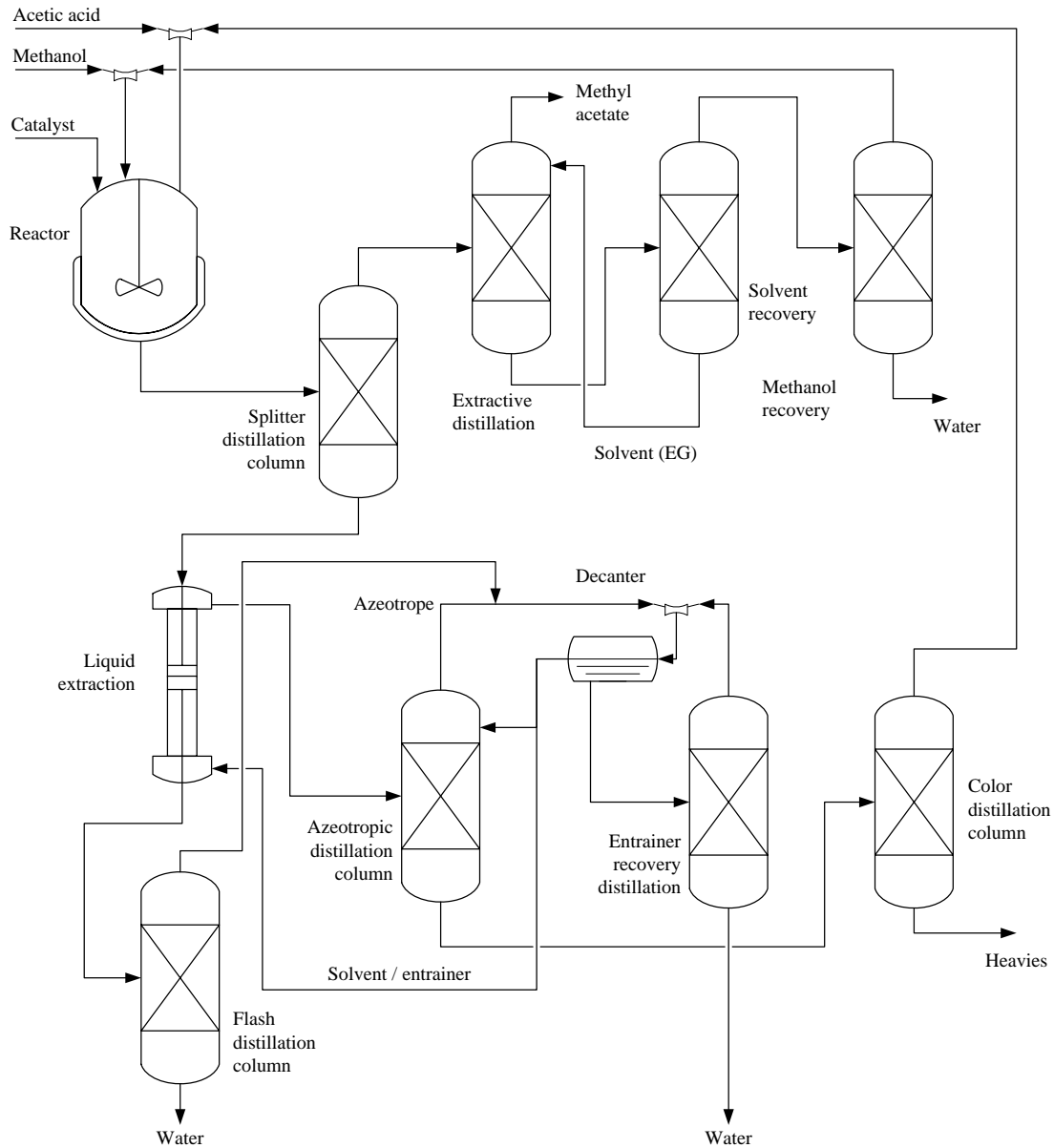
Figure 4-1: Methyl acetate production: conventional process.
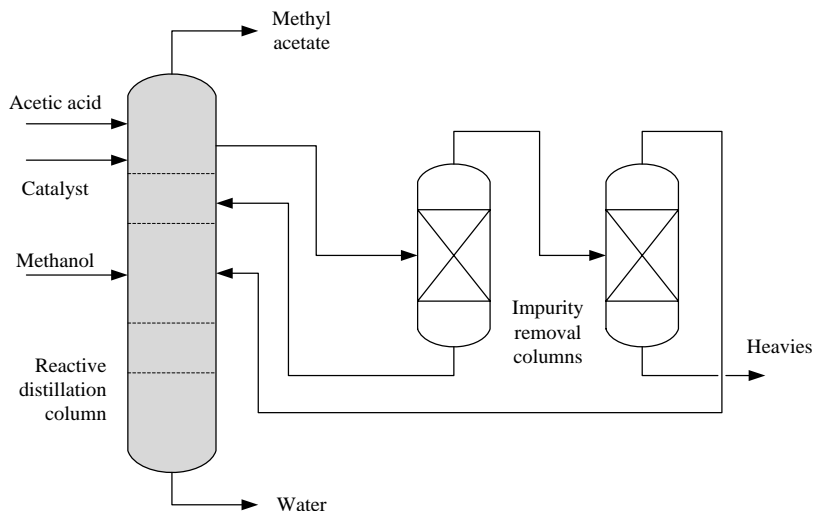
Figure 4-2: Methyl acetate production: reactive distillation.

Thermodynamic parameters

The optimal parameters found through experimentation and shown in Table 4.1 were used to predict the phase equilibrium of the considered mixtures.

Table 4-1: Fitted thermodynamic parameters for the NRTL and Peng-Robinson methods.

Model	Parameters						
	A_{12}	A_{21}	α_{12}	k_{12}	$\delta_{T+x/y}$	δ_x	δ_y
Methanol (1) – Water (2)							
NRTL	127.129	-537.528	0.1215		0.0168	0.0774	0.0257
PR – EOS				-0.0806	0.0019	0.0023	0.0023
Methanol (1) – Methyl acetate (2)							
NRTL	-443.508	261.636	0.0225		0.0105	0.0441	0.0704
PR - EOS				-0.0248	0.0009	0.0027	0.0015
Methanol (1) – Acetic acid (2)							
NRTL	57.425	-71.685	0.7835		0.0808	0.0887	0.0833
PR - EOS				-0.0047	0.0012	0.0023	0.0025
Acetic acid (1) – Methyl acetate (2)							
NRTL	-443.508	261.636	0.0225		0.0105	0.0441	0.0704
PR - EOS				-0.0248	0.0009	0.0027	0.0015
Acetic acid (1) – Water (2)							
NRTL	248.726	-204.854	0.8000		0.0261	0.0388	0.0369
PR - EOS				-0.0510	0.0028	0.0049	0.0051

The impact of inaccurate model parameters can be very serious. The parameters have a major influence on the investment and operating cost (number of stages, reflux ratio and energy consumption). Poor parameters can either lead to the calculation of non-existing azeotropes in zeotropic systems or the calculation of zeotropic behavior in azeotropic systems. The results of simulation models are strongly affected by the particular assumptions made in the plant model and by the particular assumptions made in the plant model and by the model parameters. This is the

reason why these parameters should be fitted to reliable data describing simplified systems, for example, binary mixtures. Regressing parameters to observations on the complex target system is usually not feasible, as the influence of the assumptions made on the performance of the equipment (e.g. tray efficiency in distillation) is not sufficiently isolated from the influence of the model parameters.

Chemical Kinetics: reaction rates

Auto-catalyzed reaction

The chemical reaction to be studied is the esterification of acetic acid with methanol to obtain the corresponding ester:

$$\underbrace{C_2H_4O_2}_{\text{Acetic acid}} \quad + \quad \underbrace{CH_4O}_{\text{Methanol}} \quad \rightleftharpoons \quad \underbrace{C_3H_6O}_{\text{Methyl acetate}} \quad + \quad \underbrace{H_2O}_{\text{Water}}$$

$$\underbrace{AA}_{\text{Acetic acid}} \quad + \quad \underbrace{MOH}_{\text{Methanol}} \quad \rightleftharpoons \quad \underbrace{MA}_{\text{Methyl acetate}} \quad + \quad \underbrace{H_2O}_{\text{Water}}$$
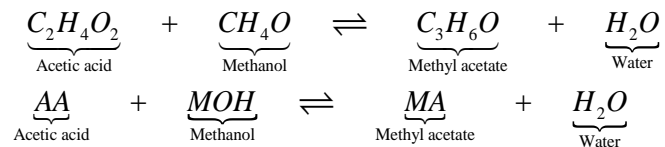
The expression auto-catalyzed kinetic makes reference while during the reaction any kind of catalyst, neither liquid nor solid is added. Esterification reactions are catalyzed by acids in general, in this case it was assumed that acetic acid catalyzes the reaction. The kinetic equation that was used was the expression reported by Pöpken et al [58]. This kinetic expression is given by:

$$r = \frac{1}{v_i}\frac{dx_i}{dt} = a_{HOAc}^{\alpha}\left(k_1 a_{HOAc} a_{MeOH} - k_{-1} a_{MeOAc} a_{H_2O}\right) \tag{0.7}$$

where the temperature dependence of the reaction rate constants are given by the Arrhenius equation:

$$k_i = k_i^0 \exp\left(\frac{-E_{Ai}}{RT}\right) \tag{0.8}$$

where k_i^0 is the frequency factor and E_{Ai} is the activation energy.

Exponent α	Activity	Relative error (%)	k_1^0 (s⁻¹)	E_{A1} (KJ/mol)	k_{-1}^0 (s⁻¹)	E_{A-1} (KJ/mol)
1.056	NRTL	2.2	6.06×10^5	63.8	9.84×10^6	80.0

The units of the eaction rate are given by the units of the rate constants. In this case, the expression has units of $\left[\dfrac{1}{s}\dfrac{kmol_i}{kmol_t}\right]$, where $kmol_i$ refers to the number of moles of component i and $kmol_t$ refers to the number of total moles in the hold-up volume of the stage. It was assumed that the kinetic equation has units of $\left[\dfrac{1}{s}\dfrac{kmol_i}{m_t^3}\right]$, where m_t^3 refers to the volume of the overall hold up of the stage.

In order adapt the kinetic expression to the model is necessary to change mole fractions to concentration units. To make this change the molar volume of the mixture is used, which is calculated as:

$$\rho_i \left(\frac{kmol_i}{m_i^3} \right) = \frac{A}{B^{\left(1+\left(1-\frac{T}{C} \right)^D \right)}}$$

$$\rho_{mixture} \left(\frac{kmol_t}{m_t^3} \right) = \frac{1}{\sum\limits_{i=1}^{c} \dfrac{x_i}{\rho_i}}$$

(0.9)

where the values of the constants A, B, C and D are reported in Table E3 Annex E. The kinetic expression in appropriate units is given as follows:

$$r = \rho_{mixture} \left(a_{HOAc}^{\alpha} \left(k_1 a_{HOAc} a_{MeOH} - k_{-1} a_{MeOAc} a_{H_2O} \right) \right) \left[\frac{1}{s} \frac{kmol_i}{m_t^3} \right]$$

(0.10)

Catalyzed reaction

The reaction is carried out in liquid phase, with an initial mixture of pure reactants. It is also possible to use a liquid catalyst (sulfuric acid or phosphoric acid), but as is well known, limitations in the storage, environmental impact, and the impact their use may have in the separation make them unfeasible for this analysis; alternatively is chosen a solid catalyst (Amberlyst 15). Hence, a solid catalyst is chosen due to its benefits of use, especially because it provides enough concentration of H^+ ions which guarantees an enhancement of the reaction rate.

The kinetics is based on the following adsorption mode [58]l:

$$r = \frac{1}{m_{cat}} \frac{1}{v_i} \frac{dn_i}{dt} = \frac{k_1 a_{HOAc}' a_{MeOH}' - k_{-1} a_{MeOAc}' a_{H_2O}'}{\left(a_{HOAc}' + a_{MeOH}' + a_{MeOAc}' + a_{H_2O}' \right)^2}$$

(0.11)

with $a_i' = \dfrac{K_i a_i}{M_i}$, where K_i is adsorption equilibrium constant for the component i, M_i and a_i are their molecular weight and activity, respectively. The rate constants k_1 and k_{-1} are defined by the Arrhenius equation:

$$k_1 = 8.497 \text{x} 10^6 \left(\frac{mol}{g_{cat} s} \right) \exp\left(\frac{-60470}{RT} \frac{Joule}{mol} \right)$$

$$k_{-1} = 6.127 \text{x} 10^5 \left(\frac{mol}{g_{cat} s} \right) \exp\left(\frac{-63730}{RT} \frac{Joule}{mol} \right)$$

K_{HOAc}	K_{MeOH}	$K_{MeOA}c$	K_{H2O}
3.15	5.64	4.15	5.24

4.2.   Analysis of the process statics

By applying the methodology described in Chapter 1 and Chapter 3 it is performed the analysis of the process statics with located reaction zone to the studied process, both manual and with graph-analytical techniques. In Annex A (Chapter 9) properties of the pure components and the mixture of the system are listed.

Location of the reaction zone

It is assumed that the reaction zone is located and corresponds to the section where the reactants are concentrated; therefore, this is the zone where reactants are fed and where the catalyst is physically located.

Analysis of the structure of the distillation diagram for the reactive system

According to the physicochemical information provided for the respective system, a phase diagram was obtained, see Figure 4.3. By observing the diagram, we can see that there is only one distillation region. The residue curves start from the azeotrope of minimum boiling point (methyl acetate - methanol) and reach the vertex of pure acetic acid. As reported by the characterization of the fixed points, are obtained a stable node (acetic acid), an unstable node (methanol – methyl acetate azeotrope) and the rest are saddle points. In the case of direct separation there are three distillation subregions, while in the case of indirect separation there are two subregions as seen in Table 4.2.

Table 4-2: Distillation subregions for direct and indirect separation

Direct separation	Indirect separation
1. MOH – AA – H_2O	1. Az_{MA-MOH} – Az_{MA-H2O} – MA
2. Az_{MA-H2O} – H_2O – AA	2. Az_{MA-MOH} – Az_{MA-H2O} – MOH – H_2O
3. Az_{MA-H2O} – MA - MOH	

In the direct separation the flow of distillate is the binary azeotrope (methyl acetate - methanol) for all the subregions and the bottoms product for the the first subregion is a ternary mixture of methanol - acetic acid – water. For the second and third distillation regions a ternary mixture composed by methyl acetate – water - acetic acid.
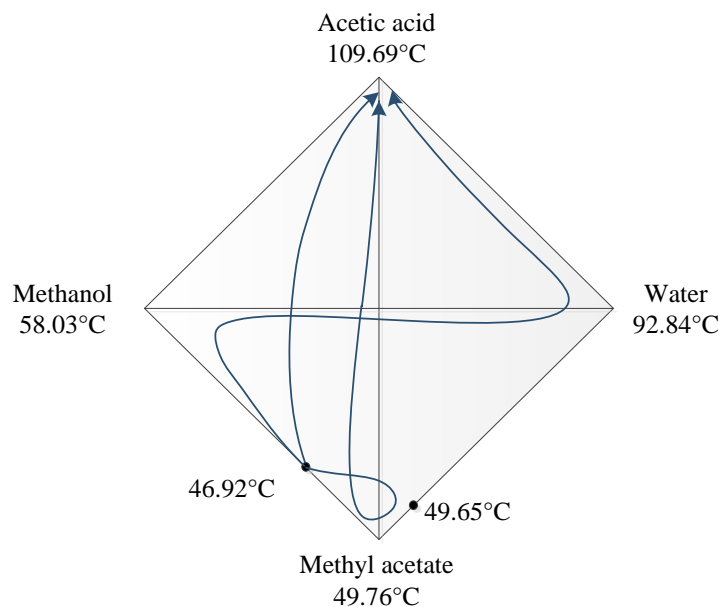
Figure 4-3: Phase diagram

Estimation of the boundaries of the subregions in the concentration simplex

For both direct and indirect separation, the boundaries of the subregions are two segments of field; the first of them is formed by projecting the thermodynamic constraint (first degree separatrix) of the ternary system (methanol – methyl acetate - water) in the quaternary diagram, see Figure 4.4a, while the second is the projection of the existing geometric separatrix in this system that goes from the azeotrope methyl acetate - methanol, acetic acid and pure water (see Figure 4.4b). In the same way, for both direct and indirect separation the boundaries of the subregions are a segment of the field formed by projecting the thermodynamic constraint (first degree separatrix) of the ternary system (methanol-methyl acetate-water) and the geometric constraint in the quaternary diagram. The physical meaning of the first separatrix and how it changes its order by passing from a thermodynamic limit to a geometric limit is observed in Figure 4.4a.
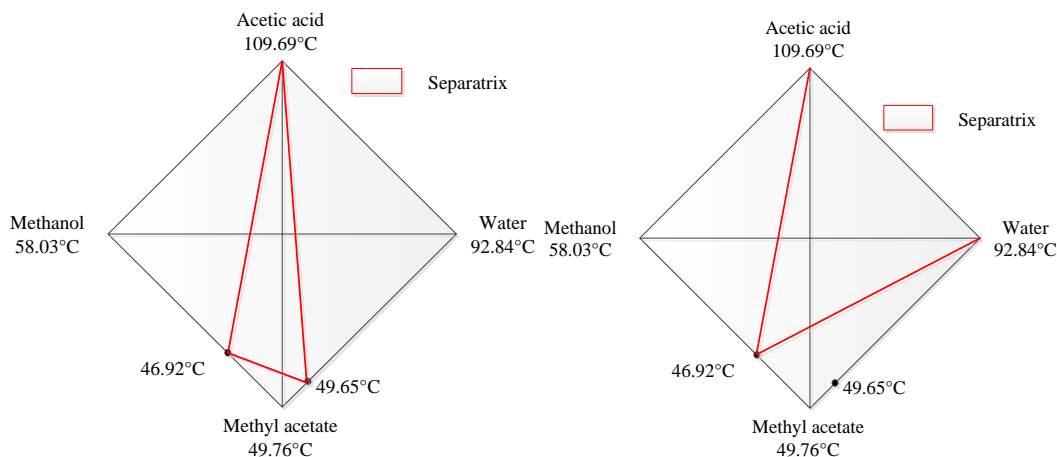
Figure 4-4: First degree separatrix and Geometric projection of the first degree separatrix

Construction of the line (or surface) of chemical equilibrium

In this study, the representation of chemical equilibrium corresponds to a surface (see Figure 4.5), which was built by taking the value of the equilibrium constant ($K_{equ} = 5.2$) reported in [28] for the system and solving the system of relevant equations proposed in Chapter 3.
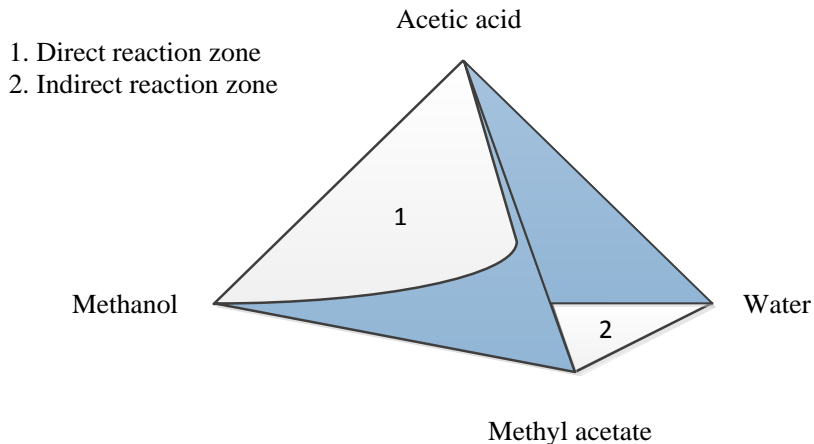
Figure 4-5: Chemical equilibrium surface

In the above representation is clearly observed in sections where the reaction has a direct and an indirect direction.

Construction of the reaction path

By using Equation 3.1, 3.2 and 3.4, the direction and extent of the interaction lines are determined based on the stoichiometry of the reaction:

$$L_1 = L_2 \frac{2}{2-2} \quad \rightarrow \quad L_1 = \infty \cdot L_2$$

Since the pole does not exist $\Pi = \infty$, the extent of reaction lines are parallel to the extent of reaction line for the equimolar case (Figure 4.6).
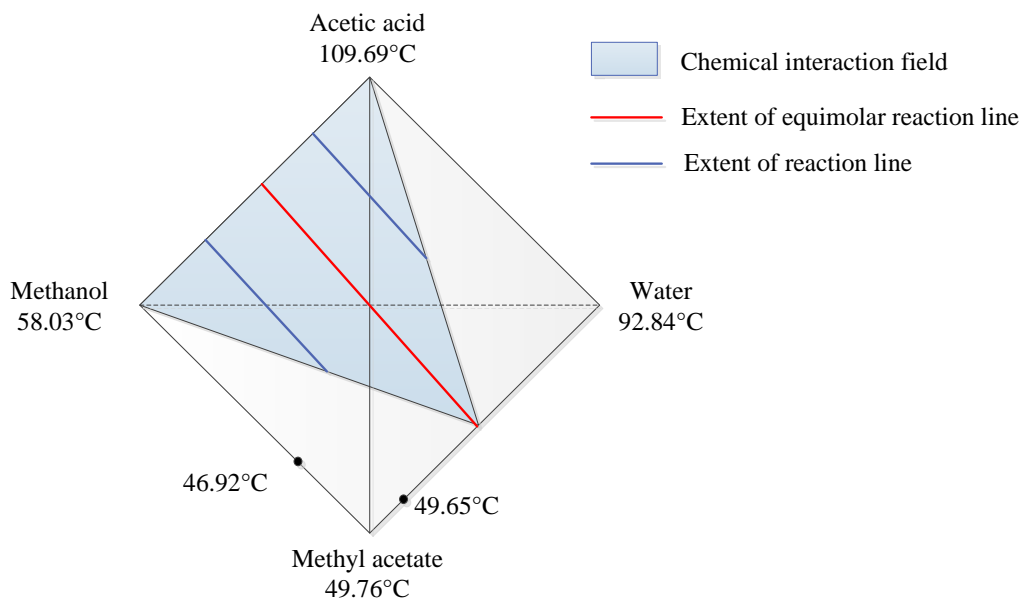
Figure 4-6: Chemical interaction field and extent of reaction lines

Calculation of the P/W relation as a function of the pseudoinitial compositions and estimation of the limiting steady states

For a set of initial mixtures (Table 4.3) were plotted the corresponding extent of reaction lines for the system under study. Over these lines were located the respective mixtures with a pseudoinitial composition (X^*_i), tracing the corresponding balance lines for direct and indirect separation. By means of Equation 1.1 and 1.2 were obtained different values of *P/W* for each pseudoinitial composition proposed, see Figure 4.7 and 4.8. With these values the respective graphs of *P/W* as a function of X^* are formed, see Figure 4.9. From the graphic representation, limiting steady states are selected (maximum or minimum points SI and end points SII). The limiting steady states found for the system under consideration are summarized in Table 4.4.
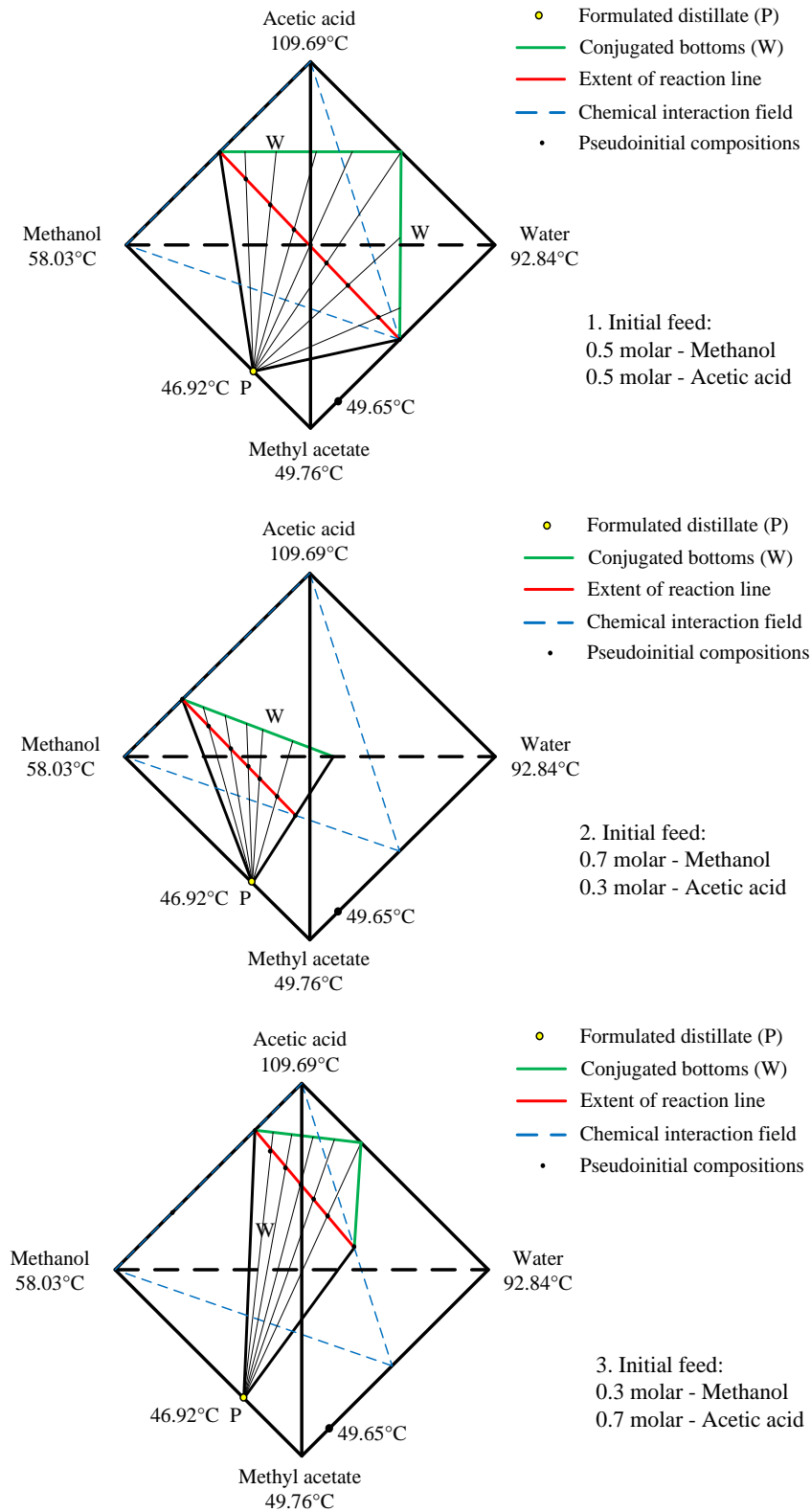
Figure 4-7: Calculation of the P/W relation for direct separation and feed conditions 1 to 3
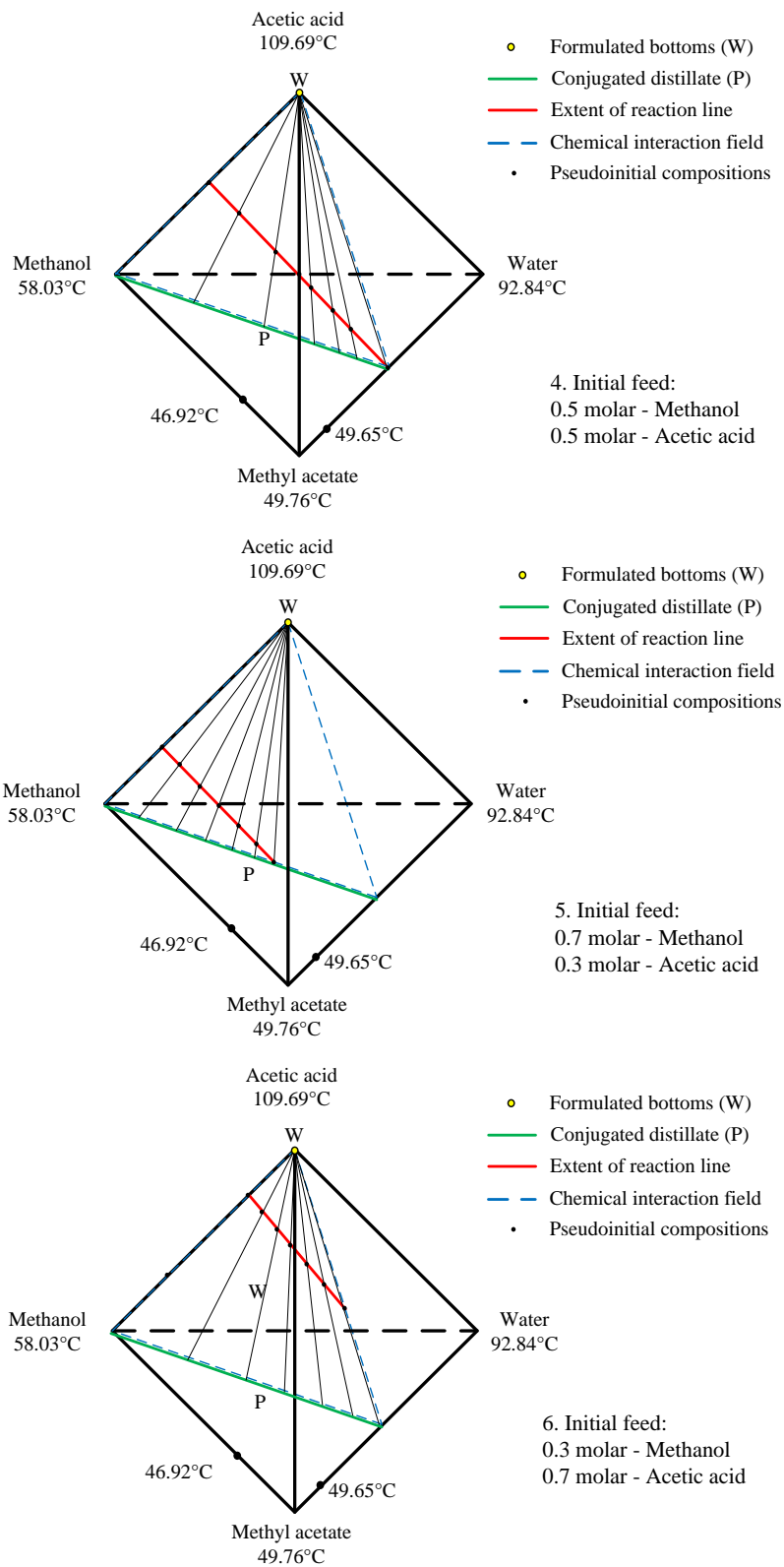
Figure 4-8: Calculation of the P/W relation for indirect separation and feed conditions 4 to 6
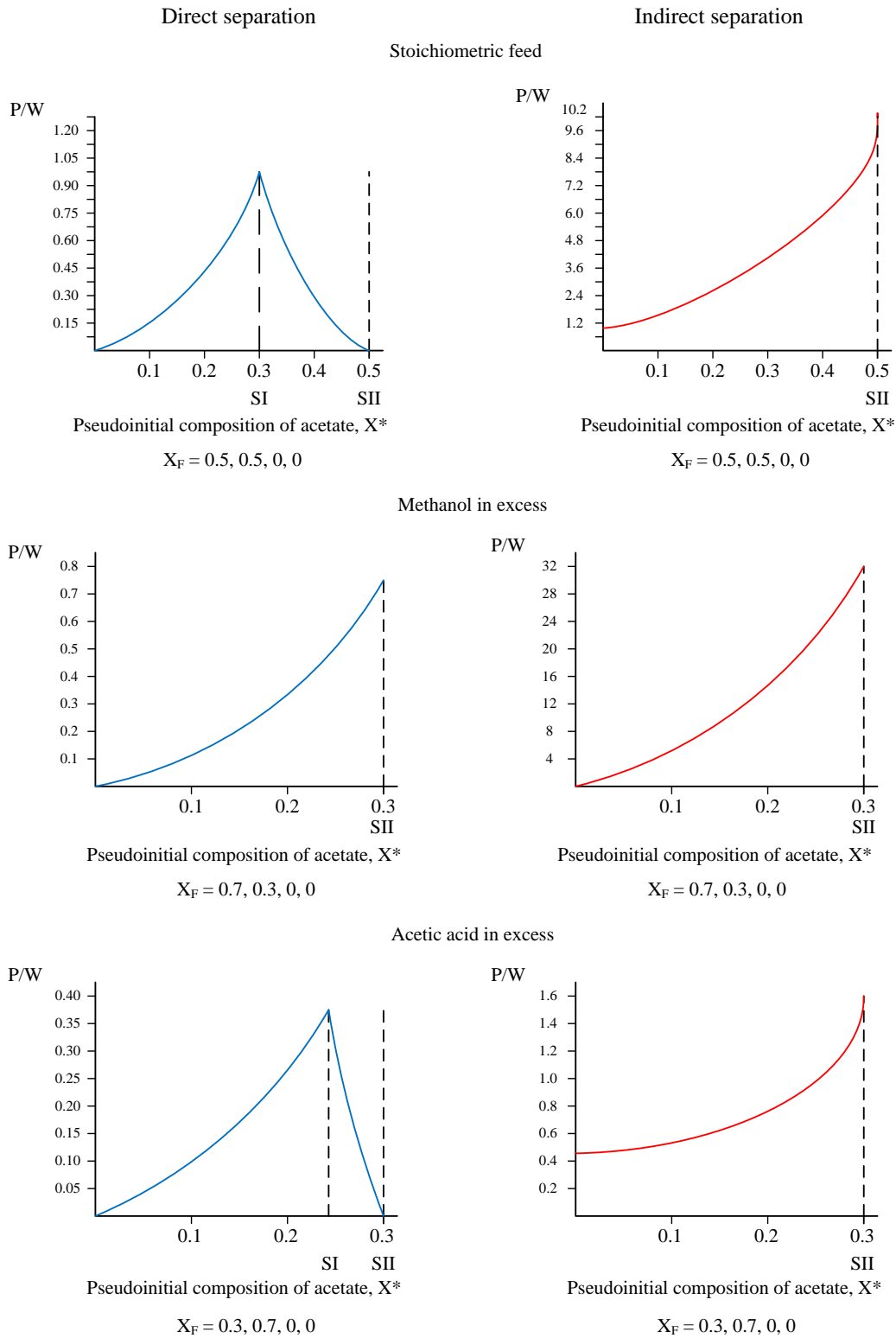
Figure 4-9: P/W relation as a function of the pseudoinitial compositions

Table 4-3: Values of the pseudoinitial compositions and P/W relation for direct and indirect separation

Initial mixture composition X_F				Pseudoinitial mixture composition X^*				Direct separation	Indirect separation
Methanol	Acetic acid	Methyl acetate	Water	Methanol	Acetic acid	Methyl acetate	Water	P/W	P/W
0.5	0.5	0	0	0.5	0.5	0	0	0	1
				0.4	0.4	0.1	0.1	0.16	1.4423
				0.31	0.31	0.19	0.19	0.4643	2.2
				0.21	0.21	0.29	0.29	1.0139	3.6
				0.16	0.16	0.34	0.34	0.6056	5.2174
				0.1	0.1	0.4	0.4	0.274	8.9333
				0	0	0.5	0.5	0	∞
0.7	0.3	0	0	0.7	0.3	0	0	0	2.4146
				0.64	0.24	0.06	0.06	0.075	3.2581
				0.59	0.19	0.11	0.11	0.1625	4.2917
				0.54	0.14	0.16	0.16	0.303	6.4118
				0.49	0.09	0.21	0.21	0.4286	9.5833
				0.44	0.04	0.26	0.26	0.4058	24.6
				0.4	0	0.3	0.3	0.75	∞
0.3	0.7	0	0	0.3	0.7	0	0	0	0.4646
				0.24	0.64	0.06	0.06	0.069	0.5422
				0.2	0.6	0.1	0.1	0.1322	0.6494
				0.16	0.54	0.15	0.15	0.2124	0.7838
				0.11	0.51	0.19	0.19	0.2991	0.9306
				0.08	0.46	0.23	0.23	0.4078	1.1594
				0	0.38	0.31	0.31	0	1.6154

Table 4-4: Limiting steady states of the system

Initial mixture composition X_F				Pseudoinitial mixture composition X^*				Representation	Direct separation P/W	Indirect separation P/W
Methanol	Acetic acid	Methyl acetate	Water	Methanol	Acetic acid	Methyl acetate	Water			
				0.21	0.21	0.29	0.29	A	1.0139	-
0.5	0.5	0	0	0	0	0.5	0.5	B	0	∞
0.7	0.3	0	0	0.4	0	0.3	0.3	C	0.75	∞
0.3	0.7	0	0	0.08	0.46	0.23	0.23	D	0.4078	-
				0	0.38	0.31	0.31	E	0	1.6164

Evaluation of the practical feasibility for the limiting steady states

To determine the practical feasibility of such limiting steady states, it is necessary to draw the tentative paths to carry out the reactive distillation for the limiting states selected in Table 4.4, and their respective behavior is also analyzed in the concentration simplex determining then the feasibility of these states according to criteria set out in the methodology, see Figure 4.10 and 4.11.
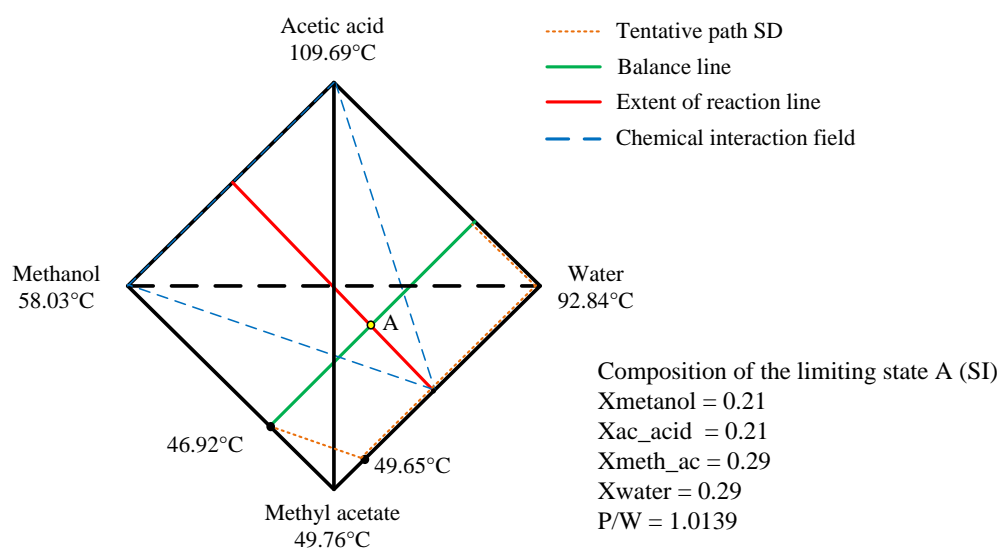
Figure 4-10: Tentative path – Stoichiometric feeding for direct separation. Limiting state A.
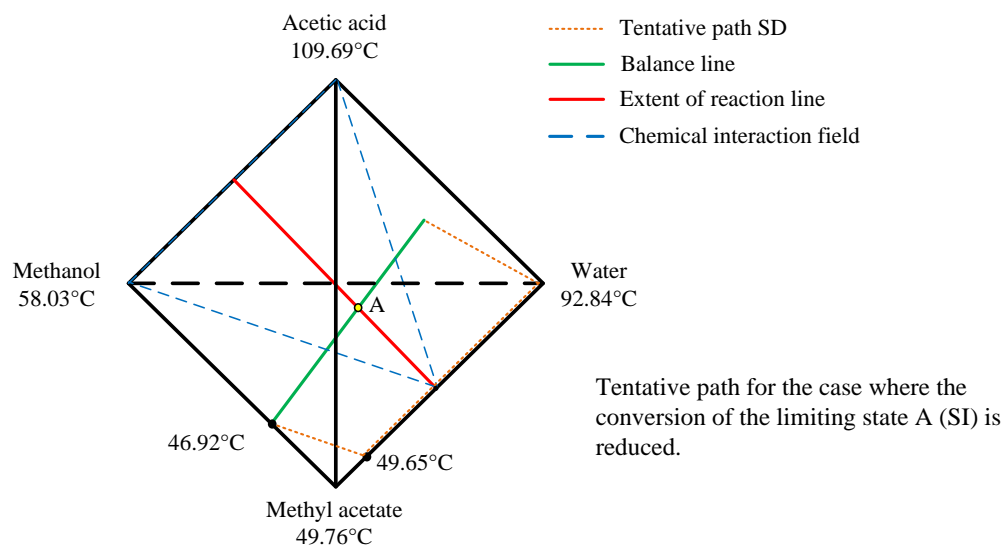
Figure 4-11: Tentative path – Stoichiometric feeding for direct separation. Limiting state A with lower conversion.

Point A (Figure 4.10): This trajectory goes around the concentration simplex and part of it is located over the chemical equilibrium. It should be noted that it is required an infinite volume to reach this steady state, therefore it must be considered a lower conversion point (Figure 4.11) to which the new path falls on the area of forward reaction having then an achievable limiting state.
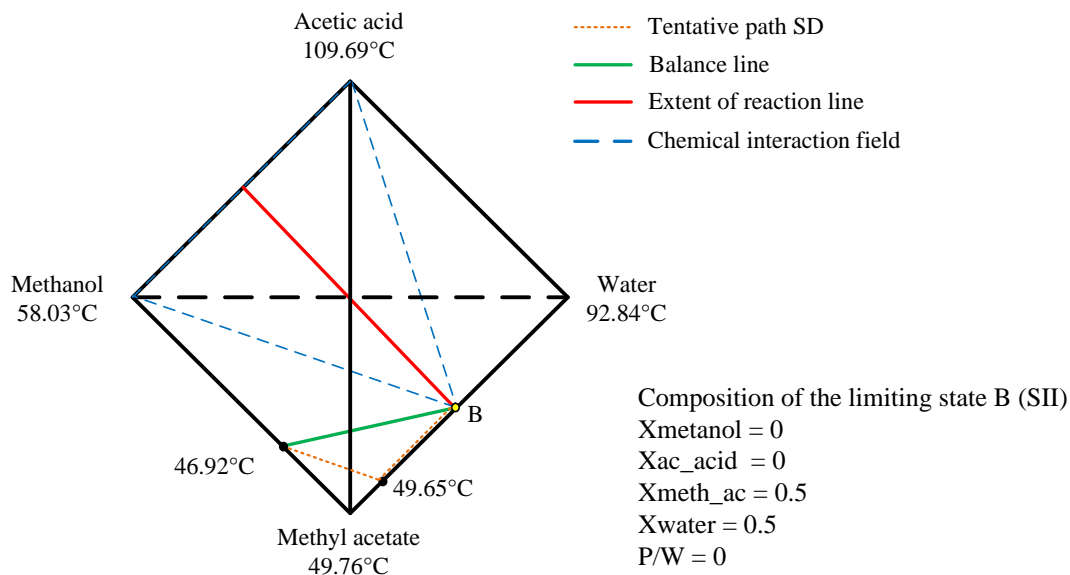
Figure 4-12: Tentative path – Stoichiometric feeding for direct separation. Limiting state B.
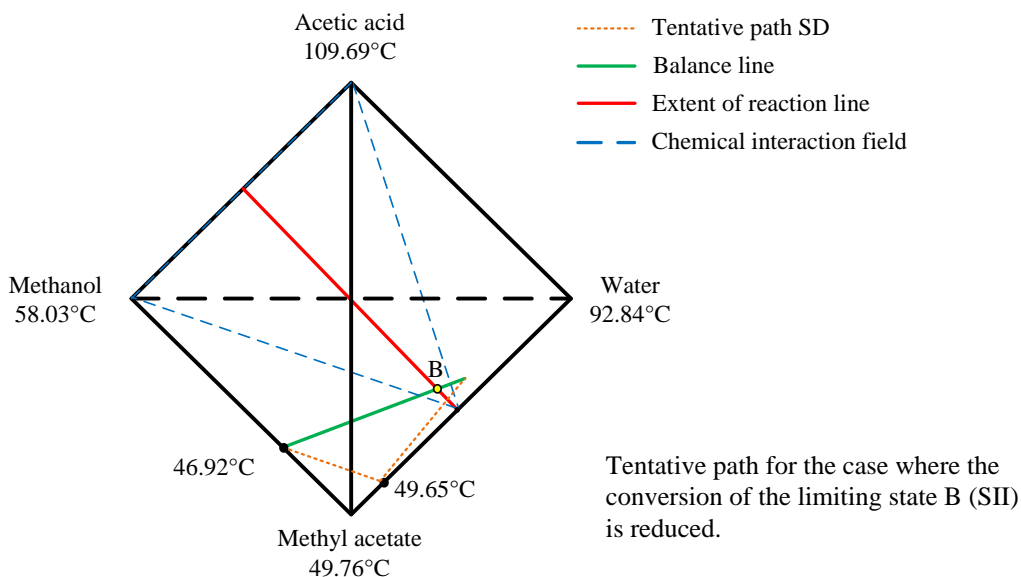
Figure 4-13: Tentative path – Stoichiometric feeding for direct separation. Limiting state B with lower conversion.

Point B (Figure 4.12): This path does not go around all the concentration simplex and no segment of it is located within the area of forward reaction. Considering a point with lower conversion (Figure 4.13) it is possible to note that the path goes around the simplex but is located entirely in the reverse reaction. Due to this, this limiting steady state is not performed.
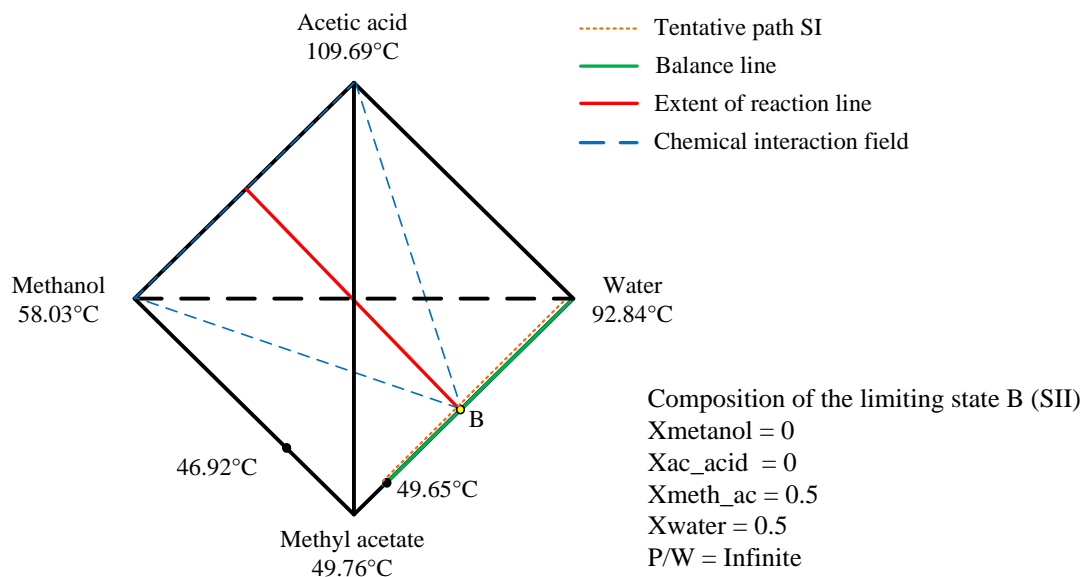
Figure 4-14: Tentative path – Stoichiometric feeding for indirect separation. Limiting state B.
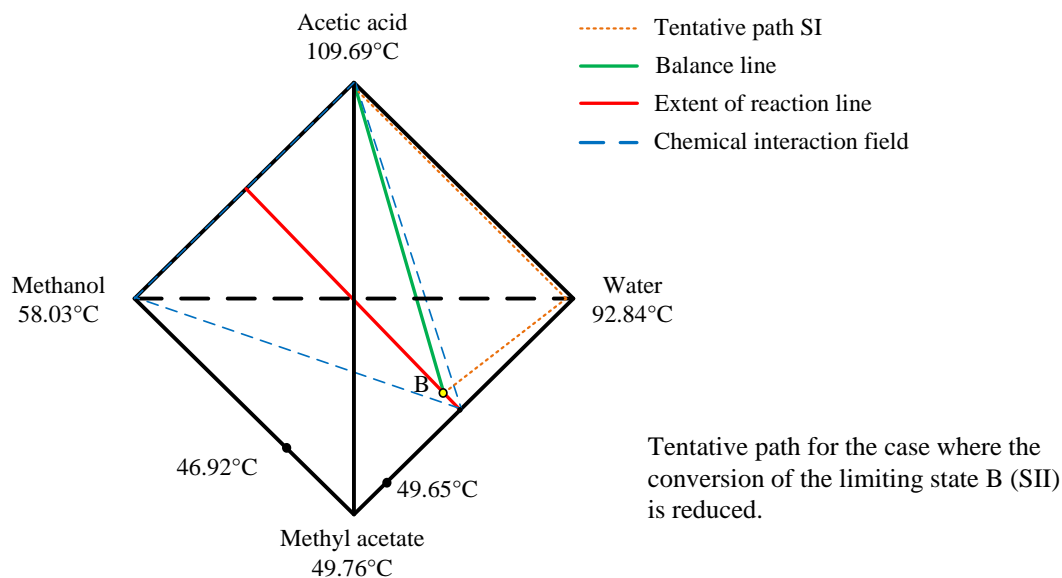
Figure 4-15: Tentative path – Stoichiometric feeding for indirect separation. Limiting state B with lower conversion.

Point B indirect separation (Figure 4.14): This path does not go around all the concentration simplex and no segment of it is located within forward reaction zone. Considering a point with lower conversion (Figure 4.15) it is possible to note that the path goes throughout the simplex and part of is located on the chemical equilibrium, which infers that it would take an infinite volume to perform this limiting steady state.

Composition of the limiting state C (SII)
$X_{metanol} = 0.4$
$X_{ac\_acid} = 0$
$X_{meth\_ac} = 0.3$
$X_{water} = 0.3$
$P/W = 0.75$
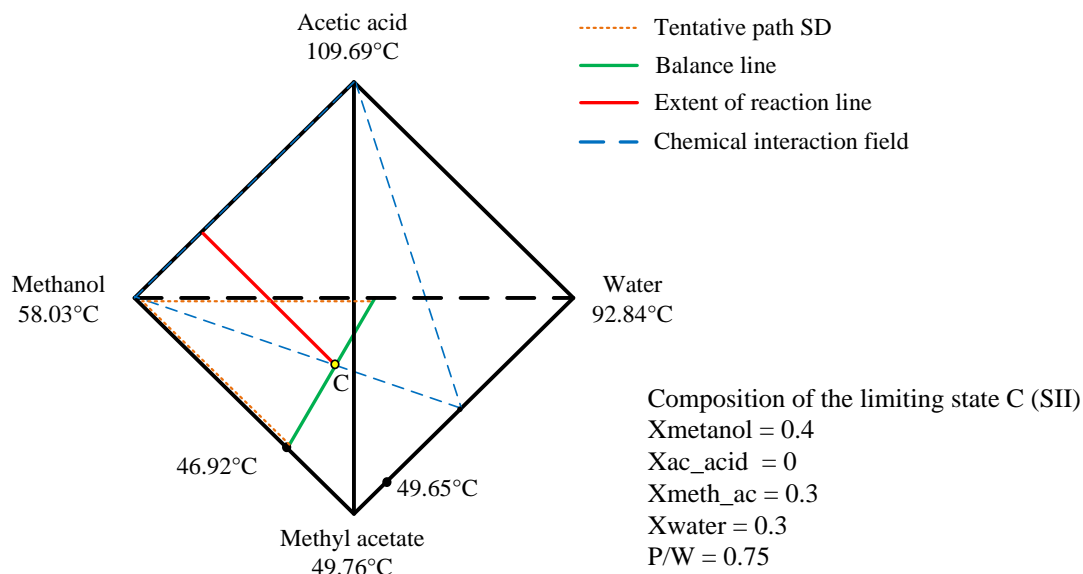
Figure 4-16: Tentative path – Methanol in excess for direct separation. Limiting state C.

Tentative path for the case where the conversion of the limiting state C (SII) is reduced.
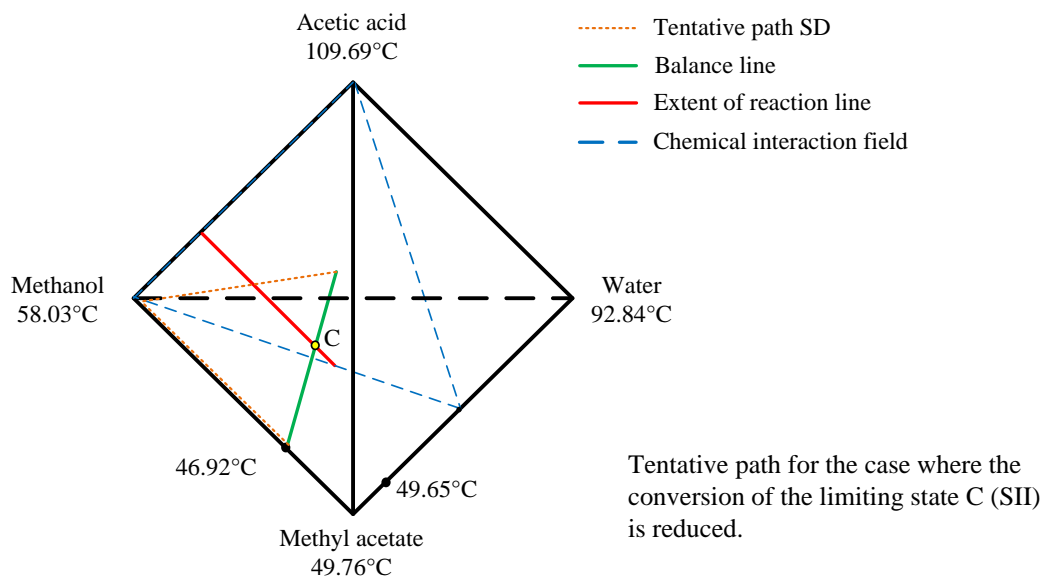
Figure 4-17: Tentative path – Methanol in excess for direct separation. Limiting state C with lower conversion.

Point C (Figure 4.16): This path does not go around all the concentration simplex although the total of it is located on the chemical equilibrium. Considering a point with less conversion (Figure 4.17), the path will go around all the simplex and will be located within the zone of forward reaction, whereby this limiting steady state would be achievable.
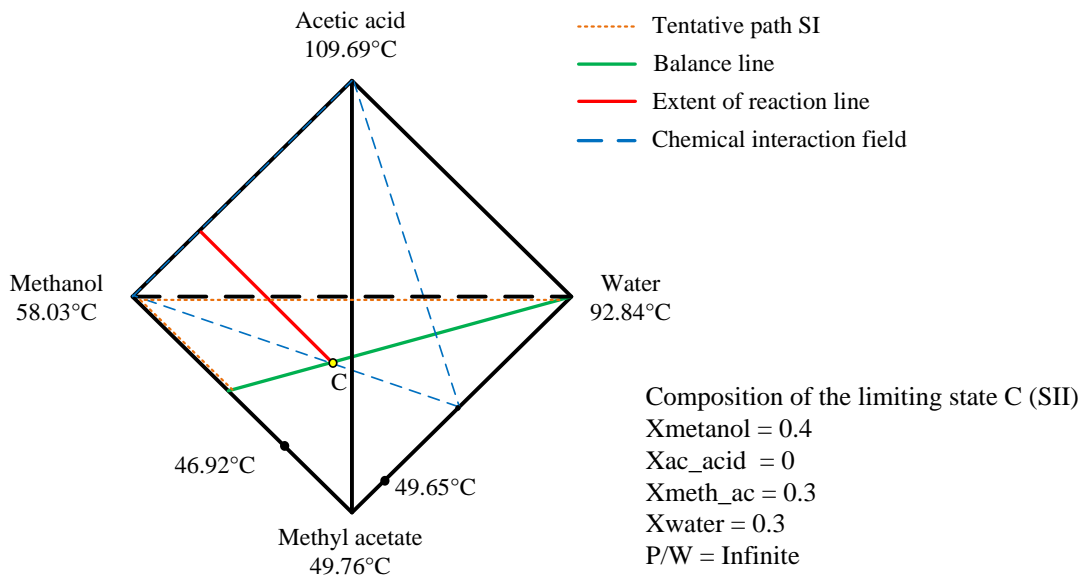
Figure 4-18: Tentative path – Methanol in excess for indirect separation. Limiting state C.
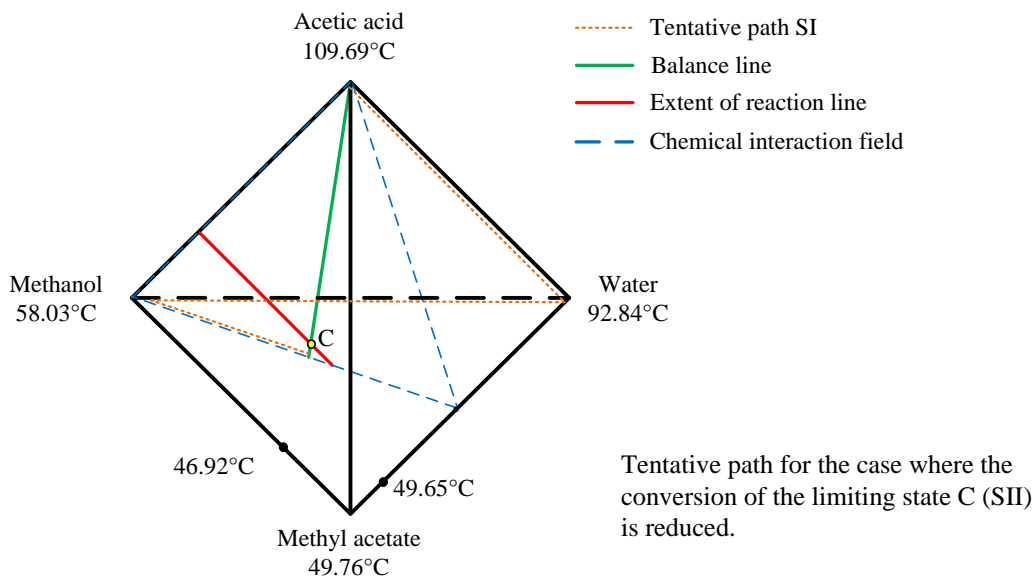
Figure 4-19: Tentative path – Methanol in excess for indirect separation. Limiting state C with lower conversion.

Point C indirect separation (Figure 4.18): This path does not go around all the simplex although the total of it is located on the chemical equilibrium. Considering a point with lower conversion (Figure 4.19), it is shown that the path is carried out throughout the entire simplex and is located on the chemical equilibrium, requiring then an infinite volume to reach that limiting steady state.
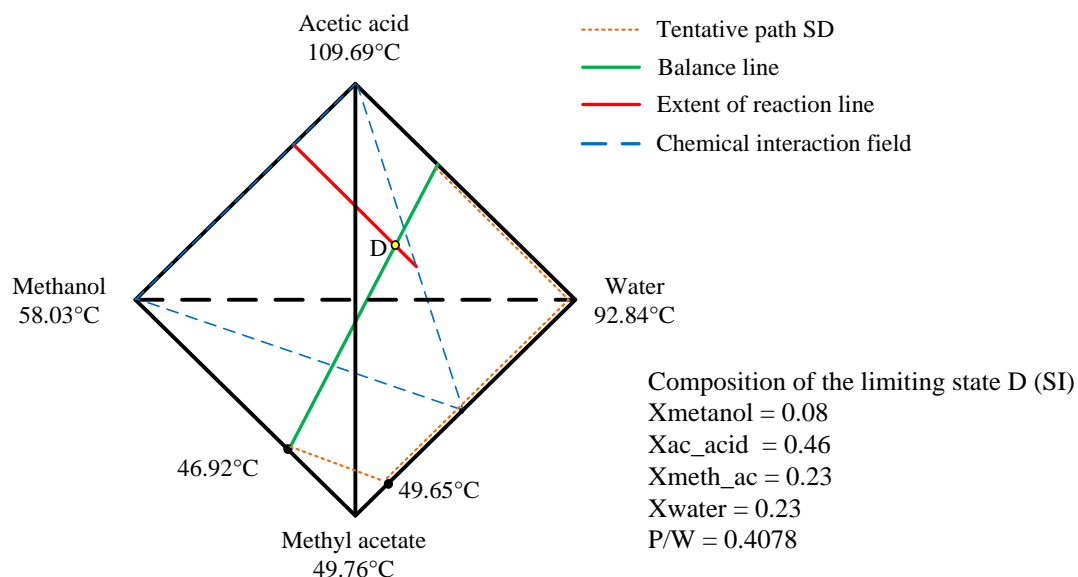
Figure 4-20: Tentative path – Acetic acid in excess for direct separation. Limiting state D.
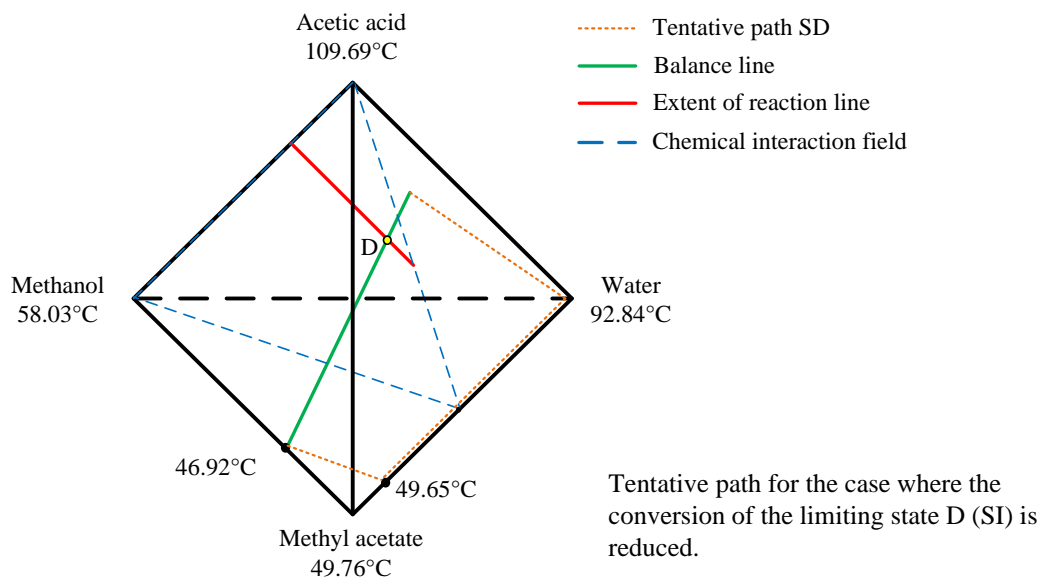
Figure 4-21: Tentative path – Acetic acid in excess for direct separation. Limiting state D with lower conversion.

Point D (Figure 4.20): The path goes around the concentration simplex and part of the path is located on the chemical equilibrium. Considering a point with less conversion (Figure 4.21), it would ensure that part of the new path will be located within the area of forward reaction, being then a reachable limiting steady state.
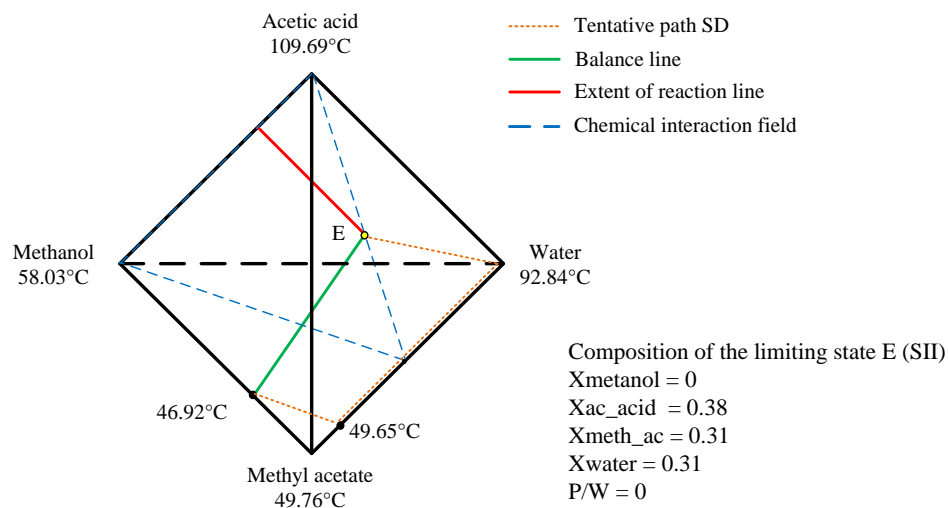
Figure 4-22: Tentative path – Acetic acid in excess for direct separation. Limiting state E.

Point E (Figure 4.22): Although this course goes around the concentration simplex for both this point and another point with lower conversion, none of the cases guarantee that the path is located the zone of forward reaction, being impossible the practical performance of the limiting steady state.
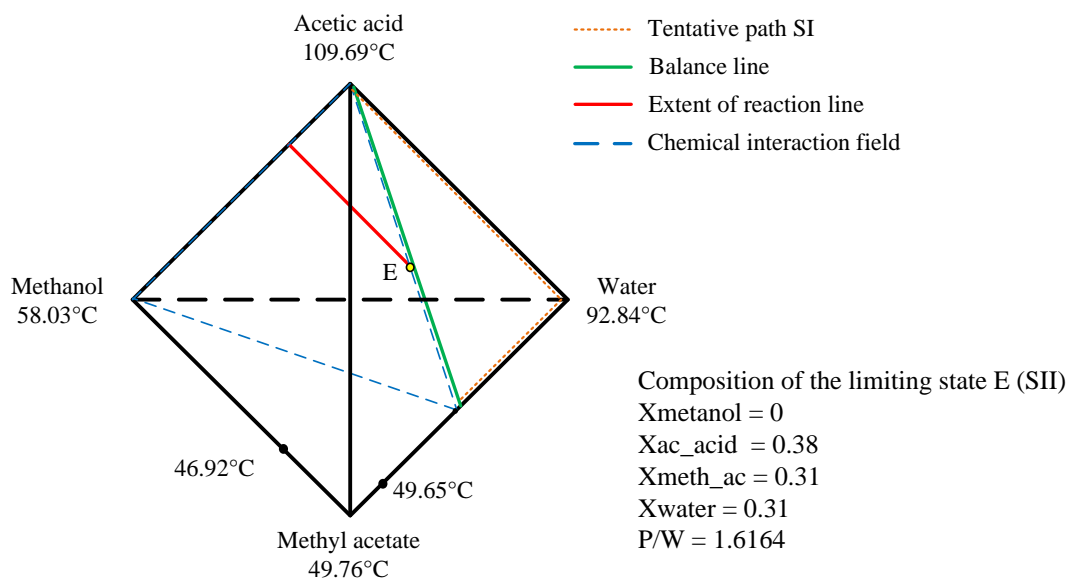
Figure 4-23: Tentative path – Acetic acid in excess for indirect separation. Limiting state E.
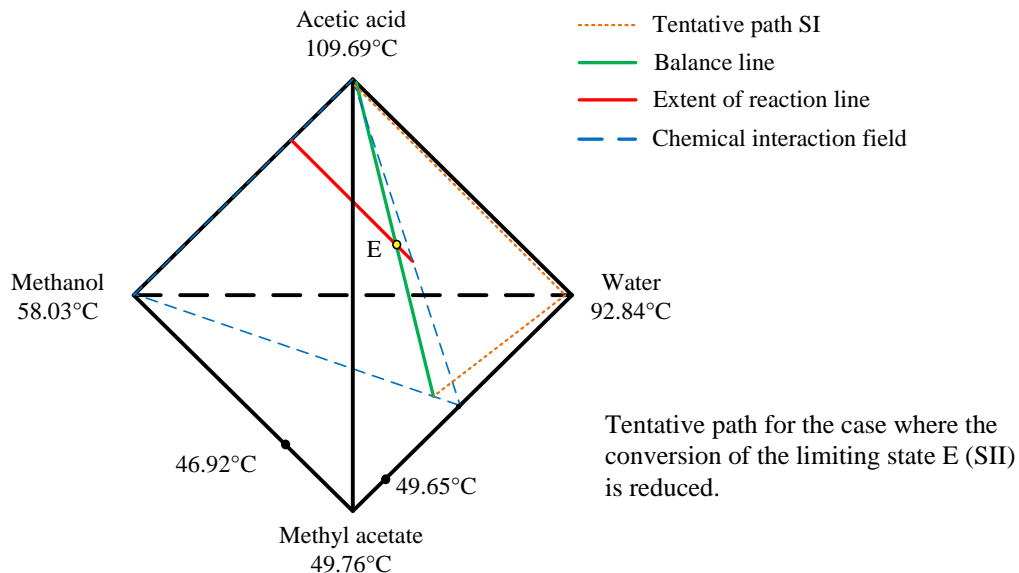
Figure 4-24: Tentative path – Acetic acid in excess for indirect separation. Limiting state E with lower conversion.

Point E indirect separation (Figure 4.23): This path does not go around all the concentration simplex and part of it is located on the chemical equilibrium. Considering a point with lower conversion (Figure 4.24), it is obtained a path that goes around the simplex and part of it is located on the chemical equilibrium, requiring then an infinite volume to obtain this limiting steady state.

The steady states represented by points A, C and D for direct separation are chosen as limiting steady states to fulfill the requirements of reaction and separation, as well as points B, C and E in indirect separation. Then, it is necessary to establish the corresponding flow diagram for the different limiting steady states that are feasible in the practice. This is carried out by analyzing the location of the tentative path for the reactive distillation in the concentration simplex for each selected limiting steady states. The location of the reaction zone is performed considering the segment of the path that is located in the zone of forward reaction. The products obtained for both distillate and bottoms are determined by the initial and end points of the balance line in the respective mode of separation. Therefore, the configurations obtained for each limiting steady states are shown in Figures 4.25, 4.26 and 4.27, according to the results found and shown in the previous section.

For all the feasible limiting steady states, the segment of the tentative path for the reactive distillation located in the zone of forward reaction corresponds to the end of it; therefore, the reaction zone is located across the lower section of the column. However, it is necessary to leave

some stage at the end of the column without catalyst in order to have a separation in them (stripping zone).
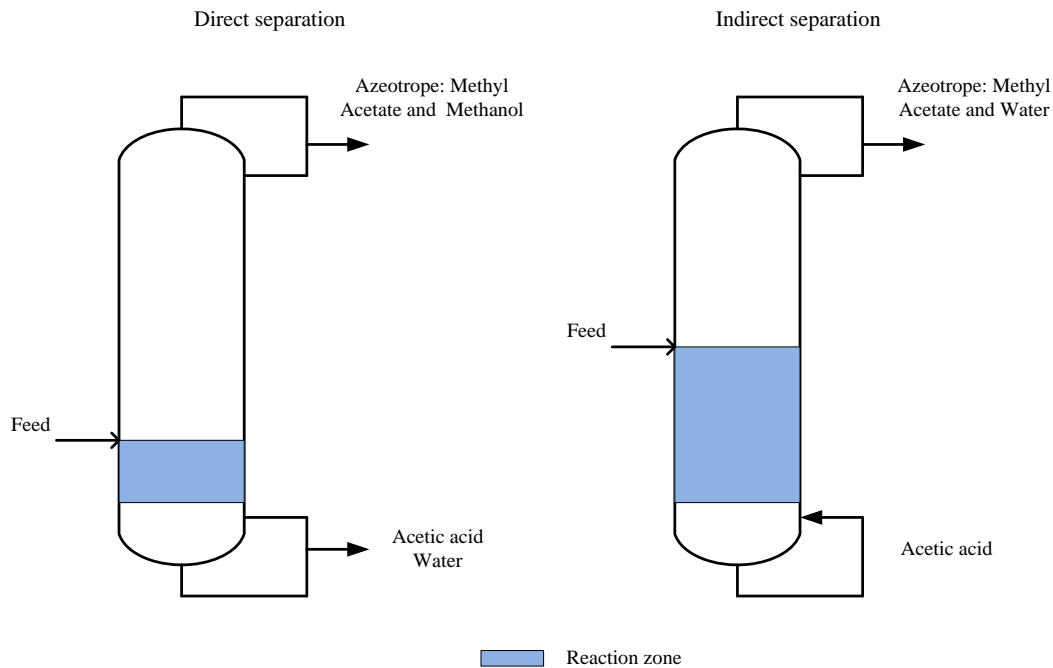
Figure 4-25: Distillation scheme for stoichiometric feed
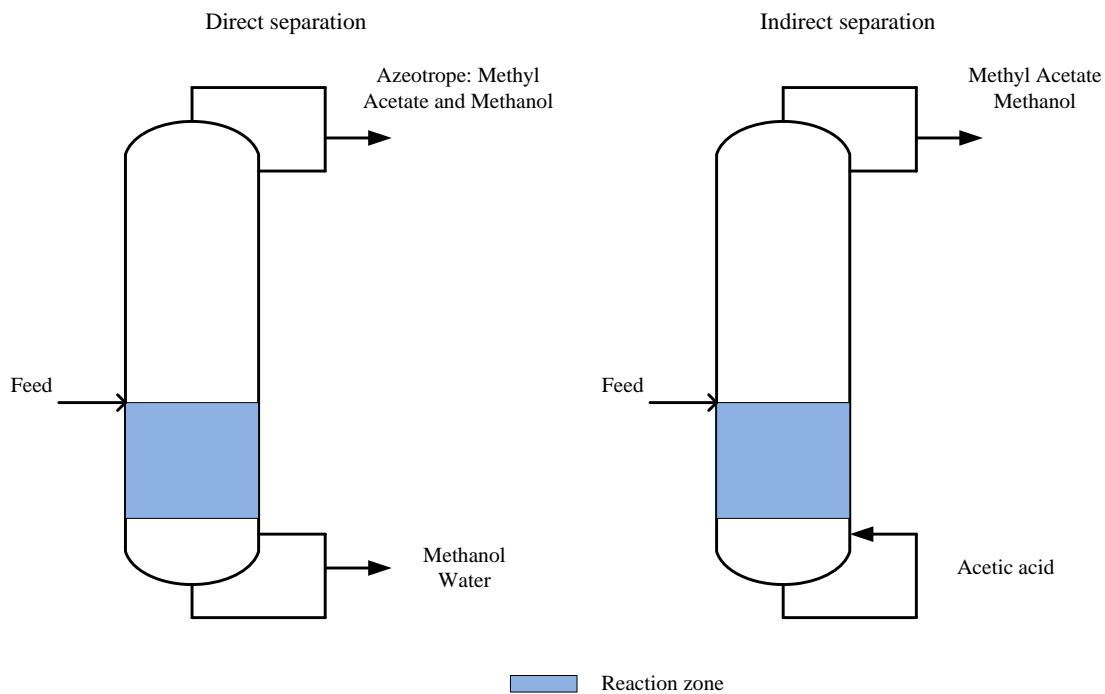
Figure 4-26: Distillation scheme for feed with methanol in excess
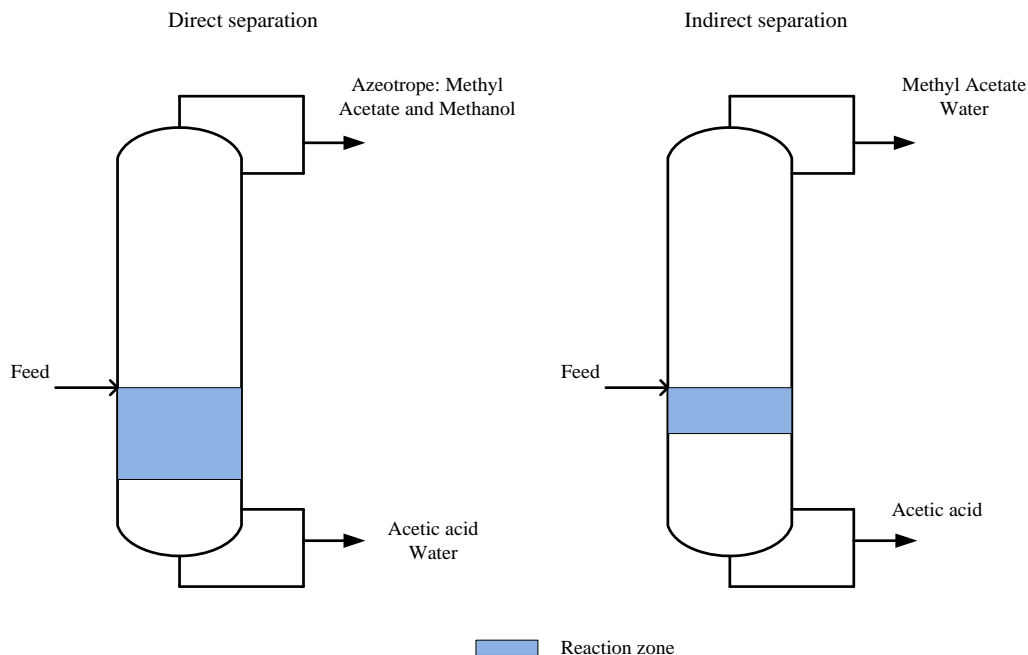
Figure 4-27: Distillation scheme for feed with acetic acid in excess

Selection of the limiting steady state with higher conversion

By using Equations 1.1, 1.2 and 1.3 it was determined the limiting steady state with maximum conversion; the results are summarized below:

Table 4-5: Conversion reached for every limiting steady states and P/W relations

Separation mode	Point	Conversion referred to Acetic Acid	Conversion referred to Methanol	P/W
Direct	A	58%	58%	1.0139
Direct	C	100%	43%	0.75
Direct	D	34%	73%	0.4078
Indirect	B	100%	100%	∞
Indirect	C	100%	43%	∞
Indirect	E	46%	100%	1.6164

The limiting steady state with the higher conversion is the point B, which can be considered optimal for the process, but if its trajectory is analyzed, it is concluded that it would need an infinite volume for its practical realization as already stated above. This phenomenon also occurs when considering the points C and E in indirect modes of separation, which ultimately leads us to conclude that these limiting steady states will not be taken into account in choosing the optimal limiting steady state for the process. Even though the remaining limiting steady states have high conversion rates for one of the reactants, except point A where conversion of reactants is the same,

point A is chosen because the condition of stoichiometric feed prevails. Besides, the P/W relation has a reasonable value considering the energy consumption of the column.

Construction of the flowsheet for the stated objective (desired product)

Analyzing the tentative path for the reactive distillation, see Figure 4.10, for the limiting steady state chosen as the optimal to carry out the process, the following observations are made for the proposed technological scheme according to the principles set out in the methodology:

- It is noted that the tentative path for the reactive distillation that takes place in the zone of forward reaction is located in the segment water - acetic acid, and therefore the catalyst bed must be located at the bottom of the column, so that the reagents are concentrated in this area. Furthermore, it is considered that in the bottom of the column no catalyst is added, so that those stages help in the separation.

- According to the balance line for direct separation, the bottoms product is an acetic acid-water mixture which must be fed to another column in order to recover acetic acid and then recycle it to the reactive distillation column.

- The distillate product is a mixture of methyl acetate – methanol (azeotrope), which must be subsequently fed to a second column to separate the methyl acetate from methanol and thus obtain a product with the desired purity specifications. The methanol obtained is recycled to the first column.
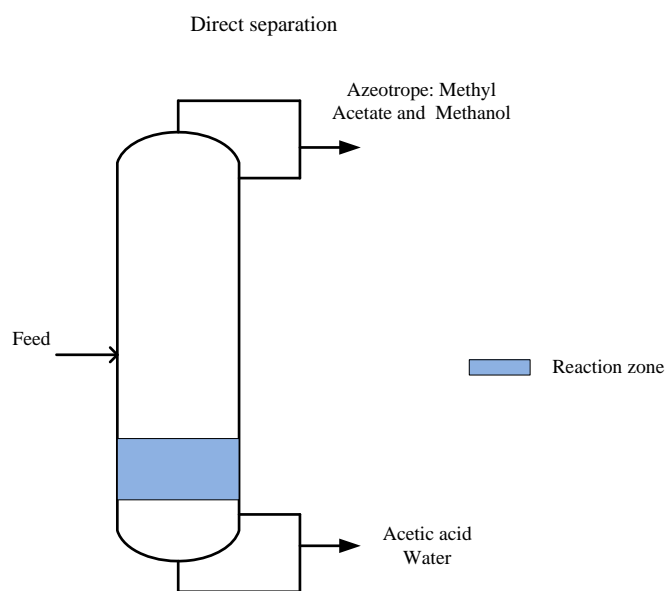
Figure 4-28: Distillation scheme for stoichiometric feed in direct separation

As a result of this graph-analytical analysis it is concluded that:

- − The location of the reaction zone, i.e., the catalyst is determined according to the tentative path of the limiting steady state chosen, see Figure 4.10. In that path there is a segment located in the zone of forward reaction which also corresponds to the bottoms of the column; it is clear then from this analysis that the catalyst must be located in this section.

- − Although conversions of reactants are increased compared to those presented in the chemical equilibrium, the final configuration of the column shows that the degree of conversion and selectivity desired (both 100%) are not achieved. This is due to the thermodynamic constraint imposed on the system (methyl acetate - methanol azeotrope) which is not overcome during the process. Hence, it is necessary the use of more columns to obtain the desired product, leading to an increase in the investment and operating costs. Notably, the technological scheme proposed decreases the use of separation and reaction units necessary in the conventional configuration.

- − A good possibility to reach higher conversion and selectivity in the reactive distillation column, it would be the implementation of an unconventional separation method in separation, such as the addition of a solvent for breaking the constraints imposed on the system.

- − If the configuration of the obtained column is compared with the industrial case, it can be seen that there are huge differences (conversions below 100%, impure distillate and bottoms products). Then, it is necessary to implement new methods of analysis that consider other phenomena (auto-extractive) in the development of the process and which have not been considered in this analysis.

Auto-Extractive phenomenon in the production of methyl acetate by reactive distillation

As was previously shown, the acetic acid which is part of the reacting mixture has physical and chemical properties that interact positively in the breaking of thermodynamic constraints formed in the system. According to the choice of solvents, it was found that the minimum composition of acetic acid that "breaks" the methyl acetate - methanol azeotrope was 0.4 molar and for the methyl acetate - water azeotrope was 0.18 molar. With these values it can be qualitatively explained the effect produced by the acetic acid in the reactive distillation paths and therefore in the behavior of the column, which leads to determine the distribution of the final product. Knowing in advance that the tentative reactive distillation lines proposed in the analysis of the process statics give a basic idea of the inner separation scheme inside of the tower showing the path of separation at

extreme conditions (∞ / ∞), it is possible then to divide them into segments and to understand the influence of acetic acid on the development of these lines. Then, the above described is performed having as a basis the trajectory established for the limiting steady state limit chosen in the analysis of the process statics.

Change in the tentative path considering a single feed stream to the distillation column

The analysis begins with the layout of the field that represents the required concentration of acetic acid (i.e.>0.4), to achieve the extractive phenomenon; see Figure 4.29, which exceeds the minimum concentration necessary to "break" the azeotrope to ensure that the phenomenon occurs.
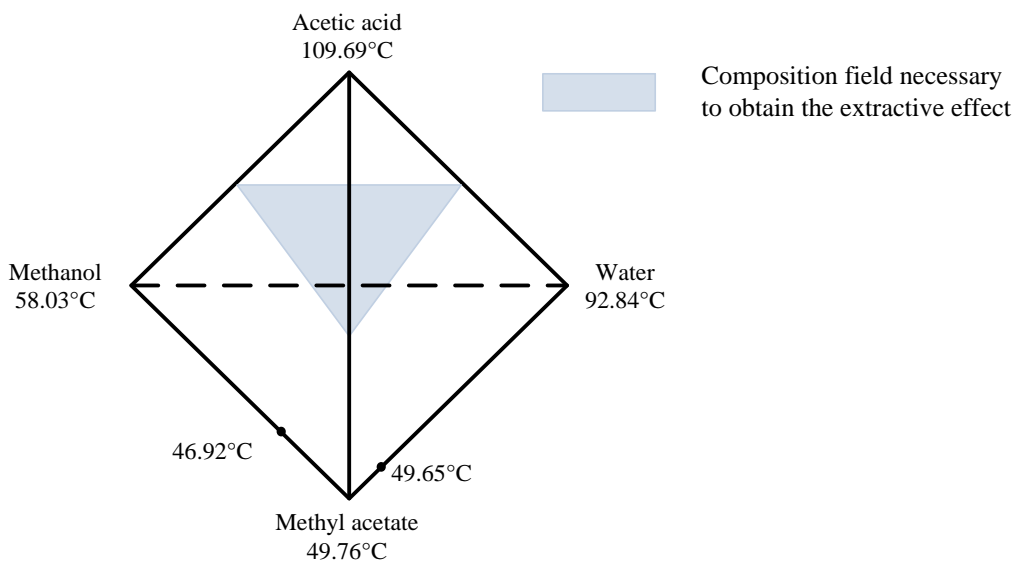
Figure 4-29: Field of minimum concentration of acetic acid required to break the azeotrope.

The analysis continues with the layout of the tentative reactive distillation path, see Figure 4.30, for the limiting steady state chosen for the process. This limiting steady state was found for a stoichiometric feed of reactants to the column, where conversion of 58% was established for both reactants.
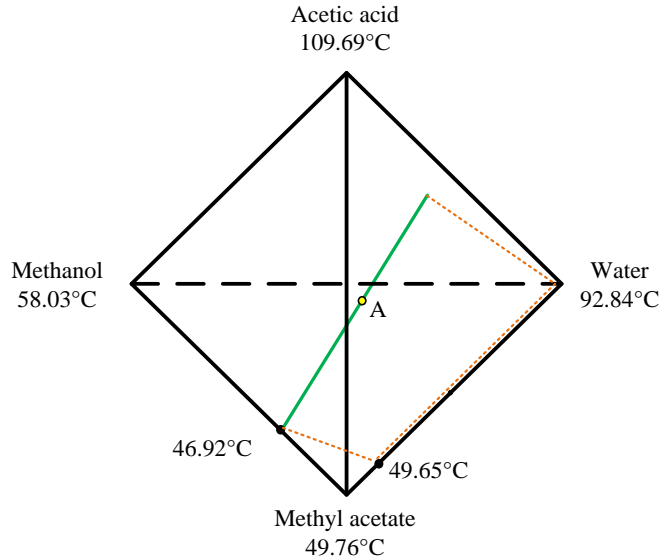
Figure 4-30: Tentative path for the limiting steady state chosen.
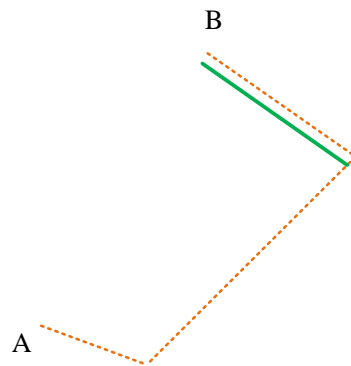
Figure 4-31: Tentative path for the limiting steady state chosen in an independent field.

By removing this path, see Figure 4.31, in an independent field it is understood the following:

Point A: represents the components obtained as distillate products (methyl acetate – methanol azeotrope). Point B: represents the components obtained as bottoms products (acetic acid - water – methanol mixture). Green line: Segment of the path that is located in the forward reaction zone.

Thus, each segment of the path represents the separation in the column. Considering that the analysis of the process statics is performed by a single feed and the azeotrope (methyl acetate - methanol) is located at the end of the path, it could be added to a stage in this region an amount of acid acetic in order to break the thermodynamic limit (azeotrope methyl acetate-ethanol) achieving the extractive effect. This can be represented by taking a point (i.e. a stage) located on the top of the column and then drawing a feeding line to the pure acetic acid; the cutoff point of this line with

the field represents the amount of acid needed to "break" the azeotrope, which also creates a region where the path is modified arriving then to the pure methyl acetate and not to the azeotrope as initially was established, see Figure 4.32.
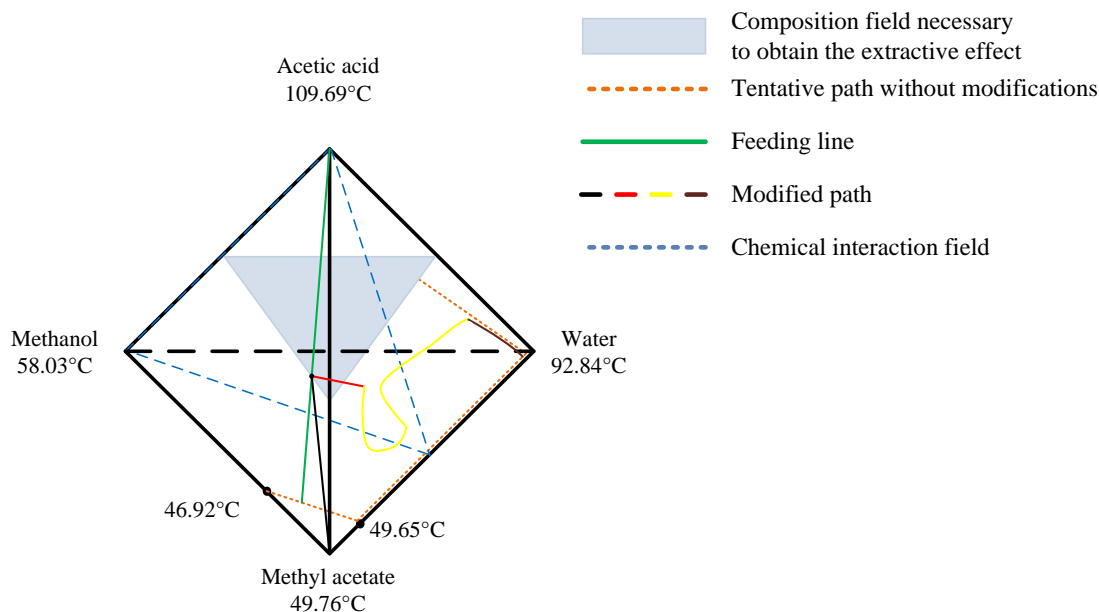
Figure 4-32: Modified tentative path for the limiting steady state chosen.

The foregoing figure shows the influence of acetic acid in the separating component of the process, so it can be considered that from this plate and a few above is located the extractive section of the column. Therefore, the trend of the path in this area is relatively constant (red) referred to a concentration of acetic acid which can be easily explained since in this region of the column the acetic acid acts as extracting agent separating the methyl acetate from the other components without a change in the concentration. In addition, acetic acid shows no evaporative effect due to its physicochemical conditions (high difference in boiling point), making convenient its choice as solvent for the process. It can also be noted that there is a small slope because the reaction occurs at a lower rate than in the reaction zone with the methanol which ascended to this section of the column, so it should be considered a small decrease in the concentration of acetic acid. The descending behavior exhibited by the path (yellow) can be explained as follows: the leaving stream enriched in acetic acid in the previous section drops inside the column as it is the heaviest component of the system, reacted with the methanol present in these stages and therefore the content of acid and methanol decreases rapidly. The residual acetic acid reacts with the remaining methanol, having then no more content of it in this section of the column. The segment of the tentative path (green) indicates that in this section water is separated from the other components in

this section of the column. Hence, it is concluded that pure water is obtained as bottoms product as it becomes the new compound with higher boiling point, and not a mixture of acid acetic acid and water as initially proposed. It should be noted that the segments studied are located largely in the forward reaction zone so higher conversions are achieved than those established.

Analysis of the distribution of local products along the column considering two feed steams

Since the analysis of the process static is only applicable to a single feed, it is intended to propose alternatives only at qualitative level for understanding the process considering two feeds, because the variables that influence the development of the reactive - extractive process are located in the feeding area of both reactants and solvents. As an initial step it is necessary to analyze a feed to the column with methanol in excess. Although as already stated, the steady state with greater advantages for the process is found at stoichiometric feed, so it is proposed the use of that feeding condition (a small excess of methanol). Then, the hypothetically initial feed is divided into two feeds, one comprised entirely of methanol with a small percentage of acetic acid, and the other composed of pure acetic acid. With these initial conditions (excess of methanol), the limiting steady state with greater conversion and its respective tentative distillation path is qualitatively determined. It should be noted that the steady state is possible at a practical level in direct separation mode, therefore all the analysis is referred to this type of separation. As this analysis was previously performed the results are taken and shown below:
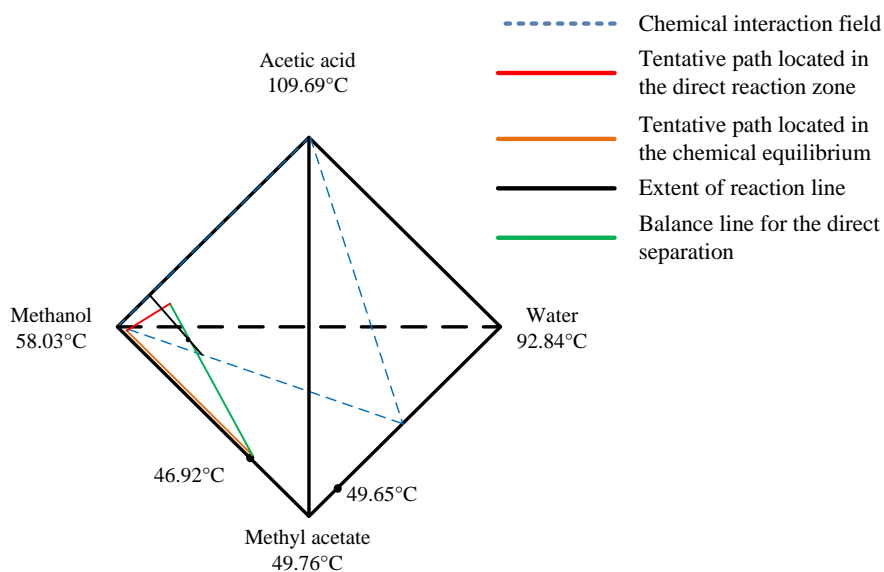
Figure 4-33: Tentative path for an excess of methanol.

According to the location of the tentative path in the concentration simplex, it is possible to set that the reactants are fed in the lower section of the column as this section of the path is in the forward reaction zone (green line in Figure 4.33).

In order to achieve the initially set feeding conditions, the missing acetic acid is added to the upper stages of the tower (black line in Figure 4.34). The feed in such location is considered in order to use the acetic acid as separating agent of the existing azeotrope as top product. Since due to its characterization as unstable node (methyl acetate – methanol azeotrope), it will always be obtained as top product for any initial composition of a quaternary or ternary mixture considering the components of the azeotropes to be separated within the column as direct separation regardless the effect of the acid.
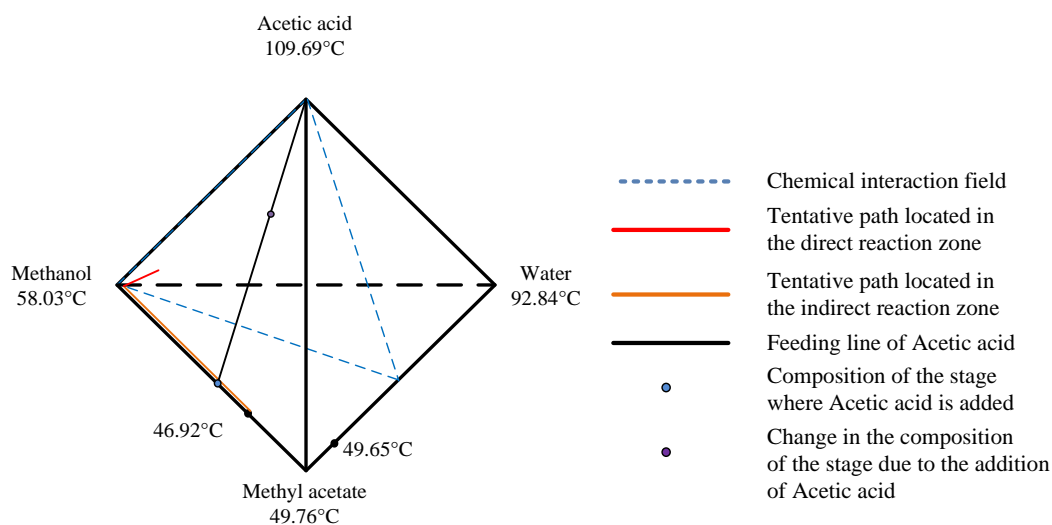
Figure 4-34: Tentative path for an excess of methanol and feeding line of acetic acid.

This allows us to analyze the behavior of the column from the top to the end of it. The addition of acetic acid in this stage displaces the local composition of it (blue dot in Figure 4.34) enriching it in acetic acid (endpoint in Figure 4.34), which produces a change in the tentative path as the minimum condition of acetic acid necessary to achieve the extractive effect is reached in this stage and some stages below as it was seen in the first analysis. For this new point, a balance line is drawn formulating the distillate, see Figure 4.35, obtaining pure methyl acetate as top product and a mixture of acetic acid and methanol as a bottom product. It should be clarified that these bottoms are local, i.e. they are not the bottoms of the distillation column but the bottoms of the section where the extractive phenomenon is achieved, see Figure 4.36.
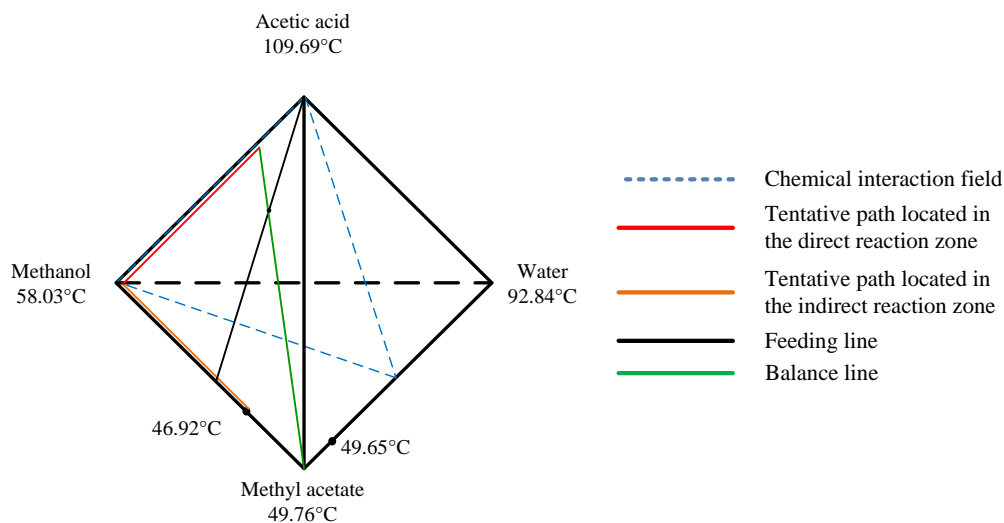
Figure 4-35: Modified tentative path by the addition of acetic acid.
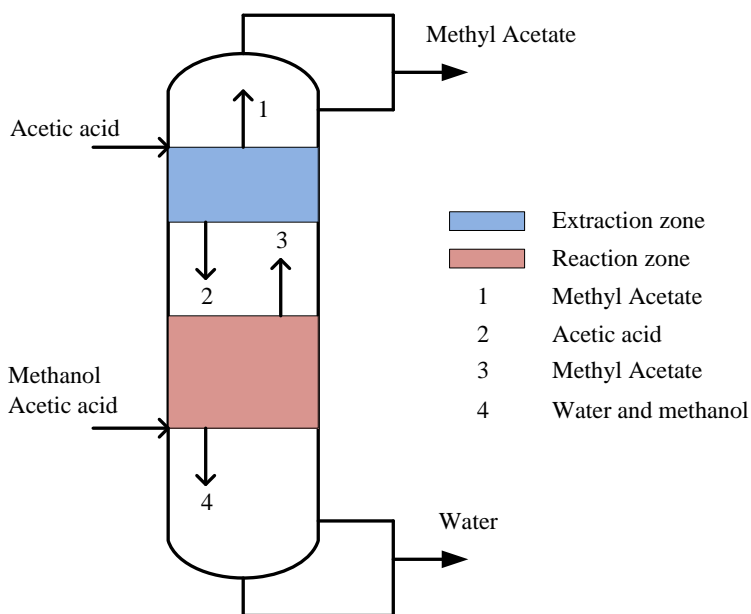
Figure 4-36: Local behavior in the column because of the addition of acetic acid.

An analogous way to understand this phenomenon is by considering an extractive distillation column where the mixture to be separated is the methyl acetate - methanol azeotrope and the solvent using acetic acid to "break" the azeotrope. If it is established that the local composition of the reactants obtained in the bottoms of these stages are fed to another section of the column (lower than the previous) and setting it as a new initial composition (with an excess of acetic acid), the result obtained for this point by its higher extent of reaction and the corresponding tentative path

for the new point are shown in Figure 4.37. From Figure 4.37 it is concluded that the top product obtained for this composition is the methyl acetate - methanol azeotrope and the bottoms (local) is a ternary mixture of acid acetic acid, water and methanol. The new tentative path is located at a higher percentage in the forward reaction section. The result of this is described graphically, understanding that it is analyzed a small segment of the behavior inside the column, see Figure 4.38.
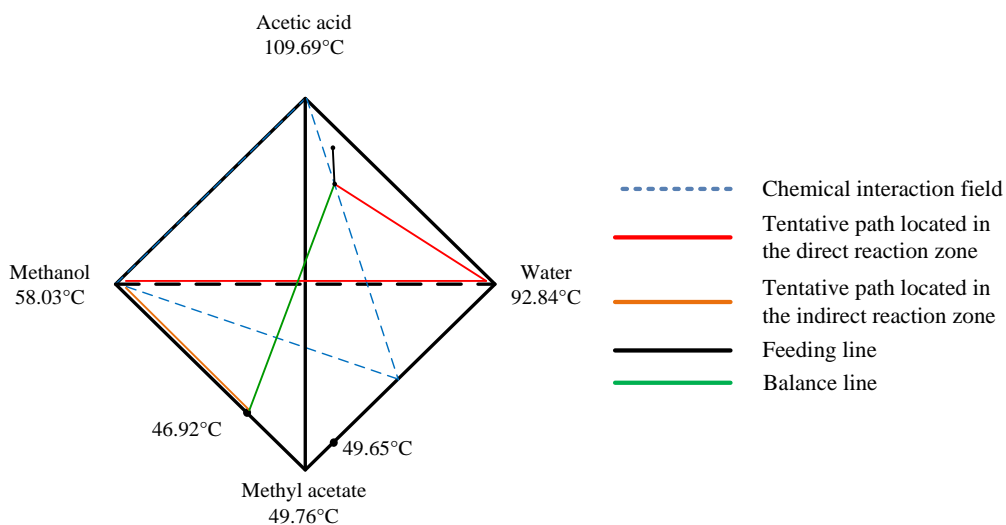
Figure 4-37: New tentative path due to the local composition analysis.
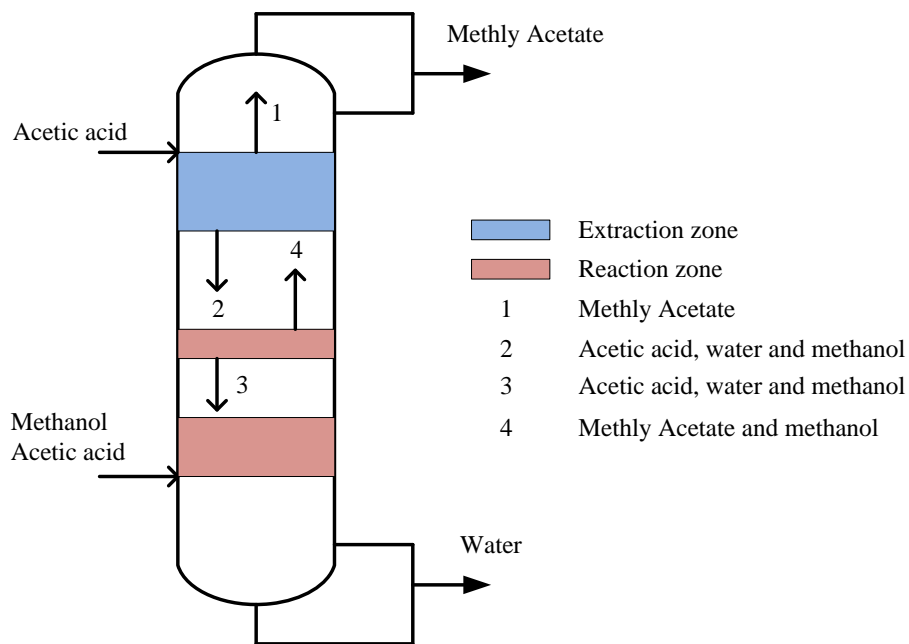
Figure 4-38: Configuration of the column for the local composition analysis.

If the composition of bottoms is taken and fed again into another section of the tower and is performed the same procedure described above, it is obtained a ternary mixture consisting of acetic acid, methanol and water as a product of bottoms for this section (local) and the distillate can be pure methyl acetate if the concentration of acetic acid has not fallen below the required value to reach the extractive phenomenon, or the methyl acetate - methanol azeotrope if the acetic acid concentration has decreased considerably exceeding the established value. Likewise a significant segment of the path is located in the forward reaction zone, see Figure 4.39.
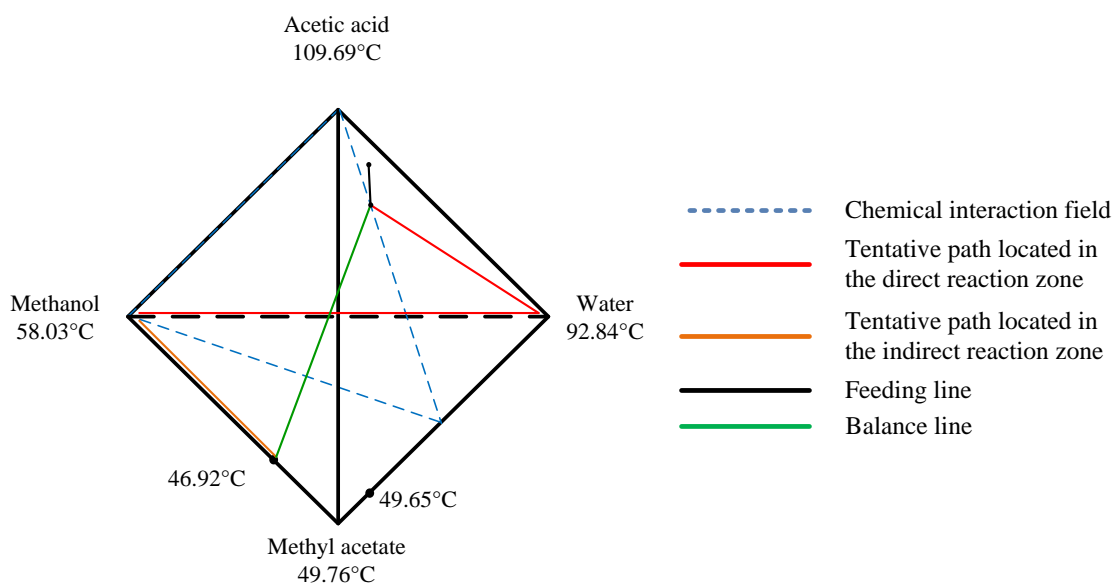
Figure 4-39: New tentative path due to the local composition analysis.

Following the same procedure for each point obtained in each section of the tower, analyzing a lower section to another previously considered section it is found that the distribution of products for each section will be similar to the compounds obtained, seeing that as the process goes to lower sections the content of acetic acid and methanol is exhausted which eventually leads to obtain pure water as a product of bottoms and methyl acetate - water azeotrope as top (local) product which ascends in the column and is eliminated in the top of the column, see Figures 4.40 and 4.41.
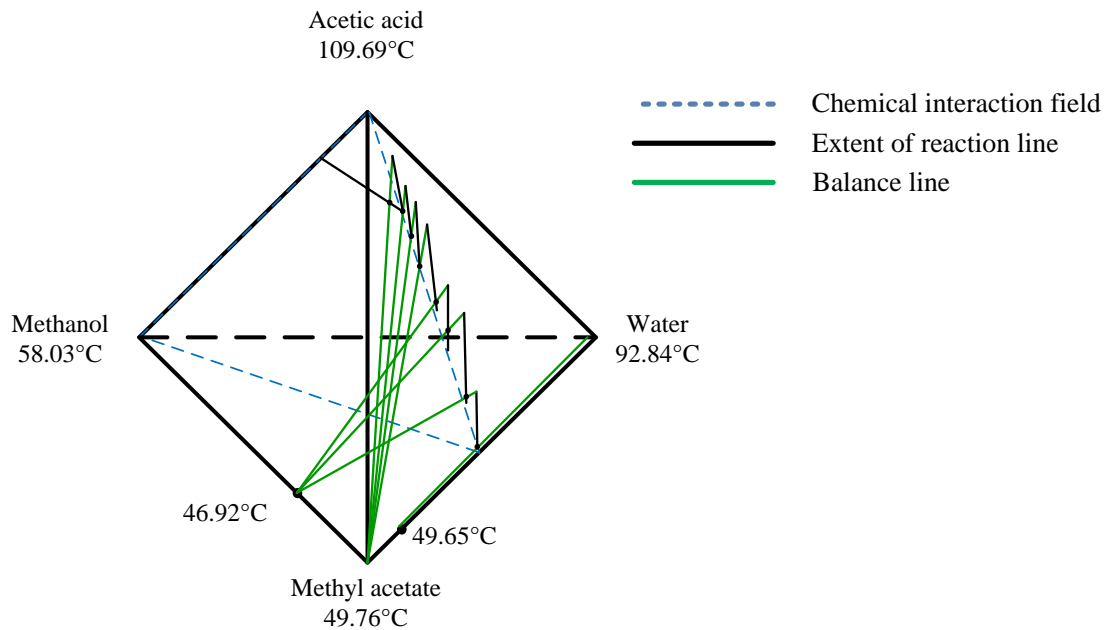
Figure 4-40: Extent of reaction and balance lines for each point of local composition.
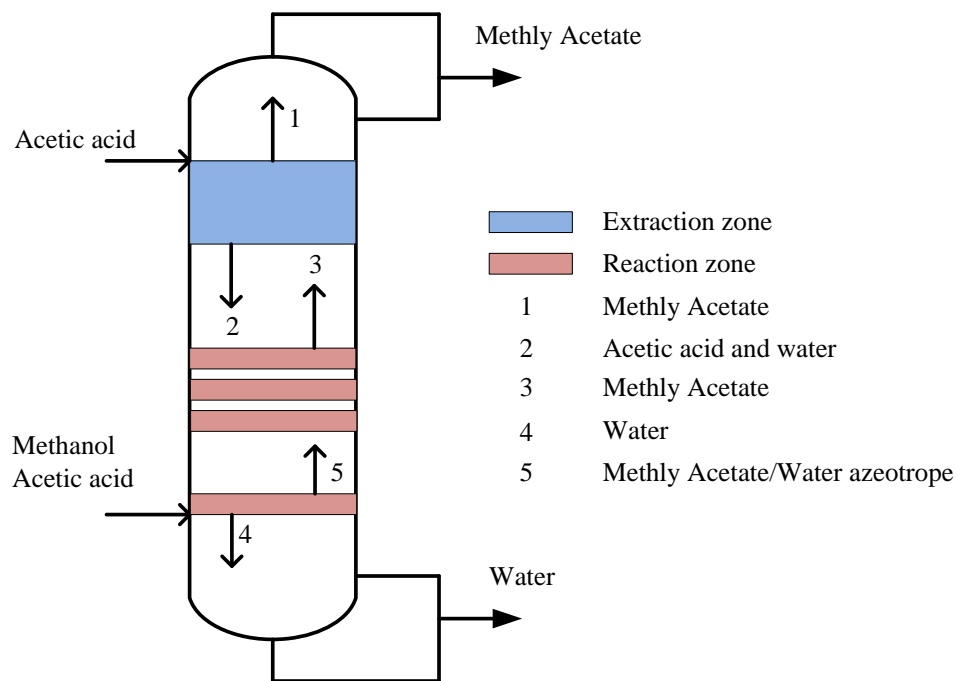
Figure 4-41: Behavior of the column according to the local composition analysis.

By joining all the points of local composition obtained in each section column, it is provided a general description of the tentative distillation path, see Figure 4.42. This representation allows to distinguish the different regions where both separation and reaction phenomena occur. The segment in red indicates the rectifying section of the column where are separated the methyl acetate from those components which it does not form azeotropes. The segment in blue represents the section where the auto-extractive phenomenon occurs; as can be observed, the concentration of acetic acid in these stages will always be higher than the minimum amount required to achieve this effect. Then, it is shown one region in green where the concentration of acetic acid has a strong decrease, which represents that this acid is descending down the column and reacting with the methanol in each one of these stages forming the reaction products, therefore this section of the path describes the reaction zone of the column, confirming the location of this section of the path in the forward reaction on the concentration simplex. Finally, the last segment of the path (yellow) represents the stripping section of the column where the water is separated from the methyl acetate and the remaining content of methanol that may be present in this section of the column.
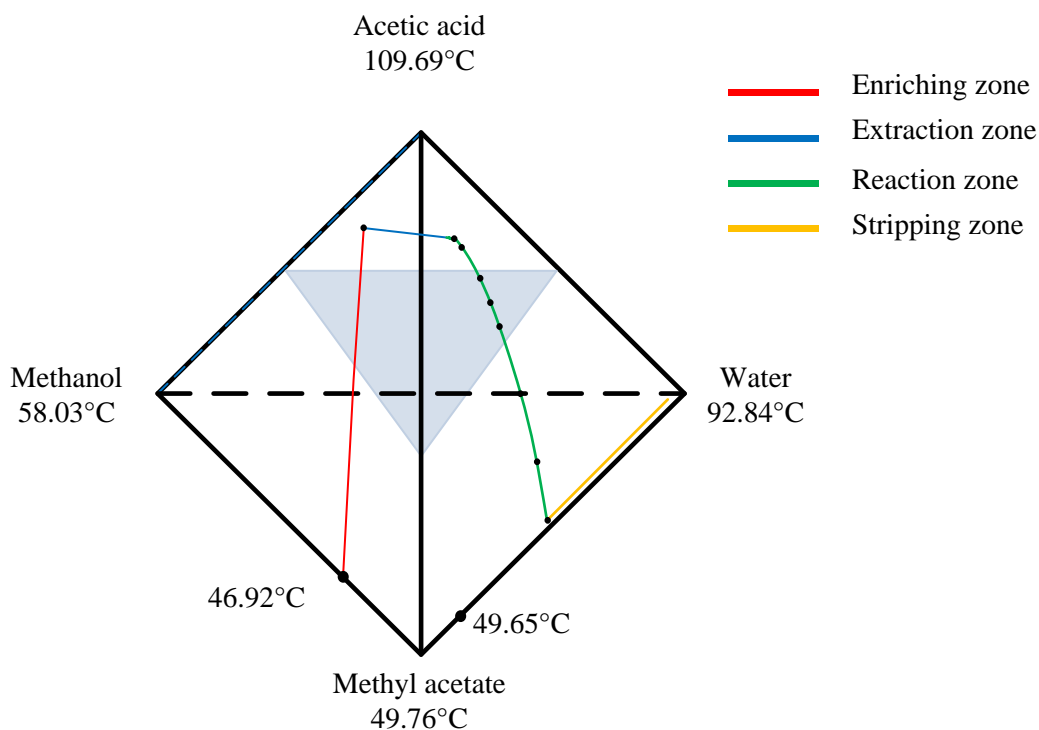
Figure 4-42: Tentative path of the extractive – reactive distillation according to the points of local composition.

Hence, the final configuration of the column is represented by the following Figure:
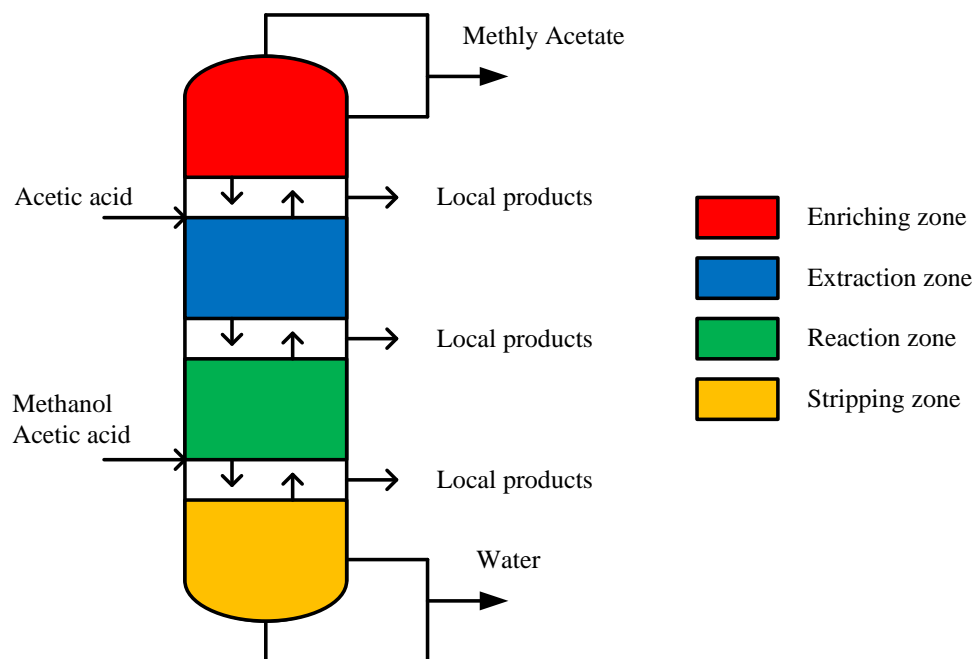
Figure 4-43: Tentative path of the column according to the points of local composition.

Comparing the first analysis with this one a similar result is obtained, understanding in a clearer way the true behavior inside the column.

The effect obtained by considering two feeds can show the influence produced by the feeding of the two reactants in different parts of the columns in the inner product distribution in the column, showing the dual function of the acid acetic acid in the process for both separation component (solvent) and the reaction component (reactive).

Then, it is set the difference in the results between the analysis of the process statics considering a single feed and the results obtained in this analysis considering two feeds. It is clear that the configuration with two feeds has an excess of one of the reactants (methanol), although with a small amount.
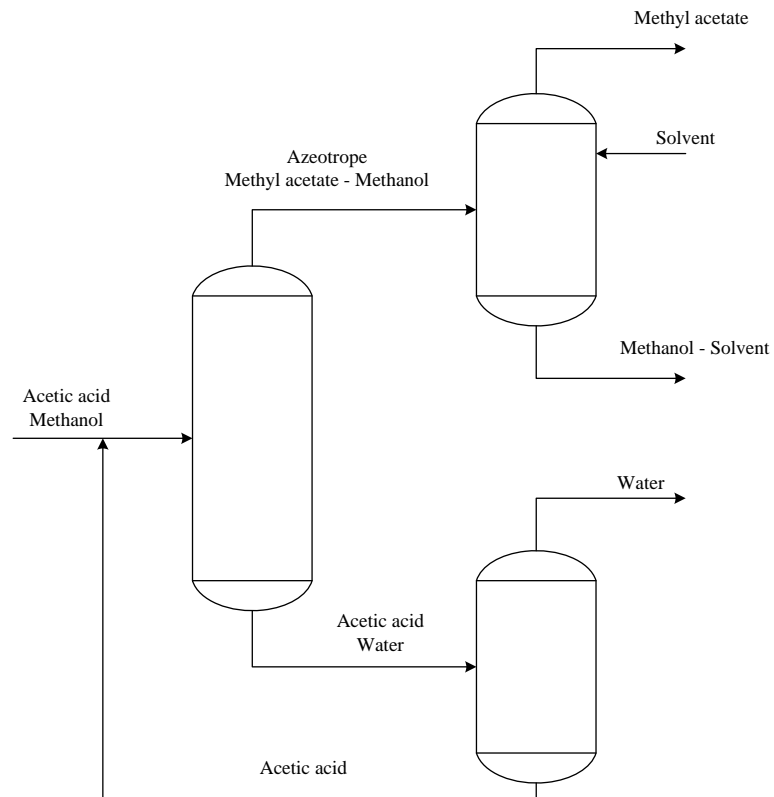
Separation scheme using a single feed stream
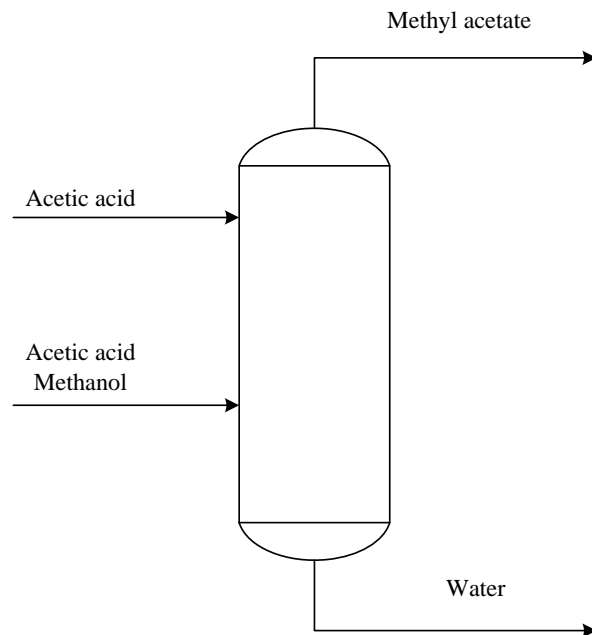
Separation scheme using two feed streams

Final analysis of the change in the tentative path considering two feed streams to the distillation column

As was stated in the previous section, it is intended to describe qualitatively the behavior of the column by dividing the feed of the reactants into two separate feeds. Initially, it is considered a main feed with a small excess of methanol to the column for reasons explained in the previous item. This is divided into three independent feeds, the first composed of the two reactants in small percentages, and which will be considered as a hypothetical feed to explain the general behavior of the tower. The second feed is comprised by pure acetic acid and the third by pure methanol. For the first feeding conditions where there are stoichiometric amounts of the two reactants, it is performed the corresponding analysis of the process statics for such feed, obtaining then the respective limiting steady stable that has the highest degree of conversion with its respective tentative distillation line.

From the location of the tentative distillation path in the concentration simplex it is concluded:
- – The location of the reaction zone takes place in the bottom of the column, according to the segment of the tentative path located within the area of forward reaction.
- – Distillate product: methyl acetate – methanol azeotrope.
- – Bottoms product: acetic acid - water mixture.

Based on the fact that the top product is the azeotrope and to meet the feeding requirements established, the acetic acid is fed to the upper stages (Figure 4.44) of the column which leads to change the trend of the tentative trajectory showing the effect explained in the previous section. As can be seen in Figure 4.44, the behavior of the trajectory in this section must be practically constant referred to the concentration of the acid as being in the stages where the extractive phenomenon occurs, however it must be taken into account that some methanol reacts with acetic acid and hence it is concluded that the trajectory should have a small slope.

Subsequently, the remaining methanol is added to the bottom (feed line Figure 4.44, red color) of the column producing a significant change in the trajectory, an increase in the concentration of methanol in this section, which consequently makes it react with the acetic acid from the top of the column, consuming the total amount of acid and achieving full conversion relative to acetic acid. Thus, the bottoms product will be pure water.
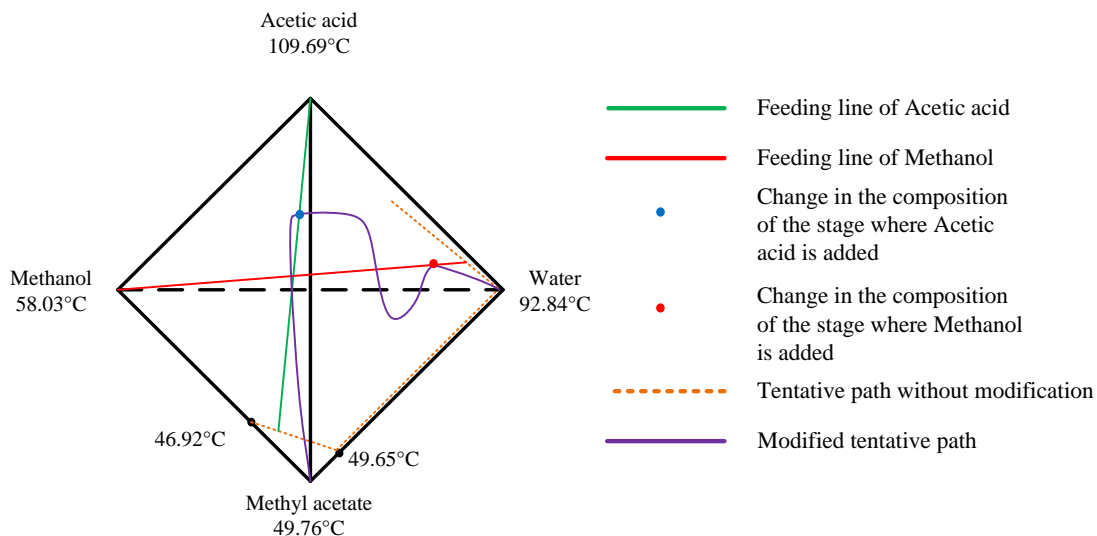
Figure 4-44: Final behavior of the modified tentative path.

As a final result, it can be seen that acetic acid at first has an extractive function, and then it is re-enriched to fully interact with the fed methanol forming the desired products of the reaction. Thus, it is clearly stated that the feeding of the two products must be made in an independent way.

4.3.   Rigorous simulation of a reactive distillation column

Reactive distillation column with a single feed

Case 1: Column with a single feed, auto-catalyzed reaction and 10 separating stages

The first studied case for this system is a reactive distillation column with 8 stages plus the condenser and the boiler. The column is fed on the stage 6 with a mixture of saturated liquid, with a molar flow of *132 gmol/h*, whose composition is reported in Table 4.6. In Figure 4.45 it is shown the reactive distillation scheme for this case:

Table 4-6: Feed composition for Case 1.

Component	Molar fraction	Molar flow (*gmol/h*)
Methanol	0.43	56.76
Acetic acid	0.56	73.92
Methyl acetate	0.00	0.00
Water	0.01	1.32
Total		132

In the following figures are presented the temperature profiles, vapor and liquid phase composition profiles, and liquid and vapor flow profiles in the distillation column (Figures 4.46, 4.47, 4.48 and 4.49). The data to build these figures are reported in Table 10.1 in Annex E.
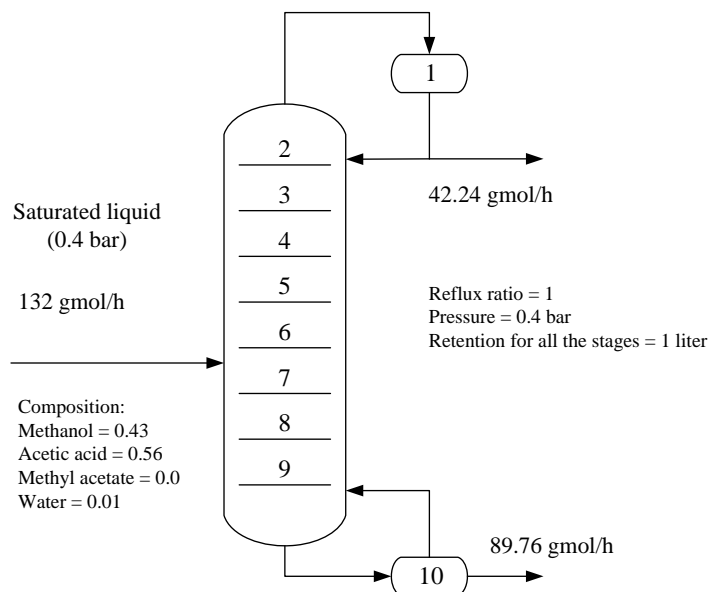
Figure 4-45: Reactive distillation column for Case 1.
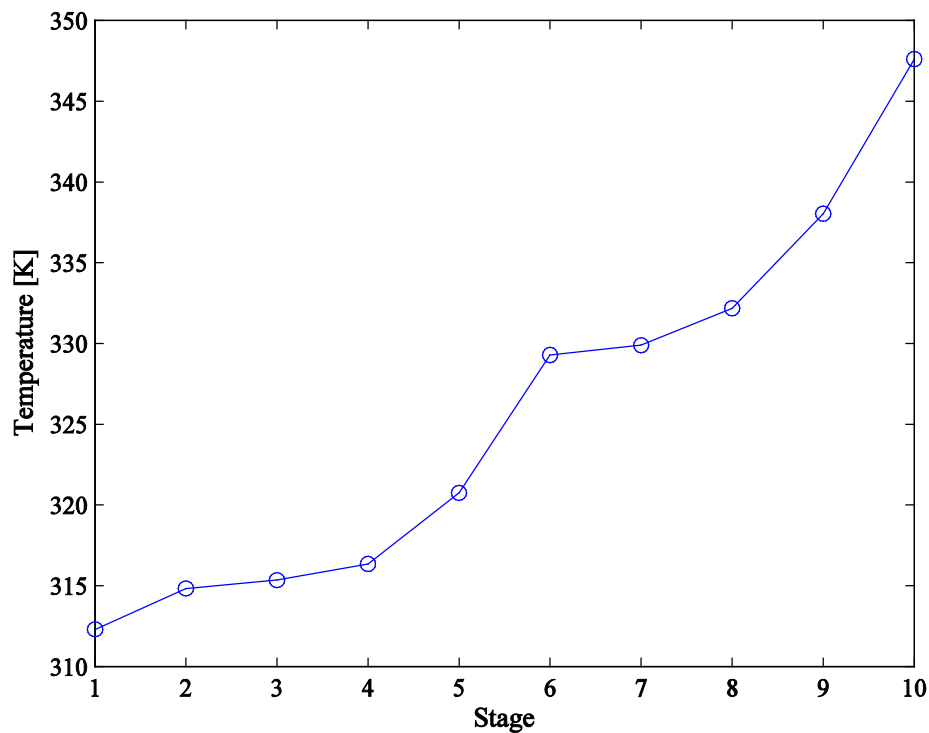
Figure 4-46: Temperature profile along the reactive distillation column for Case 1.
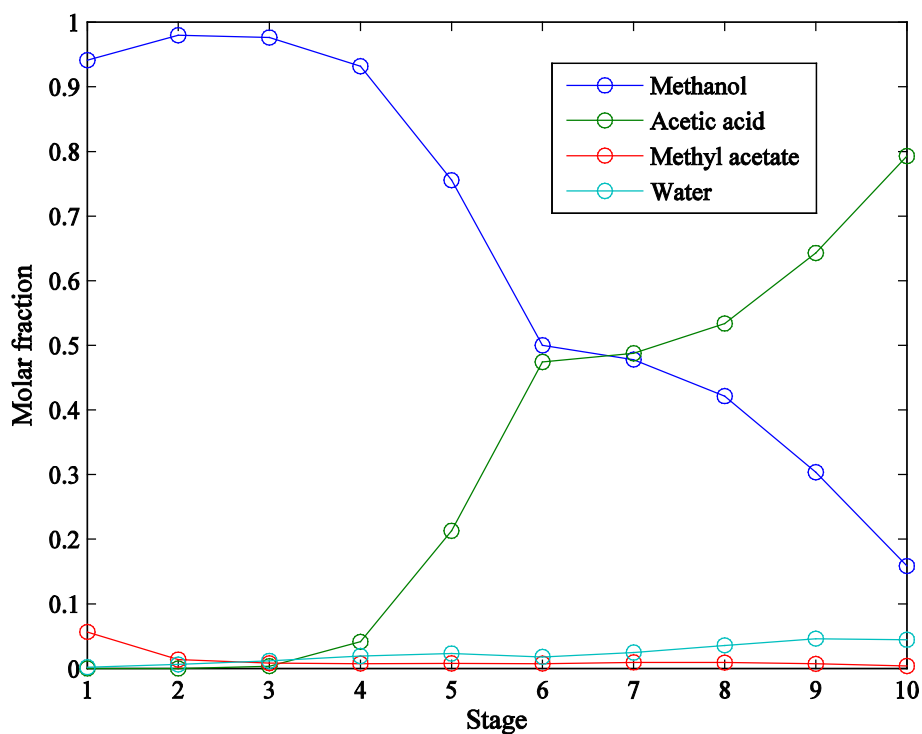
Figure 4-47: Liquid phase composition profiles along the column for Case 1.
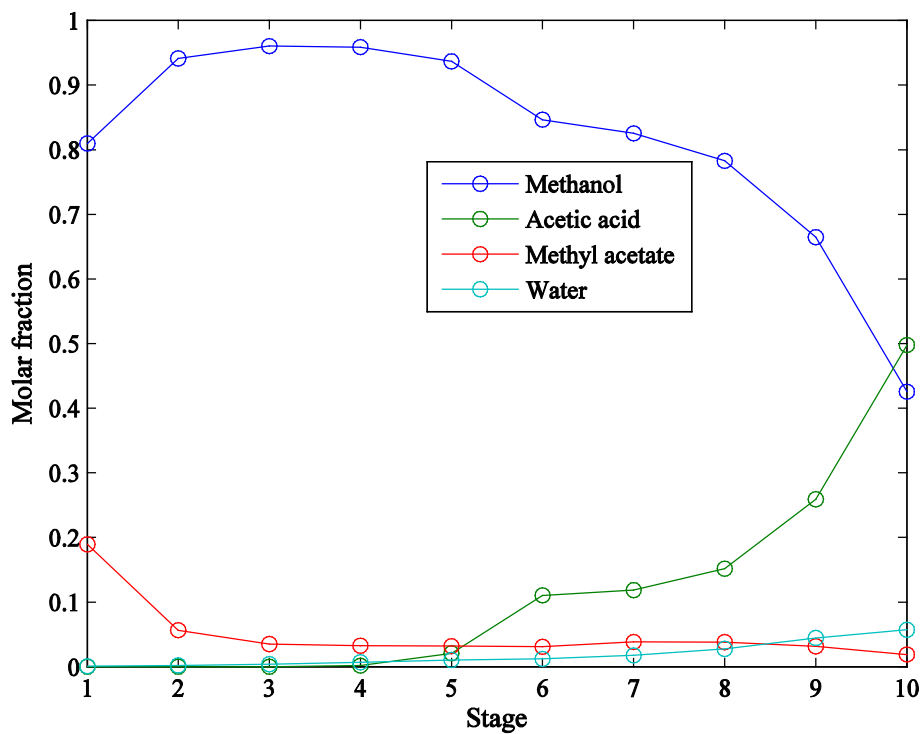
Figure 4-48: Vapor phase composition profiles along the column for Case 1.
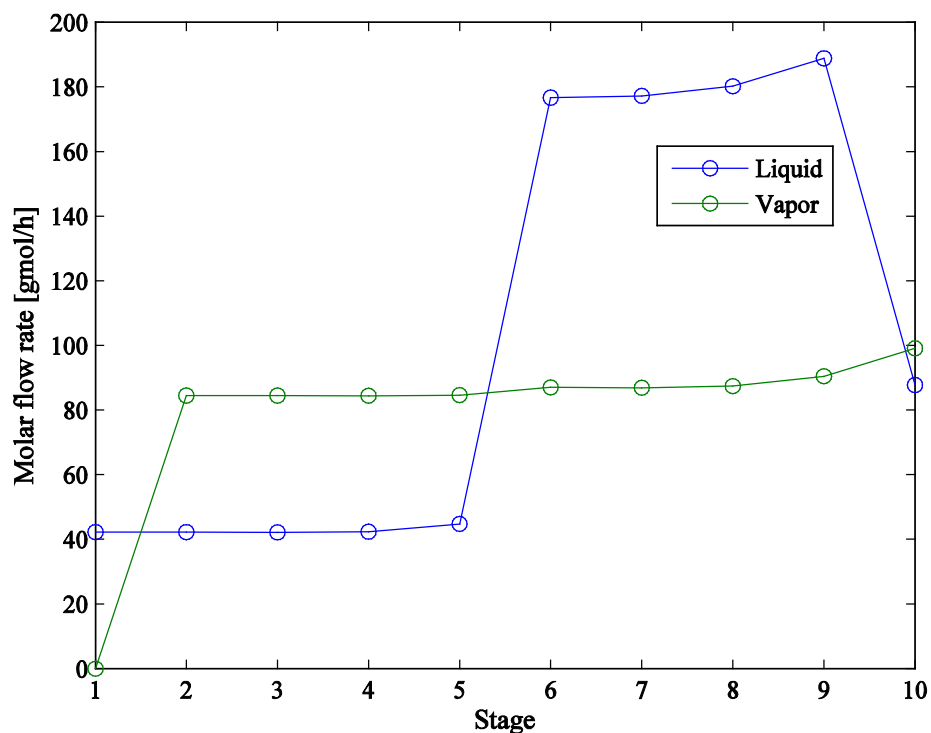
Figure 4-49: Liquid and vapor flow profiles along the column for Case 1.

Table 4-7: Summary of results obtained for Case

Component	Molar fraction	
	Distillate	**Bottoms**
Methanol	0.941	0.159
Acetic acid	9.00E-06	0.793
Methyl acetate	0.057	0.004
Water	0.002	0.044

Component	Flow rate [gmol/h]	
	Distillate	**Bottoms**
Methanol	39.757	14.242
Acetic acid	3.72E-04	71.158
Methyl acetate	2.394	0.368
Water	0.089	3.992
Total	42.240	89.760
Conversion		4.80%
Recovery		86.67%

There were defined the variables conversion and recovery percentage in order to compare the processes. The first term makes reference to the amount of methyl acetate produced with respect to the highest possible amount of it, which is equal to the sum of the methyl acetate as distillate and bottoms divided by the maximum amount of methyl acetate to be produced with full conversion of the limiting reactant. The second term is used to evaluate the amount of methyl acetate recovered as distillate with respect to all the methyl acetate that leaves the column. These terms have the following expressions:

$$\% \text{ Conversion} = \frac{\text{Produced acetate (distillate + bottoms)}}{\text{Produced acetate at maximum conversion}} \tag{0.12}$$

$$\% \text{ Recovery} = \frac{\text{Methyl acetate (distillate)}}{\text{Methyl acetate (distillate)} + \text{Methyl acetate (bottoms)}} \tag{0.13}$$

As it can be seen in Table 4.7, the conversion reached in the column is not good enough – 5% –, with a concentration (molar fraction) of only 5.7% in the flow of distillate. This behavior shows that the acetic acid by itself is not a good catalyst for this reaction. In Table 4.8 it is presented how the methyl acetate molar fraction, conversion percentage and recovery percentage as a function of the volume of the stage vary in the column. The reactive distillation column of Figure 4.45 has a retention volume of 1 liter, which corresponds to a total residence time in the column of 1.5 hours, as shown in Table 4.8.

Table 4-8: Behavior of the methyl acetate molar fraction, conversion and recovery percentage as a function of the volumetric retention and the total residence time in the column.

Retention of the stage [L]	Total retention of the column [L]	Molar fraction of Methyl acetate		Total residence time [h]	Conversion	Recovery
		Distillate	Bottoms			
0.1	1	0.0064	0.0005	0.15	0.5%	86.6%
0.5	5	0.0302	0.0022	0.76	2.6%	86.6%
1	10	0.0567	0.0041	1.53	4.9%	86.7%
5	50	0.1985	0.0145	7.63	17.1%	86.6%
10	100	0.2984	0.0226	15.26	25.8%	86.1%
50	500	0.5438	0.0548	76.28	49.1%	82.4%
100	1000	0.6261	0.0749	152.55	58.4%	79.7%
500	5000	0.7244	0.1237	762.76	73.5%	73.4%
1000	10000	0.7512	0.1358	1525.52	77.4%	72.3%
2000	20000	0.7763	0.1417	3051.03	80.2%	72.1%
5000	50000	0.8039	0.1447	7627.58	82.7%	72.3%
10000	100000	0.8151	0.1447	15255.17	83.6%	72.6%

It is noticed in Figure 4.50 that to obtain high conversions it is necessary to used long residence times, which is equivalent to use high retention volumes. Though high retention volumes improve conversion, they could harm the column hydraulics because it increases the pressure drop inside the column, which also has a negative effect in the economy of the process.
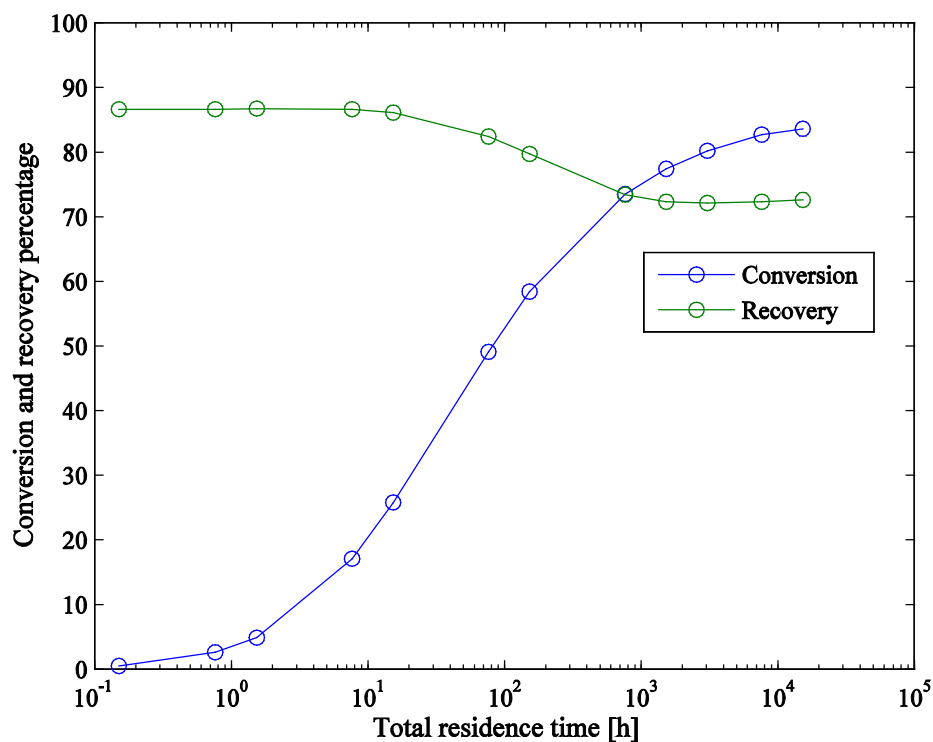
Figure 4-50: Behavior of the conversion and recovery percentage as a function of the total residence time in the column.

Case 2: Column with a single feed, catalyzed reaction and 10 separating stages

In this case it was used the same distillation scheme presented in Case 1 considering a catalyzed reaction. The amount of catalyst per stage is 25 *g*. In the following figures are presented the temperature profiles, vapor and liquid phase composition profiles, and liquid and vapor flow profiles in the distillation column. The data to build these figures are reported in Table 10.2 in Annex E.
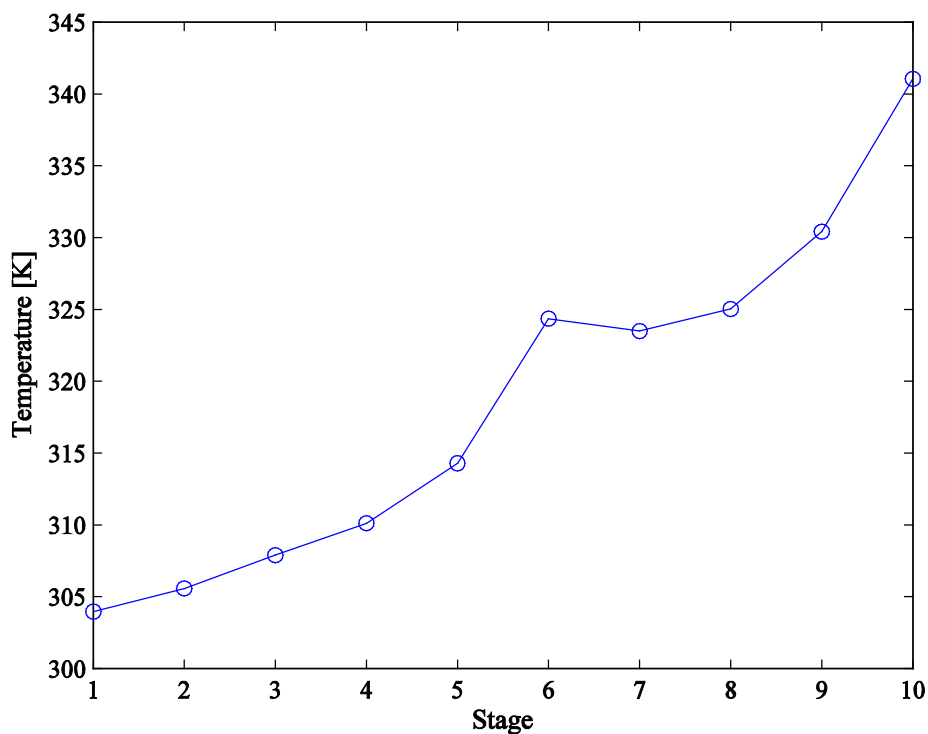
Figure 4-51: Temperature profile along the reactive distillation column for Case 2.
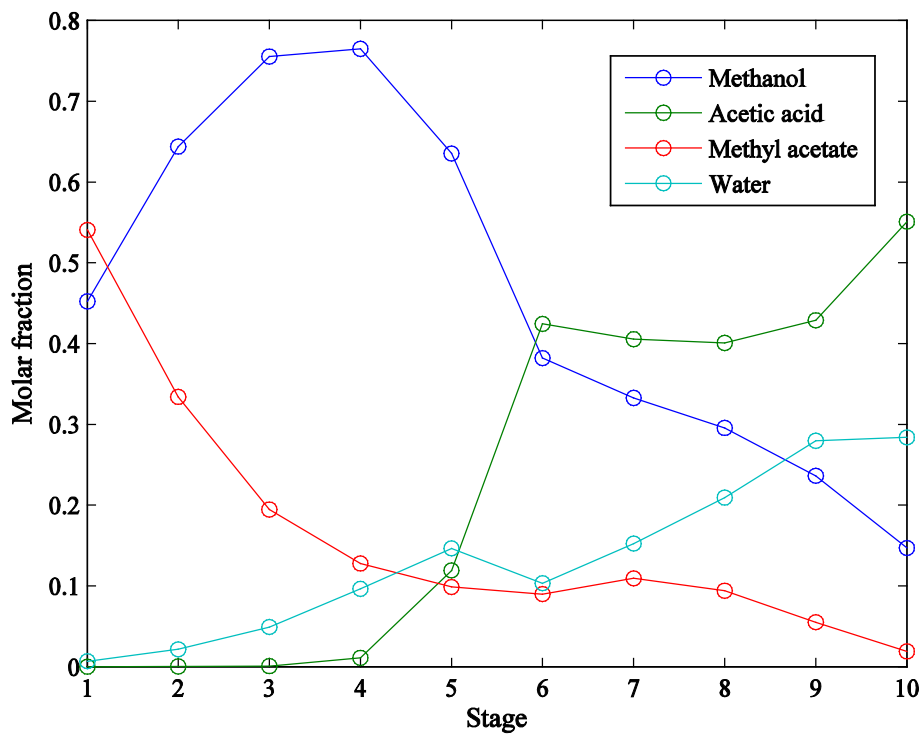
Figure 4-52: Liquid phase composition profiles along the column for Case 2.
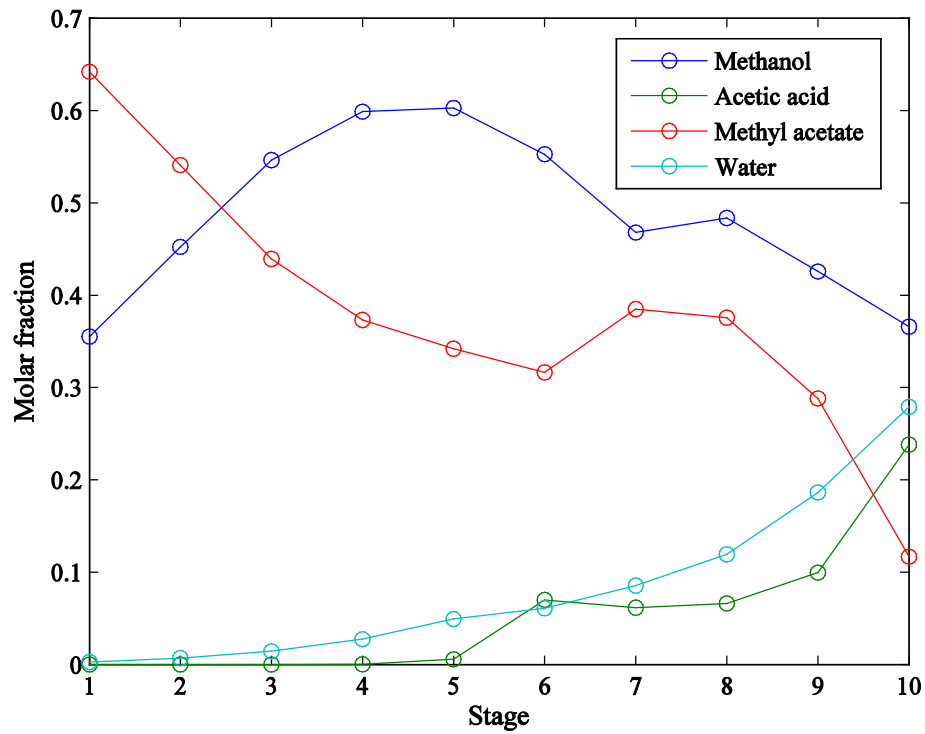
Figure 4-53: Vapor phase composition profiles along the column for Case 2.
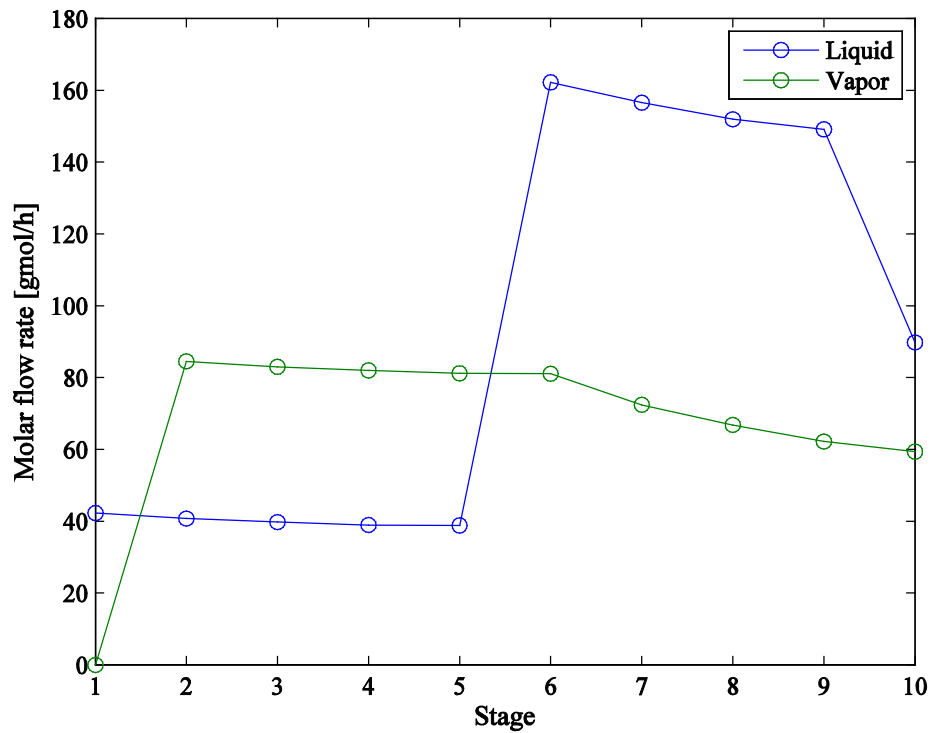
Figure 4-54: Liquid and vapor flow profiles along the column for Case 2.

Table 4-9: Summary of results obtained for Case 2.

Component	Molar fraction	
	Distillate	Bottoms
Methanol	0.452	0.147
Acetic acid	5E-06	0.551
Methyl acetate	0.541	0.018
Water	0.007	0.284

Component	Flow rate [gmol/h]	
	Distillate	Bottoms
Methanol	19.90	13.192
Acetic acid	1.97E-04	49.451
Methyl acetate	22.844	1.625
Water	0.296	25.493
Total	42.24	89.760
Conversion		43.1%
Recovery		93.35%

As it can be seen in Table 4.9, the conversion reached in the column is so much higher than the conversion reached when the auto-catalyzed reaction was used. This result demonstrates that the use of catalyst is required so as to obtain high conversions. The concentration (molar fraction) of methyl acetate in the flow of distillate is 54.1%, which is greater than 5.7% for the auto-catalyzed reaction in Case 1.

1.1. Case 3: Column with a single feed, catalyzed reaction and 25 separating stages

The general configuration of the reactive distillation column is shown in Figure 4.55, its only variation with respect to the column in Case 2 is the number of stages. This case was developed in order to evaluate the effect the number of stages has on the conversion, and to compare the result obtained in Case 2 for a column with only 10 stages. In Table 4.10 is presented the summary of results for Case 3. The profiles are reported in Table 10.3 and Figures 10.1, 10.2, 10.3 and 10.4 in Annex E.
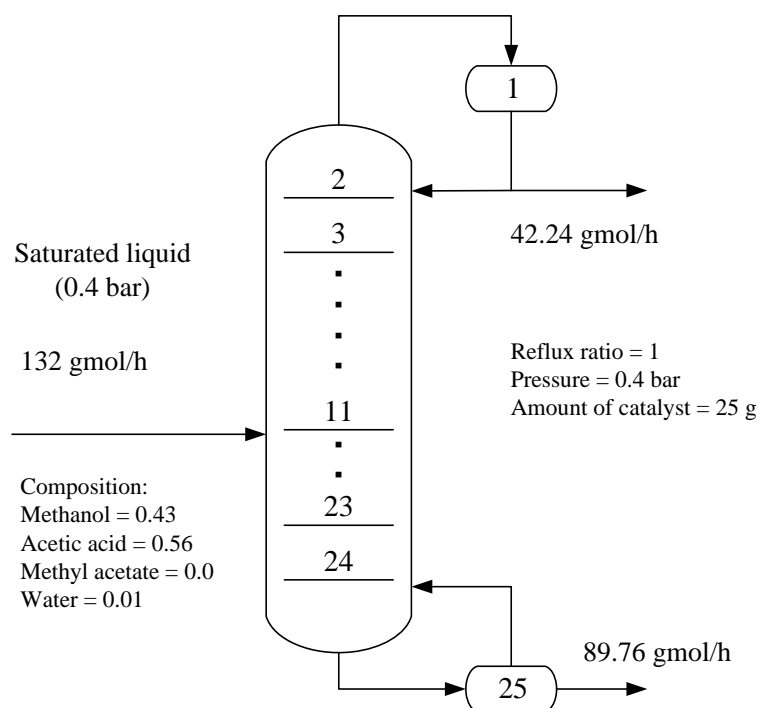
Figure 4-55: Reactive distillation column for Case 3.

Table 4-10: Summary of results obtained for Case 3.

Component	Molar fraction	
	Distillate	**Bottoms**
Methanol	0.406	0.109
Acetic acid	4E-07	0.491
Methyl acetate	0.593	0.053
Water	5E-04	0.347

Component	Flow rate [gmol/h]	
	Distillate	**Bottoms**
Methanol	17.154	9.786
Acetic acid	1.85E-05	44.100
Methyl acetate	25.063	4.757
Water	0.023	31.117
Total	42.24	89.760
Conversion		52.53%
Recovery		84.04%

Even though there is an increase in the number of stages of the column, there is not a significant enhancement in the conversion. In Case 2 conversion is 43% and in Case 3 is 53%. Besides, the

recovery of methyl acetate is reduced from 93% to 84%; this means that part of the methyl acetate is lost in the flow of bottoms. The change in the concentration of methyl acetate is also unnoticeable. In Case 2 there is a concentration (molar fraction) of 0.54 and in Case 3 there is a concentration (molar fraction) of 0.59.

1.2. Case 4: Column with a single feed, catalyzed reaction and 50 separating stages

As an additional example to demonstrate that there is not a significant effect of the number of stages on the conversion and the concentration of methyl acetate, it is considered a last reactive distillation column with 50 stages. This column has the same configuration as the one presented in Figure 4.55 but using 50 stages and feeding on stage 24. In Table 4.11 is presented the summary of results for Case 4. The profiles are reported in Table 10.4 and graphics Table 10.5, 10.6, 10.7 and 10.8 in Annex E.

Table 4-11: Summary of results obtained for Case 4.

Component	Molar fraction	
	Distillate	Bottoms
Methanol	0.407	0.077
Acetic acid	5E-10	0.459
Methyl acetate	0.593	0.085
Water	6E-07	0.379

Component	Flow rate [gmol/h]	
	Distillate	Bottoms
Methanol	17.173	6.898
Acetic acid	2.22E-08	41.231
Methyl acetate	25.067	7.622
Water	2.76E-05	34.009
Total	42.24	89.760
Conversion		57.59%
Recovery		76.68%

It is observed that the molar fraction of methyl acetate in the distillate does not increase in comparison to Case 3. In Table 4.12 it is summarized the behavior of both conversion and recovery percentage as a function of the number of stages using a catalyzed reaction, and in Figure 4.56 it is shown the tendency of these behaviors.

Table 4-12: Behavior of conversion and recovery percentage as a function of the number of stages.

Stage	Conversion	Recovery
10	42.86%	92.63%
25	52.75%	83.94%
50	57.59%	76.61
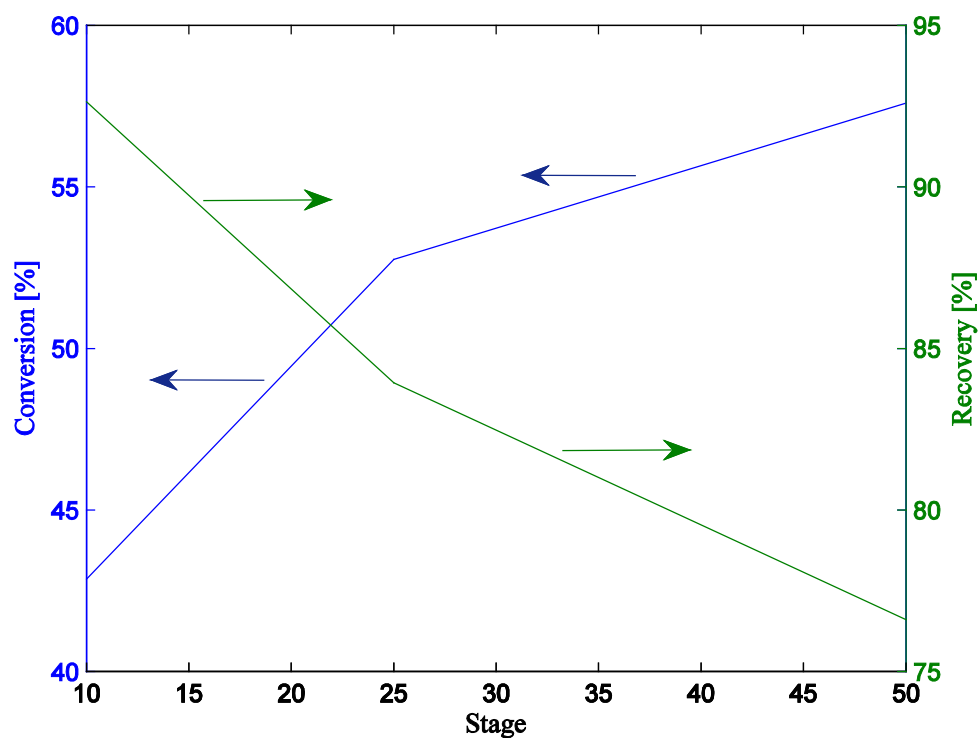
Figure 4-56: Behavior of conversion and recovery percentage as a function of the number of stages.

Though there is a huge increase in the number of stages, the respective enhancement of the conversion is only 35%. This shows that an increase in the number of stages of a reactive distillation for a system with a single feed stream, does not improve the overall conversion. Also, it can be noticed that an increase in the number of the stages leads to a decrease in the recovery of methyl acetate, which affects the yield of the process. Though the increase in the conversion percentage from 10 to 25 stages is about 23%, the respective increase in the flow of methyl acetate as distillate was only 10%, because while the conversion grows the recovery falls.

In Figure 4.57 it is shown the behavior of the conversion percentage for Cases 2, 3 and 4 as a function of the amount of catalyst. In this graphic it is observed how the conversion percentage is not a function of the number of stages but the total amount of catalyst in the column.

The column with 50 stages has the lowest conversion percentage in all the range of used catalyst. It was also found that for all the configurations that the conversion does not increase after a certain amount of catalyst. In Table 10.5 (Annex E) are reported the behavior of the molar fraction of methyl acetate in distillate and bottoms, and the conversion and recovery percentages for Cases 2, 3 and 4 as a function of the total amount of catalyst.
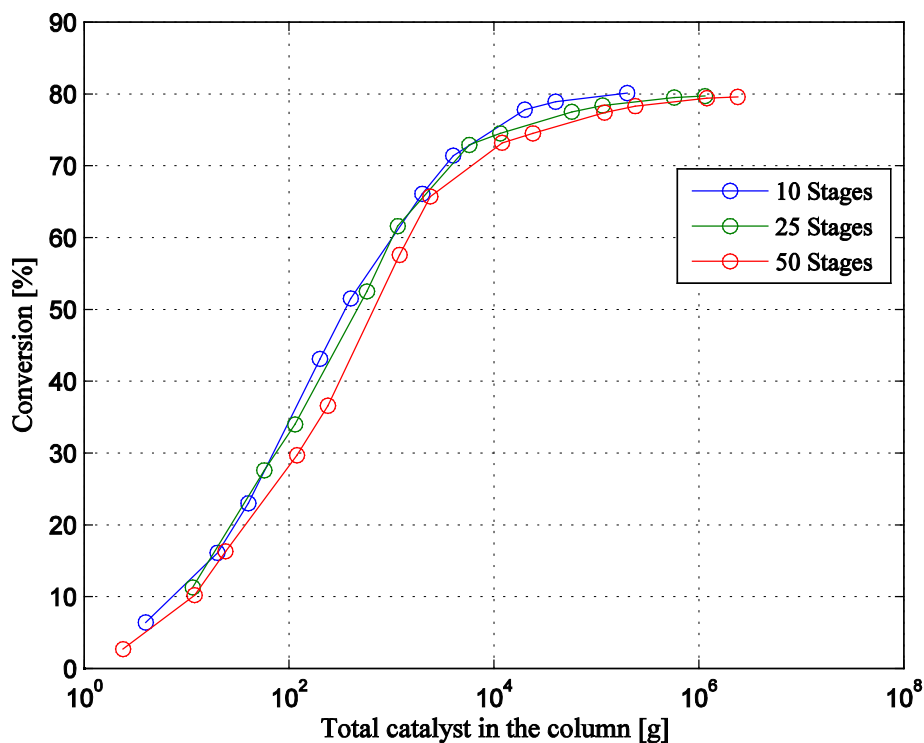
Figure 4-57: Behavior of conversion percentage for three distillation columns as a function of the total amount of catalyst.

2. Reactive distillation column with two feed streams

2.1. Case 5: Column with two feed streams, auto-catalyzed reaction and 25 separating stages

This distillation column has 25 stages, two feed streams on stages 7 and 20. In Table 4.13 are reported the specifications of each feed stream. Every stage has a volumetric retention of 0.5 liters, with a total residence time in the column of 4.1 hours.

The following Figure shows the configuration used in this case:
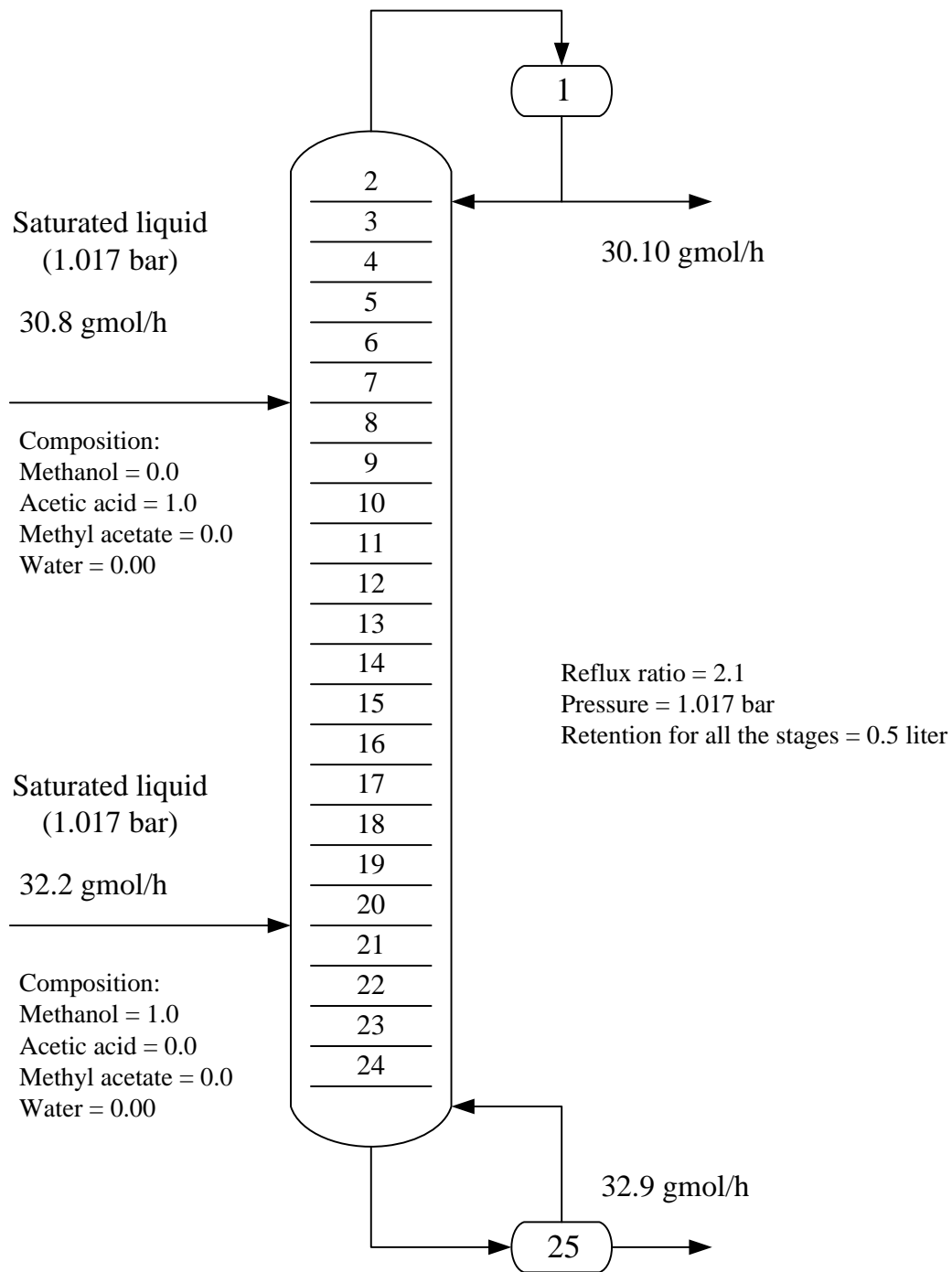
Figure 4-58: Reactive distillation column for Case 5.

Table 4-13: Specifications of the feed streams for Case 5.

	Molar fraction	
Component	**Feed 1**	**Feed 2**
Methanol	0	1
Acetic acid	1	0
Methyl acetate	0	0
Water	0	0

	Flow rate [gmol/h]	
Component	**Feed 1**	**Feed 2**
Methanol	0	32.2
Acetic acid	30.8	0
Methyl acetate	0	0
Water	0	0
Temperature [K]	**294.25**	**293.25**
Density [gmol/L]	**17.4**	**24.7**

In Table 10.6 (Annex E) are reported the detailed result for this case and in the following graphics will be presented the temperature profiles, vapor and liquid phase composition profiles, and liquid and vapor flow profiles in the distillation column.
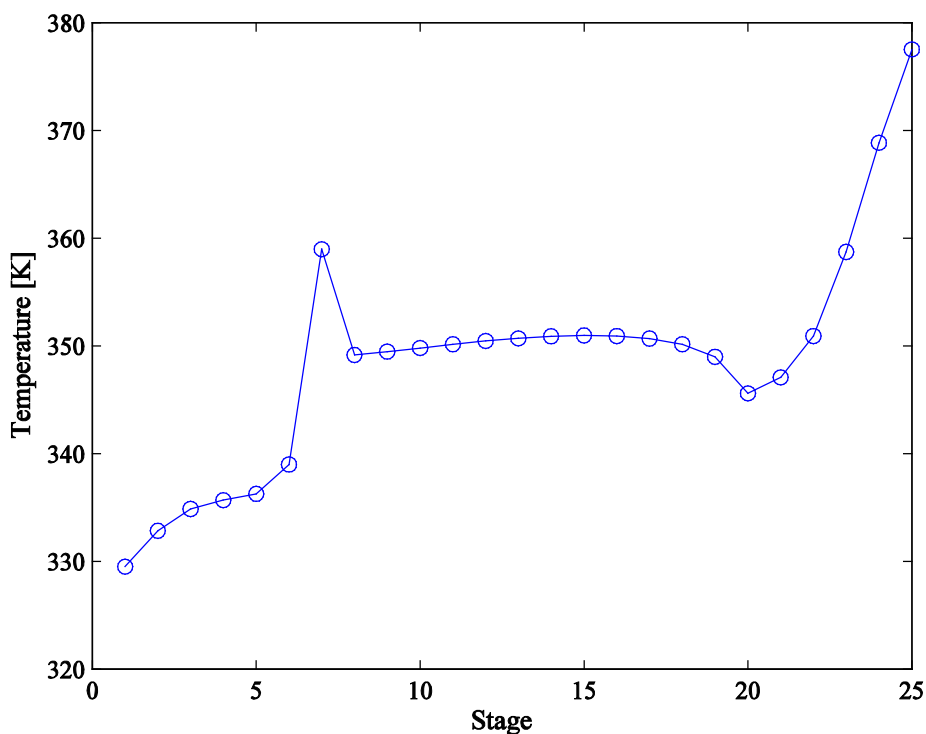
Figure 4-59: Temperature profile along the reactive distillation column for Case 5.
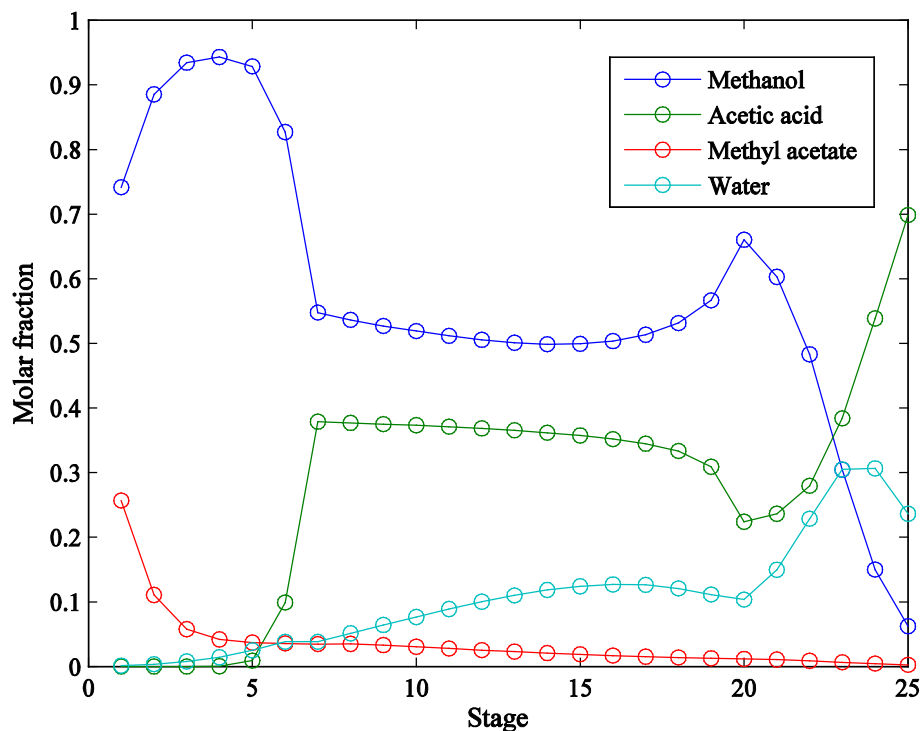
Figure 4-60: Liquid phase composition profiles along the column for Case 5.
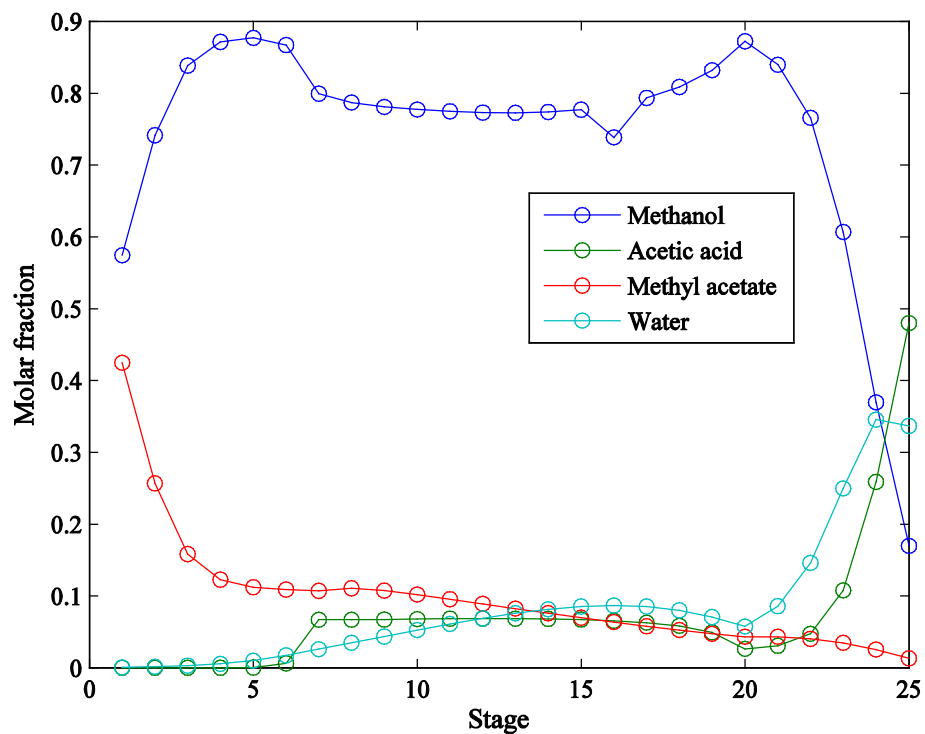
Figure 4-61: Vapor phase composition profiles along the column for Case 5.
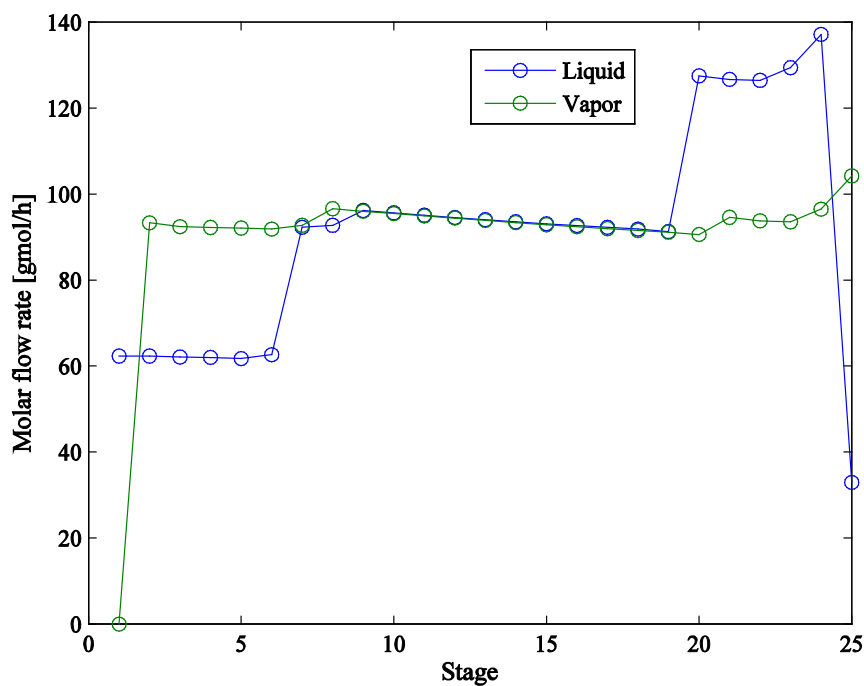
Figure 4-62: Liquid and vapor flow profiles along the column for Case 5.

In Table 4.14 is presented the summary of results for Case 4. This configuration has a relative small conversion percentage but a high recovery percentage, i.e. almost all the methyl acetate produced in the column leaves it as distillate.

Table 4-14: Summary of results obtained for Case 5.

Component	Molar fraction	
	Distillate	**Bottoms**
Methanol	0.741	0.063
Acetic acid	7E-08	0.699
Methyl acetate	0.257	0.003
Water	0.001	0.236

Component	Flow rate [gmol/h]	
	Distillate	**Bottoms**
Methanol	22.32	2.06
Acetic acid	2E-06	22.98
Methyl acetate	7.73	0.09
Water	0.05	7.77
Total	30.10	32.90
Conversion		25.38%
Recovery		98.84%

In Table 4.15 and Figure 4.63 it is observed that the conversion percentage with two feed streams grows faster with the residence time in comparison to the conversion percentage when applying a single feed stream, where the maximum conversion is 80% for higher retention times.

Table 4-15: Behavior of the methyl acetate molar fraction, conversion and recovery percentage as a function of the volumetric retention and the total residence time in the column.

Retention of the stage [L]	Total retention of the column [L]	Molar fraction of Methyl acetate		Total residence time [h]	Conversion	Recovery
		Distillate	Bottoms			
0.1	2.5	0.0735	0.0012	0.81	7.3%	98.3%
0.5	12.5	0.2570	0.0026	4.07	25.4%	98.9%
1	25	0.4109	0.0028	8.14	40.5%	99.3%
5	125	0.7555	0.0030	40.72	74.2%	99.6%
10	250	0.8423	0.0031	81.43	82.6%	99.6%
15	375	0.8816	0.0031	122.15	86.5%	99.6%
20	500	0.9035	0.0030	162.87	88.6%	99.6%
50	1250	0.9434	0.0034	407.17	92.6%	99.6%
100	2500	0.9357	0.0049	814.34	93.7%	99.4%
500	12500	0.9603	0.0095	4071.71	94.9%	98.9%
1000	25000	0.9610	0.0104	8143.42	95.0%	98.8%
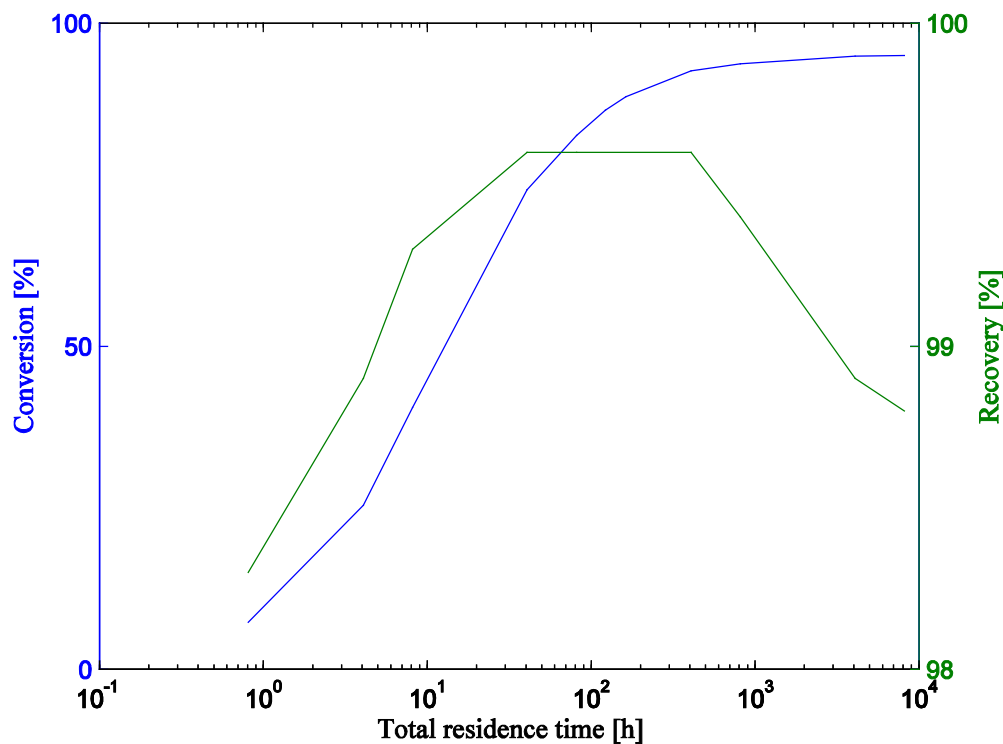
Figure 4-63: Behavior of the conversion and recovery percentage as a function of the total residence time in the column.

It can be seen in Figure 4.63 that the recovery percentage of methyl acetate remains at higher levels, which shows the good efficiency of the separation in this column. Besides, the recovery percentage also has a maximum value. Figure 4.64 shows the behavior of the temperature and the reaction as a function of the total residence time. The reaction rate and the maximum and average temperatures decrease while the total residence time increases. The fact that the conversion percentage does not decrease with an increase in the total residence time is due to the column operates under chemical equilibrium. In Table 10.7 (Annex E) are reported in detail the values in which Figure 4.64 is based.
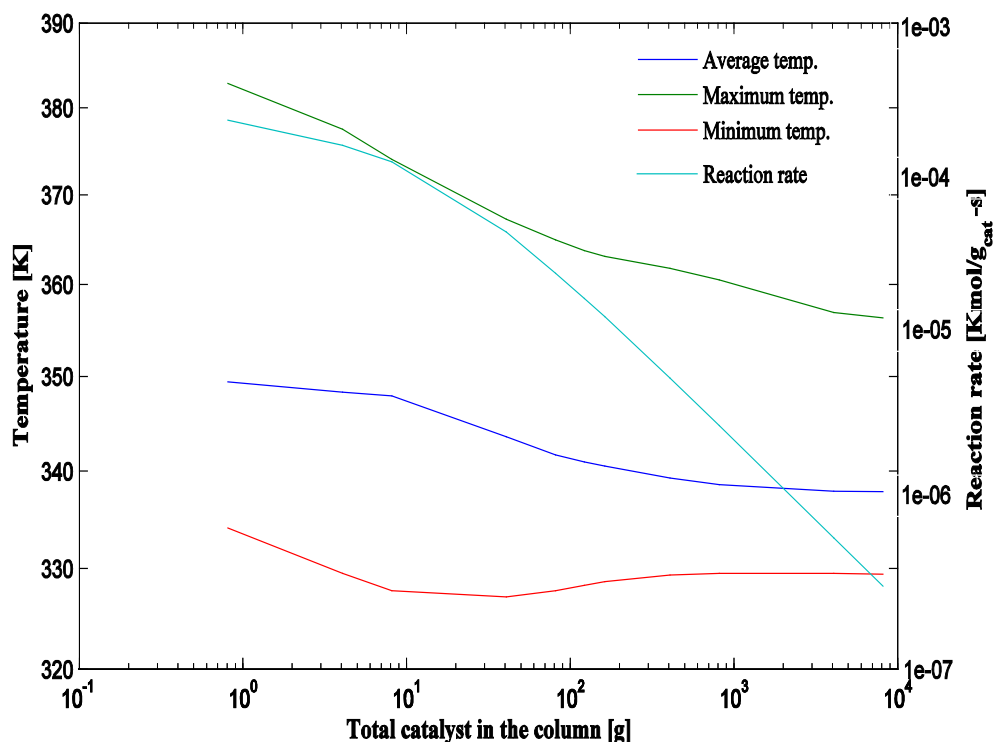
Figure 4-64: Behavior of the temperature and the average reaction rate as a function of the total residence time in the column.

2.2. Case 6: Column with two feed streams, catalyzed reaction and 25 separating stages

For this case was used the same configuration of the column for Case 5. It was employed a catalyzed reaction with 50 g of catalyst in every of the 23 stages. It was also assumed a volumetric retention of 0.5 liters in the boiler and the condenser. The following graphics show the temperature profiles, vapor and liquid phase composition profiles, and liquid and vapor flow profiles in the distillation column. The graphics were built using the data provided in Table 10.8 (Annex E).
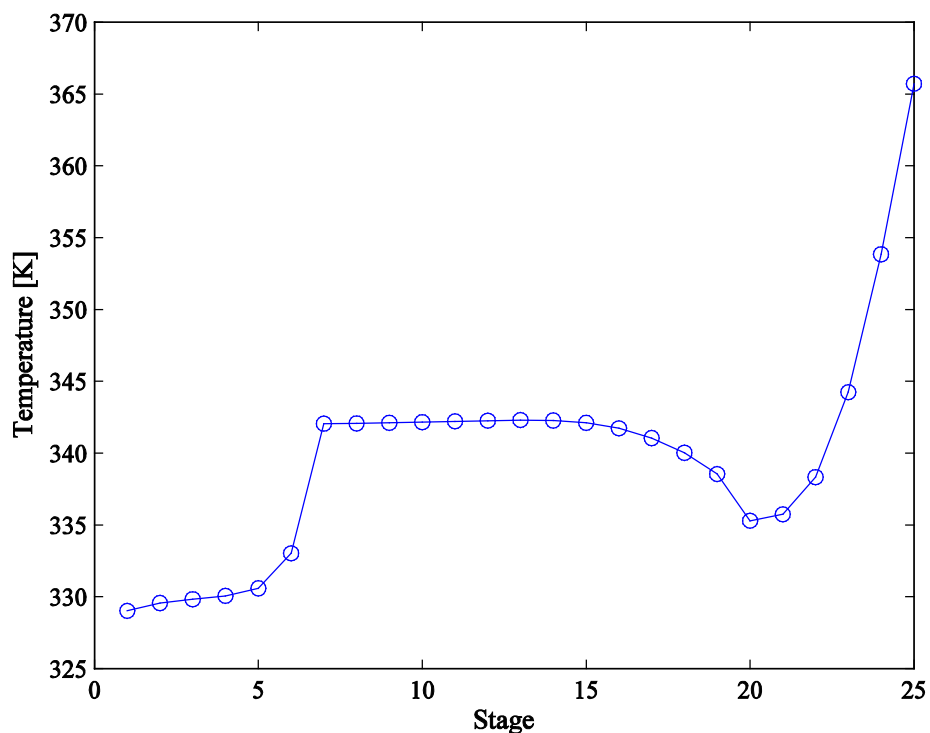
Figure 4-65: Temperature profile along the reactive distillation column for Case 6.
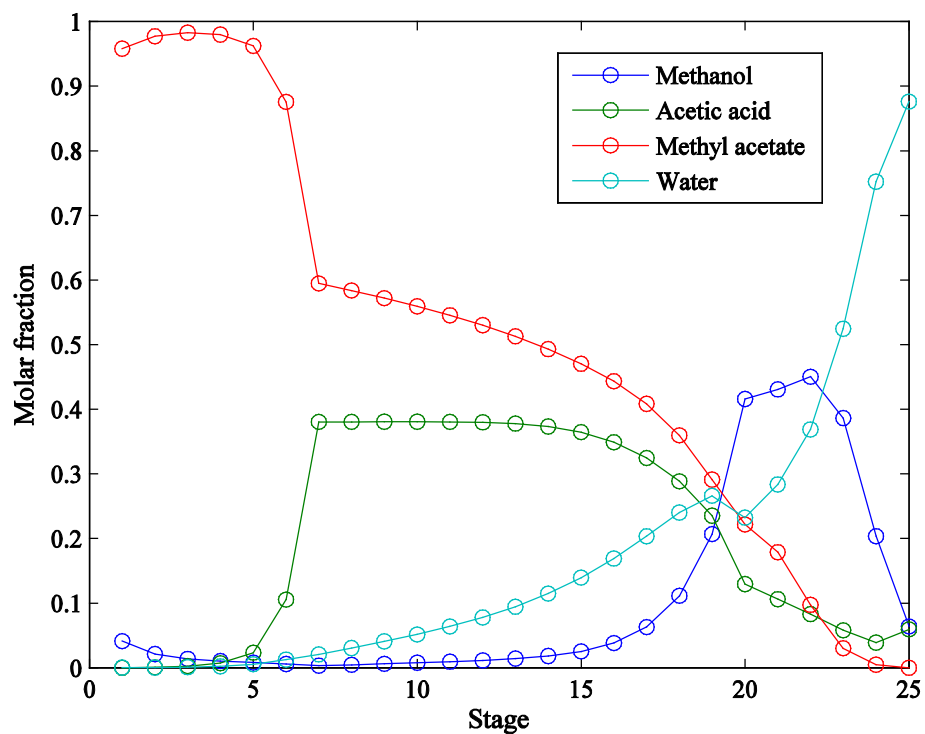
Figure 4-66: Liquid phase composition profiles along the column for Case 6.
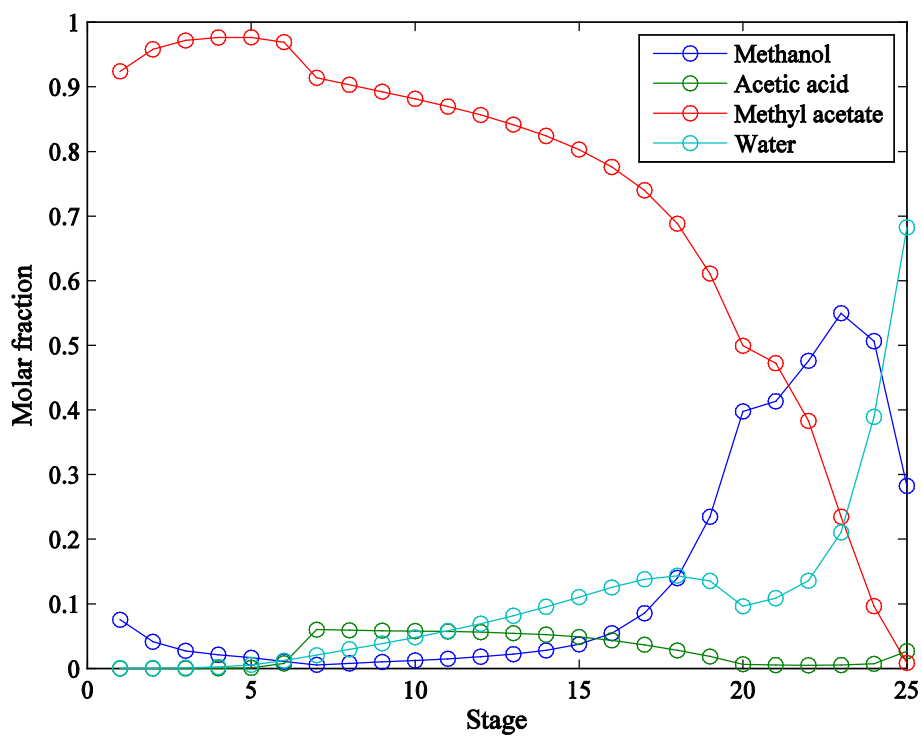
Figure 4-67: Vapor phase composition profiles along the column for Case 6.
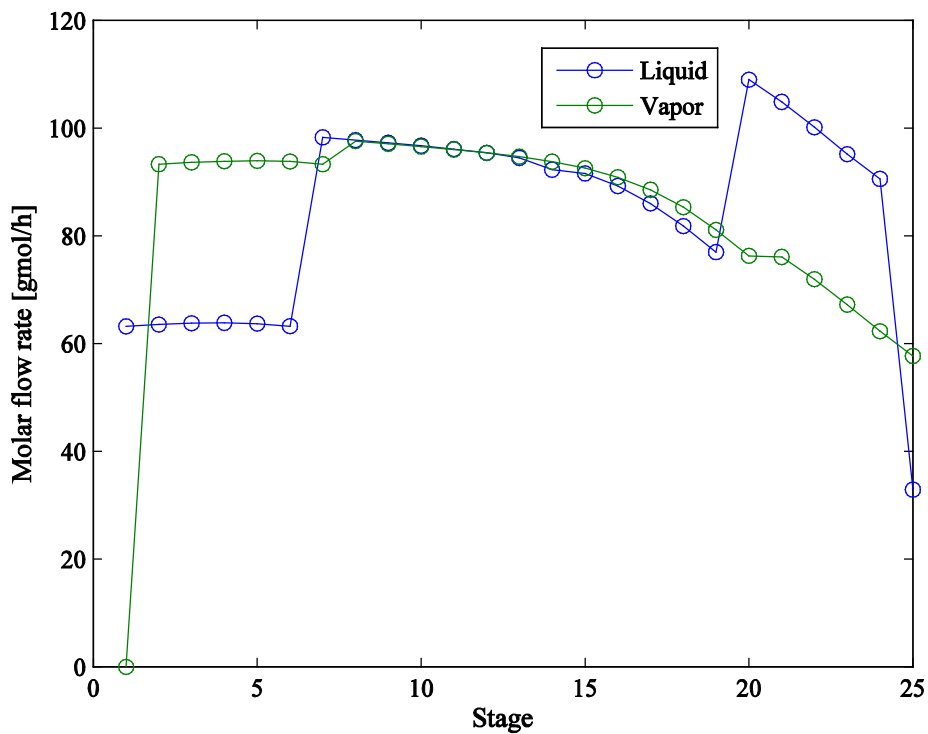
Figure 4-68: Liquid and vapor flow profiles along the column for Case 6.

Table 4.16 shows the result for Case 6, having a high degree of conversion and recovery.

Table 4-16: Summary of results obtained for Case 6.

Component	Molar fraction	
	Distillate	Bottoms
Methanol	0.0415	0.0642
Acetic acid	4.0E-05	0.0595
Methyl acetate	0.958	0.0002
Water	0.0006	0.8761

Component	Flow rate [gmol/h]	
	Distillate	Bottoms
Methanol	1.25	2.11
Acetic acid	1.20E-03	1.96
Methyl acetate	28.83	0.01
Water	1.71E-02	28.82
Total	30.10	32.90
Conversion		93.63%
Recovery		99.96%

Table 4-17: Behavior of the conversion and recovery percentage as a function of the total amount of catalyst in the column.

Catalyst in the stage [g]	Total catalyst in the column [g]	Molar fraction of Methyl acetate		Conversion	Recovery
		Distillate	Bottoms		
0.05	1.15	0.1172	0.0034	11.8%	96.96%
0.25	5.75	0.2634	0.0023	26.0%	99.07%
0.5	11.5	0.3689	0.0017	36.2%	99.51%
2.5	57.5	0.6952	0.0007	68.0%	99.89%
5	115	0.8125	0.0004	79.4%	99.95%
7.5	172.5	0.8696	0.0003	85.0%	99.97%
8	184	0.8770	0.0002	85.7%	99.97%
10	230	0.8992	0.0002	87.9%	99.98%
15	345	0.9272	0.0001	90.6%	99.98%
20	460	0.9399	0.0001	91.9%	99.98%
30	690	0.9509	0.0002	92.9%	99.98%
40	920	0.9555	0.0002	93.4%	99.98%
50	1150	0.9579	0.0002	93.6%	99.97%
100	2300	0.9619	0.0005	94.1%	99.94%
250	5750	0.9643	0.0010	94.3%	99.88%
500	11500	0.9652	0.0013	94.5%	99.85%
2500	57500	0.9661	0.0018	94.6%	99.80%
5000	115000	0.9662	0.0018	94.6%	99.79%

In Figure 4.69 is presented the behavior of the conversion and recovery percentage as a function of the amount of catalyst present in the column. It is observed that are not necessary huge amounts of catalyst to reach high conversions. In the same way, the recovery percentage has maximum values. This demonstrates that this configuration has a high efficiency, because besides reaching high conversions in the reaction, it also achieves an excellent separation of the products.
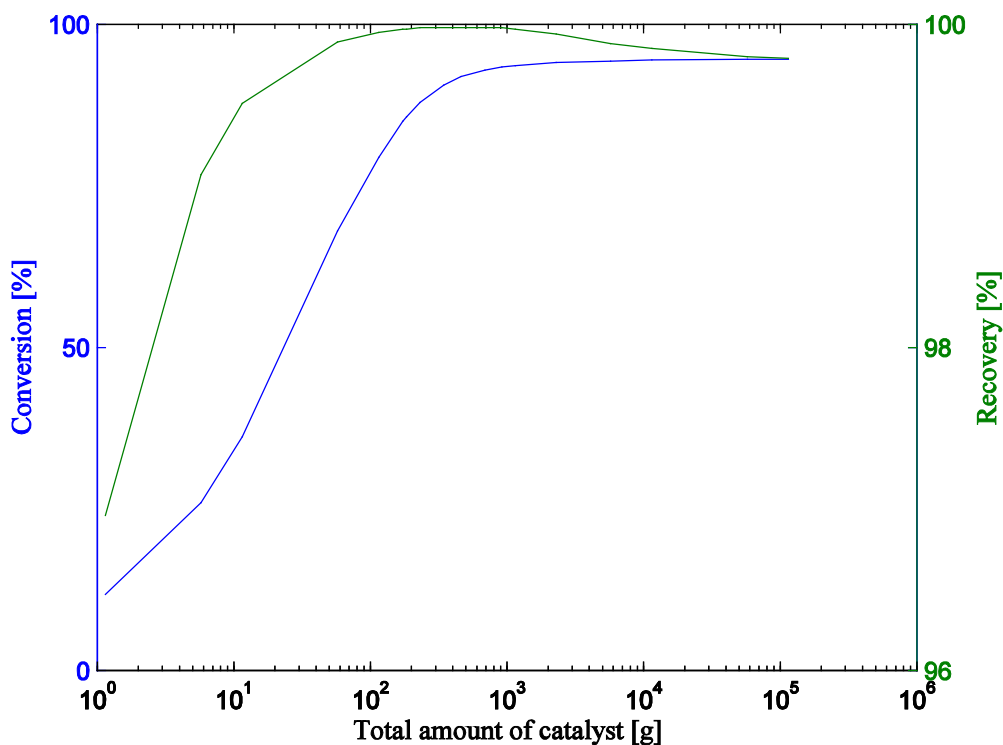
Figure 4-69: Behavior of the conversion and recovery percentage as a function of the total amount of catalyst in the column.

The recovery percentage has a maximum value, i.e., it is achieved a condition of optimal separation. In Figure 4.69, which is based on Table 10.9 (Annex E), it can be seen how the amount of catalyst affects the temperature and the average reaction rate. The average temperature has a maximum in the same section where the recovery percentage has it. On the other hand, the maximum temperature also has a minimum in this section. A higher temperature in the column leads to a re-concentration of methyl acetate in the upper section enriching the distillate stream. Furthermore, the reaction rate decreases as the amount of catalyst increases because of a fall in the average temperatures.
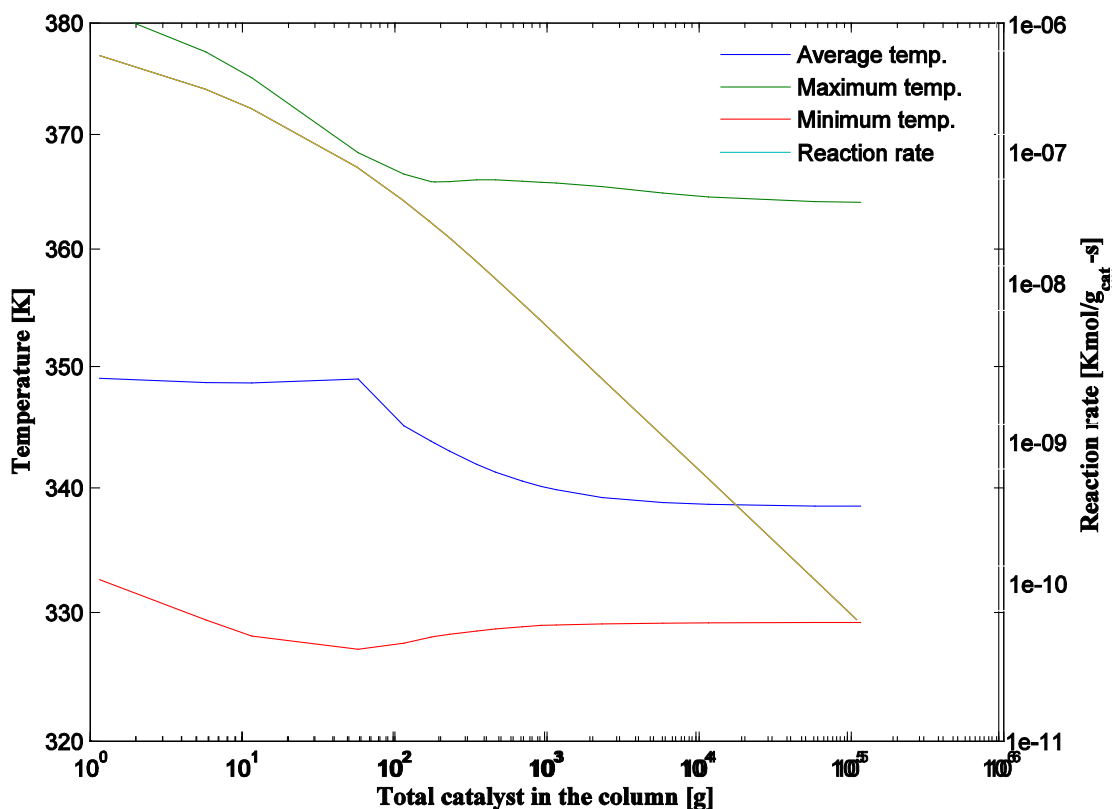
Figure 4-70: Behavior of the average temperature and reaction rate as a function of the total amount of catalyst in the column.

When the amount of catalyst is low the reaction rate is slow, hence the concentration of reactants is high along the column, and thus the forward reaction is favored. When the amount of catalyst is high the reactants are consumed faster, hence the concentration of reactants is low, and thus the forward reaction will be less favored than in the other case.

The reflux ratio was also analyzed. In Figure 4.71 it is shown the behavior of the conversion and recovery percentage as a function of the reflux ratio. The optimum reflux ratio is located between 1.5 and 2.0. In Table 10.10 are reported the data to build Figure 4.71.
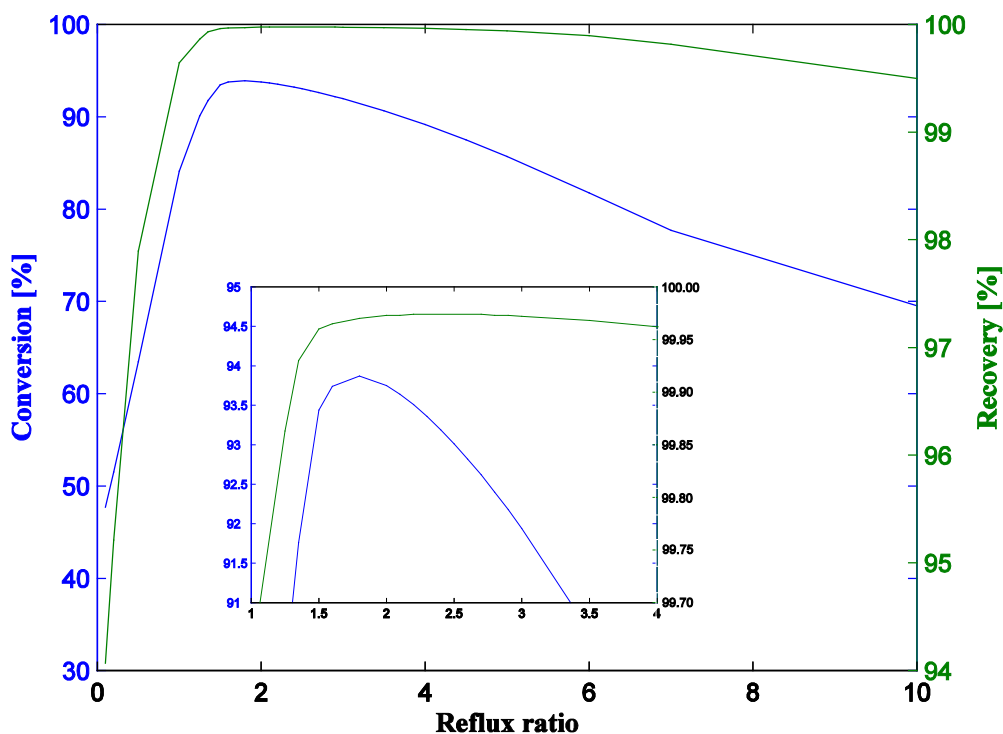
Figure 4-71: Behavior of conversion and recovery percentage as a function of the reflux ratio in the column.

The behavior exhibited in Figure 4.71 indicates that an initial increase in the reflux ratio leads to a fast increase in conversion and recovery reaching maximum values, having then a small fall.

The reflux ratio is a very important constraint to design reactive distillation columns because both liquid and vapor flows inside the column are dependent on this parameter, which also helps to calculate the heat duties in the condenser and boiler. It must be said that the highest operating cost in a reactive distillation column is related to the heat duty of the boiler.
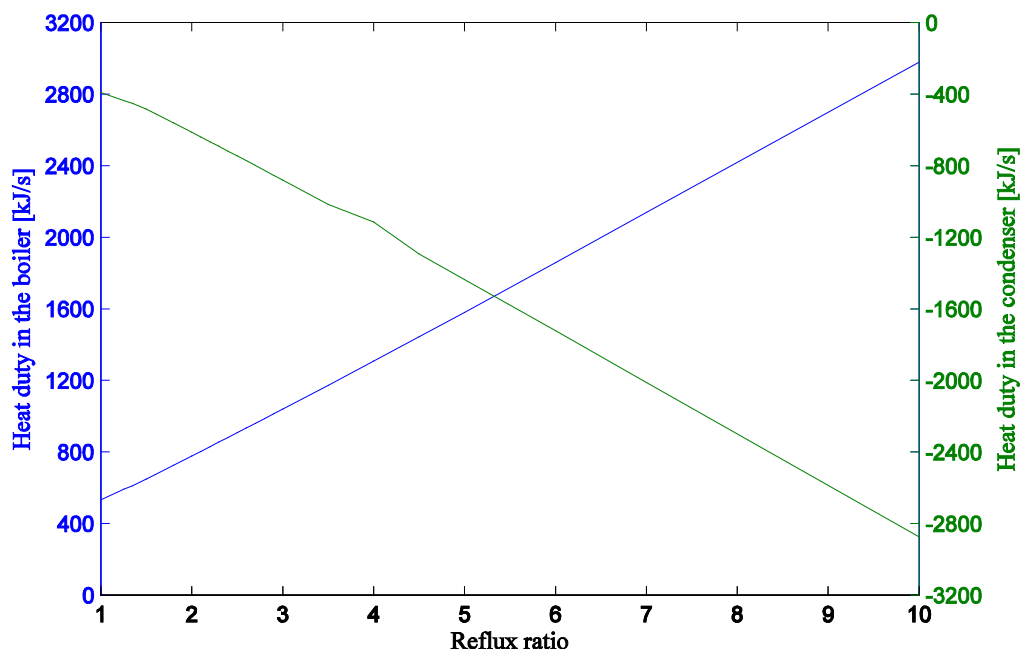
Figure 4-72: Behavior of the heat duties as a function of the reflux ratio in the column.

In Figure 4.72, based on Table E.27 (Annex E), for low reflux ratios are obtained low heat duties. In general, it is convenient to fix, if possible, the lowest reflux ratio. Hence, an economic analysis must be performed so as to find an optimum value of this design parameter.

2.3. Case 7: Column with two feed streams, catalyzed and auto-catalyzed reaction, 25 separating stages with enriching and reaction zones

The general configuration of this column is given in Figure 4.45 but in this case it was employed a catalyzed reaction in 18 out of 25 stages with 50 g of catalyst per stage, and also it was used auto-catalyzed reaction in the enriching zone, the boiler and the condenser with a volumetric retention of 0.5 liters.

The enriching zone goes from stages 2 to 6, the reaction zone from stages 7 to 24. In Table 4.18 is reported the kinetics used in every stage of the reactive distillation column for this case.

Table 4-18: Type of kinetics used in the reactive distillation column for Case 7.

Stage	Type of kinetics	Stage	Type of kinetics	Stage	Type of kinetics
1	Autocatalyzed	10	Catalyzed	19	Catalyzed
2	Autocatalyzed	11	Catalyzed	20	Catalyzed
3	Autocatalyzed	12	Catalyzed	21	Catalyzed
4	Autocatalyzed	13	Catalyzed	22	Catalyzed
5	Autocatalyzed	14	Catalyzed	23	Catalyzed
6	Autocatalyzed	15	Catalyzed	24	Catalyzed
7	Catalyzed	16	Catalyzed	25	Autocatalyzed
8	Catalyzed	17	Catalyzed		
9	Catalyzed	18	Catalyzed		

The following graphics show the temperature profiles, vapor and liquid phase composition profiles, and liquid and vapor flow profiles in the distillation column. The graphics were built using the data provided in Table 10.12 (Annex E).
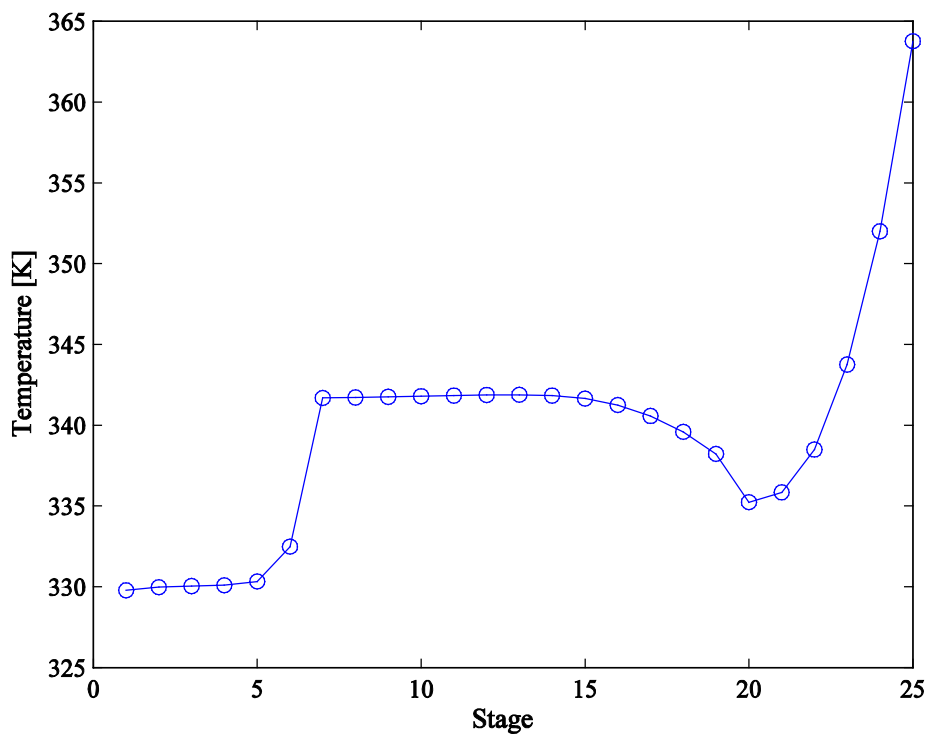
Figure 4-73: Temperature profile along the reactive distillation column for Case 7.
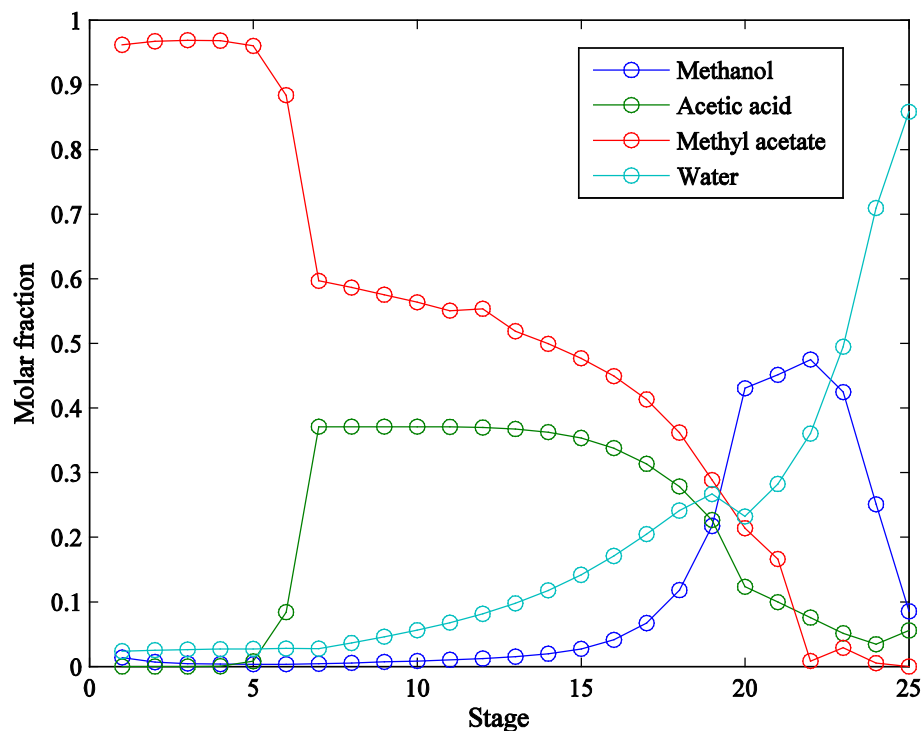
Figure 4-74: Liquid phase composition profiles along the column for Case 7.
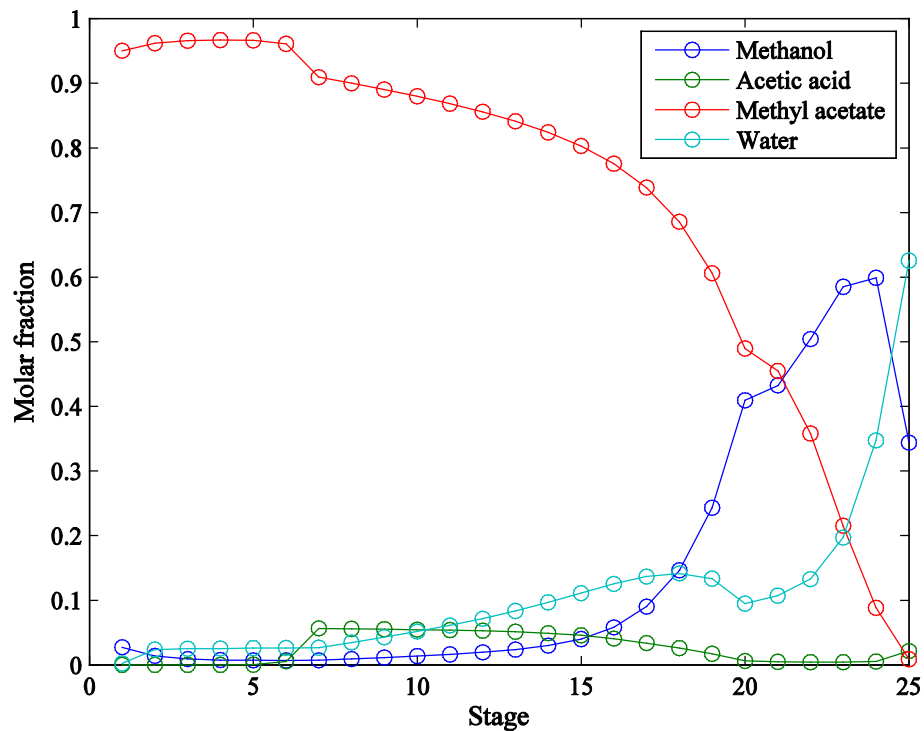
Figure 4-75: Vapor phase composition profiles along the column for Case 7.
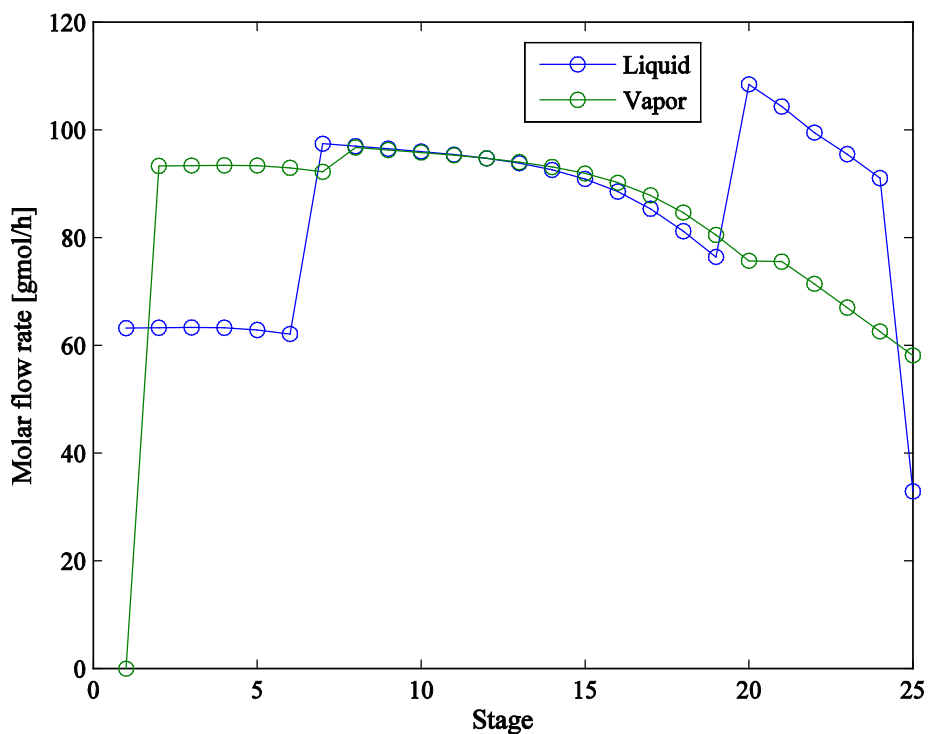
Figure 4-76: Liquid and vapor flow profiles along the column for Case 7.

Table 4-19: Summary of results obtained for Case 7.

Component	Molar fraction	
	Distillate	**Bottoms**
Methanol	0.014	0.0855
Acetic acid	1.27E-07	0.0559
Methyl acetate	0.962	0.0003
Water	2.4E-02	0.8583

Component	Flow rate [gmol/h]	
	Distillate	**Bottoms**
Methanol	0.43	2.81
Acetic acid	3.5E-06	1.84
Methyl acetate	28.95	0.01
Water	7.2E-01	28.24
Total	30.10	32.90
Conversion		94.03%
Recovery		99.97%

In Figure 4.77 it is presented the performance of the conversion and recovery as a function of the amount of catalyst. In this graph it can be seen how the conversion at the beginning increases its

value with an increase in the catalyst reaching a constant value. The recovery has a maximum achieving then an optimal condition for the separation.
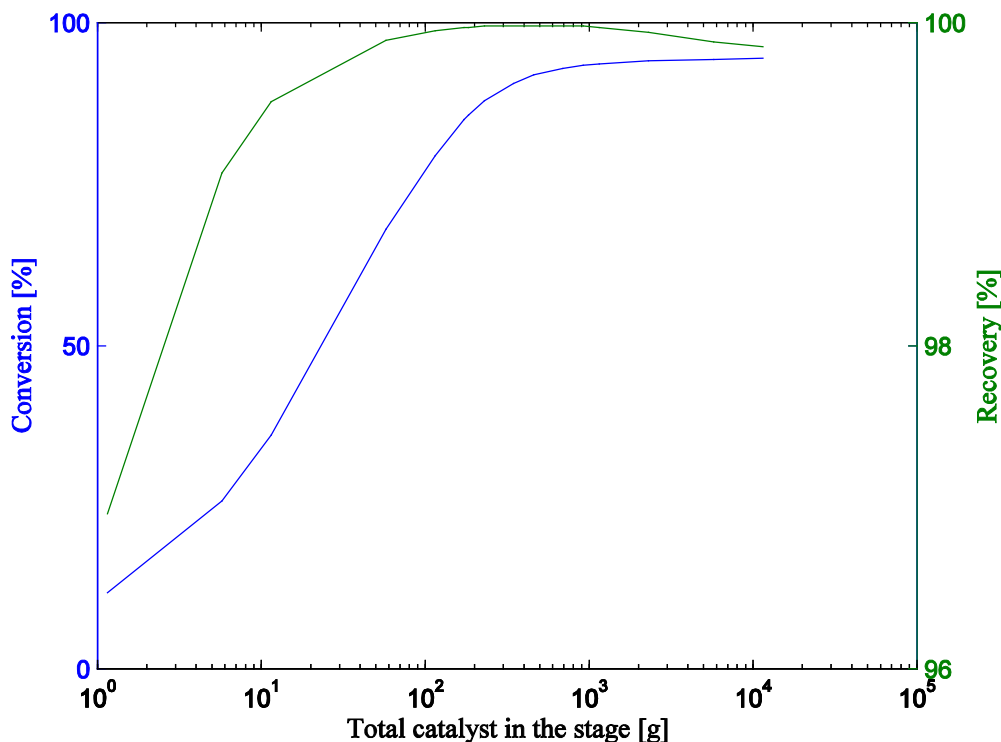
Figure 4-77: Behavior of the conversion and recovery percentage as a function of the amount of catalyst in the column.

2.4. Case 8: Column with two feed streams, catalyzed and auto-catalyzed reaction, 25 separating stages with enriching, extraction, reaction and stripping zones

The general configuration of this column is given in Figure 4.4 but in this case it was employed a catalyzed reaction in 8 out of 25 stages with 50 g of catalyst per stage, and also it was used auto-catalyzed reaction in the enriching, extraction and stripping zones, and the boiler and the condenser with a volumetric retention of 0.5 liters.

The enriching zone goes from stages 2 to 6, the extraction zone from stages 7 to 12, the reaction zone from stages 13 to 20 and the stripping zone from stages 21 to 24. In Table 4.20 is reported the kinetics used in every stage of the reactive distillation column for this case.

Table 4-20: Type of kinetics used in the reactive distillation column for Case 8.

Stage	Type of kinetics	Stage	Type of kinetics	Stage	Type of kinetics
1	Autocatalyzed	10	Autocatalyzed	19	Catalyzed
2	Autocatalyzed	11	Autocatalyzed	20	Catalyzed
3	Autocatalyzed	12	Autocatalyzed	21	Autocatalyzed
4	Autocatalyzed	13	Catalyzed	22	Autocatalyzed
5	Autocatalyzed	14	Catalyzed	23	Autocatalyzed
6	Autocatalyzed	15	Catalyzed	24	Autocatalyzed
7	Autocatalyzed	16	Catalyzed	25	Autocatalyzed
8	Autocatalyzed	17	Catalyzed		
9	Autocatalyzed	18	Catalyzed		

The following graphics show the temperature profiles, vapor and liquid phase composition profiles, and liquid and vapor flow profiles in the distillation column. The graphics were built using the data provided in Table 10.14 (Annex E).
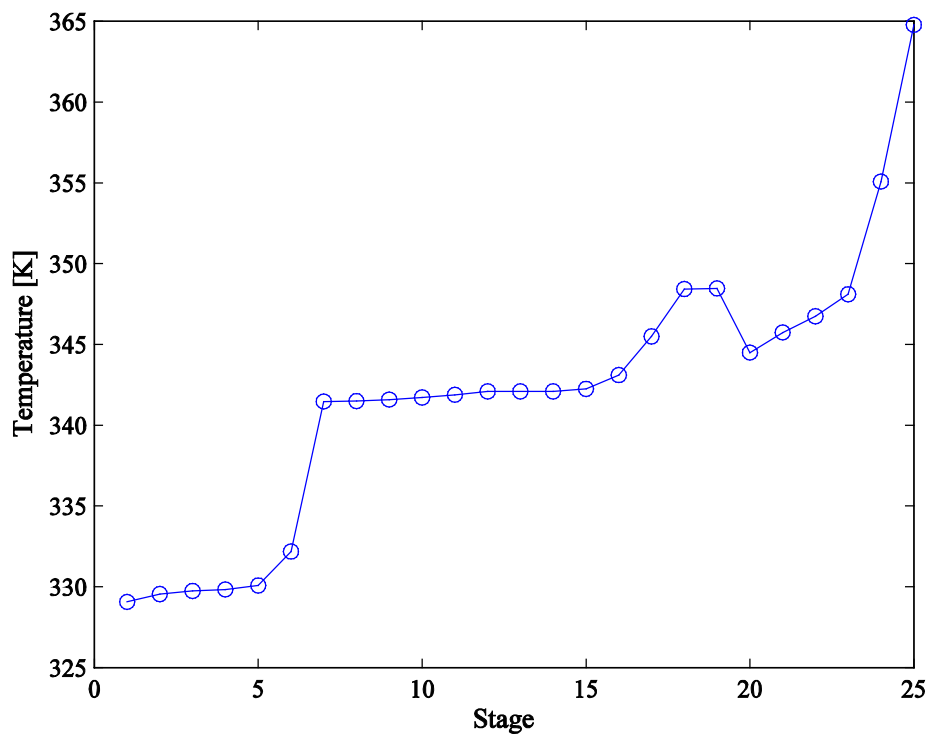
Figure 4-78: Temperature profile along the reactive distillation column for Case 8.
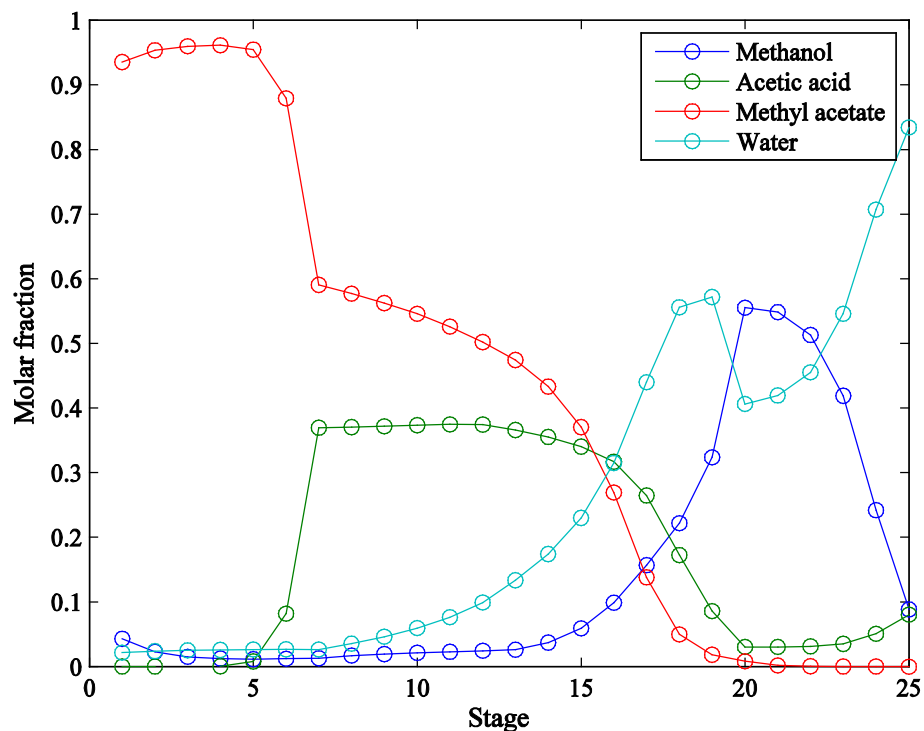
Figure 4-79: Liquid phase composition profiles along the column for Case 8.
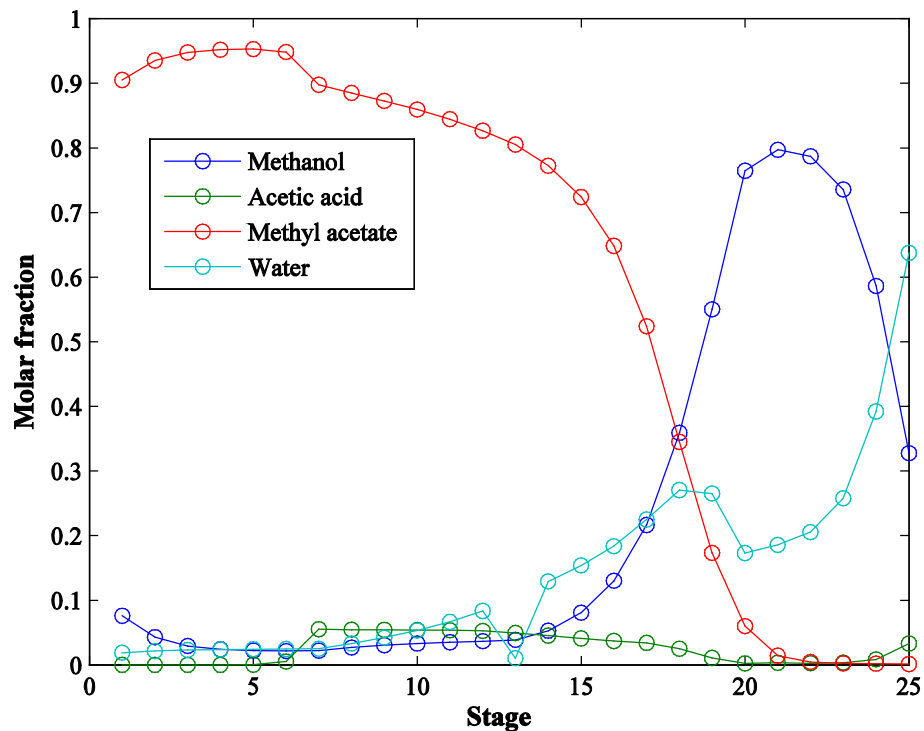
Figure 4-80: Vapor phase composition profiles along the column for Case 8.
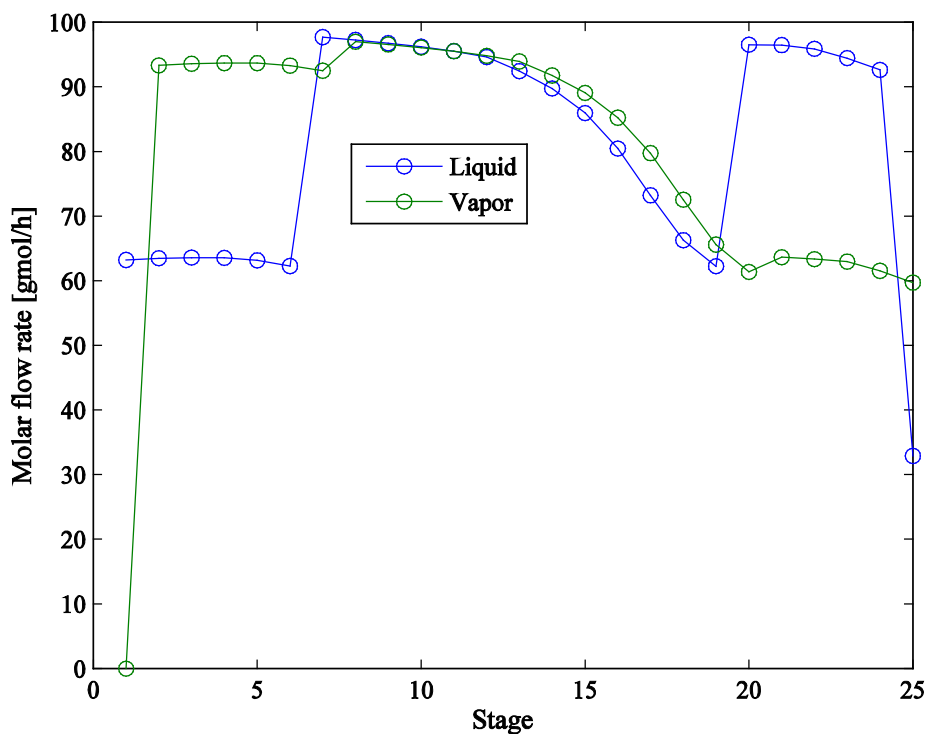
Figure 4-81: Liquid and vapor flow profiles along the column for Case 8.

Table 4-21: Summary of results obtained for Case 8.

Component	Molar fraction	
	Distillate	**Bottoms**
Methanol	0.0430	0.0836
Acetic acid	9.43E-08	0.0804
Methyl acetate	0.9353	5.05E-05
Water	2.17E-02	0.8359

Component	Flow rate [gmol/h]	
	Distillate	**Bottoms**
Methanol	1.30	2.75
Acetic acid	2.84E-06	2.65
Methyl acetate	28.15	1.63E-03
Water	6.52E-01	27.50
Total	30.10	32.90
Conversion		91.43%
Recovery		99.99%
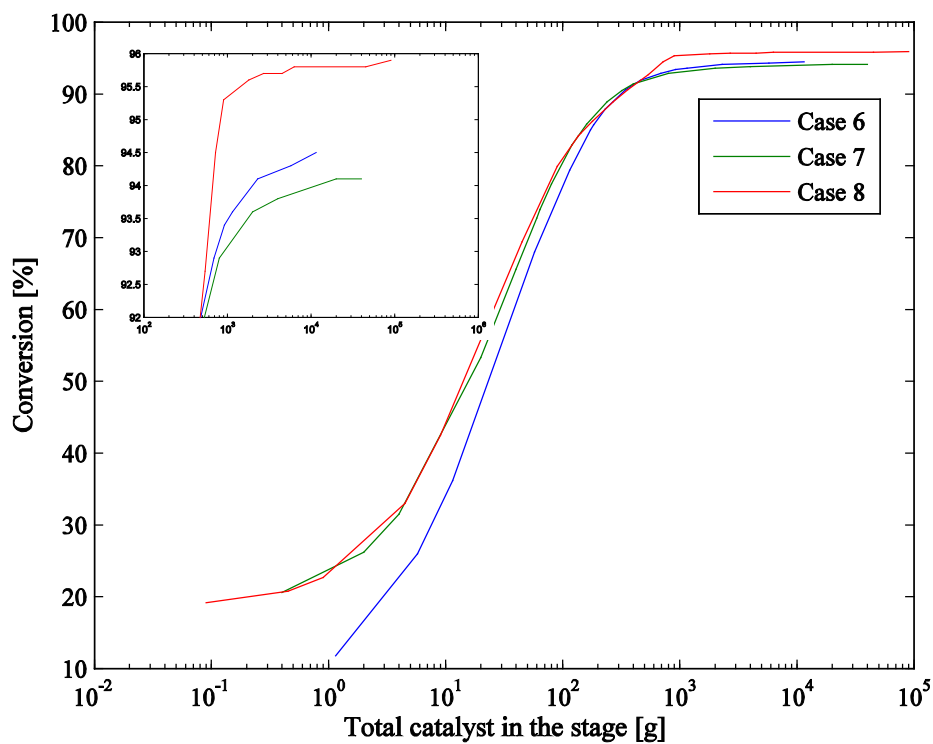
Figure 4-82: Comparison of the conversion percentages for Cases 6, 7 and 8.
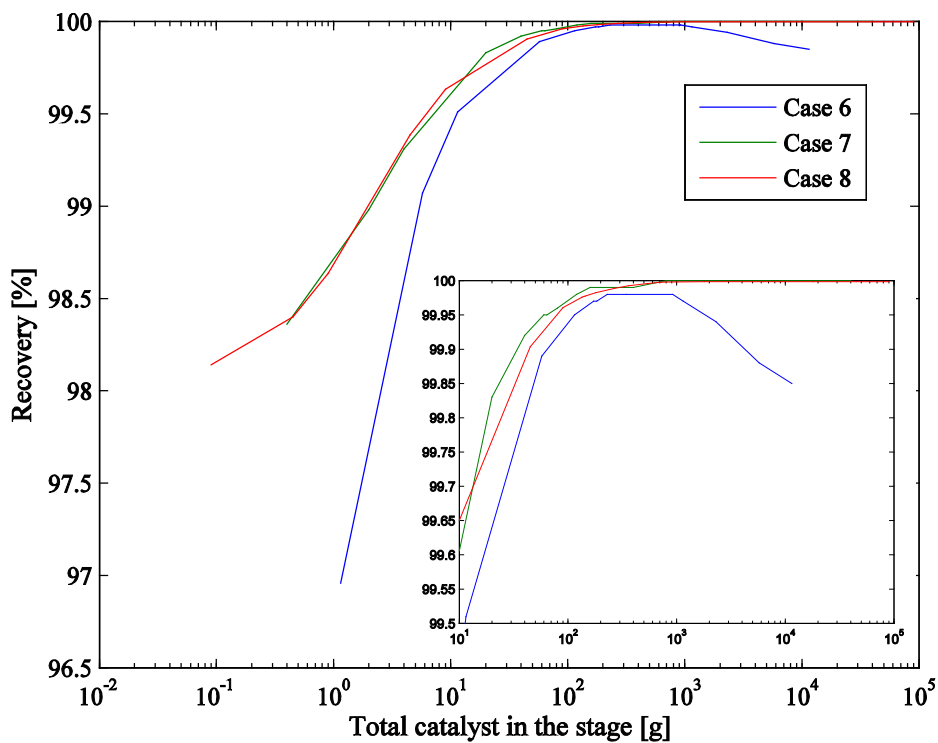
Figure 4-83: Comparison of the recovery percentages for Cases 6, 7 and 8.

There is a behavior in this case that has not been present in other configurations. The recovery percentage has an asymptote at an amount of catalyst greater than 1000 g, therefore it does not have a maximum value. In this way, it is demonstrate that an extraction zone (stages 6 to 12) is required in order to achieve an efficient separation. However, it is observed in Figure 4.82 that the conversion percentage in Case 8 reaches higher values at small amounts of catalyst that in Cases 6 and 7. By increasing the catalyst, these configurations reach better conversions than in Case 8. Information from Case 8 used in Figures 4.82 and 4.83 is presented in Table 10.15 (Annex E).

2.5. Case 9: Column with two feed streams, catalyzed and auto-catalyzed reaction, 35 separating stages with enriching, extraction, reaction and stripping zones

The general configuration of the reactive distillation column is given by Figure 4.84. The reaction zone is located from stages 13 to 30, from stages 1 to 6 the enriching zone, from stages 7 to 12 the extraction zone and from stages 31 to 35 the stripping zone. Stages 1 to 6 (enriching zone) have a volumetric retention of 0.2 liter, and stages 7 to 12 (extraction zone) and stages 31 to 35 (stripping zone) have a volumetric retention of 0.5 liters.
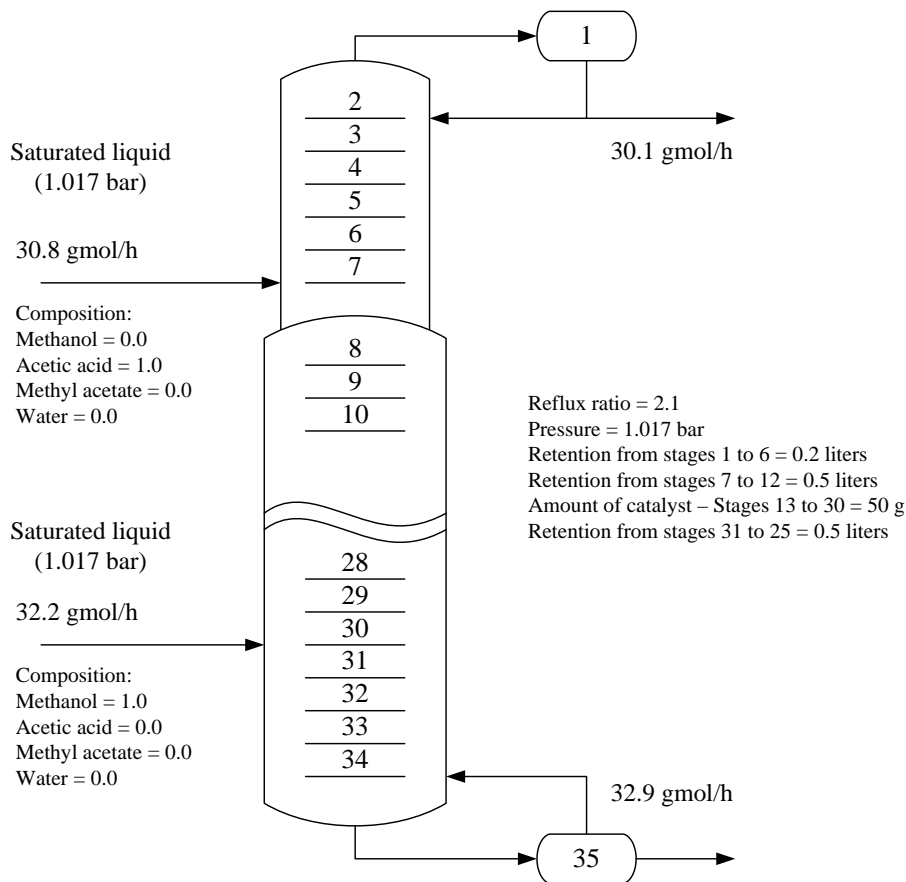
Figure 4-84: General configuration of the reactive distillation column for Case 9.

In Table 10.15 (Annex E), where are reported the data from Case 8, it can be seen that the reaction rates from stages 1 to 6 are negative, therefore in this zone of the column methyl acetate and water are reacting to form methanol and acetic acid. Thus, so as to increase the conversion, it was considered a lower volumetric retention for this enriching zone.

Another strategy that was applied to this case to improve conversion was to increase the number of stages where catalyst is present, having then 18 catalyzed stages in this case. Table4.22 shows the type of kinetics applied in every stage of the column.

Table 4-22: Type of kinetics used in the reactive distillation column for Case 9.

Stage	Type of kinetics	Stage	Type of kinetics	Stage	Type of kinetics
1	Autocatalyzed	13	Catalyzed	25	Catalyzed
2	Autocatalyzed	14	Catalyzed	26	Catalyzed
3	Autocatalyzed	15	Catalyzed	27	Catalyzed
4	Autocatalyzed	16	Catalyzed	28	Catalyzed
5	Autocatalyzed	17	Catalyzed	29	Catalyzed
6	Autocatalyzed	18	Catalyzed	30	Catalyzed
7	Autocatalyzed	19	Catalyzed	31	Autocatalyzed
8	Autocatalyzed	20	Catalyzed	32	Autocatalyzed
9	Autocatalyzed	21	Catalyzed	33	Autocatalyzed
10	Autocatalyzed	22	Catalyzed	34	Autocatalyzed
11	Autocatalyzed	23	Catalyzed	35	Autocatalyzed
12	Autocatalyzed	24	Catalyzed		

The following graphics show the temperature profiles, vapor and liquid phase composition profiles, and liquid and vapor flow profiles in the distillation column. The graphics were built using the data provided in Table 10.16 (Annex E).
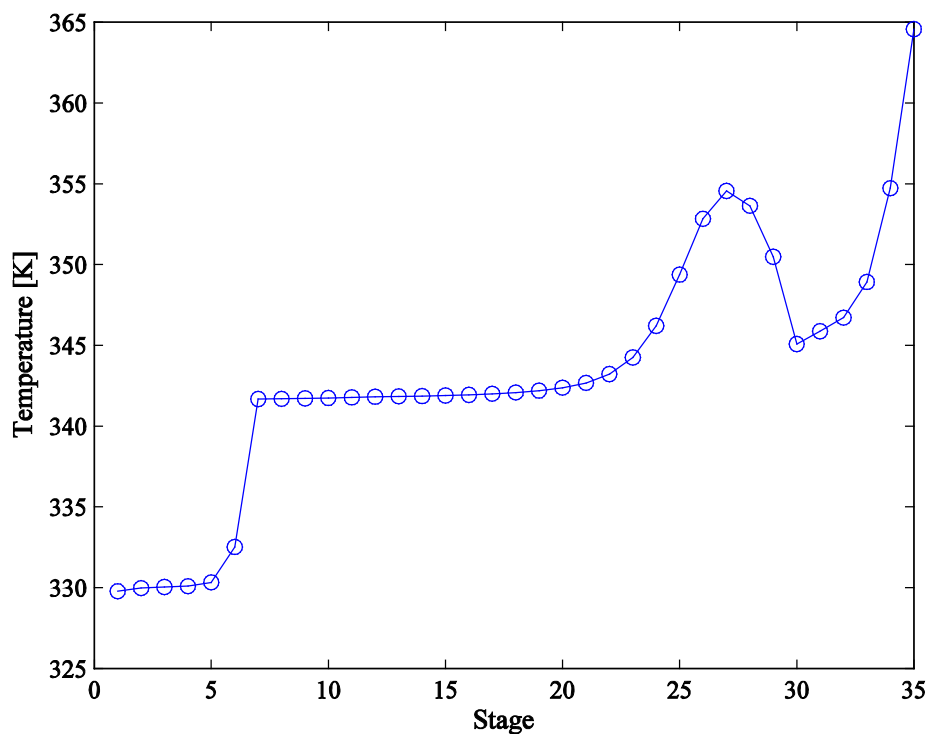
Figure 4-85: Temperature profile along the reactive distillation column for Case 9.
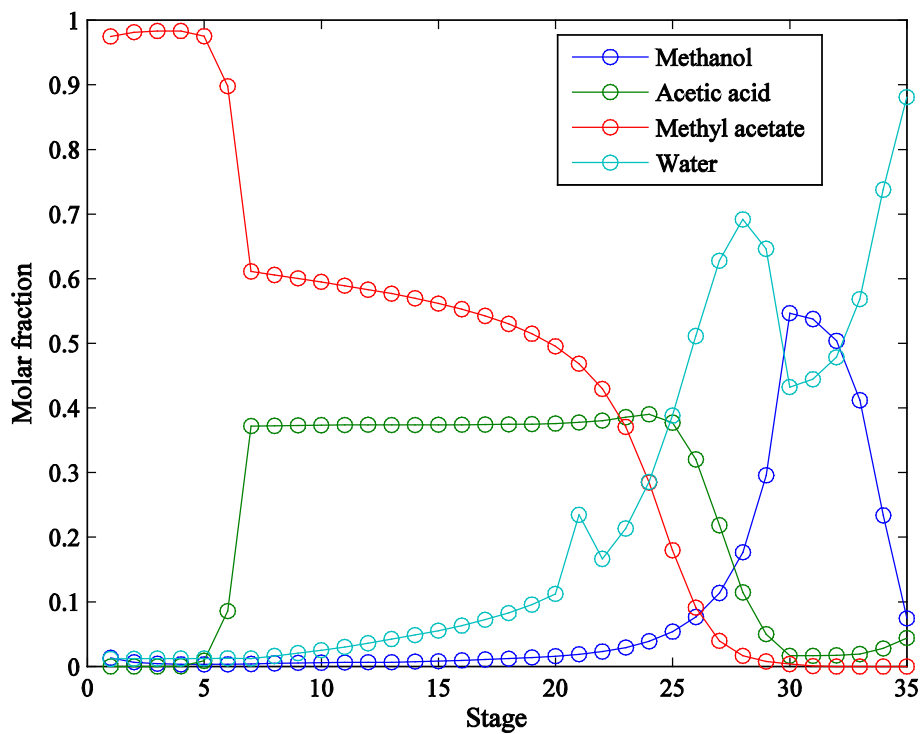
Figure 4-86: Liquid phase composition profiles along the column for Case 9.
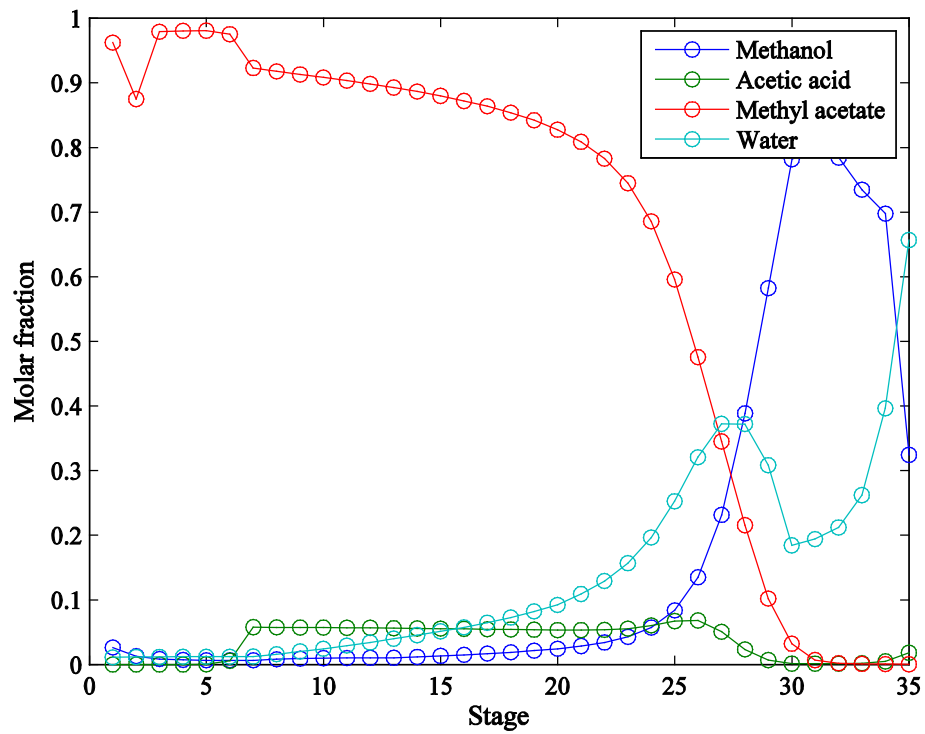
Figure 4-87: Vapor phase composition profiles along the column for Case 9.
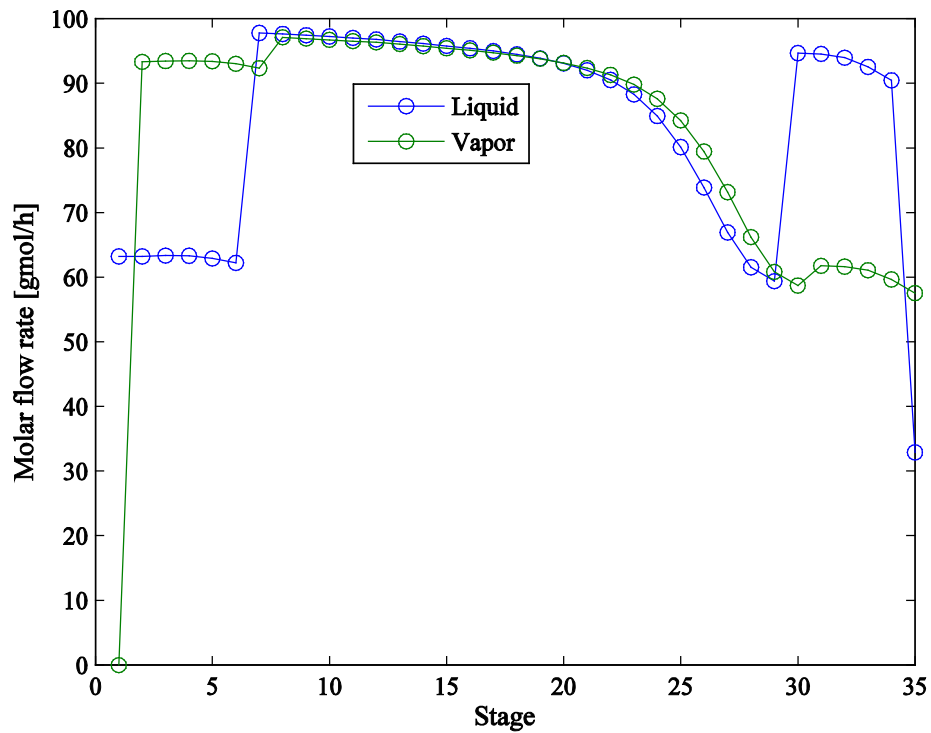
Figure 4-88: Liquid and vapor flow profiles along the column for Case 9.

Table 4-23: Summary of results obtained for Case 9.

Component	Molar fraction	
	Distillate	**Bottoms**
Methanol	0.0134	0.0746
Acetic acid	1.3E-07	0.0443
Methyl acetate	0.9748	1.6E-05
Water	1.2E-02	0.8811

Component	Flow rate [gmol/h]	
	Distillate	**Bottoms**
Methanol	0.40	2.45
Acetic acid	3.9E-06	1.46
Methyl acetate	29.34	0.00
Water	3.6E-01	28.99
Total	30.10	32.90
Conversion		95.42%
Recovery		99.99%
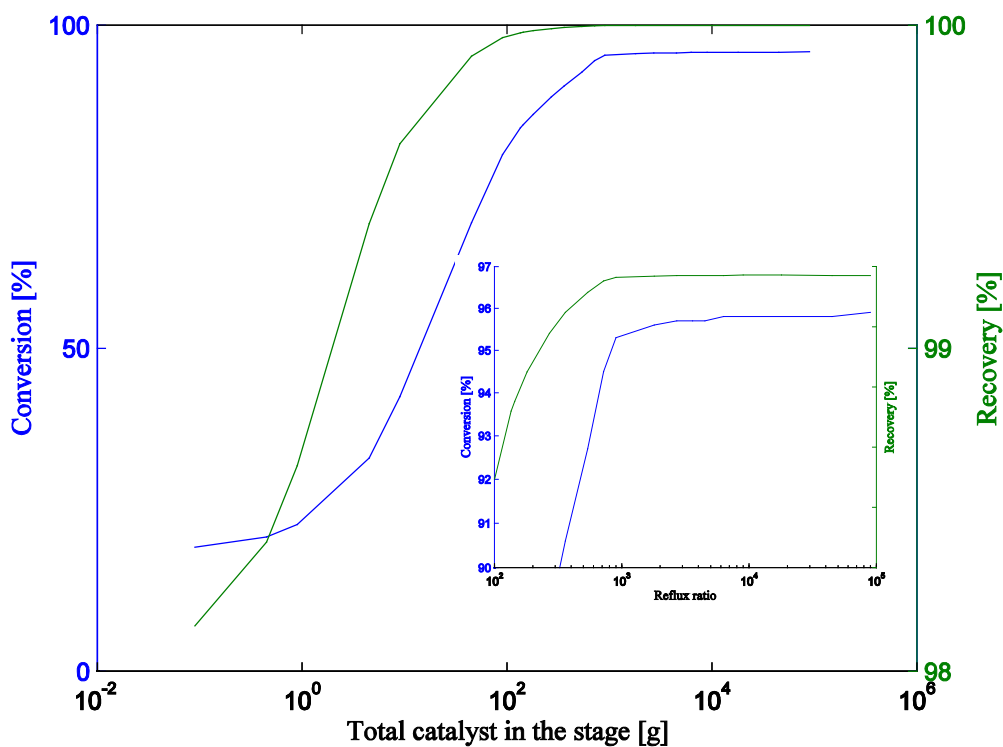
Figure 4-89: Behavior of conversion and recovery percentage as a function of the total amount of catalyst in the column.

The summary of results in Table 4.23 shows that this configuration has a higher conversion than in previous cases, also the recovery indicates that almost all the methyl acetate produced in the reactive process leaves the column as top product.

Graphic Figure 4.89 is based on the data reported in Table 10.17 (Annex E). According to this graphic it is possible to see that both conversion and recovery percentages grow fast when the amount of catalyst is below 1000 g, however when the amount of catalyst is over 1000g there is not a significant increase in them.

Case 9 is applied at an industrial scale because in the middle section of the column the reaction takes place and in the upper and lower sections the separation happens. In general, this scheme is more efficient to produce methyl acetate by reactive distillation. This process is limited by the thermodynamic constraints imposed by the binary azeotrope (methyl acetate – methanol) in the upper section of the column. As demonstrated in the studied cases, the reaction without catalyst is pretty small, so when the upper section of the column does not have catalyst it behaves like an extractive – enriching zone due to the presence of acetic acid. Thus, in distillation columns with a single feed it is not possible to reach conversions higher than 80% despite the use of high volumetric retentions or huge amounts of catalyst. Thereby, the acetic acid located in the upper section of the column reacts with the methanol, breaking the methyl acetate - methanol azeotrope so as to obtain distillates with a minimum concentration of methanol.

Table 4.24 shows the final concentration (mass fraction) for Case 9:

Table 4-24: Compositions obtained for Case 9.

Component	Mass fraction	
	Distillate	Bottoms
Methanol	0.0059	0.1143
Acetic acid	0	0.1271
Methyl acetate	0.9912	0.01
Water	0.0029	0.7586

According to Table 4.24 a final composition of 99% of methyl acetate in the flow of distillate was obtained in this case, achieving also an almost complete separation between the products of reaction (methyl acetate and water).

4.4. Comparison of the results obtained under finite reflux

In Figure 4.90 are presented the liquid phase composition profiles obtained which were calculated under finite efficiency using a non-equilibrium model. In order to compare the results evaluated under ∞/∞ conditions using an equilibrium model please see Figure 4.44.
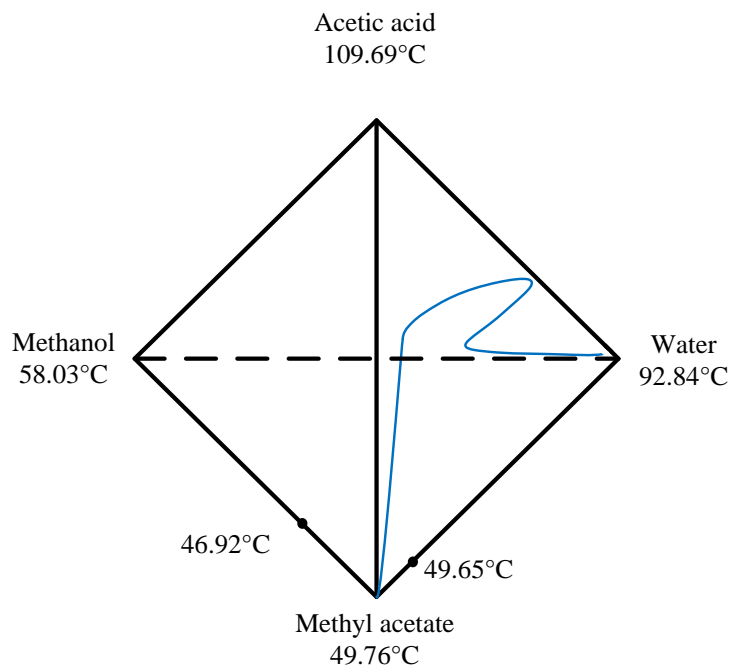
Figure 4-90: Liquid phase composition profiles under finite efficiency.

The general configuration of the reactive distillation column in given in Figure 4.91. The reaction zone is located from stage 13 to 30, from stage 1 to 6 the enriching zone, from stage 7 to 12 the extraction zone and from stage 31 to 35 the stripping zone.

As can be seen in both diagrams there is a qualitative similarity between composition profiles for both conditions. There are some differences in the behavior of these paths due to the nature of the equilibrium models used to calculate them. With regard to the final configuration of the column, the different reaction and separation zones presented in the final results of both studies show similarity to as the location of the feeding zone of the reactants.

The qualitative similarity between the two methods, can give more validity to the procedure and analysis employed in this work. As it has been proposed, the formulation and application of a short-cut method requires the validity of the result obtained from the simulation.
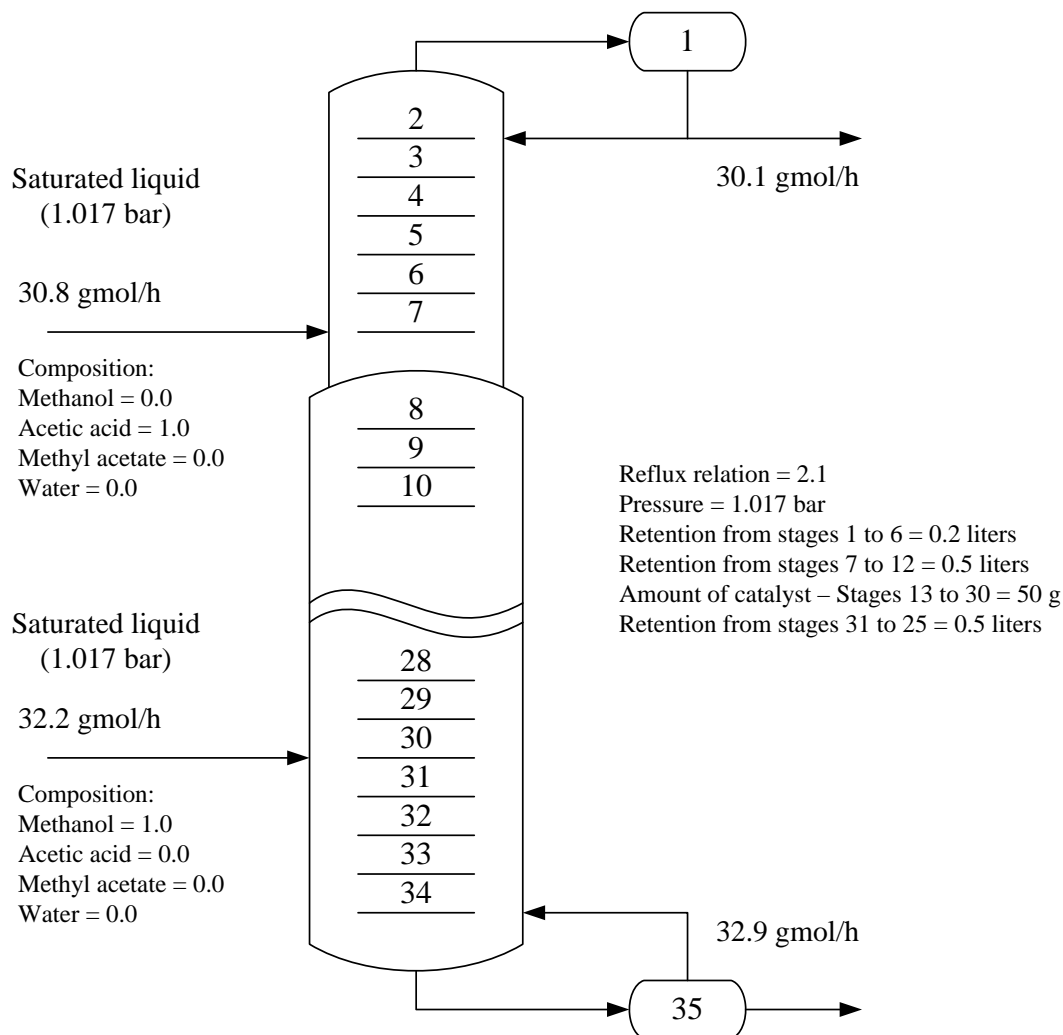
Figure 4-91: General configuration of the reactive distillation column under finite conditions.

On the other hand, it should be noted the importance in the use of short-cut methods for determining the practical feasibility of a process, since this type of methodology only requires minimal information and time spent in its development is the bare minimum, contrary to what happens when the implementation of a process is performed directly by the simulation of it, requiring then more work and time. As well, it is noteworthy that these short-cut methods can be employed as initial steps in process simulation.

5. Results – Generation of optimal for the downstream processing of the ABE fermentation.

5.1. ABE Fermentation

Fermentation

Corn is first steeped in water until its kernels attain certain moisture content. The softened corn kernels are subsequently milled to yield corn endosperm for the fermentation. The endosperm is enzymatically hydrolyzed to solubilize the starch to hydrolyzate. The fermentation is carried out in 4 stages. Then, fresh water and corn steep liquor are mixed with a percentage of the hydrolyzate, and fed to the first stage of the fermenters in series. The lasting fraction of the hydrolyzate is mixed again with water, stillage, and corn steep liquor and fed to the next phase of the fermentation. The strain of bacteria used in the fermentation is the improved strain of *Clostridium Acetobutylicum*. In the initial fermentation stage there is an inoculum or seed step where bacteria grow at measured conditions to have a good assimilation of the carbohydrates, small residence time, and an undesired production of solvent. The second and third stages are also continuous fermentation stages where the carbohydrate-rich media and organic acids are transformed into butanol, ethanol and acetone. The fourth stage is a batch storage stage consisting of a set of storage tanks where the residual carbohydrates are spent to produce a solvent maximizing then its conversion. The completed fermentation broth contains butanol (1.5% weight), acetone (0.6% weight), ethanol (0.2% weight), acetic acid (0.18% weight), and butyric acid (0.08% weight). This fermentation broth is constantly treated for product recovery. The major chemical reactions involved in the fermentation process are as follows.

Chemistry of starch hydrolysis:

$$-\left(C_6H_{10}O_5\right)_n - \left(\text{Starch}\right) + nH_2O \xrightarrow{\textit{Enzyme}} nC_6H_{12}O_6\left(\text{Glucose}\right)$$
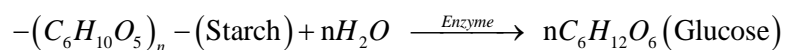
Chemistry of fermentation: anaerobic; microorganism *Clostridium beijerinckii*:

$$C_6H_{12}O_6 + H_2O \rightleftharpoons 2C3H6O \text{ (Acetone)} + 3CO_2 + 4H_2$$

$$C_6H_{12}O_6 \rightleftharpoons C_4H_{10}O \text{ (Butanol)} + 2CO_2 + H_2O$$

$$C_6H_{12}O_6 \rightleftharpoons 2C_2H_5O \text{ (Ethanol)} + 2CO_2 + H_2$$
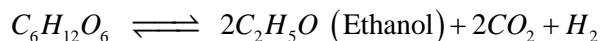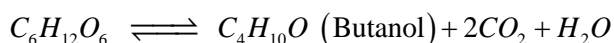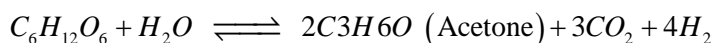
Downstream processing

The components leaving the fermenters are purified in the downstream processing section of the process.

– Feed

The stream to be fed to the separation processes is the fermentation broth which includes a liquid phase where the remaining solids of corn are suspended. This phase is composed by butanol, ethanol, acetone, and organics acids such as butyric acid and acetic acid. Throughout the downstream processing, these organic acids are transformed into ethanol and butanol, respectively.

– Processing

The fermentation broth is heated in a heat exchanger and then is fed to the gas stripper and the extractor. In the gas stripper the mixture composed by butanol, acetone, and ethanol is stripped to the top of this unit having them as a top product or "distillate" whit a composition of 36% weight of butanol, 14% weight of acetone, 3% of ethanol, and 47% weight of water. The stream that leaves the unit as bottoms is composed by a mixture of insoluble protein, fiber, cells from the fermentation broth, and organic acids like acetic and butyric acid; The bottoms can be re-processed separately using centrifuges, evaporators and dryers, in order to obtain dry distiller's dried grains (DDG) that can be sold as fertilizer or food for animals. The resulting distillate is exposed to a sequence of separation tasks with different arrangements of operating units, mostly distillation columns, of diverse kinds. In the hypothetical case the broth that leaves the fermentation is fed to an extractor rather than to the gas stripper using X as entrainer, it is possible to extract butanol, ethanol, acetone, and organic acids like butyric acid and acetic acid, into the extract phase. The extract phase, comprising 98.3% weight of entrainer and the butanol, ethanol and acetone, is subjected them to a sequence of separation tasks with different arrangements of operating units such as gas stripping, extraction and distillation. The raffinate phase comprising a 99.6% weight of water and solids in suspension is treated as waste and is sent to a waste treatment system or reprocessed to produce the dry

distiller's grains. Hence, it is not included in the design of the consequent separation task; logically, it has no effect on the assessment of the downstream processing flowsheets.

– **Products to be obtained**

The downstream processing has butanol, ethanol and acetone as main yields. Though the desired product is butanol, ethanol and acetone are high-priced products as well.

5.2. Application of the method

The following steps are required so as to apply the methodology to design the separation scheme of the ABE fermentation.

1. Identification of the components present in the process

Fermentation broth is the mixture to be treated in the downstream section of the flowsheet. Pure butanol, ethanol, acetone and water (W) are the products to be considered. Intermediate materials are all other compounds necessary to perform the downstream processing.

2. Selection of unit operations in downstream processing

The selection of the right operating units is crucial to generate flowsheets. To generate a group of optimal and near-optimal structures, it is necessary to clearly identify to the maximum detail all the processing units required to carry out the process. The operating units required to separate the mixture can be proposed by heuristical or theoretical methods coupling them in order to add rigorous criteria to the design. As pointed in the previous segment of this chapter, only conventional operating units such gas stripping, extraction and distillation are considered to perform this analysis.

– **Gas Stripping**

Gas stripping is considered as a flash distillation which efficiently acts as a way to remove a component or components if the volatilities of these components are considerably dissimilar from the volatilities of the other components. Water (W) and the solids of corn represent the 98% weight of the fermentation broth; therefore, it is coherent to separate the water and the solids from the broth by gas stripping. The gas stripping employed for this is labeled "Gas Stripper G1" and uses a stripper. The solids and the remaining water leave

the gas stripper as a bottoms stream for additional processing to obtain Dried Distiller's Grains. On the other hand, the chosen products to be separated - butanol, ethanol and acetone- are stripped and obtained as a top product stream. This stream has a composition of 36% weight % of butanol, 3% weight of ethanol, 14% weight of acetone and 47% weight of water. It must be pointed out that the mixture water - ethanol and water - butanol form azeotropes, so, with regard to obtain pure components and a full separation of them, it is necessary to include an azeotropic distillation.

– **Extraction**

An extraction can be used starting the downstream processing to separate small solid particles which remain in suspension in water coming out the fermentation broth; this operating unit requires an extractor and is labeled as "Extractor E1". Then, by using 2-ethyl-1-hexanol (X) as entrainer it is possible to remove a significant quantity of the desired products – butanol, ethanol and acetone – originated at the fermenter into the extract stream, thus having a raffinate stream composed by water and suspended solids, and traces of butanol, ethanol and acetone. Additionally, there are no azeotropes in this phase (44); hence, conventional distillation is enough to separate these components.

– **Distillation**

The components considered in the downstream processing can be separated by conventional distillation or by complex configurations. There are two binary azeotropes ethanol – water and water – butanol in the resulting mixture, so thermodynamic information is required to select a realistic distillation scheme for separating these azeotropes. In this sense, it is proposed an Azeotropic Distillation Unit A1 to separate the mixture ethanol – water - butanol into their pure components. Also, an Azeotropic Distillation Unit A2 is proposed to separate the mixture water – butanol into their pure components.

Table 5.1 summarizes the units selected in the previous analysis. In total, there are 22 operating units comprising 33 processing subunits. Hydrolysis and fermentation were not taken into account in the design of the flowsheet. However, the units to carry out the hydrolysis (Hydrolysis Reactor H1) and fermentation (Fermenter 1) were incorporated in the analysis for handiness. The economic evaluation of these units was performed following a simulation procedure on the commercial software Aspen Plus®. These costs are also presented in Table 5.1.

Table 5-1: Operating units and their associated costs.

	Operating units		Cost			
#	# Subunit	Designation of equipment	Capital (10^3 US$)	Annualized capital (10^3 US$/year)	Operating (10^3 US$/year)	Total (10^3 US$/year)
1		H-1				
2		F-1				
3		G-1	2180	727	871	1598
4		D-1	2088	696	973	1569
5		A-1	49653	16551	218800	235351
6		D-2	2294	765	891	1656
7		D-3	1831	610	864	1474
8		A-2	19681	6620	87520	94140
9		E-1	1189	396	5231	5627
10		S-1	1914	638	864	1502
11	11-1	D-5	2392	797	902	1699
	11-2	D-6	2058	686	873	1559
12	12-1	D-7	1684	561	852	1413
	12-2	D-8	2275	758	892	1650
13	13-1, 13-2	D-9, D-10	6684	2228	2666	4894
14	14-1, 14-2	D-11, D-12	6301	2100	2513	4613
15		D-13	6079	2026	2415	1451
16		D-14	6412	2137	2558	1695
17	17-1, 17-2	D-15, D-16	6862	2287	2737	5024
18	18-1, 18-2	D-17, D-18	6746	249	2691	4940
19	19-1, 19-2	D-19, D-20	8068	2689	3218	5907
20	20-1, 20-2	D-21, D-22	314	1041	1246	2287
21	21-1, 21-2	D-25, D-26	4210	1403	1679	3082
22	22-1, 22-2, 22-3	D-27, D-28, D-29	4156	1385	1658	3043

3. P-Graph representation of the process

All operating units are symbolized as a conventional diagram with the corresponding process graph. The process graphs illustrations of the units are the most important requirement to perform the algorithms MSG and ABB described in the methodology. The optimal and near-optimal structures are evaluated from the full structure or the alleged maximal flowsheet, by the employment of the algorithm ABB.

– **Generation of the complete flowsheet**

The algorithm MSG is used in this step to build the maximal flowsheet containing all the specification for the materials and the 20 operating units established in the second step. The complete flowsheet equivalent to the comprehensive structure is shown in Figures 5.1 and 5.2. The maximal structure includes all possible conventional units necessary to separate the mixture.
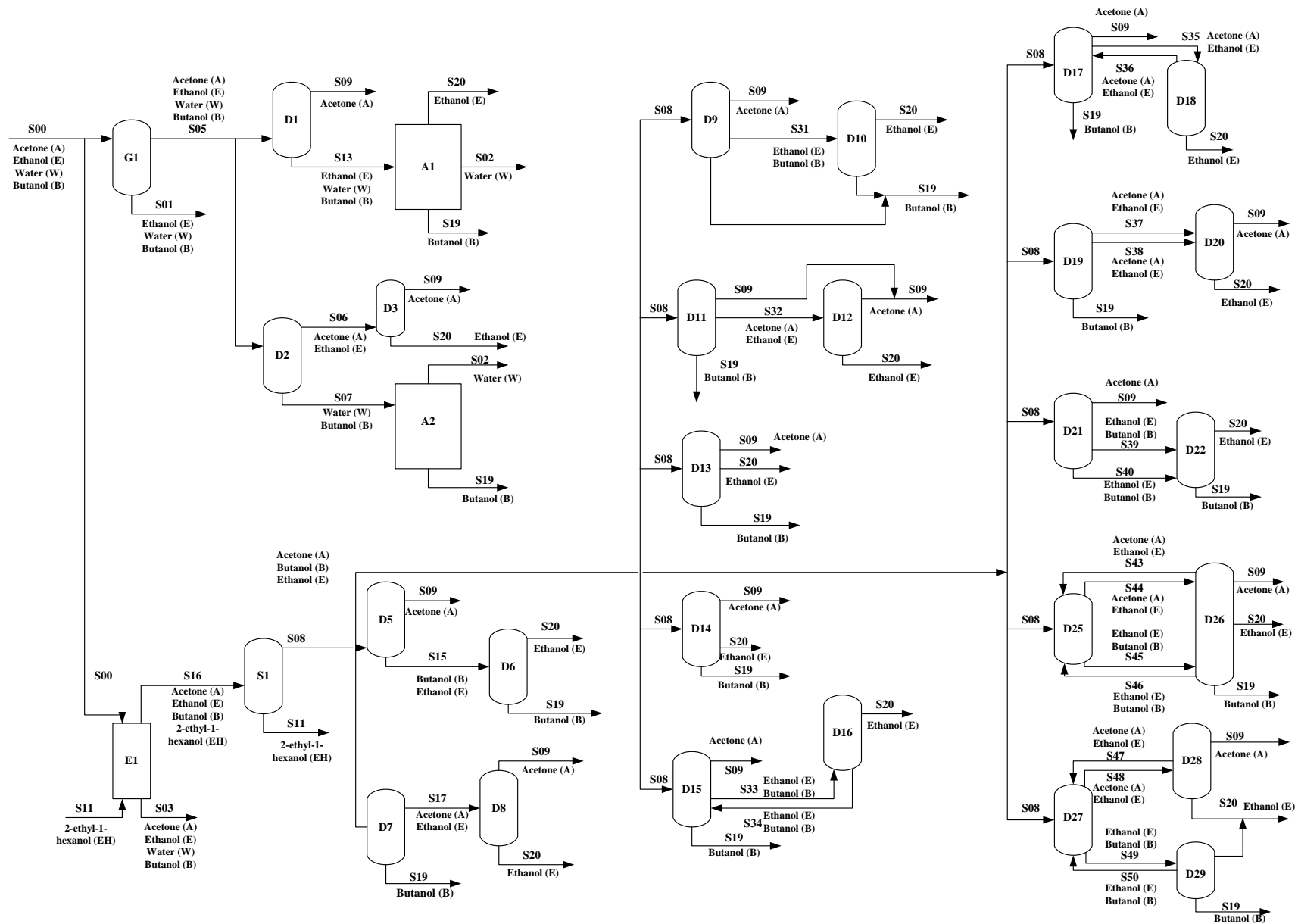
Figure 5-1: Conventional representation of the ABE fermentation corresponding to the maximal flowsheet.
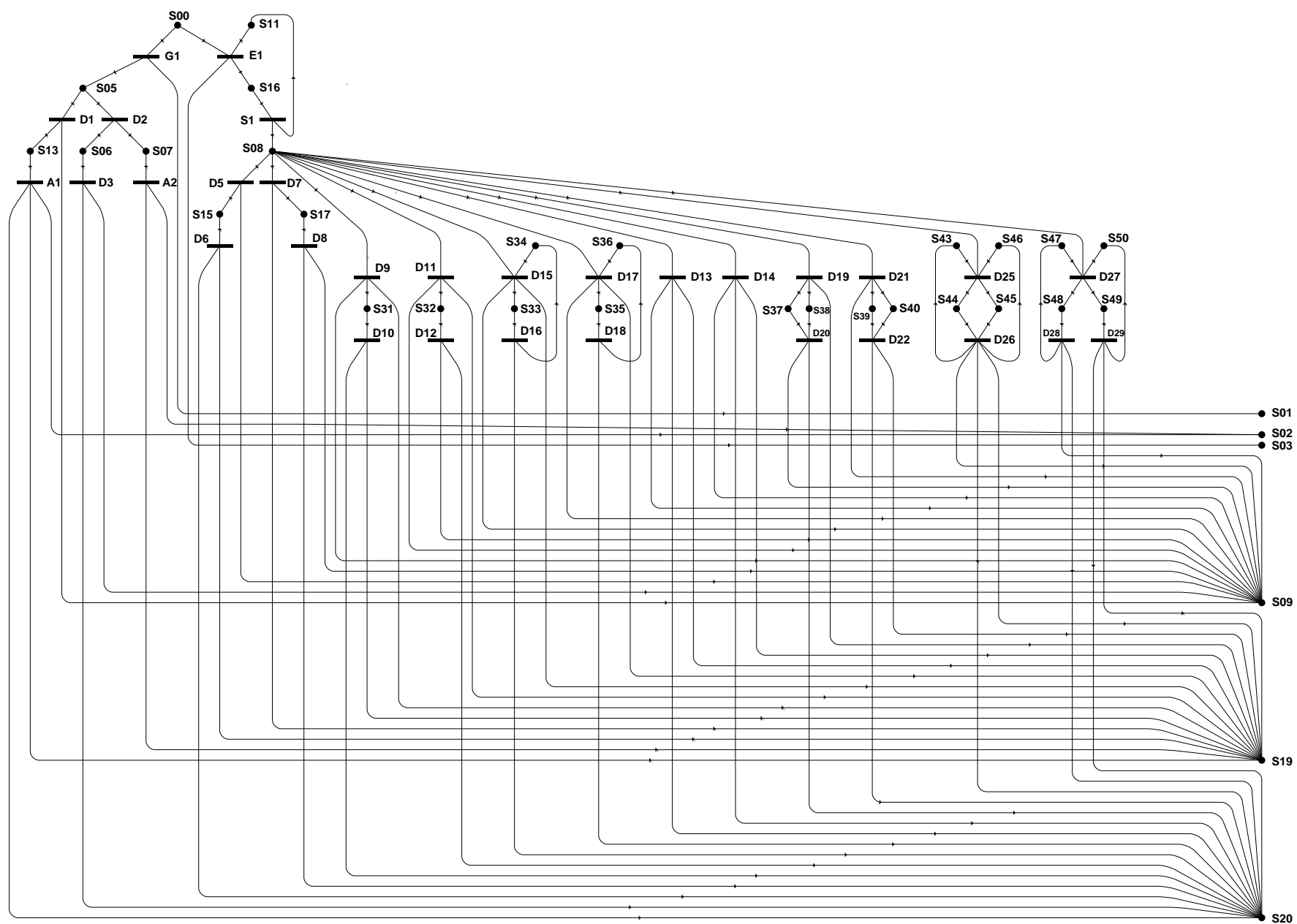
Figure 5-2: Process graph representation of the ABE fermentation corresponding to the maximal flowsheet.

In Figures 5.1 and 5.2 *G* represents the gas stripper, *E* the extractor, *D* the distillation columns and *S* the streams.

The final product (butanol) or Stream *S09* can be produced exclusively by one of the operating units *D-1, D-3, D-5, D-8, D-9, D-11, D-13, D-14, D-15, D-17, D-19, D-21, D-26*, and *D-28*. After selecting any of these operating units for the production of *S09*, no further decision is needed. For example, if it is decided to produce stream *S09* by operating unit *D1*, operating unit *G1* is automatically included as the only candidate for producing material S05 consumed by *D1*. According to the mutual exclusions, operating units, *D2* and *E1* are excluded. This, in turn, leads to the exclusion of all other operating units except operating units *D1, G1*, and *A1*. At this critical operating unit A1 is included as the only candidate for producing final products *S19* and *S2*0. As a result, the feasible structure including operating units *A1, D1*, and *G1* was generated.

The flowsheet generated from the maximal structure is void of splitting and merging of the material streams. This implies that a stream at any point in the flowsheet would be processed only by a single operating unit. This is in accord with a well-known structural feature of a downstream processing system. Such a structural feature is attributable to the production of pure products.

4. Generation of optimal structures

Objective function

To determine the cost of a structure it must be minimized an objective function that can be estimated as the overall value of the investment and running costs for all the units in the separation scheme. The costs of adding pipes, pumps or compressors to the operating units in all the structures can be ignored in this analysis. The investment cost of a unit t is the amount of money necessary for acquiring and setting up such unit or subunit in the network. The running cost of a unit comprises some other annual costs like payments for labors and administration, and costs for acquiring raw materials and services such as vapor and gas. In case the extractor is included in the structure, it must also be considered the costs of purchasing the entrainer.

5. Costs estimation

The strategy to design a chemical process is regularly performed in phases, starting from the least detailed to the most rigorous with their associated economic evaluations. The process flowsheet synthesis approach represents the first phase of design where a basic process engineering method is made by filtering a huge number of process options.

The economic evaluation was performed based on the simulation created to obtain 200 million pounds of butanol per year as main product, working 325 days and handling purities of 99.9% weight of butanol, 99.6% weight of ethanol and 99.9% weight of acetone. The value of an operating unit is assessed by two methods that can be founded on simulation and heuristics. The use of each method depends on the accessibility of data or the nature of the process. If there is not enough data to perform the heuristics-based method, a simulation must be performed using the commercial packages Aspen Plus and Aspen Economic Evaluator.

The simulation-based method to evaluate the capital and operating costs was used for the following operating units: gas stripper 3 (G1); distillation column 4 (D1); distillation column 6 (D2); distillation column (D3); extractor 10 (S1); unit 11, counting distillation column 11-1 (D5) and distillation column 11-2 (D6); and unit 12, including distillation column 12-1 (D7) and distillation column 12-2 (D8). In the simulations on Aspen Plus, there must be specified some conditions of the feed like the feed flow, concentration, temperature, and pressure; the compositions of the light and heavy key components in the distillation columns; and design condition of the distillation columns as reflux ratio or the number of stages. The units are simulated on Aspen Plus to calculate the mass and heat balances, and hence the energy consumption and the size of the equipment. The data obtained from the simulation are the entered into Aspen Economic Evaluator to estimate the operating cost and the investment cost. Hence, the minimized objective function is obtained by iterating the sizing and costing simulations and establishing trade-offs between the operating and the capital costs.

The heuristics-based method to evaluate the capital and operating costs was used for the following operating units: Group a) azeotropic distillation column 8 (A2); azeotropic distillation column 5 (A1); extractor 9 (E1); Group b) units 13, including distillation column 13-1 (D9) and distillation column 13-2 (D10); units 14, including distillation column 14-1 (D11) and distillation column 14-2 (D12); distillation column 15 (D13); distillation column 16 (D14); unit 17, including distillation column 17-1 (D15) and distillation column 17-2 (D16); unit 18, including distillation column 18-1 (D17) and distillation column 18-2 (D18); unit 19, including distillation column 19-1 (D19) and distillation column 19-2 (D20); unit 20, including distillation column 20-1 (D21) and distillation column 20-2 (D22); unit 21, including distillation column 21-1 (D25) and distillation column 21-2 (D26); and unit 22, including distillation column 22-1 (D27), distillation column 22-2 (D28), and distillation column 22-3 (D29).

The units included in group (a) are commonly used and well understood; therefore the existing data for these units can be independently calculated. In the case of the units of group b), the existing data for calculating the costs of units are the cost scaling factors dependent on the cost of a "reference" unit. The cost of a unit is calculated by multiplying the cost of that selected unit by the cost scaling factor. It was proposed the conventional-direct scheme of distillation columns 11, comprising 11-1 (D5) and 11-2 (D6), as the "reference" unit to estimate the other costs based on this "reference" unit. The cost information and their calculation approaches are presented in the above presented Table 5.1.

Generation of Optimal Flowsheets

The set of optimal flowsheets contained in the maximal structure are input into software to carry out the algorithm ABB. The list is renewed every time iteration in the maximal structure takes place. If the total cost of a flowsheet is higher than one of the optimal flowsheets already calculated to that point, the flowsheet will not branch further. The corresponding optimal flowsheet is presented in Figure 5.3.
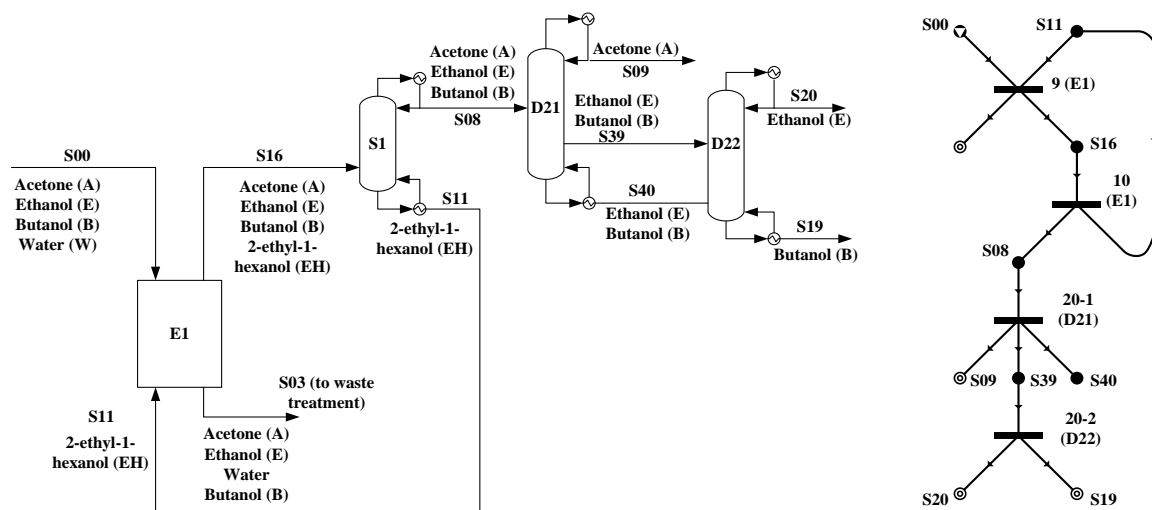
Figure 5-3: Ordinary and process graph representations of the optimal flowsheet.

Efficacy of Methodology

The methodology applied to find optimal and near-optimal separation flowsheets is capable of creating a huge amount of flowsheets optimizing them following an economic criterion and some rules established by the graph-theory and by the application of a polynomial algorithm which helped to find a superstructure comprising all the process alternatives. This superstructure encloses

all the combinatorially possible flowsheets with the operating units previously established for the original process leading to a huge reduction in the exploration for possible flowsheets. The later suggests that finding all achievable flowsheets among all the combinatorially feasible networks is a challenging task.

Evaluation of Flowsheets

In Table 5.2 are listed the best flowsheets generated using the total costs as the condition to rank them in ascendant order. It shows that usually the inclusion of an extractor removes the requirement of a stripper and azeotropic distillation comprising the optimal flowsheets. The azeotropic distillation is not included in the ranking due to its associated costs.

Table 5-2: Optimal flowsheets obtained by the application of the algorithms.

Flowsheet	Operating units	Cost (1000 US$/year)
1	E1, S1, D21-D22,	9416
2	E1, S1, D27-D29	10172
3	E1, S1, D7, D8	10192
4	E1, S1, D25-D26	10211
5	E1, S1, D5, D6	10387
6	E1, S1, D13	11580
7	E1, S1, D11-D12	11742
8	E1, S1, D14	11824
9	E1, S1, D9-10	12023
10	E1, S1, D17-D18	12069

Figure 5.4 compares the costs of the resultant optimal estructures.
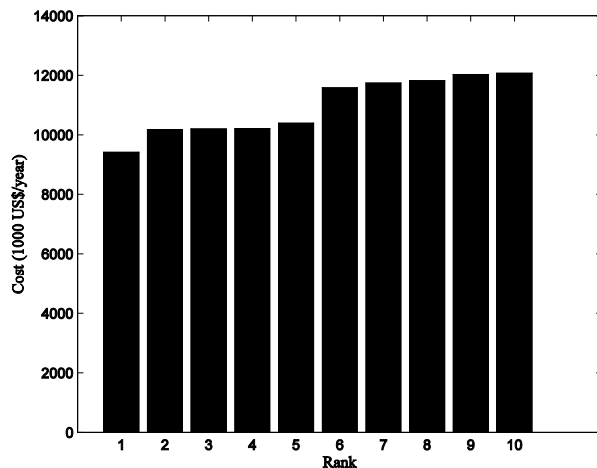
Figure 5-4: Comparisson between the optimal flowsheets.

The optimal flowsheet is remarkably cheaper than the others. It can be also observed in Table 5.2 that the variances in the costs of the structures can be endorsed to the changes in the schemes of distillation after the extraction and the gas stripping. The best structure is composed by an extractor E1, a stripper S1, and two complex-direct distillation columns D21 and D22. The total cost of the optimal downstream processing is, in turn, US$756x10^3 (7%) and US$776x10^3 (8%) less than the second and third optimal structure. These distillation columns in these structures are considered complex-Petlyuk and simple-indirect, correspondingly. These two schemes were synthetized using the heuristics-based method, indicating then the significance of heuristics in Chemical Process Engineering and its application on re-designing mature and full developed technologies.

6. Concluding remarks

The use of applied thermodynamics outlined in this work is designed to provide a macroscopic treatment of the subject in which the physical concepts and laws are clearly delineated and set in a simple mathematical structure. The theory is such that all the concepts and statements used could initially be demonstrated directly by observation and experimentation. It is also intended to be logically rigorous, although complete rigor cannot be attempted in this short exposition.

Process Engineering is a crucial empowering methodology to synthetize, design, calculate, rate and optimize chemical and biotechnological processes. Process modeling is very dependent on precise characterization of the thermodynamic properties and behavior of the compounds involved in the process. Historically, thermodynamics has developed a variety of contributions that to this day have not been sorted out into a theory generally accepted as satisfactory for design purposes. There is confusion in many expositions of the subject even though the principles are essentially understood and are no longer topics of fundamental research. The use of thermodynamics leads to a deeper understanding of the characteristics of process networks. Given that, thermodynamics is a key enabling knowledge to model processes and to perform experimental and simulation measurements. Once experimentation, theory and simulation are combined, the engineer is able to design better processes which also leads to an integral understanding of the process.

Unlikely, there were two main problems with this approach. First, even the most precise mathematics were too slow for processes with a realistic model like it was presented when applying the Wang – Henke algorithm to calculate a reactive distillation column. Second, heuristics make sense in isolating a single unit, but these rules fail when the system is composed by a large number of units like the ABE fermentation because the methods trying to overcome these problems through a mathematical approach often add complication to the issue by mixing the microscopic concepts given by the thermodynamics with global concepts given by the overall

process synthesis in their attempt to solve design problems. Mathematical and statistical treatments of thermodynamics are, of course, valid by themselves, but it is improper to use statistical concepts to patch up holes in a complex network.

It is necessary, therefore, that structures of complex flowsheets be theoretically analyzed and studied from the combinatorial perspective in process synthesis. In this regard, the graph-theory provides an efficient way to answer the above questions, thereby arising enormous savings in the computational effort required by a mathematical programming method for solving the model of the problem. This technique, however, requires rigorous, theoretical analysis of process synthesis.

The graph-theory applied to process synthesis is aimed at generalized procedures which, for any process, will lead to a 'best' network. Early research in Process Synthesis accepted the argument that there might many different possible designs. Thus, a large number of networks were generated and evaluated on the computer. Hence, the research is focused on the employment of mathematically efficient search techniques to scan quickly as many designs as possible. Simulations and rigorous calculations give a measurement of the behavior of a process in a defined thermodynamic state. However, experimental measurements restrain the process into a single thermodynamic state, and the interaction rules are defined from the response the experiment has. Therefore, both simulation and rigorous calculations allow the engineer to understand what it is known, while experimentation finds what it is unknown.

Lately, several methodical techniques have been used as theoretical instruction to the synthesis of chemical process. In this work were applied to the general synthesis of a single unit and a complex network of unit a system synthesis principle like the analysis of the process statics in the case of the reactive distillation, called to be a basic decomposition theory; a rigorous calculation method like the Wang-Henke algorithm; a design technique using a heuristic approach and the operation of a branch and bound algorithm to the synthesis of optimal flowsheets For the studied cases some specific characteristics of these theories were used. Though the results, presented as rules, have restricted applications different than the specific problems proposed, they do provide a theoretical guidance for process engineering modeling using the thermodynamics and the graph-theory.

The final diagram obtained for both studied cases is very simplified and has only the most essential process steps shown, even though it is a complex network of reactors, distillation columns, compressors, heat exchangers, driers, furnaces, quench units, etc. When designing such processes,

the chemical engineer faces two tasks. First, there is the conventional engineering task of designing the individual pieces of equipment. Second, there is the task of designing the overall process. This involves decisions of where and how to integrate the various pieces of equipment or, quite frequently, whether to integrate at all. Generally, integrated processes cannot readily accommodate changes in operating conditions and consequently local equipment failure can more easily affect the entire plant, maintenance procedures become more difficult, etc. In addition, integration can be costly in terms of capital. In practice 'best' networks are hardly ever found. It takes many years, and many different consecutive installations, before the design of a chemical process evolves towards the 'best'.

It was confirmed that the methodology used in this work is useful to design other chemical processes. In practical terms, retrofitting a process through this approach is technically more feasible with relatively less effort, time a cost than designing and building an entire novel process due to the similarities the optimal flowsheet has with the original structure. In this sense, the graph-theoretic approach and the analysis of the process statics applied to process synthesis makes easier the choice between retrofitting or designing a new process because this methodology is able to generate optimal flowsheets with a degree of simplicity. The cost is certainly a proper standard for selecting the flowsheets to reduce the unfeasible alternatives. In addition to the costs function, the flowsheets can also be evaluated using other optimization criteria as controllability, operability or sustainability. Hence, the resultant flowsheets should be evaluated by means of the other criteria, having as a result a multiobject optimization problem.

The construction of a flowsheet can be supported by schemes that contain relevant heuristics as well as thermodynamic laws and strategies of generation. As the underlying rule sets are known to be not complete and fail-proof in a rigorous sense, these methodologies will not guarantee the finding of the global optimum by themselves but strongly enhance the quality and speed of finding very good solutions to the problem in question. The aim of presenting both methodologies is to develop structure-optimized solutions for a given chemical engineering task treated on an abstract thermodynamic level. It is based on the use of process synthesis knowledge combined with an optimizing technique. Thus it is the aim of this combined approach to exploit the advantages of a powerful and robust optimization method like the one provided by the graph theory, which belong to the group of probabilistic techniques, and another based on the topological thermodynamics based on a rule-based knowledge system, to avoid the generation of too many non-feasible solutions to the chemical task.

7. Annex A – Detailed information of chemical and thermodynamic properties

Physical, chemical and thermodynamical properties

The components of the system are enumerated this way:

Methanol (1) / Acetic acid (2) / Methyl acetate (3) / Water (4)

Table 7-1: Properties of pure component.

Component	Property				
	T_C *(K)*	P_C *(bar)*	R_D *(Å)*	*μ (Debye)*	*Zra*
Methanol (1)	512.8	80.94	1.536	1.71	0.2318
Acetic acid (2)	594.8	57.85	2.595	1.74	0.2240
Methyl acetate (3)	506.9	49.60	2.862	1.72	0.2560
Water (4)	647.37	221.20	0.615	1.83	0.2380

– Vapor pressure - Antoine's Equation:

$$\ln P^{sat}(atm) = a - \frac{b}{T(K)+c}$$

(0.14)

The values of these parameters are reported in Table D.2:

Table 7-2: Constants for the Antoine Equation for vapor pressures of pure species.

Component	Parameter (atm)		
	a	*b*	*c*
Methanol (1)	11.9738	3643.3136	-33.424
Acetic acid (2)	10.7733	3785.565	-39.63
Methyl acetate (3)	9.6350	2665.5416	-53.424
Water (4)	11.7109	3481.1955	-45.14

– Liquid molar density:

$$\rho\left(\frac{kmol}{m^3}\right) = \frac{A}{B^{\left(a+\left(1-\frac{T}{C}\right)^D\right)}} \qquad\qquad \rho_{mixture} = \frac{1}{\displaystyle\sum_{i=1}^{c}\frac{x_i}{\rho_i}} \tag{0.15}$$

Table 7-3: Constants – Liquid molar density.

Component	Parameter			
	A	*B*	*C*	*D*
Methanol (1)	2.3003	0.2714	512.64	0.2328
Acetic acid (2)	1.5791	0.2695	592.71	0.2684
Methyl acetate (3)	1.121	0.2585	506.8	0.2745
Water (4)	5.459	0.3054	647.13	0.081

– Vapor and liquid enthalpy:

For the vapor it is used the Aly-Lee correlation for the isobaric – ideal gas heat capacity:

$$C_p^{g-id} = A + B\left(\frac{C/T}{\text{Senh}\left(C/T\right)}\right)^2 + D\left(\frac{E/T}{\text{Cosh}\left(E/T\right)}\right)^2 \tag{0.16}$$

The vapor enthalpy can be calculated by integration:

$$\hat{H}(T) = AT + BT\left(C/T\right)\text{Coth}\left(C/T\right) - DT\left(E/T\right)\text{Tanh}\left(E/T\right) -$$
$$\left[AT_{REF} + BT_{REF}\left(C/T_{REF}\right)\text{Coth}\left(C/T_{REF}\right) - DT_{REF}\left(E/T\right)\text{Tanh}\left(E/T\right)\right] \tag{0.17}$$

Table 7-4: Constants – Isobaric ideal gas heat capacity.

Component	Parameter				
	A	*B*	*C*	*D*	*E*
Methanol (1)	37980	87150	1717	45440	802
Acetic acid (2)	40200	136750	1262	70030	569.7
Methyl acetate (3)	69630	197000	2053	154030	845
Water (4)	33363	26790	2610.5	8896	1169

The liquid enthalpy is obtained by subtracting to the vapor enthalpy the vaporization enthalpy calculated from:

$$\Delta H_{vap}(T) = A\left(1-T_R\right)^{\left(B+CT_R+DT_R^2+ET_R^3\right)} \quad \text{where } T_R = \frac{T}{T_C}$$

Table 7-5: Parameters – Vaporization enthalpy.

Component	Parameter					
	A	**B**	**C**	**D**	**E**	$T_C(K)$
Methanol (1)	5.239×10^7	0.3682	0	0	0	512.58
Acetic acid (2)	1.117×10^7	-1.424	0.15	1.45	0	592.71
Methyl acetate (3)	4.491×10^7	0.315	0.0749	0	0	506.80
Water (4)	5.2053×10^7	0.3199	-0.212	0.2579	0	647.13

Table 7-6: Standard enthalpy of formation.

Component	kJ/mol	J/kmol	kcal/mol
Methanol (1)	-201.166720	-201166720	-48.08
Acetic acid (2)	-434.84312	-43484312	-103.93
Methyl acetate (3)	-409.613600	-409613600	-97.90
Water (4)	-241.8352	-2418352	-57.80

Equations of State, Mixing rules and Activity models used in this work

Equations of State (EOS) and Mixing rules

The Peng-Robinson (PR) equation of state [59] has the following form:

$$P = \frac{RT}{v-b} - \frac{a}{v(v+b)+b(v-b)} \tag{0.18}$$

where P is the pressure, T the absolute temperature and R is the ideal gas constant. a and b are the energy and size parameters, respectively, which are calculated from:

$$a = 0.457235 \frac{R^2 T_c^2}{P_c} \alpha(T_r) \tag{0.19}$$

$$b = 0.077796 \frac{RT_c}{P_c} \tag{0.20}$$

the subscripts c and r represent critical and reduced conditions, respectively.

The correlation for the α function is:

$$\alpha(T_r) = \left[1 + \kappa\left(1 - \sqrt{T_r}\right)\right]^2 \tag{0.21}$$

$$\kappa = 0.37464 + 1.54226\omega - 0.26992\omega^2 \tag{0.22}$$

where ω is the acentric factor.

To extend the PR-EOS to mixtures the Wong-Sandler mixing rules were used [60]. Thus, the a_m and b_m parameters have the following form:

$$b_m = \frac{\sum_i \sum_j z_i z_j \left(b - \dfrac{a}{RT}\right)_{ij}}{1 - \sum_i z_i \dfrac{a_i}{b_i RT} - \dfrac{\underline{A}_\infty^E}{CRT}}$$

(0.23)

and

$$a_m = b_m \left[\sum_i z_i \frac{a_i}{b_i} + \frac{\underline{A}_\infty^E}{C} \right]$$

(0.24)

where C is a constant related to the equation:

$$C = \frac{1}{\sqrt{2}} \ln\left(\sqrt{2} - 1\right)$$

(0.25)

And

$$\left(b - \frac{a}{RT}\right)_{ij} = \frac{\left(b - \left(a/RT\right)\right)_i + \left(b - \left(a/RT\right)\right)_j}{2} \left(1 - k_{ij}\right)$$

(0.26)

where k_{ij} is a second virial coefficient binary interaction parameter, z is the molar fraction and $\underline{A}_\infty^E$ is the excess Helmholtz free energy at infinite pressure which was calculated from NRTL model:

$$\frac{\underline{A}_\infty^E}{RT} = \sum_i z_i \left(\frac{\sum_j z_j \tau_{ji} g_{ji}}{\sum_k z_k g_{ki}} \right)$$

(0.27)

with

$$g_{ij} = \exp\left(-\alpha_{ij} \tau_{ij}\right)$$

(0.28)

Activity model

EOS are very attractive for the calculation of vapor-liquid equilibrium, but they require several expressions which are able to describe the *PvT* behavior not only of the vapor but also of the liquid phase with a proper accuracy. In this sense, activity models such as nonrandom two-liquid (NRTL) and allow to an improved description of the real behavior of systems from the information of binary their binary parameters.

The first model considered is the three parameter (α, τ_{12}, τ_{21}) nonrandom two-liquid (NRTL) equation which has the analytical following expressions [61]:

$$\frac{\underline{G}^E}{RT} = x_1 x_2 \left(\frac{\tau_{21} G_{21}}{x_1 + x_2 G_{21}} + \frac{\tau_{12} G_{12}}{x_2 + x_1 G_{12}} \right)$$

(0.29)

with

$$\ln\left(G_{12}\right) = -\alpha\tau_{12} \qquad\qquad\qquad \ln\left(G_{21}\right) = -\alpha\tau_{21}$$

and

$$
\begin{aligned}
\ln\left(\gamma_1\right) &= x_2^2\left[\tau_{21}\left(\frac{G_{21}}{x_1 + x_2 G_{21}}\right)^2 + \frac{\tau_{12}G_{12}}{\left(x_2 + x_1 G_{12}\right)^2}\right] \\[2mm]
\ln\left(\gamma_2\right) &= x_1^2\left[\tau_{12}\left(\frac{G_{12}}{x_2 + x_1 G_{12}}\right)^2 + \frac{\tau_{21}G_{21}}{\left(x_1 + x_2 G_{21}\right)^2}\right]
\end{aligned}
\tag{0.30}
$$

In the case of binary mixtures α, τ_{12} and τ_{21} are the adjustable parameters of the model.

Entrainers for the extraction of the products from acetone-butanol-ethanol fermentation broth

Presented are three candidate solvents (entrainers) for the extraction of the products from ABE fermentation broth. 2-ethyl-1-hexanol is best known as the solvent for extraction of butanol from the broth. It has a large separation factor for butanol from water. The separation factor (Sf) is defined as:

$$Sf = \frac{Kd}{Er} \tag{0.31}$$

Where *Kd* is the distribution coefficient, *Er* (equilibrium ratio) and *E* stands for extract phase and *R* stands for raffinate phase.

The *Er* for 2-ethyl-1-hexanol is 0.022, which implies that very little water is being withdrawn into the extract phase. The *Kd* of 6.09 for 2-ethyl-1-hexanol to butanol shows that butanol prefers being in the organic phase. As displayed in the following table, 2-ethyl-1-hexanol is the best choice for the extraction solvent.

Table 7-7: Comparison of three candidate entrainers for the extraction of the products from ABE fermentation broth.

Solvents	Kd (mol E/mol R)			Er	Sf (Kd/Er)		
	Butanol	**Ethanol**	**Acetone**	**(H₂O E/H₂O R)**	**Butanol**	**Ethanol**	**Acetone**
2-ethyl-1-hexanol	6.09	0.47	0.58	0.022	280	21	26
Butyl acetate	3.58	0.26	0.97	0.018	200	14	54
Oleic acid	1.61	0.15	0.21	0.01	160	15	27

8.   Annex B – Basic concepts of Thermodynamics

Equilibrium conditions for heterogeneous closed systems

A heterogeneous closed system is composed by two or more phases, each one considered as an open system inside a global closed system.

In Figure B.1 is presented a heterogeneous closed system. The phase β can exchange mass and energy with phase α. But the combined system only can exchange energy as heat transfer or mechanic work with the surroundings.
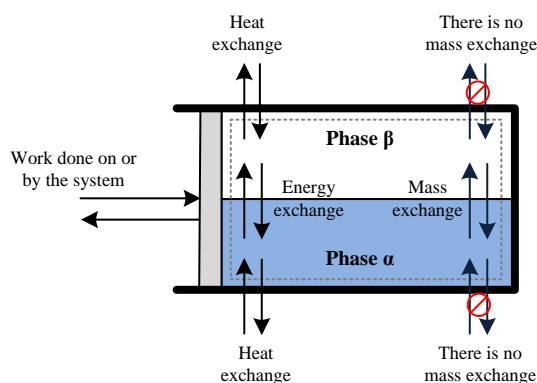
Figure 8-1: Symbolic representation of a heterogeneous closed system.

The intensive properties of a system are temperature, pressure and chemical potential. In the equilibrium, the intensive properties of the system are the same on each phase, i.e. the temperature of phase β is the same as the temperature of phase α, the pressure of phase β is the same as the pressure of phase α, and the chemical potential of a component in the phase β is the same as the chemical potential of a component in the phase α. This applies for two phases, but a system can have π phases, hence, all the intensive properties must be the same in each phase. Josiah Willard Gibbs demonstrated the previous criteria using the function U as starting point.

For each phase, the fundamental thermodynamic relation has this form:

$$dU = TdS - PdV + \sum_{i=1}^{c} \mu_i dn_i$$

(0.32)

The total derivative *dU* for global closed system comes from the sum of the previous relation for all the phases, this way:

$$dU = \sum_{k=1}^{\pi} T^{(k)} dS^{(k)} - \sum_{k=1}^{\pi} P^{(k)} dV^{(k)} + \sum_{k=1}^{\pi} \sum_{i=1}^{c} \mu_i^{(k)} dn_i^{(k)}$$

(0.33)

Where π is the total number of phases in the heterogeneous system.

Expanding equation(8.2):

$$dU = T^{(1)} dS^{(1)} - P^{(1)} dV^{(1)} + \sum_{i=1}^{c} \mu_i^{(1)} dn_i^{(1)} + T^{(2)} dS^{(2)} - P^{(2)} dV^{(2)} + \sum_{i=1}^{c} \mu_i^{(2)} dn_i^{(2)} +$$

$$\cdots T^{(k)} dS^{(k)} - P^{(k)} dV^{(k)} + \sum_{i=1}^{c} \mu_i^{(k)} dn_i^{(k)} + \cdots + T^{(\pi)} dS^{(\pi)} - P^{(\pi)} dV^{(\pi)} + \sum_{i=1}^{c} \mu_i^{(\pi)} dn_i^{(\pi)}$$

(0.34)

The equilibrium conditions can be obtained considering that $(dU)_{S,V,ni} = 0$ for the global closed system. The individual variations

$$dS^{(1)}, dS^{(2)}, \cdots, dS^{(\pi)}$$

$$dV^{(1)}, dV^{(2)}, \cdots, dV^{(\pi)}$$

$$dn_i^{(1)}, dn_i^{(2)}, \cdots, dn_i^{(\pi)}, \quad \text{for } i = 1, 2, \cdots c$$

are dependent on the restrictions imposed by the constant- total entropy *S*, the constant-total volume *V*, and the constant-total number of moles of the component i, $\sum_{i=1}^{c} n_i$. That is to say:

$$dS = dS^{(1)} + dS^{(2)} + \cdots + dS^{(k)} + \cdots + dS^{(\pi)} = 0$$

(0.35)

$$dV = dV^{(1)} + dV^{(2)} + \cdots + dV^{(k)} + \cdots + dV^{(\pi)} = 0$$

(0.36)

$$\sum_{k=1}^{\pi} dn_i = dn_i^{(1)} + dn_i^{(2)} + \cdots + dn_i^{(k)} + \cdots + dn_i^{(\pi)}, \quad \text{for } i = 1, 2, \ldots, c$$

(0.37)

There are then $\pi(c+2)$ intensive variations in equation (8.3):

$$dT^{(1)}, dT^{(2)}, \cdots, dT^{(\pi)}$$

$$dP^{(1)}, dP^{(2)}, \cdots, dP^{(\pi)}$$

$$d\mu_i^{(1)}, d\mu_i^{(2)}, \cdots, d\mu_i^{(\pi)}, \quad \text{for } i = 1, 2, \cdots c$$

And there are *c+2* restrictions imposed by equations (8.4), (8.5) and (8.6).

If equations (8.4), (8.5) and (8.6) are used to eliminate the variations *dS, dV, dn_i* in each phase, then *dU* can be expressed in terms of *(π-1) (c+2)* intensive independent variables. If the intensive properties are eliminated from phase 1, it is obtained the following:

$$dS^{(1)} = -dS^{(2)} - dS^{(3)} - \cdots - dS^{(k)} - \cdots - dS^{(\pi)}$$

(0.38)

$$dV^{(1)} = -dV^{(2)} - dV^{(3)} - \cdots - dV^{(k)} - \cdots - dV^{(\pi)}$$

(0.39)

$$dn_i^{(1)} = -dn_i^{(2)} - dn_i^{(3)} - \cdots - dn_i^{(k)} - \cdots - dn_i^{(\pi)}$$

(0.40)

Replacing equations (8.7), (8.8) and (8.9) in equation (8.3):

$$dU = T^{(1)}\left[-dS^{(2)} - dS^{(3)} - \cdots - dS^{(k)} - \cdots - dS^{(\pi)}\right] - P^{(1)}\left[-dV^{(2)} - dV^{(3)} - \cdots - dV^{(k)} - \cdots - dV^{(\pi)}\right] +$$

$$\sum_{i=1}^{c}\mu_i^{(1)}\left[-dn_i^{(2)} - dn_i^{(3)} - \cdots - dn_i^{(k)} - \cdots - dn_i^{(\pi)}\right] + T^{(2)}dS^{(2)} - P^{(2)}dV^{(2)} + \sum_{i=1}^{c}\mu_i^{(2)}dn_i^{(2)} + \cdots$$

$$+T^{(k)}dS^{(k)} - P^{(k)}dV^{(k)} + \sum_{i=1}^{c}\mu_i^{(k)}dn_i^{(k)} + \cdots + T^{(\pi)}dS^{(\pi)} - P^{(\pi)}dV^{(\pi)} + \sum_{i=1}^{c}\mu_i^{(\pi)}dn_i^{(\pi)}$$

Rearranging:

$$dU = \left(T^{(2)} - T^{(1)}\right)dS^{(2)} - \left(P^{(2)} - P^{(1)}\right)dV^{(2)} + \left(\mu_1^{(2)} - \mu_1^{(1)}\right)dn_1^{(2)} + \cdots + \left(\mu_c^{(2)} - \mu_c^{(1)}\right)dn_c^{(2)}$$

$$+\left(T^{(3)} - T^{(1)}\right)dS^{(3)} - \left(P^{(3)} - P^{(1)}\right)dV^{(3)} + \left(\mu_1^{(3)} - \mu_1^{(3)}\right)dn_1^{(3)} + \cdots + \left(\mu_c^{(3)} - \mu_c^{(1)}\right)dn_c^{(3)} + \cdots$$

$$+\left(T^{(k)} - T^{(1)}\right)dS^{(k)} - \left(P^{(k)} - P^{(1)}\right)dV^{(k)} + \left(\mu_1^{(k)} - \mu_1^{(3)}\right)dn_1^{(k)} + \cdots + \left(\mu_c^{(k)} - \mu_c^{(1)}\right)dn_c^{(k)} + \cdots$$

$$+\left(T^{(\pi)} - T^{(1)}\right)dS^{(\pi)} - \left(P^{(\pi)} - P^{(1)}\right)dV^{(\pi)} + \left(\mu_1^{(\pi)} - \mu_1^{(3)}\right)dn_1^{(\pi)} + \cdots + \left(\mu_c^{(\pi)} - \mu_c^{(1)}\right)dn_c^{(\pi)}$$

In the equilibrium, $(dU)_{S,V,ni} = 0$, since the variations

$$dS^{(2)}, dS^{(3)}, \cdots, dS^{(\pi)}$$

$$dV^{(2)}, dV^{(3)}, \cdots, dV^{(\pi)}$$

$$dn_i^{(2)}, dn_i^{(3)}, \cdots, dn_i^{(\pi)}, \text{ for } i = 2, 3, \cdots c$$

are independent, then, in the equilibrium for a closed system in which dU = 0, it is said that:

$$\frac{\delta U}{\delta S^{(1)}} = 0, \quad \frac{\delta U}{\delta V^{(1)}} = 0, \quad \frac{\delta U}{\delta n_1^{(1)}} = 0, \cdots, \quad \frac{\delta U}{\delta n_c^{(1)}} = 0$$

$$\text{for } i = 2, \cdots, \pi$$

Thus:

$$T^{(i)} - T^{(1)} = 0, \ P^{(i)} - P^{(1)} = 0, \ \mu_j^{(i)} - \mu_j^{(1)} = 0, \ \cdots, \ \mu_j^{(i)} - \mu_j^{(1)} = 0$$

$$\textit{for } i = 2, \cdots, \pi, j = 1, \ldots, c$$

Then, as a consequence:

$$T^{(1)} = T^{(2)} = \cdots = T^{(k)} \quad \text{(Thermic equilibrium)}$$

(0.41)

$$P^{(1)} = P^{(2)} = \cdots = P^{(k)} \quad \text{(Mechanic equilibrium)}$$

(0.42)

$$\mu_j^{(1)} = \mu_j^{(2)} = \cdots = \mu_j^{(k)} \quad \text{(Diffusional equilibrium)}$$

$$\text{for } j = 1, \cdots, c$$

(0.43)

These are the conditions of equilibrium for a closed heterogeneous system. It is shown that the intensive properties are all the same in the phase equilibrium.

Fugacity

The chemical potential does not have an equivalent in the physical world; therefore, it must be expressed using an auxiliary function that can be identified in the physical reality. A very useful auxiliary function is obtained by means of the concept of fugacity.

To develop an auxiliary equation for the chemical potential, it must be used the fundamental thermodynamic relation as a function of the molar properties:

$$d\hat{G} = -\hat{S}dT + \hat{V}dP + \sum_{i=1}^{c} \mu_i dx_i$$

(0.44)

Where $\mu_i = \left(\dfrac{\partial G}{\partial n_i} \right)_{T,P,n_i}$.

So, for an ideal pure gas at constant temperature:

$$d\hat{G}^{id} = \hat{V}^{id} dP \qquad @ T = \text{constant}$$

For an ideal gas hold the equation of state $\hat{V}^{id} = \dfrac{RT}{P}$. Then:

$$d\hat{G}^{id} = \frac{RT}{P}dP$$
$$d\hat{G}^{id} = RTd\left(\ln P\right)$$

(0.45)

Though this expression is only valid for an ideal gas, it suggests that for a real gas must be written another equation of the same form, defining the fugacity *f* as a new property with units of pressure:

$$d\hat{G} = RTd\left(\ln f\right)$$

(0.46)

It is possible to demonstrate that the chemical potential of a component *i* in a mixture is given by:

$$\hat{\mu}_i - \mu_i^0 = RT \ln\left(\frac{\hat{f}_i}{f_i^0}\right)$$

(0.47)

and the chemical potential of a pure component *i* is given by:

$$\mu_i - \mu_i^0 = RT \ln\left(\frac{f_i}{f_i^0}\right)$$

(0.48)

Where $\hat{f}_i$ is the fugacity of component *i* in the mixture which can be called partial fugacity, f_i is the fugacity of the pure component *i*, f_i^0 is the fugacity of pure component *i* in the reference state, and μ_i^0 is the chemical potential of pure component *i* in the reference state.

The equality of partial fugacities as a criteria for phase equilibrium

The condition of diffusional equilibrium:

$$\hat{\mu}_i^{(1)} = \hat{\mu}_i^{(2)} = \cdots = \hat{\mu}_i^{(\pi)} \tag{0.49}$$

can be written as a more useful form to calculate the phase equilibrium by considering the relation between the chemical potential μ_i and the fugacity f_i.

For a phase α the equations (8.16) and (8.17) take the following form, respectively:

$$\mu_i^{(\alpha)} - \mu_i^{o(\alpha)} = RT\left(\ln\left(\frac{f_i^{(\alpha)}}{f_i^{o(\alpha)}} \right) \right) \tag{0.50}$$

$$\hat{\mu}_i^{(\alpha)} - \mu_i^{o(\alpha)} = RT\left(\ln\left(\frac{\hat{f}_i^{(\alpha)}}{f_i^{o(\alpha)}} \right) \right) \tag{0.51}$$

and for the phase β,

$$\mu_i^{(\beta)} - \mu_i^{o(\beta)} = RT\left(\ln\left(\frac{f_i^{(\beta)}}{f_i^{o(\beta)}} \right) \right) \tag{0.52}$$

$$\hat{\mu}_i^{(\beta)} - \mu_i^{o(\beta)} = RT\left(\ln\left(\frac{\hat{f}_i^{(\beta)}}{f_i^{o(\beta)}} \right) \right) \tag{0.53}$$

Subtracting equations (8.19) and (8.21):

$$\left(\mu_i^{(\alpha)} - \mu_i^{o(\alpha)} \right) - \left(\mu_i^{(\beta)} - \mu_i^{o(\beta)} \right) = \left[RT\left(\ln\left(\frac{f_i^{(\alpha)}}{f_i^{o(\alpha)}} \right) \right) \right] - \left[RT\left(\ln\left(\frac{f_i^{(\beta)}}{f_i^{o(\beta)}} \right) \right) \right]$$

Rearranging:

$$\left(\mu_i^{(\alpha)} - \mu_i^{(\beta)} \right) - \left(\mu_i^{o(\alpha)} - \mu_i^{o(\beta)} \right) = RT\left[\ln\left(\frac{f_i^{(\alpha)} f_i^{o(\beta)}}{f_i^{o(\alpha)} f_i^{(\beta)}} \right) \right]$$

If the system is in equilibrium, $\mu_i^{(\alpha)} - \mu_i^{(\beta)}$. Since both phases α and β are defined by *T, P⁰*, it is obtained then that $\mu_i^{o(\alpha)} - \mu_i^{o(\beta)}$ and $f_i^{o(\alpha)} = f_i^{o(\beta)}$. Hence:

$$\left(\cancel{\mu_i^{(\alpha)}} - \cancel{\mu_i^{(\beta)}} \right) - \left(\cancel{\mu_i^{(\alpha)}} - \cancel{\mu_i^{(\beta)}} \right) = RT\left[\ln\left(\frac{f_i^{(\alpha)} \cancel{f_i^{o(\beta)}}}{\cancel{f_i^{o(\alpha)}} f_i^{(\beta)}} \right) \right]$$

Simplify, we have that $\ln\left(\dfrac{f_i^{(\alpha)}}{f_i^{(\beta)}} \right) = 0$, i.e. the condition of phase equilibrium in a pure component system is given by:

$$f_i^{\alpha} = f_i^{\beta} \tag{0.54}$$

If equations (8.20) and (8.22) are subtracted, then:

$$\left(\hat{\mu}_i^{(\alpha)} - \mu_i^{o(\alpha)} \right) - \left(\hat{\mu}_i^{(\beta)} - \mu_i^{o(\beta)} \right) = \left[RT \left(\ln \left(\frac{\hat{f}_i^{(\alpha)}}{f_i^{o(\alpha)}} \right) \right) \right] - \left[RT \left(\ln \left(\frac{\hat{f}_i^{(\beta)}}{f_i^{o(\beta)}} \right) \right) \right]$$

Rearranging:

$$\left(\hat{\mu}_i^{(\alpha)} - \hat{\mu}_i^{(\beta)} \right) - \left(\mu_i^{o(\alpha)} - \mu_i^{o(\beta)} \right) = RT \left[\ln \left(\frac{\hat{f}_i^{(\alpha)} f_i^{o(\beta)}}{\hat{f}_i^{(\beta)} f_i^{o(\alpha)}} \right) \right]$$

If the system is in equilibrium, $\hat{\mu}_i^{(\alpha)} - \hat{\mu}_i^{(\beta)}$. Since both phases α and β are defined by T, P^0, it is

obtained then that $\mu_i^{o(\alpha)} - \mu_i^{o(\beta)}$ and $f_i^{o(\alpha)} = f_i^{o(\beta)}$. Hence:

$$\left(\cancel{\hat{\mu}_i^{(\alpha)} - \hat{\mu}_i^{(\beta)}} \right) - \left(\cancel{\mu_i^{o(\alpha)} - \mu_i^{o(\beta)}} \right) = RT \left[\ln \left(\frac{\hat{f}_i^{(\alpha)} \, \cancel{f_i^{o(\beta)}}}{\hat{f}_i^{(\beta)} \, \cancel{f_i^{o(\alpha)}}} \right) \right]$$

Then:

$$\ln \left(\frac{\hat{f}_i^{(\alpha)}}{\hat{f}_i^{(\beta)}} \right) = 0$$

therefore, the condition of equilibrium for a multicomponent system is given by:

$$\hat{f}_i^{(\alpha)} = \hat{f}_i^{(\beta)} \qquad (0.55)$$

So, if the condition $\hat{\mu}_i^{(\alpha)} - \hat{\mu}_i^{(\beta)}$ is satisfied, then the condition of equality of the partial fugacities

$\hat{f}_i^{(\alpha)} = \hat{f}_i^{(\beta)}$ is satisfied as well.

Basic concepts

For the equilibrium between the liquid phase L and the vapor phase V, the condition of equality of
the partial fugacities is expressed as:

$$\hat{f}_{i,L} = \hat{f}_{i,V} \qquad i = 1, 2, 3, \cdots, c$$

$$(0.56)$$

For the vapor phase V, the partial fugacity coefficient $\hat{\varphi}_i$ is defined by:

$$\hat{\varphi}_i = \frac{\hat{f}_{i,V}}{y_i P} \Rightarrow \hat{f}_{i,V} = y_i \hat{\varphi}_i P$$

$$(0.57)$$

For the liquid phase L, the activity coefficient γ_i is defined by:

$$\gamma_i = \frac{\hat{f}_{i,L}}{x_i f_i^0} \Rightarrow \hat{f}_{i,L} = x_i \gamma_i f_i^0$$

$$(0.58)$$

Replacing equations (8.26) and (8.27) in equation (8.25):

$$y_i \hat{\varphi}_i P = x_i \gamma_i f_i^0$$

(0.59)

In order to apply this equation in the calculation of liquid-vapor equilibrium it is required an

equation of state for the vapor phase to find $\hat{\varphi}_i$, and an expression $\dfrac{\hat{G}^E}{RT}$ for the liquid phase to find

γ_i. Additionally, the fugacities in the state of reference f_i^0 are required as well.

In case the expression for $\dfrac{\hat{G}^E}{RT}$ is based on the state of reference defined by the Lewis-Randall rule,

f_i^0 represents the fugacity of pure component i at T and P of the mixture.

$$f_i^0 \left(\text{Lewis - Randall} \right) = f_i \left(T, P \right)$$

Note that for a pure component the Gibbs free energy is given by equation (8.15):

$$d\hat{G}_i = RTd \ln f_i$$

For a pure substance:

$$d\hat{G}_i = -\hat{S}_i dT + \hat{V}_i dP$$

(0.60)

and at constant temperature:

$$d\hat{G}_i = \hat{V}_i dP$$

(0.61)

Equaling equations (8.15) and (8.30):

$$RTd \ln f_i = \hat{V}_i dP$$

(0.62)

Thus,

$$\left(\frac{\partial \ln f_i}{\partial P} \right)_T = \frac{\hat{V}_i}{RT}$$

(0.63)

Integrating at constant temperature from the saturated liquid state to the compressed liquid state:

$$\int_{f_L^{sat}}^{f_L} d \ln f_i = \int_{P_i^{sat}}^{P} \frac{\hat{V}_{i,L}}{RT} dP$$

$$\ln \left(\frac{f_{i,L}}{f_{i,L}^{sat}} \right) = \frac{1}{RT} \int_{P_i^{sat}}^{P} \hat{V}_{i,L} \, dP$$

$$f_{i,L} = f_{i,L}^{sat} \exp \left(\frac{1}{RT} \int_{P_i^{sat}}^{P} \hat{V}_{i,L} \, dP \right)$$

(0.64)

The definition of fugacity coefficient is:

$$\varphi_i = \frac{f_i}{P}$$

Hence:

$$f_{i,L}^{sat} = \varphi_i^{sat} P_i^{sat}$$

(0.65)

Replacing this expression in equation (8.33):

$$f_{i,L} = \varphi_i^{sat} P_i^{sat} \exp\left(\frac{1}{RT}\int_{P_i^{sat}}^{P} \hat{V}_{i,L} \ dP\right)$$

(0.66)

Replacing equation (8.35) in equation (8.28), it is obtained an equation that can be used as a starting point for the vapor-liquid equilibrium calculations:

$$y_i\hat{\varphi}_i P = x_i\gamma_i\varphi_i^{sat} P_i^{sat} \exp\left(\frac{1}{RT}\int_{P_i^{sat}}^{P} \hat{V}_{i,L} \ dP\right)$$

(0.67)

Setting up $\Phi_i = \dfrac{\hat{\varphi}_i}{\varphi_i^{sat}}\exp\left(-\dfrac{1}{RT}\int_{P_i^{sat}}^{P} \hat{V}_{i,L} \ dP\right)$, then equation (8.36) can be presented as:

$$y_i\Phi_i P = x_i\gamma_i P_i^{sat}$$

(0.68)

Φ_i is related to the non-ideality of the vapor phase, and γ_i is related to the non-ideality of the liquid phase. That is to say that $\Phi_i = 1$ means that the vapor behaves like a mixture of ideal gases and $\gamma_i = 1$ means that the liquid phase behaves like an ideal solution.

It is common to find in the literature the equation (8.37) written as:

$$y_i = K_i x_i$$

(0.69)

Where:

$$K_i = \frac{\gamma_i P_i^{sat}}{\Phi_i} = \frac{\gamma_i P_i^{sat}\varphi_i^{sat}}{\hat{\varphi}_i P}\exp\left(\frac{1}{RT}\int_{P_i^{sat}}^{P} \hat{V}_{i,L} \ dP\right)$$

(0.70)

It is very important to know that $K_i = 1$ does not represent neither the ideal vapor phase nor the ideal liquid phase. Physically, K_i can be interpreted as the trend a component i has so as to stay in the vapor phase or the liquid phase in a solution. For instance, if K_i is big, it means that the substance i tends to concentrate in the vapor phase; if K_i is small, it means that the substance i tends to concentrate in the liquid phase.

Bubble point calculation

The present algorithm is used to calculate the bubble point and the vapor phase composition, knowing the pressure and liquid phase composition. The bubble point is the temperature (at a given pressure) where the first bubble of vapor is formed.

Starting from the stoichiometric restriction:

$$\sum_{i=1}^{c} y_i = 1$$

(0.71)

Replacing the equilibrium relation $y_i = K_i x_i$, in equation (8.40):

$$\sum_{i=1}^{c} K_i x_i = 1$$

(0.72)

Equation (8.39) shows that $K_i = \dfrac{\gamma_i P_i^{sat}}{\Phi_i P}$, where $\gamma_i = \gamma_i(T, x_i)$, $\Phi_i = \Phi_i(T, P, y_i)$ and

$P_i^{sat} = P_i^{sat}(T)$. Then, replacing K_i in the equation $y_i = K_i x_i$:

$$y_i = \frac{x_i \gamma_i P_i^{sat}}{\Phi_i P}$$

(0.73)

Replacing K_i in equation (8.41):

$$\sum_{i=1}^{c} \frac{x_i \gamma_i P_i^{sat}}{\Phi_i P} = 1$$

Isolating P:

$$P = \sum_{i=1}^{c} \frac{x_i \gamma_i P_i^{sat}}{\Phi_i}$$

To calculate the bubble point it is employed an auxiliary variable to make the process easier:

$$P = P_k^{sat} \sum_{i=1}^{c} \frac{x_i \gamma_i}{\Phi_i} \left(\frac{P_i^{sat}}{P_k^{sat}} \right)$$

(0.74)

where *k* is an arbitrary component. Now, setting:

$$\alpha_{k,i} = \frac{P_i^{sat}}{P_k^{sat}}$$

(0.75)

And replacing in equation (8.43):

$$P_k^{sat} = \frac{P}{\displaystyle\sum_{i=1}^{c} \frac{x_i \gamma_i}{\Phi_i \alpha_{k,i}}}$$

(0.76)

To calculate the bubble point it is necessary to have an initial estimate of *T* so as to start the iterative process. The algorithm comprises the following steps:

1. To calculate the vapor pressures P_i^{sat} of each component, the activity coefficients γ_i using $\gamma_i = \gamma_i(T, x_i)$ and the initial value of *T*.

2. To select a component of reference *k* and calculate $\alpha_{k,i}$ using equation (8.44).

3. To assume $\Phi_i = 1$ for $i = 1, 2, \cdots, c$ and calculate the molar fractions in the vapor phase y_i using equation (8.42).

4. To calculate Φ_i with the normalized values of y_i.

5. To calculate the molar fractions y_i using equation (8.42), normalize them and then recalculate Φ_i.

6. Repeat step 5 till the values of y_i do not have a significant change in their iterations. The convergence criteria that can be applied is $\sum_{i=1}^{c} \left| \dfrac{y_i^{(k)} - y_i^{(k-1)}}{y_i^{(k)}} \right| \leq \varepsilon_1$, where ε_1 is a very small number.

7. To calculate P_k^{sat} of the reference component using equation (8.45) finding then a new T isolating it from the vapor pressure equation $P_k^{sat} = P_k^{sat}(T)$.

8. To recalculate the vapor pressures P_i^{sat} with the new value of T using $P_i^{sat} = P_i^{sat}(T)$, the $\alpha_{k,i}$ using (8.44), and γ_i using $\gamma_i = \gamma_i(T, x_i)$.

9. Repeat steps 5 to 8 till T does not have a significant change in their iterations. The convergence criteria that can be applied is $\sum_{i=1}^{c} \left| \dfrac{T^{(k)} - T^{(k-1)}}{T^{(k)}} \right| \leq \varepsilon_2$, where ε_2 is a very small number.

10. To determine the final values of y_i with the final values of T using equation (8.42), and the normalize them.

To normalize y_i is applied the equation $y_i^* = \dfrac{y_i}{\sum\limits_{i=1}^{c} y_i}$.

9.   Annex C – Mathematical Model of a Reactive Distillation Column

Figure 9.1 shows the scheme of a reactive distillation column, wherein stage 1 corresponds to a total or partial condenser and the n stage corresponds to a partial reboiler. The column is considered a liquid-vapor separator, continuous and in steady state with n equilibrium stages arranged in cascade and countercurrent flow. The difference between a reactive distillation column with a conventional distillation column is that in the first one the components react between them. The feed stream to be reacted and separated into fractions is introduced into one or more points along the shell of the column. Due to the difference in gravity between the liquid and vapor phase, the liquid runs down the column, cascading from stage to stage, while vapor rises through the column, having contact with the liquid in each of the separating stages. The liquid that reaches the bottom of the column is partially vaporized in the reboiler to provide the vapor that will ascend through the column. The remaining liquid is removed as bottoms. The vapor that reaches the top of the column is cooled and condensed wholly or partially; part of this liquid is recycled to the column as reflux. The rest of the condensed liquid or uncondensed vapor is removed as top product.

This flow pattern in the reactive distillation column provides a countercurrent contact between the vapor and liquid in all sections of the column. The vapor and liquid phases at a given stage are close to reach the phase equilibrium (temperature, pressure and composition), to a point that is dependent on the efficiency of the stage.

Lighter components (lower boiling point) tend to concentrate in the vapor phase while the heavier (with higher boiling point) tend to do so in the liquid phase. Therefore, the vapor phase becomes richer in lighter components while ascending through the column, and a liquid phase that is becoming increasingly richer in heavy components as it descends to the bottom.
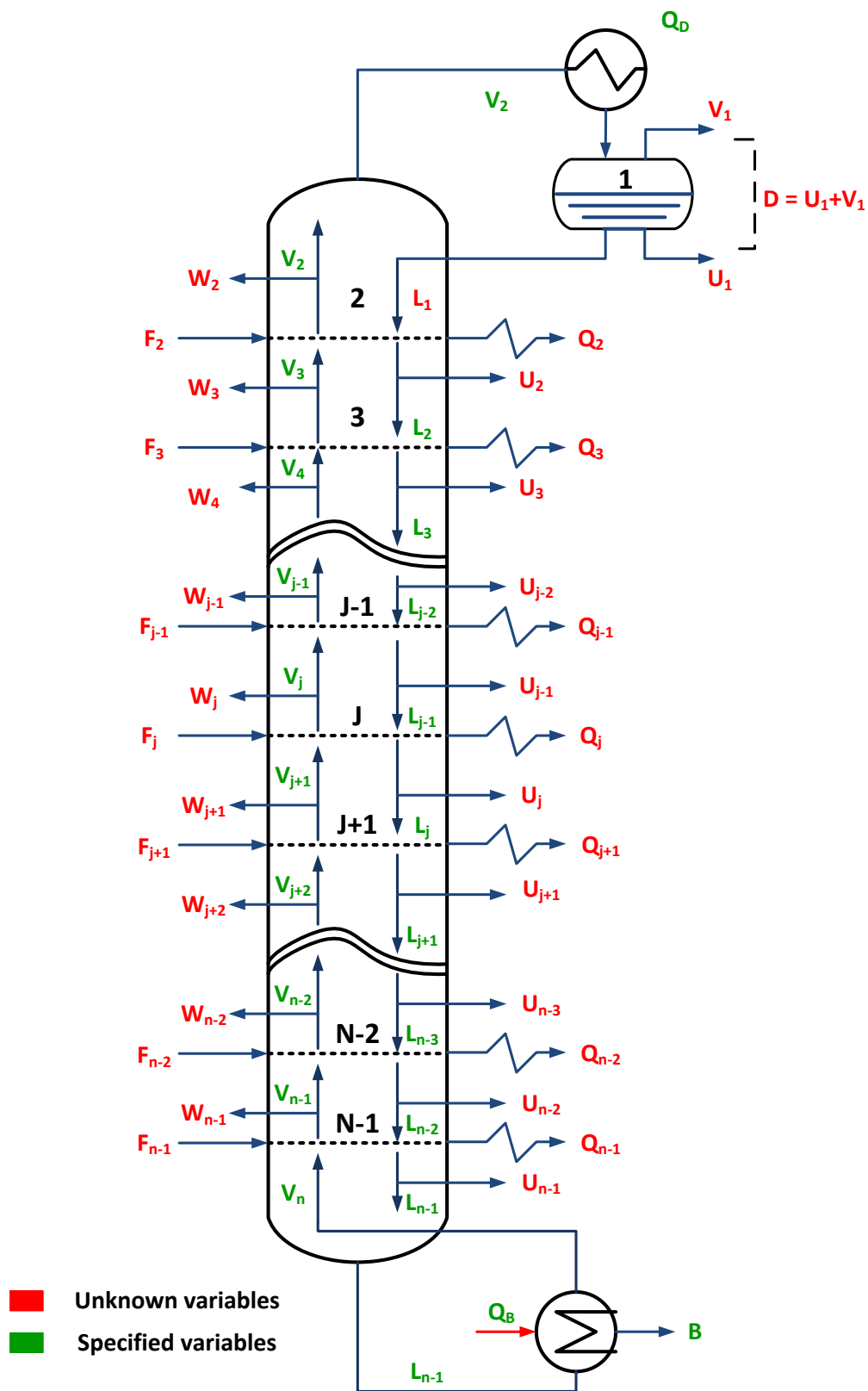
Figure 9-1: General scheme of a reactive distillation column.

When the condenser is total, the flow denoted as V_1 does not exist, and the top product is obtained by a lateral fluid outlet U_1. The rest of the condensate is returned to stage 2 as reflux L_1. Therefore, the distillate has the same composition of the vapor leaving the stage 2 and the reflux that reaches stage 2. When the condenser is partial, the top product or distillate is obtained from the flow denoted as V_1, and the output lateral flow U_1 does not exist. Therefore, the vapor flow V_1 is in equilibrium with the liquid leaving the condenser L_1 which is fed to stage 2. Stage 1 is an additional stage in equilibrium when the condenser is partial.

The reboiler of the reactive distillation column is considered as a partial reboiler, because from it is obtained a liquid stream B leaving as bottoms and a vapor stream V_n which is returned to the distillation column. These two streams are assumed to be in equilibrium, and therefore the reboiler is considered as an equilibrium stage.

Figure 9.2 presents shows the scheme of an equilibrium stage j vapor-liquid:
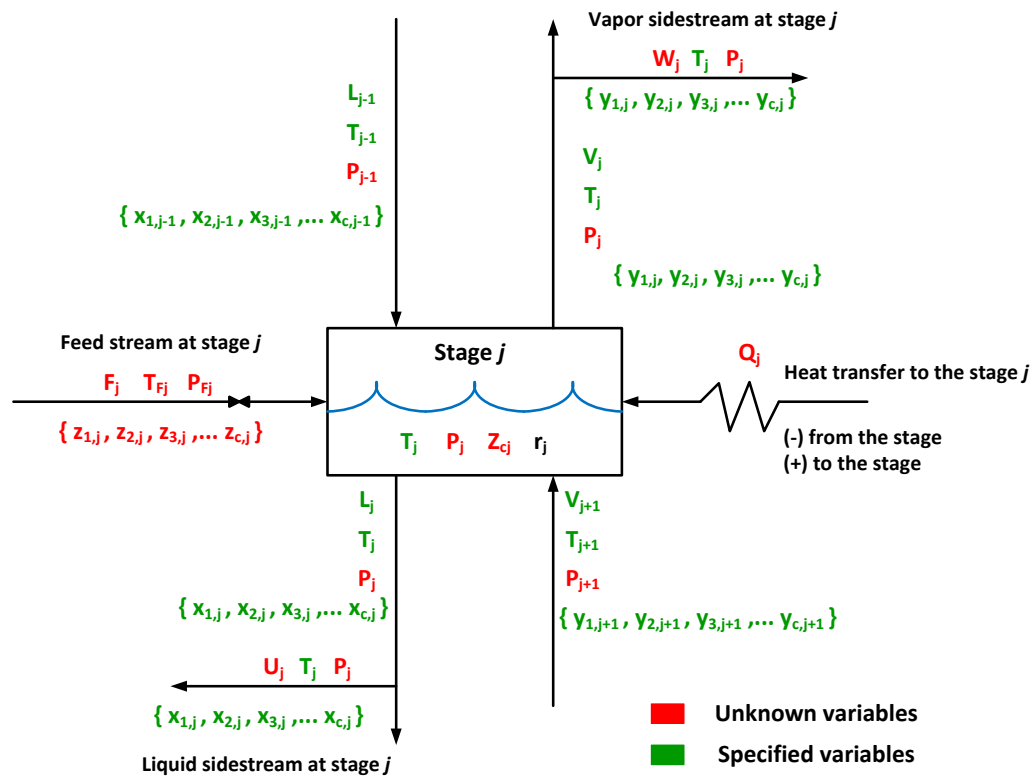
Figure 9-2: General scheme of an equilibrium stage in a distillation column.

To the stage j can enter a feed stream of one or two phases with molar flow F_j, a global molar fraction z_{ij} for the component i, temperature T_{Fj}, pressure P_{Fj}. The feed pressure must be greater or

equal to the pressure of the stage P_j. To the stage j enters a liquid from the upper stage $j\text{-}1$ with molar flow L_{j-1}, a mole fraction composition $x_{i,\,j-1}$, a temperature T_{j-1} and a pressure P_{j-1}. Likewise, from the lower phase $j+1$ enters to stage j a vapor stream with molar flow V_{j+1}, with a mole fraction $y_{i,j+1}$, a temperature T_{j+1} and a pressure P_{j+1}.

The vapor stream leaving stage j has as intensive properties y_{ij}, T_{j} and P_j. This stream can be divided into a side stream with molar flow W_j and a stream V_j to stage $j\text{-}1$, or if $j=1$ and the condenser is partial, the vapor stream leaves the column as top product V_1. If the condenser is total, there is no vapor flow from this stage. The liquid stream leaving the stage j has as intensive properties x_{ij}, T_j and P_j and is in equilibrium with the vapor. This liquid can also be divided into a liquid side stream with molar flow U_j and a stream L_j passing to stage $j+1$ or, if $n = j$, this stream leaves the separator as bottoms.

Heat Q_j can be transmitted from (-) or to (+) stage j to simulate coolers, heaters and intermediate reboilers.

Development of the mathematical model

Mass balance in the stage j:

$$M_{i,j} = L_{j-1}x_{i,j-1} + V_{j+1}y_{i,j+1} + F_j z_{i,j} - \left(L_j + U_j\right)x_{i,j} - \left(V_j - W_j\right)y_{i,j} + Z_{Cj}\frac{v_i}{\left|v_k\right|}r_j = 0 \qquad (0.77)$$

where:

Z_{Cj} : retention or ammount of catalyst
v_i : stoichiometric coefficient of component i
v_k: stoichiometric coefficient of refence component k
r_j : reaction rate

Equilibrium relation of component i for the stage j:

$$E_{i,j} = K_{i,j}x_{i,j} - y_{i,j} = 0 \qquad (0.78)$$

Summation equations for the stage j:

$$S_j^V = \sum_{i=1}^{C} y_{i,j} - 1 = 0 \qquad (0.79)$$

$$S_j^L = \sum_{i=1}^{C} x_{i,j} - 1 = 0 \qquad (0.80)$$

Energy balance in the stage j

$$H_j = L_{j-1}\hat{H}_{L,j-1} + V_{j+1}\hat{H}_{V,j-1} + F_j\hat{H}_{F,j} - \left(L_j + U_j\right)\hat{H}_{L,j} - \left(V_j + W_j\right)\hat{H}_{V,j} + Q_j = 0 \qquad (0.81)$$

The variables to model a stage of a reactive distillation column are shown in Table 9.1.

Table 9-1: Variables to model a stage of a reactive distillation column.

Variables of the stage *j*	Symbol	Value
Vapor flow rate	V_j	1
Liquid flow rate	L_j	1
Liquid side stream	U_j	1
Vapor side stream	W_j	1
Feed flow rate	F_j	1
Vapor molar fraction	$y_{i,j}$	c
Liquid molar fraction	$x_{i,j}$	c
Feed molar fraction	$z_{i,j}$	c
Temperature of the stage	T_j	1
Temperature of the feed	T_{Fj}	1
Pressure of the stage	P_j	1
Pressure of the feed	P_{Fj}	1
Heat flow	Q_j	1
Retention or amount of catalyst	Z_{Cj}	1
	TOTAL	**11+3c**

In the Table 9.1 are not included variables such as the reaction rate r_j, enthalpies H_{Lj}, H_{Vj}, H_{Fj} and the distribution coefficient $K_{i,j}$ because these variables are functions of temperature T_j, pressure P_j, vapor composition $y_{i,j}$ and liquid composition $x_{i,j}$ of the stage.

$$K_{ij} = K_{ij}\left(T_j, P_j, x_{i,j}, y_{i,j}\right)$$
$$H_{Vj} = H_{Vj}\left(T_j, P_j, y_{i,j}\right)$$
$$H_{Lj} = H_{Lj}\left(T_j, P_j, x_{i,j}\right)$$
$$H_{Fj} = H_{Fj}\left(T_F, P_F, z_{i,j}\right)$$
$$r_j = r_j\left(T_j, x_{i,j}, y_{i,j}\right)$$

The number of stages of the distillation column must be also considered as an additional variable. Thus, the total number of variables is $11+3c$ per stage plus the number of stages.

In consequence, the total number of variables to model a reactive distillation column is:

$$n(11+3c)+1 \tag{0.82}$$

Table 9.2 shows the MESH equations necessary to model a stage of a reactive distillation column:

Table 9-2: MESH equations to model a stage of a reactive distillation column.

Equations of the stage j	Value
Balance per component	c
Equilibrium equations	c
Summation equations	2
Energy balance	1
TOTAL	**3+2c**

Each stage of the distillation column has the same set of equations, so, the total number of equations to model a reactive distillation column is:

$$n(3+2c) \tag{0.83}$$

A system of equations has a unique solution when the number of independent equations is the same as the number of unknown variables. In this case, the number of unknown variables is higher than the number of equations:

$$\text{Number of equations} \quad < \quad \text{Number of variables}$$
$$n(3+2c) \quad\quad < \quad\quad n(11+3c)+1$$

Therefore, some variables must be specified to solve the system and to find the value of the variables. The number of variables to be specified it is calculated by subtracting the equations (9.6) and (9.7):

$$\left[n(11+3c)+1\right]-\left[n(c+2c)\right]=n(8+c)+1 \tag{0.84}$$

In general, the specified variables correspond to operating variables which can be manipulated by the user outside the column.

Table 9-3: Variables to specify per stage.

Variables of the stage j	Symbol	Value
Liquid side stream	U_j	1
Vapor side stream	W_j	1
Feed flow rate	F_j	1
Feed molar fraction	$z_{i,j}$	c
Temperature of the stage	T_j	1
Temperature of the feed	T_{Fj}	1
Pressure of the stage	P_j	1
Pressure of the feed	P_{Fj}	1
Heat flow	Q_j	1
Retention or amount of catalyst	Z_{Cj}	1
TOTAL		**8+c**

Table 9.3 shows all the *8+c* variables to specify per stage. Hence, for the entire column, *n(8+c)* variables must be specified. If the number of stages is also defined, the previous equation will increase its value to *n(8+c)+1*. In Table 9.3 it is also possible to notice that the heat flow is a specified variable since the stage 2 till stage *n-1*, as long as values for Q_1 and Q_n have to be calculated, therefore, two other values corresponding to two additional variables must be introduced to replace the heat flows in the condenser and the boiler. Usually, reflux (L_1) and distillate ($D = V_1 + U_1$) are also stated.

The following table shows the variables to be calculated to design a reactive distillation column.

Table 9-4: Variables to be calculated per stage.

Variables of the stage j	Symbol	Value
Vapor flow rate	V_j	1
Liquid flow rate	L_j	1
Vapor molar fraction	$y_{i,j}$	c
Liquid molar fraction	$x_{i,j}$	c
Temperature of the stage	T_j	1
TOTAL		**3+2c**

To demonstrate that it is not necessary to introduce the total mass balance as an additional equation because this equation is a linear combination of the MESH equations.

Adding the c mass balance per component of the stage j - Equation (0.85) –, it is obtained:

$$\sum_{i=1}^{C} M_{i,j} = \sum_{i=1}^{C} \left[L_{j-1} x_{i,j-1} + V_{j+1} y_{i,j+1} + F_j z_{i,j} - \left(L_j + U_j \right) x_{i,j} - \left(V_j - W_j \right) y_{i,j} + Z_{Cj} \frac{v_i}{|v_k|} r_j \right] = 0$$

Using the properties of summation:

$$\sum_{i=1}^{C} M_{i,j} = \sum_{i=1}^{C} \left[L_{j-1} x_{i,j-1} \right] + \sum_{i=1}^{C} \left[V_{j+1} y_{i,j+1} \right] + \sum_{i=1}^{C} \left[F_j z_{i,j} \right] + \dots$$
$$\dots - \sum_{i=1}^{C} \left[\left(L_j + U_j \right) x_{i,j} \right] - \sum_{i=1}^{C} \left[\left(V_j - W_j \right) y_{i,j} \right] + \sum_{i=1}^{C} \left[Z_{Cj} \frac{v_i}{|v_k|} r_j \right] = 0$$

Then, isolating the independent terms:

$$\sum_{i=1}^{C} M_{i,j} = L_{j-1} \sum_{i=1}^{C} \left[x_{i,j-1} \right] + V_{j+1} \sum_{i=1}^{C} \left[y_{i,j+1} \right] + F_j \sum_{i=1}^{C} \left[z_{i,j} \right] + \dots$$
$$\dots - \left(L_j + U_j \right) \sum_{i=1}^{C} \left[x_{i,j} \right] - \left(V_j - W_j \right) \sum_{i=1}^{C} \left[y_{i,j} \right] + \frac{Z_{Cj}}{|v_k|} r_j \sum_{i=1}^{C} \left[v_i \right] = 0$$

Replacing Equations (0.86) and (0.87) in the last expression, it is obtained:

$$\sum_{i=1}^{C} M_{i,j} = M_j = L_{j-1} + V_{j+1} + F_j \sum_{i=1}^{C} \left[z_{i,j} \right] - \left(L_j + U_j \right) - \left(V_j - W_j \right) + \frac{Z_{Cj}}{|v_k|} r_j \sum_{i=1}^{C} \left[v_i \right] = 0$$

As the feed molar composition z_{ij} is a known variable, the relation $\sum_{i=1}^{C} z_{i,j} = 1$ must be satisfied.

Thus, by applying this restriction:

$$\sum_{i=1}^{C} M_{i,j} = M_j = L_{j-1} + V_{j+1} + F_j - \left(L_j + U_j \right) - \left(V_j - W_j \right) + \frac{Z_{Cj}}{|v_k|} r_j \sum_{i=1}^{C} \left[v_i \right] = 0$$

The last equation is the same as the total mass balance of the stage j:

$$M_j = L_{j-1} + V_{j+1} + F_j - \left(L_j + U_j \right) - \left(V_j - W_j \right) + \frac{Z_{Cj}}{|v_k|} r_j v_i = 0 \tag{0.88}$$

For the energy balance - Equation (0.89) – the standard state for a component is its pure form at atmospheric pressure and the temperature of interest, which is choose to be 298 K (25°C).

As a demonstration, it will be show that the energy balance, including the heat of reaction, is equal to Equation (0.90) when the enthalpy of each component is referred to the chemical elements.

Assuming the enthalpy of mixing is ignored, the molar enthalpy for both vapor and liquid are defined as:

$$\hat{H}_{L,i} = \sum_{i=1}^{C} \left[x_{i,j} \hat{H}_{L\,i,j} \right] \tag{0.91}$$

$$\hat{H}_{V,i} = \sum_{i=1}^{C} \left[y_{i,j} \hat{H}_{V\,i,j} \right] \tag{0.92}$$

The molar enthalpy of component *i* is defined as:

$$\hat{H}_{L\,i} = \hat{H}^{\circ}_{form,i} + \widehat{\hat{H}}_{L\,i} \tag{0.93}$$

$$\hat{H}_{V\,i} = \hat{H}^{\circ}_{form,i} + \widehat{\hat{H}}_{V\,i} \tag{0.94}$$

where:

$$\widehat{\hat{H}}_{L\,i} = \left\{ \int_{T_{ref}}^{T_j} \left[\hat{C}_P^{gi}(T) dT \right] \right\} - \hat{H}_{vap,i}(T_j) \tag{0.95}$$

$$\widehat{\hat{H}}_{V\,i} = \int_{T_{ref}}^{T_j} \left[\hat{C}_P^{gi}(T) dT \right] \tag{0.96}$$

and $\hat{H}^{\circ}_{form,i}$ is the standard enthalpy of formation of component *i*.

By replacing Equations (0.97) and (0.98) in (0.99) and (0.100) respectively, it is possible to obtain the following expression:

$$\hat{H}_{L\,i} = \sum_{i=1}^{C} x_{i,j} \left(\hat{H}^{\circ}_{form,i} + \widehat{\hat{H}}_{L\,i} \right) \tag{0.101}$$

$$\hat{H}_{V\,i} = \sum_{i=1}^{C} y_{i,j} \left(\hat{H}^{\circ}_{form,i} + \widehat{\hat{H}}_{V\,i} \right) \tag{0.102}$$

Rearranging:

$$\hat{H}_{L\,i} = \sum_{i=1}^{C} \left[x_{i,j} \hat{H}^{\circ}_{form,i} \right] + \sum_{i=1}^{C} \left[x_{i,j} \widehat{\hat{H}}_{L\,i} \right] \tag{0.103}$$

$$\hat{H}_{V\,i} = \sum_{i=1}^{C} \left[y_{i,j} \hat{H}^{\circ}_{form,i} \right] + \sum_{i=1}^{C} \left[y_{i,j} \widehat{\hat{H}}_{V\,i} \right] \tag{0.104}$$

Thus:

$$\hat{H}_{L\,i} = \sum_{i=1}^{C} \left[x_{i,j} \hat{H}^{\circ}_{form,i} \right] + \widehat{\hat{H}}_{L\,i} \tag{0.105}$$

$$\hat{H}_{V\,i} = \sum_{i=1}^{C} \left[y_{i,j} \hat{H}^{\circ}_{form,i} \right] + \widehat{\hat{H}}_{V\,i} \tag{0.106}$$

where:

$$\widehat{\hat{H}}_{L\,i} = \sum_{i=1}^{C} \left[x_{i,j} \widehat{\hat{H}}_{L\,i,j} \right] \tag{0.107}$$

$$\widehat{\hat{H}}_{V\,i} = \sum_{i=1}^{C} \left[y_{i,j} \widehat{\hat{H}}_{V\,i,j} \right] \tag{0.108}$$

Equations (0.109) and (0.110) are the standard enthalpy of formation for the liquid and vapor phase.

Replacing Equations (0.111) and (0.112) in (0.113), it becomes in:

$$H_j = L_{j-1}\left[\sum_{i=1}^{C}\left[x_{i,j-1}\hat{H}^{\circ}_{form,i}\right]+\hat{\widehat{H}}_{L\,j-1}\right]+V_{j+1}\left[\sum_{i=1}^{C}\left[y_{i,j+1}\hat{H}^{\circ}_{form,i}\right]+\hat{\widehat{H}}_{V\,j+1}\right]+\dots$$
$$\dots+F_j\left[\sum_{i=1}^{C}\left[z_{i,j}\hat{H}^{\circ}_{form,i}\right]+\hat{\widehat{H}}_{F\,j}\right]-\left(L_j-U_j\right)\left[\sum_{i=1}^{C}\left[x_{i,j}\hat{H}^{\circ}_{form,i}\right]+\hat{\widehat{H}}_{L\,j}\right]+\dots \tag{0.114}$$
$$\dots-\left(V_j-W_j\right)\left[\sum_{i=1}^{C}\left[y_{i,j}\hat{H}^{\circ}_{form,i}\right]+\hat{\widehat{H}}_{V\,j}\right]+Q_j=0$$

Rearranging:

$$H_j = L_{j-1}\hat{\widehat{H}}_{L\,j-1}+V_{j+1}\hat{\widehat{H}}_{V\,j+1}+F_j\hat{\widehat{H}}_{F\,j}-\left(L_j-U_j\right)\hat{\widehat{H}}_{L\,j}-\left(V_j-W_j\right)\hat{\widehat{H}}_{V\,j}+Q_j+\dots$$
$$\dots+L_{j-1}\left[\sum_{i=1}^{C}\left[x_{i,j-1}\hat{H}^{\circ}_{form,i}\right]\right]+V_{j+1}\left[\sum_{i=1}^{C}\left[y_{i,j+1}\hat{H}^{\circ}_{form,i}\right]\right]+F_j\left[\sum_{i=1}^{C}\left[z_{i,j}\hat{H}^{\circ}_{form,i}\right]\right]+\dots \tag{0.115}$$
$$\dots-\left(L_j-U_j\right)\left[\sum_{i=1}^{C}\left[x_{i,j}\hat{H}^{\circ}_{form,i}\right]\right]-\left(V_j-W_j\right)\left[\sum_{i=1}^{C}\left[y_{i,j}\hat{H}^{\circ}_{form,i}\right]\right]=0$$

Defining $\tilde{H}_j$ as:

$$\tilde{H}_j = L_{j-1}\hat{\widehat{H}}_{L\,j-1}+V_{j+1}\hat{\widehat{H}}_{V\,j+1}+F_j\hat{\widehat{H}}_{F\,j}-\left(L_j-U_j\right)\hat{\widehat{H}}_{L\,j}-\left(V_j-W_j\right)\hat{\widehat{H}}_{V\,j}+Q_j \tag{0.116}$$

$$H_j = \tilde{H}_j + L_{j-1}\left[\sum_{i=1}^{C}\left[x_{i,j-1}\hat{H}^{\circ}_{form,i}\right]\right]+V_{j+1}\left[\sum_{i=1}^{C}\left[y_{i,j+1}\hat{H}^{\circ}_{form,i}\right]\right]+F_j\left[\sum_{i=1}^{C}\left[z_{i,j}\hat{H}^{\circ}_{form,i}\right]\right]+\dots$$
$$\dots-\left(L_j-U_j\right)\left[\sum_{i=1}^{C}\left[x_{i,j}\hat{H}^{\circ}_{form,i}\right]\right]-\left(V_j-W_j\right)\left[\sum_{i=1}^{C}\left[y_{i,j}\hat{H}^{\circ}_{form,i}\right]\right]=0 \tag{0.117}$$

$$H_j = \tilde{H}_j + \left[\sum_{i=1}^{C}\begin{array}{l}L_{j-1}\left[x_{i,j-1}\hat{H}^{\circ}_{form,i}\right]+V_{j+1}\left[y_{i,j+1}\hat{H}^{\circ}_{form,i}\right]+F_j\left[z_{i,j}\hat{H}^{\circ}_{form,i}\right]+\dots\\ \dots-\left(L_j-U_j\right)\left[x_{i,j}\hat{H}^{\circ}_{form,i}\right]-\left(V_j-W_j\right)\left[y_{i,j}\hat{H}^{\circ}_{form,i}\right]\end{array}\right]=0 \tag{0.118}$$

$$H_j = \tilde{H}_j + \sum_{i=1}^{C}\left[\hat{H}^{\circ}_{form,i}\right]\left[L_{j-1}x_{i,j-1}+V_{j+1}y_{i,j+1}+F_jz_{i,j}-\left(L_j-U_j\right)x_{i,j}-\left(V_j-W_j\right)y_{i,j}\right]=0$$
$$\tag{0.119}$$

$$M_{i,j}=L_{j-1}x_{i,j-1}+V_{j+1}y_{i,j+1}+F_jz_{i,j}-\left(L_j+U_j\right)x_{i,j}-\left(V_j-W_j\right)y_{i,j}+Z_{Cj}\frac{v_i}{|v_k|}r_j=0$$

$$-Z_{Cj}\frac{v_i}{|v_k|}r_j=L_{j-1}x_{i,j-1}+V_{j+1}y_{i,j+1}+F_jz_{i,j}-\left(L_j+U_j\right)x_{i,j}-\left(V_j-W_j\right)y_{i,j} \tag{0.120}$$

$$H_j = \tilde{H}_j + \sum_{i=1}^{C} \left\{ \left[\hat{H}^{\circ}_{form,i} \right] \left[-Z_{Cj} \frac{v_i}{|v_k|} r_j \right] \right\} = 0$$

$$H_j = \tilde{H}_j - \frac{Z_{Cj}}{|v_k|} r_j \sum_{i=1}^{C} \left[\hat{H}^{\circ}_{form,i} v_i \right] = 0$$

(0.121)

$$H_j = L_{j-1}\hat{\hat{H}}_{L\,j-1} + V_{j+1}\hat{\hat{H}}_{V\,j+1} + F_j\hat{\hat{H}}_{Fj} - \left(L_j - U_j \right)\hat{\hat{H}}_{L\,j} + \dots$$

$$\dots - \left(V_j - W_j \right)\hat{\hat{H}}_{V\,j} + Q_j - \underbrace{\frac{Z_{Cj}}{|v_k|} r_j \sum_{i=1}^{C} \left[\hat{H}^{\circ}_{form,i} v_i \right]}_{\text{Enthalpy of mixing}} = 0$$

(0.122)

Extension of the Wang – Henke algorithm to reactive distillation columns

The Wang - Henke algorithm was developed by J.C. Wang and G.E. Henke in 1966. The basic structural formulation of the algorithm uses the MESH (Mass – Energy – Entropy – Enthalpy) equations presented inabove:

Mass balance for the stage j

$$M_{i,j} = L_{j-1}x_{i,j-1} + V_{j+1}y_{i,j+1} + F_j z_{i,j} - \left(L_j + U_j \right)x_{i,j} - \left(V_j - W_j \right)y_{i,j} + Z_{Cj}\frac{v_i}{|v_k|}r_j = 0 \qquad (0.123)$$

Equilibrium relation of component i for the stage j:

$$E_{i,j} = K_{i,j}x_{i,j} - y_{i,j} = 0 \qquad (0.124)$$

Summation equations for the stage j:

$$S_j^V = \sum_{i=1}^{C} y_{i,j} - 1 = 0 \qquad (0.125)$$

$$S_j^L = \sum_{i=1}^{C} x_{i,j} - 1 = 0 \qquad (0.126)$$

Energy balance in the stage j:

$$H_j = L_{j-1}\hat{H}_{L,j-1} + V_{j+1}\hat{H}_{V,j-1} + F_j\hat{H}_{F,j} - \left(L_j + U_j \right)\hat{H}_{L,j} - \left(V_j + W_j \right)\hat{H}_{V,j} + Q_j = 0 \qquad (0.127)$$

In general, the Wang – Henke method is powerful and useful because it is easily manipulated algebraically in order to create a set of equations where independent variables are the molar fractions in liquid phase $x_{i,j}$, the vapor flow rate V_j and the temperature of the stage T_j in the reactive distillation column.

The first step in the formulation of the method is to combine the mass balance M_j from stage 1 to stage j. This equation represents the total mass balance for all the j stages. By means of this

equation, the mass balances for each component $M_{i,j}$ and the equilibrium relations $E_{i,j}$ it is possible to construct a tridiagonal system of equations where the independent variables are the molar fractions in liquid phase $x_{i,j}$. In the same way, with the energy balance equation H_j and the total mass balance for all the j stages, another system is formed where the independent variable is the vapor flow rate V_j. Then, by using the stoichiometric and equilibrium relation s an equation is established having the temperature T_j as independent variable. Initially, it must be established an auxiliary equation that makes finding the solution(s) of the system of equations easier. This new function is obtained by adding the total mass balances from the stage 1 to the stage j. Rearranging the total mass balances of the stage m:

$$M_j = L_{j-1} + V_{j+1} - L_j - V_j + \left(F_j - U_j - W_j \right) + \frac{Z_{Cj}}{|v_k|} r_j \sum_{i=1}^{C} [v_i] = 0 \qquad (0.128)$$

The total mass balances from the stage 1 to the stage j, are:

$$j = 1 \quad \rightarrow \quad M_1 = L_0 + V_2 - L_1 - V_1 + \left(F_1 - U_1 - W_1 \right) + \frac{Z_{C1}}{|v_k|} r_1 \sum_{i=1}^{C} [v_i] = 0$$

$$j = 2 \quad \rightarrow \quad M_2 = L_1 + V_3 - L_2 - V_2 + \left(F_2 - U_2 - W_2 \right) + \frac{Z_{C2}}{|v_k|} r_2 \sum_{i=1}^{C} [v_i] = 0$$

$$j = 3 \quad \rightarrow \quad M_3 = L_2 + V_4 - L_3 - V_3 + \left(F_3 - U_3 - W_3 \right) + \frac{Z_{C3}}{|v_k|} r_3 \sum_{i=1}^{C} [v_i] = 0$$

$$\begin{matrix} \vdots & \vdots & \vdots \\ \vdots & \vdots & \vdots \end{matrix}$$

$$j = m-1 \rightarrow \quad M_{m-1} = L_{m-2} + V_m - L_{m-1} - V_{m-1} + \left(F_{m-1} - U_{m-1} - W_{m-1} \right) + \frac{Z_{Cm-1}}{|v_k|} r_{m-1} \sum_{i=1}^{C} [v_i] = 0$$

$$(0.129)$$

$$j = m \quad \rightarrow \quad M_m = L_{m-1} + V_{m+1} - L_m - V_m + \left(F_m - U_m - W_m \right) + \frac{Z_{Cm}}{|v_k|} r_m \sum_{i=1}^{C} [v_i] = 0$$

$$j = m+1 \rightarrow \quad M_{m+1} = L_m + V_{m+2} - L_{m+1} - V_{m+1} + \left(F_{m+1} - U_{m+1} - W_{m+1} \right) + \frac{Z_{Cm+1}}{|v_k|} r_{m+1} \sum_{i=1}^{C} [v_i] = 0$$

$$\begin{matrix} \vdots & \vdots & \vdots \\ \vdots & \vdots & \vdots \end{matrix}$$

$$j = j-1 \rightarrow \quad M_{j-1} = L_{j-2} + V_j - L_{j-1} - V_{j-1} + \left(F_{j-1} - U_{j-1} - W_{j-1} \right) + \frac{Z_{Cj-1}}{|v_k|} r_{j-1} \sum_{i=1}^{C} [v_i] = 0$$

$$j = j \quad \rightarrow \quad M_j = L_{j-1} + V_{j+1} - L_j - V_j + \left(F_j - U_j - W_j \right) + \frac{Z_{Cj}}{|v_k|} r_j \sum_{i=1}^{C} [v_i] = 0$$

The total mass balances from the stage 1 to the stage j are summed. This summation is carried out step by step to clearly identify the resultant term. At first, the total mass balances from stages 1 and 2 are summed.

$$\sum_{q=1}^{2} M_q = M_1 + M_2 = \left(\begin{array}{l} L_0 + \cancel{V_2} - \cancel{L_1} - V_1 + \left(F_1 - U_1 - W_1 \right) + \dfrac{Z_{C1}}{|v_k|} r_1 \sum_{i=1}^{C} [v_i] + \dots \\[3mm] \dots + \cancel{L_1} + V_3 - L_2 - \cancel{V_2} + \left(F_2 - U_2 - W_2 \right) + \dfrac{Z_{C2}}{|v_k|} r_2 \sum_{i=1}^{C} [v_i] \end{array} \right) = 0$$

$$\sum_{q=1}^{2} M_q = M_1 + M_2 = L_0 - V_1 + V_3 - L_2 + \sum_{p=1}^{2} \left(F_p - U_p - W_p \right) + \sum_{p=1}^{2} \left(\dfrac{Z_{Cp}}{|v_k|} r_p \sum_{i=1}^{C} [v_i] \right) = 0$$

To the last equation is added the total mass balance of the stage 3 and then, successively, till the stage *m*, obtaining then the following expression:

$$\sum_{q=1}^{m} M_q = M_1 + M_2 + M_3 + \dots + M_{m-1} + M_m =$$

$$= \left(\begin{array}{l} L_0 - V_1 + \cancel{V_m} - \cancel{L_{m-1}} + \sum_{p=1}^{m-1} \left(F_p - U_p - W_p \right) + \sum_{p=1}^{m-1} \left(\dfrac{Z_{Cp}}{|v_k|} r_p \sum_{i=1}^{C} [v_i] \right) + \dots \\[3mm] \dots + \cancel{L_{m-1}} + V_{m+1} - L_m - \cancel{V_m} + \left(F_m - U_m - W_m \right) + \sum_{p=1}^{m} \left(\dfrac{Z_{Cp}}{|v_k|} r_p \sum_{i=1}^{C} [v_i] \right) \end{array} \right) = 0$$

$$\sum_{q=1}^{m} M_q = L_0 - V_1 + V_{m+1} - L_m + \sum_{p=1}^{m} \left(F_p - U_p - W_p \right) + \sum_{p=1}^{m} \left(\dfrac{Z_{Cp}}{|v_k|} r_p \sum_{i=1}^{C} [v_i] \right) = 0$$

In general, for the stage *j*, the next result is obtained:

$$\sum_{q=1}^{j} M_q = \left[M_1 + M_2 + M_3 + \dots + M_{m-1} + M_m + \dots + M_{j-1} \right] + M_j =$$

$$= \left(\begin{array}{l} L_0 - V_1 + \cancel{V_m} - \cancel{L_{m-1}} + \sum_{p=1}^{m-1} \left(F_p - U_p - W_p \right) + \sum_{p=1}^{m-1} \left(\dfrac{Z_{Cp}}{|v_k|} r_p \sum_{i=1}^{C} [v_i] \right) + \dots \\[3mm] \dots + \cancel{L_{m-1}} + V_{m+1} - L_m - \cancel{V_m} + \left(F_m - U_m - W_m \right) + \sum_{p=1}^{m} \left(\dfrac{Z_{Cp}}{|v_k|} r_p \sum_{i=1}^{C} [v_i] \right) \end{array} \right) = 0$$

$$\sum_{q=1}^{j} M_q = L_0 - V_1 + V_{j+1} - L_j + \sum_{p=1}^{j} \left(F_p - U_p - W_p \right) + \sum_{p=1}^{j} \left(\dfrac{Z_{Cp}}{|v_k|} r_p \sum_{i=1}^{C} [v_i] \right) = 0$$

According to the description of the reactive distillation presented in Figure 9.1 there is no *stage 0 (zero)* and as L_j represents the liquid flow rate, thus the term L_0 disappears from the previous equation.

$$\sum_{q=1}^{j} M_q = V_{j+1} - L_j - V_1 + \sum_{p=1}^{j} \left(F_p - U_p - W_p \right) + \sum_{p=1}^{j} \left(\dfrac{Z_{Cp}}{|v_k|} r_p \sum_{i=1}^{C} [v_i] \right) = 0 \qquad (0.130)$$

The physical meaning of this can be understood as a total mass balance covering the distillation column from stage 1 to *j*, as seen in Figure 9.3. Table 9.5 shows a summary of the inlet and outlet flows of the system.

$$\sum_{p=1}^{j}\left(F_p - W_p\right) = \qquad = \sum_{p=1}^{j} -U_p$$
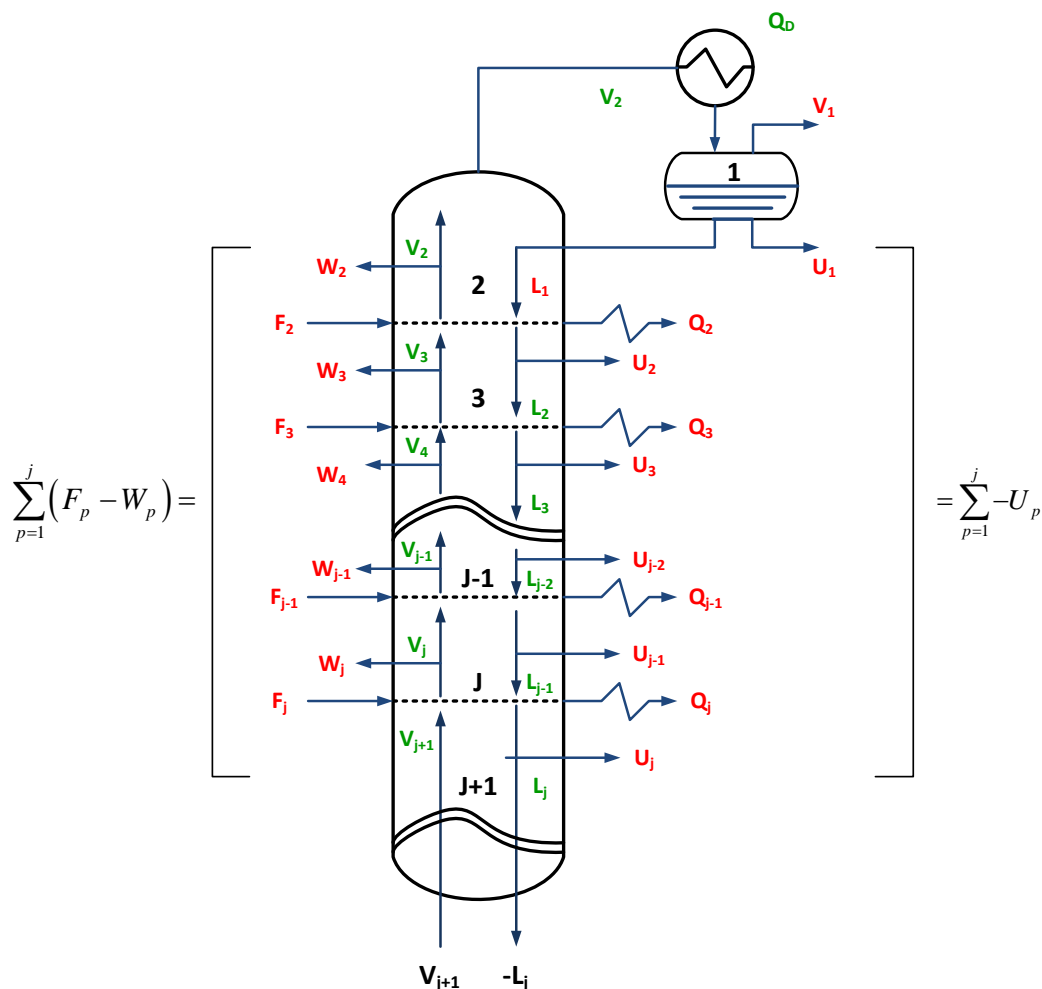
Figure 9-3: Total mass balance from stage 1 to *j*

Table 9-5: Inlet and outlet flows total of the total mass balance from stage 1 to j.

Outlet flows	
Vapor flow rate to condenser	V_1
Liquid flow rate	L_j
Liquid side stream	$\sum_{p=1}^{j} U_p$
Vapor side stream	$\sum_{p=1}^{j} W_p$

Table 9-5 (cont.)	
Inlet flows	
Vapor flow rate leaving the *j+1* stage	V_{j+1}
Liquid side stream	$\sum_{p=1}^{j} F_p$

A mass balance as its original form is described by:

$$Acummulation = Input - Output + Generation - Consumption \qquad (0.131)$$

By considering the system in steady state, the accumulation in the system is zero; the generation and consumption are determined by the reaction rate (r_j) referred to the component k. When the relation $\dfrac{v_i}{|v_k|}$ is positive it is said that component i is being generated; on the other hand, when the relation $\dfrac{v_i}{|v_k|}$ is negative it is said that component i is being consumed. v_i is the stoichiometric coefficient of component i and v_k is the stoichiometric coefficient related to the reaction rate (r_j). The mole generation or consumption of component i, in the stage j, is defined by the expression:

$$\underbrace{Z_{Cj}}_{\substack{\text{Retention or} \\ \text{amount of catalyst}}} \cdot \underbrace{\frac{v_i}{|v_k|}}_{\substack{\text{Consumption} \\ \text{or generation}}} \cdot \underbrace{r_j}_{\text{Reaction rate}}$$

The rate of mole change can be found by summing the previous equation for all the components:

$$\sum_{i=1}^{c}\left(Z_{Cj}\frac{v_i}{|v_k|}r_j \right) = \frac{Z_{Cj}}{|v_k|}r_j\sum_{i=1}^{c}[v_i]$$

Replacing then we have:

$$0 = \underbrace{V_{j+1}+\sum_{p=1}^{j}F_p}_{\text{Inputs of the system}} - \underbrace{\left(V_1+L_j+\sum_{p=1}^{j}U_p+\sum_{p=1}^{j}W_p\right)}_{\text{Outputs of the system}} + \underbrace{\sum_{p=1}^{j}\left(\frac{Z_{Cp}}{|v_k|}r_p\sum_{i=1}^{C}[v_i]\right)}_{\text{Generation and consumption}}$$

And rearranging…

$$V_{j+1}-L_j-V_1+\sum_{p=1}^{j}\left(F_p-U_p-W_p\right)+\sum_{p=1}^{j}\left(\frac{Z_{Cp}}{|v_k|}r_p\sum_{i=1}^{C}[v_i]\right)=0$$

If the liquid flow rate L_j is isolated, it is possible to find a general equation for all the liquid flows in the column:

$$L_j = V_{j+1}-V_1+\sum_{p=1}^{j}\left(F_p-U_p-W_p\right)+\sum_{p=1}^{j}\left(\frac{Z_{Cp}}{|v_k|}r_p\sum_{i=1}^{C}[v_i]\right) \qquad (0.132)$$

Considering that there is not a feed stream F_j neither a vapor side stream W_j in the condenser (stage 1), equation 9.56 becomes:

$$L_j = V_{j+1}-V_1-\cancel{F_1}-U_1-\cancel{W_1}+\sum_{p=2}^{j}\left(F_p-U_p-W_p\right)+\sum_{p=1}^{j}\left(\frac{Z_{Cp}}{|v_k|}r_p\sum_{i=1}^{C}[v_i]\right)$$

$$L_j = V_{j+1} - (V_1 + U_1) + \sum_{p=2}^{j}(F_p - U_p - W_p) + \sum_{p=1}^{j}\left(\frac{Z_{Cp}}{|v_k|}r_p\sum_{i=1}^{C}[v_i]\right)$$

Setting $D = V_1 + U_1$, with D representing the distillate flow (top):

$$L_j = V_{j+1} - D + \sum_{p=2}^{j}(F_p - U_p - W_p) + \sum_{p=1}^{j}\left(\frac{Z_{Cp}}{|v_k|}r_p\sum_{i=1}^{C}[v_i]\right) \tag{0.133}$$

To construct the tridiagonal matrix, L_j and L_{j-1} must be replaced in equation 9.1 - mass balance per component -. L_j and L_{j-1} are defined by:

$$L_j = V_{j+1} - D + \sum_{p=2}^{j}(F_p - U_p - W_p) + \sum_{p=1}^{j}\left(\frac{Z_{Cp}}{|v_k|}r_p\sum_{i=1}^{C}[v_i]\right) \tag{0.134}$$

$$L_{j-1} = V_j - D + \sum_{p=2}^{j-1}(F_p - U_p - W_p) + \sum_{p=1}^{j-1}\left(\frac{Z_{Cp}}{|v_k|}r_p\sum_{i=1}^{C}[v_i]\right) \tag{0.135}$$

Having then:

$$M_{i,j} = \left\{V_j - D + \sum_{p=2}^{j-1}(F_p - U_p - W_p) + \sum_{p=1}^{j-1}\left(\frac{Z_{Cp}}{|v_k|}r_p\sum_{i=1}^{C}[v_i]\right)\right\}x_{i,j-1} + V_{j+1}y_{i,j+1} + \ldots$$

$$\ldots + F_j z_{i,j} - \left\{V_{j+1} - D + \sum_{p=2}^{j}(F_p - U_p - W_p) + \sum_{p=1}^{j}\left(\frac{Z_{Cp}}{|v_k|}r_p\sum_{i=1}^{C}[v_i]\right) + U_j\right\}x_{i,j-1} + \ldots \tag{0.136}$$

$$\ldots + (Vj - Wj)y_{i,j+1} + Z_{Cj}\frac{v_i}{|v_k|}r_j = 0$$

From the phase equilibria $y_{i,j}$ can be defined as:

$$y_{i,j} = K_{i,j}x_{i,j}$$
$$y_{i,j+1} = K_{i,j+1}x_{i,j+1}$$

And replacing them in equation 9.33:

$$M_{i,j} = \left\{V_j - D + \sum_{p=2}^{j-1}(F_p - U_p - W_p) + \sum_{p=1}^{j-1}\left(\frac{Z_{Cp}}{|v_k|}r_p\sum_{i=1}^{C}[v_i]\right)\right\}x_{i,j-1} + V_{j+1}\left(K_{i,j+1}x_{i,j+1}\right) + \ldots$$

$$\ldots + F_j z_{i,j} - \left\{V_{j+1} - D + \sum_{p=2}^{j}(F_p - U_p - W_p) + \sum_{p=1}^{j}\left(\frac{Z_{Cp}}{|v_k|}r_p\sum_{i=1}^{C}[v_i]\right) + U_j\right\}x_{i,j-1} + \ldots$$

$$\ldots + (V_j - W_j)\left(K_{i,j}x_{i,j}\right) + Z_{Cj}\frac{v_i}{|v_k|}r_j = 0$$

Grouping similar terms:

$$\left\{V_j - D + \sum_{p=2}^{j-1}\left(F_p - U_p - W_p\right) + \sum_{p=1}^{j-1}\left(\frac{Z_{Cp}}{|v_k|}r_p\sum_{i=1}^{C}[v_i]\right)\right\}x_{i,j-1} + \dots$$

$$\dots - \left\{V_{j+1} - D + \sum_{p=2}^{j}\left(F_p - U_p - W_p\right) + \sum_{p=1}^{j}\left(\frac{Z_{Cp}}{|v_k|}r_p\sum_{i=1}^{C}[v_i]\right) + U_j - \left(V_j - W_j\right)K_{i,j}\right\}x_{i,j} + \dots \qquad (0.137)$$

$$\dots + \left(V_{j+1}K_{i,j+1}\right)x_{i,j+1} = -\left(F_j z_{i,j} + Z_{Cj}\frac{v_i}{|v_k|}r_j\right)$$

Hence, the mass balances equations per component can be reduced to a system of equations having as a general form:

$$A_j x_{i,j-1} + B_j x_{i,j} + C_j x_{i,j+1} = D_j \qquad (0.138)$$

where,

$$A_j = \left\{V_j - D + \sum_{p=2}^{j-1}\left(F_p - U_p - W_p\right) + \sum_{p=1}^{j-1}\left(\frac{Z_{Cp}}{|v_k|}r_p\sum_{i=1}^{C}[v_i]\right)\right\} \qquad (0.139)$$

$$-\left\{V_{j+1} - D + \sum_{p=2}^{j}\left(F_p - U_p - W_p\right) + \sum_{p=1}^{j}\left(\frac{Z_{Cp}}{|v_k|}r_p\sum_{i=1}^{C}[v_i]\right) + U_j - \left(V_j - W_j\right)K_{i,j}\right\} \qquad (0.140)$$

$$C_j = \left(V_{j+1}K_{i,j+1}\right) \qquad (0.141)$$

$$D_j = -\left(F_j z_{i,j} + Z_{Cj}\frac{v_i}{|v_k|}r_j\right) \qquad (0.142)$$

By analyzing these equations it is observed that Aj is the same for both equations 1.16 and 1.12, thus $A_j = L_{j-1}$.

If $j = 1$, $A_1 = L_0$ and known that there is no stage 0 (zero), it is possible to say that A_1 does not exist. When $j = n$, i.e. the last stage of the column as shown in Figure 9.3, $C_n = V_{n+1}K_{i,n+1}$ which is illogical because there is no possibility of existence of a vapor flow V_{n+1}, therefore, C_n does not exist. In general, the system of linear equations has the following form:

$$B_j x_{i,1} + C_1 x_{i,2} = D_1 \qquad \text{for} \quad j = 1 \qquad (0.143)$$

$$A_j x_{i,j-1} + B_j x_{i,j} + C_j x_{i,j+1} = D_j \quad \text{for} \quad 2 \le j \le n\text{-}1 \qquad (0.144)$$

$$A_n x_{i,n-1} + B_n x_{i,n} = D_n \qquad \text{for} \quad j = n \qquad (0.145)$$

Or as in matrix notation:

$$
\begin{pmatrix}
B_1 & C_1 & & & & \\
A_2 & B_2 & C_2 & & & \\
 & \vdots & \vdots & & & \\
 & & A_j & B_j & C_j & \\
 & & & \vdots & \vdots & \\
 & & & A_{n-1} & B_{n-1} & C_{n-1} \\
 & & & & A_n & B_n
\end{pmatrix}
\begin{pmatrix}
x_{i,1} \\
x_{i,2} \\
\vdots \\
x_{i,j} \\
\vdots \\
x_{i,n-1} \\
x_{i,n}
\end{pmatrix}
=
\begin{pmatrix}
D_1 \\
D_2 \\
\vdots \\
D_j \\
\vdots \\
D_{n-1} \\
D_n
\end{pmatrix}
\tag{0.146}
$$

Replacing L_j and L_{j-1}, expressed by equations 9.31 and 9.32, in the energy balance (Equation 9.5) :

$$
H_j = \left\{ V_j - D + \sum_{p=2}^{j-1} (F_p - U_p - W_p) + \sum_{p=1}^{j-1} \left(\frac{Z_{Cp}}{|v_k|} r_p \sum_{i=1}^{C} [v_i] \right) \right\} \hat{H}_{L,j-1} + \dots
$$

$$
\dots - \left\{ V_{j+1} - D + \sum_{p=2}^{j} (F_p - U_p - W_p) + \sum_{p=1}^{j} \left(\frac{Z_{Cp}}{|v_k|} r_p \sum_{i=1}^{C} [v_i] \right) \right\} \hat{H}_{L,j} + \dots
$$

$$
\dots + V_{j+1} \hat{H}_{V,j+1} + F_j \hat{H}_{F,j} - U_j \hat{H}_{L,j} - (V_j + W_j) \hat{H}_{V,j} + Q_j = 0
$$

Rearranging:

$$
(\hat{H}_{L,j-1} - \hat{H}_{V,j}) V_j + (\hat{H}_{V,j+1} - \hat{H}_{L,j}) V_{j+1} = -\left\{ \sum_{p=2}^{j-1} (F_p - U_p - W_p) - D + \sum_{p=1}^{j-1} \left(\frac{Z_{Cp}}{|v_k|} r_p \sum_{i=1}^{C} [v_i] \right) \right\} \hat{H}_{L,j-1} + \dots
$$

$$
\dots + \left\{ \sum_{p=2}^{j} (F_p - U_p - W_p) - D + \sum_{p=1}^{j} \left(\frac{Z_{Cp}}{|v_k|} r_p \sum_{i=1}^{C} [v_i] \right) \right\} \hat{H}_{L,j} - F_j \hat{H}_{F,j} + U_j \hat{H}_{L,j} + W_j \hat{H}_{V,j} - Q_j
\tag{0.147}
$$

So:

$$
\sum_{p=2}^{j} (F_p - U_p - W_p) = \sum_{p=2}^{j-1} (F_p - U_p - W_p) + F_j - U_j - W_j
\tag{0.148}
$$

$$
\sum_{p=1}^{j} \left(\frac{Z_{Cp}}{|v_k|} r_p \sum_{i=1}^{C} [v_i] \right) = \sum_{p=1}^{j-1} \left(\frac{Z_{Cp}}{|v_k|} r_p \sum_{i=1}^{C} [v_i] \right) + \frac{Z_{Cj}}{|v_k|} r_j \sum_{i=1}^{C} [v_i]
\tag{0.149}
$$

Replacing equations 9.45 and 9.46 in 9.44 it is obtained:

$$
(\hat{H}_{L,j-1} - \hat{H}_{V,j}) V_j + (\hat{H}_{V,j+1} - \hat{H}_{L,j}) V_{j+1} = -\left\{ \sum_{p=2}^{j-1} (F_p - U_p - W_p) - D + \sum_{p=1}^{j-1} \left(\frac{Z_{Cp}}{|v_k|} r_p \sum_{i=1}^{C} [v_i] \right) \right\} \hat{H}_{L,j-1} + \dots
$$

$$
\dots + \left\{ \sum_{p=2}^{j-1} (F_p - U_p - W_p) - D + \sum_{p=1}^{j-1} \left(\frac{Z_{Cp}}{|v_k|} r_p \sum_{i=1}^{C} [v_i] \right) \right\} \hat{H}_{L,j} + (F_j - \cancel{U}_j - W_j) \hat{H}_{L,j} + \left(\frac{Z_{Cj}}{|v_k|} r_j \sum_{i=1}^{C} [v_i] \right) \hat{H}_{L,j} - \dots
$$

$$
\dots - F_j \hat{H}_{F,j} + \cancel{U}_j \hat{H}_{L,j} + W_j \hat{H}_{V,j} - Q_j
$$

 Grouping similar terms:

$$\left(\hat{H}_{L,j-1} - \hat{H}_{V,j}\right)V_j + \left(\hat{H}_{V,j+1} - \hat{H}_{L,j}\right)V_{j+1} =$$

$$-\left\{\sum_{p=2}^{j-1}\left(F_p - U_p - W_p\right) - D + \sum_{p=1}^{j-1}\left(\frac{Z_{Cp}}{|v_k|}r_p\sum_{i=1}^{C}[v_i]\right)\right\}\left(\hat{H}_{L,j} - \hat{H}_{L,j-1}\right) + \ldots \quad (0.150)$$

$$\ldots + \left(\hat{H}_{L,j} - \hat{H}_{F,j}\right)F_j + \left(\hat{H}_{V,j} - \hat{H}_{L,j}\right)W_j + \left(F_j - \cancel{U}_j - W_j\right)\hat{H}_{L,j} + \left(\frac{Z_{Cj}}{|v_k|}r_j\sum_{i=1}^{C}[v_i]\right)\hat{H}_{L,j} - Q_j$$

Defining the variables:

$$\alpha_j = \hat{H}_{L,j-1} - \hat{H}_{V,j}$$

$$\beta_j = \hat{H}_{V,j+1} - \hat{H}_{L,j}$$

$$\gamma_j = \left\{\sum_{p=2}^{j-1}\left(F_p - U_p - W_p\right) - D + \sum_{p=1}^{j-1}\left(\frac{Z_{Cp}}{|v_k|}r_p\sum_{i=1}^{C}[v_i]\right)\right\}\left(\hat{H}_{L,j} - \hat{H}_{L,j-1}\right) + \ldots \quad (0.151)$$

$$\ldots + \left(\hat{H}_{L,j} - \hat{H}_{F,j}\right)F_j + \left(\hat{H}_{V,j} - \hat{H}_{L,j}\right)W_j + \left(\frac{Z_{Cj}}{|v_k|}r_j\sum_{i=1}^{C}[v_i]\right)\hat{H}_{L,j} - Q_j$$

Substituting them in equation 9.47:

$$\alpha_j V_j + \beta_j V_{j+1} = \gamma_j$$

Isolating V_{j+1}:

$$V_{j+1} = \frac{\gamma_j - \alpha_j V_j}{\beta_j} \quad (0.152)$$

Setting $j = j+1$

$$V_j = \frac{\gamma_{j-1} - \alpha_{j-1}V_{j-1}}{\beta_{j-1}} \quad (0.153)$$

It is observed in Figure 9.4 that the vapor leaving the stage 2 is equal to the sum of the distillate D and the reflux L1 minus the total mole consumption or accumulation in the condenser (equation 9.26), having then:

$$V_2 = D + L_1 - \frac{Z_{Cj}}{|v_k|}r_j\sum_{i=1}^{c}v_i \quad (0.154)$$
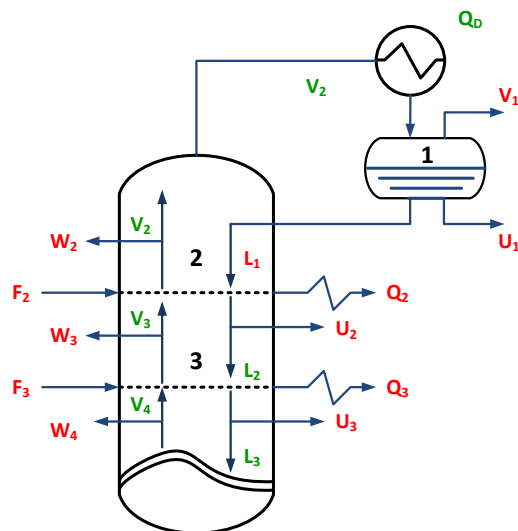
Figure 9-4: Upper zone of the reactive distillation column.

Equation 9.50 can be used to calculate V_j from V_{j+1}, thus it is possible to successively calculate all the vapor flow in the column by having calculated V_2 from equation 9.51.

In general, the equations that describe the Wang – Henke method are expressed as:

$$M_{i,j}\left(x_{i,j}, V_j, T_j\right) = \left[A_{B_C}\right] x_i - D = 0 \tag{0.155}$$

With $1 \le i \le c$ and $1 \le i \le n$

$$S\left(x_{i,j}, T_j\right) = \sum_{i=1}^{c} K_{i,j} x_{i,j} - 1 = 0 \tag{0.156}$$

With $1 \le j \le n$

$$H_j\left(x_{i,j}, V_j, T_j\right) \alpha_j V_j + \beta_j V_{j+1} - \gamma_j = 0 \tag{0.157}$$

There are c tridiagonal matrices, each one with n equations and n unknown variables, n relationships of sum and n enthalpy balances equations, for a total of $n(c+2)$ equations. So that, the number of independent variables is reduced as seen in the following table:

Independent variable	Symbol	Value
Vapor flow rate	V_j	1
Liquid molar fraction	$x_{i,j}$	c
Temperature of the stage	T_j	1
	TOTAL	*c+2*

Since the number of variables and equations is the same, the system has an algebraic solution. The energy requirement of the condenser and reboiler, Q_1 and Q_n respectively, are calculated using the corresponding energy balances. This calculation is carried out once the iterations are finished.

From the energy balance equation (equation 9.5):

$$H_j = L_{j-1}\hat{H}_{L,j-1} + V_{j+1}\hat{H}_{V,j-1} + F_j\hat{H}_{F,j} - \left(L_j + U_j\right)\hat{H}_{L,j} - \left(V_j + W_j\right)\hat{H}_{V,j} + Q_j = 0$$

And for the condenser (stage $j = 1$):

$$L_0\hat{H}_{L,0} + V_2\hat{H}_{V,2} + F_1\hat{H}_{F,1} - \left(L_1 + U_1\right)\hat{H}_{L,1} - \left(V_1 + W_1\right)\hat{H}_{V,1} + Q_1 = 0$$

Since there is no stage 0 (zero), the term $L_0\hat{H}_{L,0}$ is eliminated. Then, assuming that there is not a feed stream F_1 neither a vapor side stream W_1 in the condenser, Q_1 can be expressed as:

$$Q_c = Q_1 = V_1\hat{H}_{V,1} + \left(L_1 + U_1\right)\hat{H}_{L,1} - V_2\hat{H}_{V,2} \tag{0.158}$$

The heat duty of the condenser Q_c is calculated from the above presented equation. From Figure 9.4, it is stated that $V_2 = V_1 + U_1 + L_1$, hence, replacing in equation 9.58:

$$Q_c = V_1\hat{H}_{V,1} + \left(L_1 + U_1\right)\hat{H}_{L,1} - \left(V_1 + U_1 + L_1\right)\hat{H}_{V,2}$$

Rearranging:

$$Q_c = \left(\hat{H}_{V,1} - \hat{H}_{V,2}\right)V_1 - \left(\hat{H}_{V,2} - \hat{H}_{L,1}\right)\left(L_1 + U_1\right)$$

As the vapor enthalpy is greater than the liquid enthalpy, we have:

$$\left(\hat{H}_{V,2} - \hat{H}_{L,1}\right) \geq 0$$

On the other hand, the enthalpy of the flow $V_2\left(\hat{H}_{V,2}\right)$ is greater than the enthalpy of the flow $V_1\left(\hat{H}_{V,1}\right)$ because its temperature is higher, therefore, $\left(\hat{H}_{V,1} - \hat{H}_{V,2}\right) \leq 0$. So, regardless of the values of V_1, L_1 and U_1, $Q_c \leq 0$. It is demonstrated then that the heat duty in the condenser is negative, i.e. energy is removed from the system.

For the boiler (stage $j = n$) the equation 3.5 has the following form:

$$L_{n-1}\hat{H}_{L,n-1} + V_{n+1}\hat{H}_{V,n+1} + F_n\hat{H}_{F,n} - \left(L_n + U_n\right)\hat{H}_{L,n} - \left(V_n + W_n\right)\hat{H}_{V,n} + Q_n = 0$$

With reference to the mentioned above, the column consists of n stages, hence, there is not a vapor flow V_{n+1}, so the term $V_{n+1}\hat{H}_{V,n+1}$ disappears. Suddenly, assuming that there is not a feed stream F_n, vapor and liquid side streams - W_n and U_n -in the condenser:

$$L_{n-1}\hat{H}_{L,n-1} - L_n\hat{H}_{L,n} - V_n\hat{H}_{V,n} + Q_n = 0$$

Isolating the heat duty of the boiler is obtained:

$$Q_B = Q_n = L_n\hat{H}_{L,n} + V_n\hat{H}_{V,n} - L_{n-1}\hat{H}_{L,n-1} \tag{0.159}$$

Equation 9.59 is applied to calculate the heat duty of the boiler Q_B. From Figure 9.5 it can be seen that $L_{n-1} = V_n + L_n$, so, by replacing in equation 9.59:

$$Q_B = L_n\hat{H}_{L,n} + V_n\hat{H}_{V,n} - (L_n + V_n)\hat{H}_{L,n-1}$$

Rearranging,

$$Q_B = (\hat{H}_{V,n} - \hat{H}_{L,n-1})V_n + (\hat{H}_{L,n} - \hat{H}_{L,n-1})L_n$$

As the vapor enthalpy is greater than the liquid enthalpy, then it holds that:

$$(\hat{H}_{V,n} - \hat{H}_{L,n-1}) \geq 0$$

On the other hand, the enthalpy of the flow $L_n(\hat{H}_{L,n})$ is greater than the enthalpy of the flow $L_{n-1}(\hat{H}_{L,n-1})$ because its temperature is higher. So, regardless of the values of V_n and L_n, $Q_B \geq 0$.

It is demonstrated then that the heat duty in the boiler is positive, i.e. energy is added to the system.
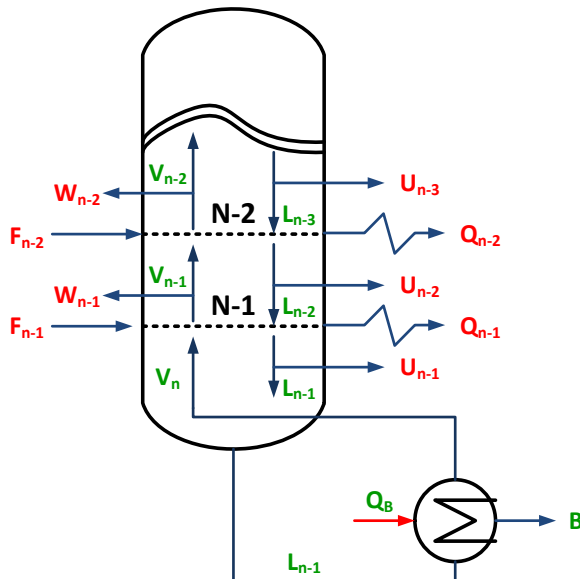
Figure 9-5: Lower zone of the reactive distillation column.

Algorithm

To design a reactive distillation column by the Wang-Henke method, it is necessary to follow an iterative procedure consisting of the following steps:

1. To start the algorithm the vapor flow rate V_j and the temperature T_j in each stage must be assumed. As the distillate flow D and reflux L_1 are known, it is possible to find the vapor flow rate of stage 2 as seen in Figure 9.2. Usually, a constant vapor flow rate along the column is also assumed and if there is a feed stream in vapor phase, its flow must be subtracted in order to find the next vapor flow rate. The vapor side streams are summed to calculate the next vapor flow rate:

$$V_2 = V_1 + U_1 + L_1 = D + L_1$$

$$V_j = V_2 + \sum_{k=2}^{j} \left(W_k - qF_k \right)$$

(0.160)

For $j = 3, 4, ..., n$. Where $q = 0$ if the feed is in liquid phase and $q = 1$ if the feed is in vapor phase. To obtain the temperatures profile, the temperature in the condenser T_1 and the temperature in the boiler T_n are supposed, constructing then a linear profile. The temperature in the boiler T_n is assumed as the same as the boiling point of the less volatile component. In the same way, the temperature in the condenser T_1 is assumed as the same as the boiling point of the most volatile component. Setting $T_D = T_1$ and $T_B = T_n$ it is obtained:

$$T_j = T_{j-1} + \frac{T_B - T_D}{n-1}$$

(0.161)

for $j = 2, 3, 4, ..., n\text{-}1$.

2. Calculate the values of the vapor – liquid distribution coefficients $K_i = \dfrac{\gamma_i P_i^{sat}}{\phi_i P}$. For the first iteration, it is considered the vapor as a mixture of ideal gases and the liquid as an ideal solution, which reduces the last expression to $K_i = \dfrac{P_i^{sat}}{P}$.

3. Solve the c tridiagonal matrices given by equation 9.43. For the first iteration, knowing that the values of $x_{i,j}$ are unknown, is assumed that the reaction rate is zero ($r_j = 0$) for $1 \leq j \leq n$. Now the c tridiagonal matrices are solved the values of $x_{i,j}$ must be normalized:

$$x_{i,j}^* = \frac{x_{i,j}}{\sum_{i=1}^{c} x_{i,j}}$$

4. Find the bubble temperature for each stage of the reactive distillation column. From this calculation it is possible to obtain the temperature of each stage T_j and the vapor composition $y_{i,j}$ leaving the stage.

5. Calculate the enthalpies of vapor, liquid and feed streams.

6. Calculate the vapor flow rates V_j for stages $3 \leq j \leq n$ using equation 9.50. For stage 2 it is applied the relation $V_2 = D + L_1$.

7. Calculate the liquid flow rates by means of equation 9.30.

8. Repeat steps 3 to 6 a number of times previously defined.

9. Calculate the heat duty of the condenser and boiler applying equations 9.58 and 9.59 respectively.

The Wang-Henke method has a good performance when is applied to solve systems with a high degree of linearity, therefore it is better to establish a number of iteration prior solving the model instead of selecting a convergence criteria.

Newton – Raphson method for multiple variables applied to reactive distillation columns

The Newton – Raphson method for multiple variables is a well suited approach to solve the model of a reactive distillation column by iterations. The method uses as initial estimates different parameters of the column that can be calculated then by the extension of the Wang – Henke model.

In general, the MESH equations used to perform the Newton – Raphson method for multiple variables are:

Total mass balance for the stage *j*:

$$M_j = L_{j-1} + V_{j+1} + F_j - \left(L_j + U_j \right) - \left(V_j - W_j \right) + \frac{Z_{Cj}}{|v_k|} r_j \sum_{i=1}^{c} v_i = 0 \qquad (0.162)$$

Mass balance of the component *i* for the stage *j*:

$$M_{i,j} = L_{j-1} x_{i,j-1} + V_{j+1} y_{i,j+1} + F_j z_{i,j} - \left(L_j + U_j \right) x_{i,j} - \left(V_j - W_j \right) y_{i,j} + Z_{Cj} \frac{v_i}{|v_k|} r_j = 0 \qquad (0.163)$$

Equilibrium relation of the component *i* for the stage *j*:

$$E_{i,j} = K_{i,j} x_{i,j} - y_{i,j} = 0 \qquad (0.164)$$

Relations of sum for the stage *j*:

$$S_j^{L-V} = \sum_{i=1}^{c} \left(x_{i,j} - y_{i,j} \right) = 0 \qquad (0.165)$$

Energy balance for the stage *j*:

$$H_j = L_{j-1}\hat{H}_{L,j-1} + V_{j+1}\hat{H}_{V,j-1} + F_j\hat{H}_{F,j} - \left(L_j + U_j\right)\hat{H}_{L,j} - \left(V_j + W_j\right)\hat{H}_{V,j} + Q_j = 0 \tag{0.166}$$

In the solution of the method it is used the total mass balance in each stage (M_j) (Equation 9.6). It was previously mentioned that the total mass balance (M_j), mass balance per component ($M_{i,j}$) and the relations of sum (S_j^L and S_j^V) form a linear dependent system of equations. In order to eliminate this linear dependence, Equations 3.3 and 3.4 are combined forming equation 9.62.

The variables that model the system are presented in Table 9.6.

Table 9-6: Variable that model a reactive distillation column.

Variables of the stage *j*	Symbol	Value
Vapor flow rate	V_j	1
Liquid flow rate	L_j	1
Vapor molar fraction	$y_{i,j}$	c
Liquid molar fraction	$x_{i,j}$	c
Temperature of the stage	T_j	1

In the formulation of the algorithm the condenser and boiler must be considered as special stages. So, stages 2 to *n-1* are calculated first, and then these two special stages. Stages 2 to *n-1* are the plates of the reactive distillation column.

Development of the algorithm for the reactive distillation plates

It is defined a vector of variables $\vec{X}_j$ for the stage j:

$$\vec{X}_j = \left(V_j, y_{1,j},\ldots,y_{c,j},T_j,x_{1,j},\ldots x_{c,j},L_j\right)^T_{1\times(3+2c)} \tag{0.167}$$

Or in abbreviated notation:

$$\vec{X}_j = \left(V_j, y_{i,j},T_j,x_{i,j},L_j\right)^T_{1\times(3+2c)} \tag{0.168}$$

For $2 \le j \le n-1$, $1 \le i \le c$ and a vector of functions for the stage *j*:

$$\vec{F}_j = \left(\underbrace{M_j}_{\substack{\text{Total mass}\\\text{balance}}}, \underbrace{M_{1,j},\ldots,M_{c,j}}_{\substack{\text{Mass balance per}\\\text{component}}}, \underbrace{H_j}_{\substack{\text{Energy}\\\text{balance}}}, \underbrace{E_{1,j},\ldots,E_{c,j}}_{\text{Equilibrium relations}}, \underbrace{S_j^{L-V}}_{\substack{\text{Relations}\\\text{of sum}}} \right)^T_{1\times(3+2c)} \tag{0.169}$$

$$\vec{X}_j = \left(V_j, y_{i,j},T_j,x_{i,j},L_j\right)^T_{1\times(3+2c)} \tag{0.170}$$

For $2 \le j \le n-1$ and $1 \le i \le c$. Then, grouping the variables of the n stages:

$$\vec{X} = \left(\vec{X}_1, \vec{X}_2, \ldots, \vec{X}_n \right)^T_{1 \times n} \tag{0.171}$$

And grouping the equations of the n stages:

$$\vec{F} = \left(\vec{F}_1, \vec{F}_2, \ldots, \vec{F}_n \right)^T_{1 \times n} \tag{0.172}$$

To evaluate the Jacobian matrix, it is necessary to calculate the partial derivatives of each function with respect of each variable:

In general, the Jacobian matrix for this system has the following form:

$$\underline{J} = \begin{pmatrix} \dfrac{\partial \vec{F}_1}{\partial \vec{X}_1} & \dfrac{\partial \vec{F}_1}{\partial \vec{X}_2} & \dfrac{\partial \vec{F}_1}{\partial \vec{X}_3} & \cdots & \dfrac{\partial \vec{F}_1}{\partial \vec{X}_{n-1}} & \dfrac{\partial \vec{F}_1}{\partial \vec{X}_n} \\[2mm] \dfrac{\partial \vec{F}_2}{\partial \vec{X}_1} & \dfrac{\partial \vec{F}_2}{\partial \vec{X}_2} & \dfrac{\partial \vec{F}_2}{\partial \vec{X}_3} & \cdots & \dfrac{\partial \vec{F}_2}{\partial \vec{X}_{n-1}} & \dfrac{\partial \vec{F}_2}{\partial \vec{X}_n} \\[2mm] \dfrac{\partial \vec{F}_3}{\partial \vec{X}_1} & \dfrac{\partial \vec{F}_3}{\partial \vec{X}_2} & \dfrac{\partial \vec{F}_3}{\partial \vec{X}_3} & \cdots & \dfrac{\partial \vec{F}_3}{\partial \vec{X}_{n-1}} & \dfrac{\partial \vec{F}_3}{\partial \vec{X}_n} \\[2mm] \vdots & \vdots & \vdots & \ddots & \vdots & \vdots \\[2mm] \dfrac{\partial \vec{F}_{n-1}}{\partial \vec{X}_1} & \dfrac{\partial \vec{F}_{n-1}}{\partial \vec{X}_2} & \dfrac{\partial \vec{F}_{n-1}}{\partial \vec{X}_3} & \cdots & \dfrac{\partial \vec{F}_{n-1}}{\partial \vec{X}_{n-1}} & \dfrac{\partial \vec{F}_{n-1}}{\partial \vec{X}_n} \\[2mm] \dfrac{\partial \vec{F}_n}{\partial \vec{X}_1} & \dfrac{\partial \vec{F}_n}{\partial \vec{X}_2} & \dfrac{\partial \vec{F}_n}{\partial \vec{X}_3} & \cdots & \dfrac{\partial \vec{F}_n}{\partial \vec{X}_{n-1}} & \dfrac{\partial \vec{F}_n}{\partial \vec{X}_n} \end{pmatrix}_{n \times n} \tag{0.173}$$

Where the derivatives of the functions for the stage k with respect of the variables for the stage t are defined by:

$$\frac{\partial \vec{F}_k}{\partial \vec{X}_t} = \left(\frac{\partial M_k}{\partial \vec{X}_t}, \frac{\partial M_{1,k}}{\partial \vec{X}_t}, \ldots, \frac{\partial M_{c,k}}{\partial \vec{X}_t}, \frac{\partial H_k}{\partial \vec{X}_t}, \frac{\partial E_{1,k}}{\partial \vec{X}_t}, \ldots, \frac{\partial E_{c,k}}{\partial \vec{X}_t}, \frac{\partial S_k^{L-V}}{\partial \vec{X}_t} \right)^T_{1 \times (3+2c)}$$

Or in abbreviated notation:

$$\frac{\partial \vec{F}_k}{\partial \vec{X}_t} = \left(\frac{\partial M_k}{\partial \vec{X}_t}, \frac{\partial M_{i,k}}{\partial \vec{X}_t}, \frac{\partial H_k}{\partial \vec{X}_t}, \frac{\partial E_{i,k}}{\partial \vec{X}_t}, \frac{\partial S_k^{L-V}}{\partial \vec{X}_t} \right)^T_{1 \times (3+2c)} \tag{0.174}$$

Where $i = 1,2,\ldots,c$.

Expanding equation 3.98:

$$\frac{\partial \vec{F}_k}{\partial \vec{X}_t} = \begin{pmatrix} \dfrac{\partial M_k}{\partial V_t} & \dfrac{\partial M_{i,k}}{\partial V_t} & \dfrac{\partial H_k}{\partial V_t} & \dfrac{\partial E_{i,k}}{\partial V_t} & \dfrac{\partial S_k^{L-V}}{\partial V_t} \\[2ex] \dfrac{\partial M_k}{\partial y_{i,t}} & \dfrac{\partial M_{i,k}}{\partial y_{i,t}} & \dfrac{\partial H_k}{\partial y_{i,t}} & \dfrac{\partial E_{i,k}}{\partial y_{i,t}} & \dfrac{\partial S_k^{L-V}}{\partial y_{i,t}} \\[2ex] \dfrac{\partial M_k}{\partial T_t} & \dfrac{\partial M_{i,k}}{\partial T_t} & \dfrac{\partial H_k}{\partial T_t} & \dfrac{\partial E_{i,k}}{\partial T_t} & \dfrac{\partial S_k^{L-V}}{\partial T_t} \\[2ex] \dfrac{\partial M_k}{\partial x_{i,t}} & \dfrac{\partial M_{i,k}}{\partial x_{i,t}} & \dfrac{\partial H_k}{\partial x_{i,t}} & \dfrac{\partial E_{i,k}}{\partial x_{i,t}} & \dfrac{\partial S_k^{L-V}}{\partial x_{i,t}} \\[2ex] \dfrac{\partial M_k}{\partial L_t} & \dfrac{\partial M_{i,k}}{\partial L_t} & \dfrac{\partial H_k}{\partial L_t} & \dfrac{\partial E_{i,k}}{\partial L_t} & \dfrac{\partial S_k^{L-V}}{\partial L_t} \end{pmatrix}_{(3+2c)\times(3+2c)} \tag{0.175}$$

Where $i = 1, 2,...,c$.

The MESH equations for the stage j depend on the variables of the stage j, the variables of the previous stage $j-1$ and the variables of the next stage $j+1$.

Hence, $\dfrac{\partial \vec{F}_k}{\partial \vec{X}_t} = 0$ if $\begin{cases} t \neq k-1 \\ t \neq k \\ t \neq k+1 \end{cases}$, i.e. for each row in the matrix represented by equation 9.99, there

are only there submatrices represented by equation 9.71, being null the other submatrices in the Jacobian matrix. In this way, it is obtained the following scheme for the Jacobian matrix of the system:

$$\underline{J} = \begin{pmatrix} \underline{B}_1 & \underline{C}_1 & \underline{0} & \cdots & \underline{0} & \underline{0} & \underline{0} \\ \underline{A}_2 & \underline{B}_2 & \underline{C}_2 & \cdots & \underline{0} & \underline{0} & \underline{0} \\ \underline{0} & \underline{A}_3 & \underline{B}_3 & \cdots & \underline{0} & \underline{0} & \underline{0} \\ \vdots & \vdots & \vdots & \ddots & \vdots & \vdots & \vdots \\ \underline{0} & \underline{0} & \underline{0} & \cdots & \underline{B}_{n-2} & \underline{C}_{n-2} & \underline{0} \\ \underline{0} & \underline{0} & \underline{0} & \cdots & \underline{A}_{n-1} & \underline{B}_{n-1} & \underline{C}_{n-1} \\ \underline{0} & \underline{0} & \underline{0} & \cdots & \underline{0} & \underline{A}_n & \underline{B}_n \end{pmatrix}_{n\times n} \tag{0.176}$$

Where:

$$\underline{A}_j = \frac{\partial \vec{F}_j}{\partial \vec{X}_{j-1}} \tag{0.177}$$

$$\underline{B}_j = \frac{\partial \vec{F}_j}{\partial \vec{X}_j} \tag{0.178}$$

$$\underline{C}_j = \frac{\partial \vec{F}_j}{\partial \vec{X}_{j+1}} \tag{0.179}$$

The structure of $\underline{A}_j$ for $j = 3, 4,..., n-1$ is defined by:

$$\underline{A}_j = \dfrac{\partial \vec{F}_j}{\partial \vec{X}_{j-1}} =$$

		$\dfrac{\partial F_j}{\partial V_{j-1}}$	$\dfrac{\partial F_j}{\partial y_{i,j-1}}$						$\dfrac{\partial F_j}{\partial T_{j-1}}$	$\dfrac{\partial F_j}{\partial x_{i,j-1}}$						$\dfrac{\partial F_j}{\partial L_{j-1}}$
			1	2	3	.	.	c		1	2	3	.	.	c	
M_j		0	0	0	0	.	.	0	0	0	0	0	.	.	0	1
$M_{i,j}$	1	0	0	0	0	.	.	0	0	L_{i-1}	0	0	.	.	0	$x_{1,i-1}$
	2	0	0	0	0			0	0	0	L_{i-1}	0			.	$x_{2,i-1}$
	3	0	0	0	0			0	0	0	0	L_{i-1}			.	$x_{3,i-1}$
	.	.	.	.				.	.	.						.
	.	.	.	.				.	.	.						.
	c	0	0	.	.	.	.	0	0	0	.		.	.	L_{i-1}	$x_{c,i-1}$
H_j		0	0	0	0	.	.	0	$L_{j-1}\dfrac{\partial \hat{H}_{L,j-1}}{\partial T_{j-1}}$	$L_{j-1}\dfrac{\partial \hat{H}_{L,j-1}}{\partial x_{i,j-1}}$						$\hat{H}_{L,j-1}$
$E_{i,j}$	1	0	0	0	0	.	.	0	0	0	0	0	.	.	0	0
	2	0	0	0	0		.	.	0	0	0	0			.	0
	3	0	0	0	0		.	.	0	0	0	0			.	0
	.	.	.	.				.	.	.					.	.
	.	.	.	.				.	.	.					.	.
	c	0	0	.	.	.	.	0	0	0					.	0
S_j^{L-V}		0	0	0	0	.	.	0	0	0	0	0	.	.	0	0

(0.180)

The structure of $\underline{B}_j$ for $j = 2,3,\ldots, n\text{-}1$ is defined by:

$$\underline{B}_j = \frac{\partial \vec{F}_j}{\partial \vec{X}_j} =$$

			$\dfrac{\partial F_j}{\partial V_{j-1}}$	$\dfrac{\partial F_j}{\partial y_{i,j}}$ $i =$						$\dfrac{\partial F_j}{\partial T_j}$	$\dfrac{\partial F_j}{\partial x_{i,j}}$ $i =$						$\dfrac{\partial F_j}{\partial L_j}$
				1	2	3	.	.	c		1	2	3	.	.	c	
M_j			-1	0	0	0	.	.	0	$\left(\dfrac{Z_{Cj}}{\|v_k\|}\displaystyle\sum_{i=1}^{c} v_s\right)\dfrac{\partial r_j}{\partial T_j}$	$\left(\dfrac{Z_{Cj}}{\|v_k\|}\displaystyle\sum_{i=1}^{c} v_s\right)\dfrac{\partial r_j}{\partial x_{i,j}}$						-1
$M_{i,j}$	i*	1	$-y_{1,j}$	$\left. -V_j + W_j \right/_{\text{For }i=i^*} \;\; \underset{\text{For }i\neq i^*}{0}$						$\left(Z_{Cj}\dfrac{v_{i^*}}{\|v_k\|}\right)\dfrac{\partial r_j}{\partial T_j}$	$\left. -L_j + U_j + \left(Z_{Cj}\dfrac{v_i}{\|v_k\|}\right)\dfrac{\partial r_j}{\partial x_{i,j}} \right/ \underset{\text{For }i=i^*}{}\left(Z_{Cj}\dfrac{v_{i^*}}{\|v_k\|}\right)\dfrac{\partial r_j}{\partial x_{i,j}} \underset{\text{For }i\neq i^*}{}$						$-x_{1,j}$
		2	$-y_{2,j}$														$-x_{2,j}$
		3	$-y_{3,j}$														$-x_{3,j}$
		.	.														.
		.	.														.
		c	$-y_{c,j}$														$-x_{c,j}$
Hj			$-\hat{H}_{V,j}$	$-\left(V_j + W_j\right)\dfrac{\partial \hat{H}_{V,j}}{\partial y_{i,j}}$						$-\left(L_j + U_j\right)\dfrac{\partial \hat{H}_{L,j}}{\partial T_j}$ $-\left(V_j + W_j\right)\dfrac{\partial \hat{H}_{V,j}}{\partial T_j}$	$-\left(L_j + U_j\right)\dfrac{\partial \hat{H}_{L,j}}{\partial x_{i,j}}$						$-\hat{H}_{L,j}$
$E_{i,j}$	i*	1	0	$\left. x_{i,j}\dfrac{\partial K_{i,j}}{\partial y_{i,j}} - 1 \right/ \underset{\text{For }i=i^*}{} x_{i^*,j}\dfrac{\partial K_{i^*,j}}{\partial y_{i,j}} \underset{\text{For }i\neq i^*}{}$						$x_{i^*,j}\dfrac{\partial K_{i^*,j}}{\partial T_{i,j}}$	$\dfrac{\partial\left(x_{i^*,j}K_{i^*,j}\right)}{\partial x_{i,j}}$						0
		2	0														0
		3	0														0
		.	.														.
		.	.														.
		c	0														0
S_j^{L-V}			0	-1	-1	-1	.	.	-1	0	1	1	1	.	.	1	0

$$(0.181)$$

The structure of $\underline{C}_j$ for $j = 2,3,\ldots, n\text{-}1$ is defined by:

$$\underline{C}_j = \frac{\partial \vec{F}_j}{\partial \vec{X}_{j+1}} =$$

		$\dfrac{\partial F_j}{\partial V_{j+1}}$	$\dfrac{\partial F_j}{\partial y_{i,j+1}}$						$\dfrac{\partial F_j}{\partial T_{j+1}}$	$\dfrac{\partial F_j}{\partial x_{i,j+1}}$						$\dfrac{\partial F_j}{\partial L_{j-1}}$
			1	2	3	.	.	c		1	2	3	.	.	c	
M_j		1	0	0	0	.	.	0	0	0	0	0	.	.	0	0
$M_{i,j}$	1	$y_{1,j+1}$	V_{j+1}	0	0	.	.	0	0	0	0	0	.	.	0	0
	2	$y_{2,j+1}$	0	V_{j+1}	0			0	0	0	0	0			.	0
	3	$y_{3,j+1}$	0	0	V_{j+1}			0	0	0	0	0			.	0
	.	.	.					.	.	.					.	.
	.	.	.					.	.	.					.	.
	c	$y_{c,j+1}$	0	.	.	.	.	V_{j+1}	0	0	.	.	.	.	0	0
H_j		$\hat{H}_{V,j+1}$	$V_{j+1}\dfrac{\partial \hat{H}_{V,j+1}}{\partial y_{i,j+1}}$						$V_{j+1}\dfrac{\partial \hat{H}_{V,j+1}}{\partial T_{j+1}}$	0	0	0	.	.	.	0
$E_{i,j}$	1	0	0	0	0	.	.	0	0	0	0	0	.	.	0	0
	2	0	0	0	0		.	.	0	0	0	0			.	0
	3	0	0	0	0		.	.	0	0	0	0			.	0
	.	.	.	.			.	.	.	.					.	.
	.	.	.	.			.	.	.	.					.	.
	c	0	0	.	.	.	.	0	0	0					.	0
S_j^{L-V}		0	0	0	0	.	.	0	0	0	0	0	.	.	0	0

$$(0.182)$$

Special stages of the reactive distillation column

The condenser and boiler are considered as two special stages because the equations to model them are not the same as for the rest of the column. The condenser can be total or partial and the boiler is treated as partial for every case.

Total condenser

In the case of the total condenser, the entire vapor flow rate V_1 in this stage is condensed and removed as two flows: the distillate flow U_1 and the flow that returns to the column L_1. Both distillate and reflux flows are known values and do not belong to the unknown variables to perform iterative calculations. The heat duty in the condenser is not an iterative variable. It must be

calculated at the end of the process using the energy balance in the condenser by means of equation 9.58 and setting $V_1 = 0$:

$$Q_1 = \left(L_1 + U_1\right)\hat{H}_{L,1} - V_2\hat{H}_{V,2}$$ (0.183)

Since there is not an outlet flow, there are not vapor molar fractions. The following Table shows the variables that model a total condenser:

Table 9-7: Variables that model a total condenser.

Variables of the stage j	Symbol	Value
Liquid molar fraction	$x_{i,j}$	c
Temperature of the stage	T_j	1

The equations to solve these variables are the c mass balances per component and the bubble temperature. The mass balance per component in the total condenser is defined by equation .1 with $V_1 = W_1 = 0$, $L_0 = 0$ and $F_0 = 0$:

$$M_{i,1} = V_2 y_{i,2} - \left(L_1 + U_1\right)x_{i,1} + Z_{Cj}\frac{v_i}{\left|v_k\right|}r_1 = 0$$ (0.184)

And the bubble temperature for the total condenser is expressed as:

$$TB_1 = \sum_{i=1}^{c} K_{i,1}\,x_{i,1} - 1 = 0$$ (0.185)

Thus, the number of equation $c+1$ is the same as the number of unknown variables $c+1$. Then, by grouping variables:

$$\vec{X}_1 = \left(x_{1,1}, \cdots x_{c,1}, T_1\right)^T_{1\times(1+c)}$$ (0.186)

And by grouping equations:

$$\vec{F}_1 = \left(M_{i,1}, TB_1\right)^T_{1\times(1+c)}$$ (0.187)

The section of the Jacobian matrix where the condenser is included is determined by the submatrices built by the partial derivatives of the functions in the next stages with respect of the variables in stage 1 $\underline{A}_2$, the partial derivatives of the functions that model the condenser with respect of the variables of the condenser $\underline{B}_1$ and the partial derivatives of the functions that model the condenser with respect of the variables in the next stage $\underline{C}_1$. These submatrices are:

$$\underline{A}_2 = \frac{\partial \vec{F}_2}{\partial \vec{X}_1}$$ (0.188)

$$\vec{B}_1 = \frac{\partial \vec{F}_1}{\partial \vec{X}_1}$$ (0.189)

$$C_1 = \frac{\partial \vec{F}_1}{\partial \vec{X}_2} \tag{0.190}$$

The structure of $\underline{A}_2$ is given by:

$$\underline{A}_2 = \frac{\partial \vec{F}_2}{\partial \vec{X}_1} =$$

		$\dfrac{\partial F_2}{\partial x_{i,1}}$						$\dfrac{\partial F_2}{\partial T_1}$
		1	2	3	.	.	c	
M_2		0	0	0	.	.	0	0
$M_{i,2}$	1	L_1	0	0	.	.	0	0
	2	0	L_1	0			0	0
	3	0	0	L_1			0	0
	.	.				.		.
	.	.				.		.
	c	0	.	.	.	.	L_1	0
H_2		$L_1 \dfrac{\partial \hat{H}_{L,1}}{\partial x_{i,1}}$						$L_1 \dfrac{\partial \hat{H}_{L,1}}{\partial T_1}$
$E_{i,2}$	1	0	0	0	.	.	0	0
	2	0	0	0		.		0
	3	0	0	0		.		0
	.	.				.		.
	.	.				.		.
	c	0	.	.	.	.	0	0
S_2^{L-V}		0	0	0	.	.	0	0

$$\tag{0.191}$$

The structure of $\underline{B}_1$ is given by:

$$\underline{B}_j = \frac{\partial \vec{F}_j}{\partial \vec{X}_j} =$$

			$\dfrac{\partial F_1}{\partial T_1}$	$\dfrac{\partial F_1}{\partial x_{i,1}}$					
				$i =$					
				1	2	3	.	.	c
$M_{i^*,1}$	i^*	1 2 3 . . . c	$\left(Z_{Cj} \dfrac{v_{i^*}}{\lvert v_k \rvert} \right) \dfrac{\partial r_1}{\partial T_1}$	$-L_1 + U_1 + \left(Z_{C1} \dfrac{v_i}{\lvert v_k \rvert} \right) \dfrac{\partial r_1}{\partial x_{i,1}}$ For $i=i^*$			$\Big/$	$\left(Z_{C1} \dfrac{v_{i^*}}{\lvert v_k \rvert} \right) \dfrac{\partial r_1}{\partial x_{i,1}}$ For $i \neq i^*$		
TB_1			$\displaystyle\sum_{i=1}^{c} x_{i,1} \dfrac{\partial K_{s,1}}{\partial T_1}$	$\displaystyle\sum_{i=1}^{c} \dfrac{\partial \left(K_{i,1}\, x_{i,1} \right)}{\partial x_{i,1}}$					

$$(0.192)$$

The structure of $\underline{C}_1$ is given by:

$$\underline{C}_j = \frac{\partial \vec{F}_j}{\partial \vec{X}_2} =$$

M_{jl}		$\frac{\partial F_1}{\partial V_2}$	$\frac{\partial F_1}{\partial y_{i,2}}$						$\frac{\partial F_1}{\partial T_2}$	$\frac{\partial F_1}{\partial x_{i,2}}$						$\frac{\partial F_1}{\partial L_2}$
			1	2	3	.	.	c		1	2	3	.	.	c	
	1	$y_{1,2}$	V_2	0	0	.	.	0	0	0	0	0	.	.	0	0
	2	$y_{2,2}$	0	V_2	0			0	0	0	0	0			.	0
	3	$y_{3,2}$	0	0	V_2			0	0	0	0	0			.	0
	.	.	.					.	.	.				.		.
	.	.	.					.	.	.				.		.
	c	$y_{c,2}$	0	.	.	.	.	V_2	0	0	.	.	.	.	0	0
TB_1		0	0	0	0	.	.	0	0	0	0	0	.	.	.	0

$$(0.193)$$

Partial condenser

In the case of the partial condenser, a part of the flow V_2 is condensed to be then returned as a reflux L_1 to the reactive distillation column and the other part leaves the column as distilled product in vapor phase V_1, having then $U_1 = 0$. The distillate flow V_1 and the reflux L_1 are known; therefore it is not necessary to iterate them.

Heat duty in the partial condenser is not an iterative variable. It must be calculated at the end of the process using the energy balance in the condenser by means of equation 9.58 and setting $U_1 = 0$:

$$Q_1 = L_1 \hat{H}_{L,1} - V_2 \hat{H}_{V,2} + V_1 \hat{H}_{V,1} \qquad (0.194)$$

The following Table shows the variables that model a partial condenser:

Table 9-8: Variable that model a partial condenser.

Variables of the stage j	Symbol	Value
Liquid molar fraction	$x_{i,j}$	c
Vapor molar fraction	$y_{i,j}$	c
Temperature of the stage	T_j	1

The equations to solve these variables are the c mass balances per component, the c relations of phase equilibrium relations and the relations of sum. The mass balance per component in the partial condenser is defined by equation 9.1 with $U_1 = 0$, $W_1 = 0$ and $L_0 = 0$:

$$M_{i,1} = V_2 y_{i,2} - L_1 x_{i,1} - V_1 y_{i,1} + Z_{Cj} \frac{v_i}{|v_k|} r_1 = 0 \qquad (0.195)$$

The relations of phase equilibrium are defined as:

$$E_{i,1} = K_{i,1} x_{i,1} = y_{i,1} = 0 \qquad (0.196)$$

And the relations of sum:

$$S_1^{L-V} = \sum_{i=1}^{c} \left(x_{i,1} - y_{i,1} \right) = 0 \qquad (0.197)$$

In this sense, the number of equations $2c+1$ is the same as the number of unknown variables $2c+1$. Then, by grouping variables:

$$\vec{X}_1 = \left(y_{1,1}, \ldots, y_{c,1}, T_1, x_{1,1}, \ldots x_{c,1} \right)^T_{1 \times (1+2c)} \qquad (0.198)$$

And by grouping equations:

$$\vec{F}_1 = \left(M_{i,1}, S_1^{L-V}, E_{i,1} \right)^T_{1 \times (1+2c)} \qquad (0.199)$$

The section of the Jacobian matrix where the partial condenser is included is determined by the submatrices built by the partial derivatives of the functions in the stage 2 with respect of the variables in stage 1 $\underline{A}_2$, the partial derivatives of the functions that model the condenser with respect of the variables of the condenser $\underline{B}_1$ and the partial derivatives of the functions that model the condenser with respect of the variables in the stage 2 $\underline{C}_1$. These submatrices are:

$$\underline{A}_2 = \frac{\partial \vec{F}_2}{\partial \vec{X}_1} \qquad (0.200)$$

$$\vec{B}_1 = \frac{\partial \vec{F}_1}{\partial \vec{X}_1} \qquad (0.201)$$

$$C_1 = \frac{\partial \vec{F}_1}{\partial \vec{X}_2} \qquad (0.202)$$

The structure of $\underline{A}_2$ is given by:

$$\underline{A}_2 = \frac{\partial \vec{F}_2}{\partial \vec{X}_1} =$$

		$\dfrac{\partial F_2}{\partial y_{i,1}}$						$\dfrac{\partial F_2}{\partial T_1}$	$\dfrac{\partial F_2}{\partial x_{i,1}}$					
		1	2	3	.	.	c		1	2	3	.	.	c
M_2		0	0	0	.	.	0	0	0	0	0	.	.	0
$M_{i,2}$	1	0	0	0	.	.	0	0	L_1	0	0	.	.	0
	2	0	0	0			0	0	0	L_1	0			.
	3	0	0	0			0	0	0	0	L_1			.
	.	.					.	.	.					
	.	.					.	.	.					
	c	0	.	.	.	.	0	0	0	.		.	.	L_1
H_2		0	0	0	.	.	0	$L_1\dfrac{\partial \hat{H}_{L,1}}{\partial T_1}$	$L_1\dfrac{\partial \hat{H}_{L,1}}{\partial x_{i,1}}$					
$E_{i,2}$	1	0	0	0	.	.	0	0	0	0	0	.	.	0
	2	0	0	0		.	.	0	0	0	0			.
	3	0	0	0		.	.	0	0	0	0			.
	.	.			.			.	.					.
	.	.			.			.	.					.
	c	0	.	.	.	.	0	0	0					.
S_2^{L-V}		0	0	0	.	.	0	0	0	0	0	.	.	0

(0.203)

The structure of $\underline{B}_2$ is given by:

$$\underline{B}_j = \frac{\partial \vec{F}_1}{\partial \vec{X}_1} =$$

			$\dfrac{\partial F_1}{\partial y_{i,1}}$						$\dfrac{\partial F_j}{\partial T_j}$	$\dfrac{\partial F_1}{\partial x_{i,1}}$					
			$i=$							$i=$					
			1	2	3	.	.	c		1	2	3	.	.	c
$M_{i,1}$	i^*	1	$-V_1$	0	0	.	.	0	$\left(Z_{C1}\dfrac{v_{i^*}}{\lvert v_k\rvert}\right)\dfrac{\partial r_1}{\partial T_1}$	$-L_1+\left(Z_{C1}\dfrac{v_i}{\lvert v_k\rvert}\right)\dfrac{\partial r_1}{\partial x_{i,1}}\Big/\left(Z_{C1}\dfrac{v_{i^*}}{\lvert v_k\rvert}\right)\dfrac{\partial r_1}{\partial x_{i,1}}$					
		2	0	$-V_1$	0			.		For $i=i^*$ For $i\neq i^*$					
		3	0	0	$-V_1$			.							
		.	.					.							
		.	.					.							
		c	0	.	.	.	.	$-V_1$							
$E_{i,1}$	i^*	1	$x_{i,1}\dfrac{\partial K_{i,1}}{\partial y_{i,1}}-1\Big/x_{i^*,1}\dfrac{\partial K_{i^*,1}}{\partial y_{i,1}}$						$x_{i^*,1}\dfrac{\partial K_{i^*,1}}{\partial y_{i,1}}$	$\dfrac{\partial\left(x_{i^*,1}K_{i^*,1}\right)}{\partial x_{i,1}}$					
		2													
		3	For $i=i^*$ For $i\neq i^*$												
		.													
		.													
		c													
S_1^{L-V}			-1	-1	-1	.	.	-1	0	1	1	1	.	.	1

(0.204)

The structure of $\underline{C}_1$ is given by:

$$\underline{C}_1 = \frac{\partial \vec{F}_1}{\partial \vec{X}_2} =$$

			$\dfrac{\partial F_1}{\partial V_2}$	$\dfrac{\partial F_1}{\partial y_{i,2}}$						$\dfrac{\partial F_1}{\partial T_2}$	$\dfrac{\partial F_1}{\partial x_{i,2}}$						$\dfrac{\partial F_1}{\partial L_3}$
				1	2	3	.	.	c		1	2	3	.	.	c	
$M_{i,1}$		1	$y_{1,2}$	V_3	0	0	.	.	0	0	0	0	0	.	.	0	0
		2	$y_{2,2}$	0	V_3	0			0	0	0	0	0			.	0
		3	$y_{3,2}$	0	0	V_3			0	0	0	0	0			.	0
		.	.	.					.	.	.					.	.
		.	.	.					.	.	.					.	.
		c	$y_{c,2}$	0	.	.	.	.	V_3	0	0	.	.	.	.	0	0
$E_{i,1}$		1	0	0	0	0	.	.	0	0	0	0	0	.	.	0	0
		2		0	0	0		.		0	0	0	0			.	0
		3		0	0	0		.		0	0	0	0			.	0
		.		.					.	.	.					.	.
		.		.					.	.	.					.	.
		c		0	.	.	.	.	0	0	0					.	0
S_1^{L-V}						0				0	0	0	0	.	.	0	0

(0.205)

Partial boiler

The boiler is the main source of energy in a reactive distillation column. Its function is to boil the liquid flow from the stage n-1 in order to generate a vapor flow that is returned to the column and a liquid flow that leaves the column as bottom product. The returned vapor and the exiting flow are in phase equilibrium, thus, the boiler is measured as a stage in equilibrium. The variables to be considered so as to model a partial boiler are the same as for the stages of the reactive distillation column.

Table 9-9: Variables to model a boiler.

Variables of the stage j	Symbol	Value
Vapor flow rate	V_n	1
Liquid flow rate	L_j	1
Vapor molar fraction	$y_{i,j}$	c
Liquid molar fraction	$x_{i,j}$	c
Temperature of the stage	T_j	1

Starting from the energy balance of the boiler it is possible to calculate the heat duty (equation 9.59):

$$Q_n = L_n \hat{H}_{L,n} - V_n \hat{H}_{V,n} - L_{n-1} \hat{H}_{L,n-1} \tag{0.206}$$

The energy balance is then replaced by the total mass balance in the column. In equation 3.27 it is demonstrated that the mass balance covers all the first j stages of the reactive distillation column:

$$\sum_{i=1}^{j} M_q = V_{j+1} - L_j - V_1 + \sum_{p=1}^{j}(F_p - U_p) - (L_j + U_j - W_p) + \sum_{p=1}^{j}\left(\frac{Z_{Cp}}{|v_k|} r_p \sum_{i=1}^{c} v_i\right) = 0$$

When $j = n$ this equation represents the total mass balance in the column. The term V_{n+1} do not exist, therefore, it is not considered in the last equation. Then:

$$M^T = -L_n - V_1 + \sum_{p=1}^{j}(F_p - U_p) + \sum_{p=1}^{j}\left(\frac{Z_{Cp}}{|v_k|} r_p \sum_{i=1}^{c} v_i\right) = 0 \tag{0.207}$$

The equations to solve the model are the total mass balance in the boiler, the c mass balances per component in the boiler, the c relations of equilibrium and the total mass balance in the column. In this sense, the number of equations $2c+3$ is the same as the number of unknown variables $2c+3$.

Total mass balance in the boiler:

$$M_n = L_{n-1} - L_n - V_n + \frac{Z_{Cp}}{|v_k|} r_p \sum_{i=1}^{c} v_i = 0 \tag{0.208}$$

Mass balance per component in the boiler:

$$M_{i,n} = L_{n-1} x_{i,n-1} - L_n x_{i,n} - V_n y_{i,n} + Z_{Cn} \frac{v_i}{|v_k|} r_n = 0 \tag{0.209}$$

Relation of equilibrium for the component i in the boiler:

$$E_{i,n} = K_{i,n} x_{i,n} - y_{i,n} = 0 \tag{0.210}$$

Relation of sum for the boiler:

$$S_n^{L-V} = \sum_{i=1}^{c} \left(x_{i,n} - y_{i,n} \right) = 0 \tag{0.211}$$

The variables can be grouped as:

$$\vec{X}_n = \left(V_n, y_{i,n}, T_n, x_{i,n}, L_n \right)^T_{1 \times (3+2c)} \tag{0.212}$$

Also, the functions can be grouped as:

$$\vec{F}_n = \left(M_n, M_{i,n}, M^T, E_{i,n}, S_n^{L-V} \right)^T_{1 \times (3+2c)} \tag{0.213}$$

Unlike the rest of stages in the column, to model the boiler it is required an equation dependent on the temperature T_j and the liquid phase composition $x_{i,j}$ in all the stages of the column. The total mass balance in the column M^T is dependent on the reaction rate r_j in each of the stages. Hence, in the Jacobian matrix it must be performed the calculation of the partial derivatives of this equation with respect of each temperature and liquid phase composition. For a stage j the derivatives are given by:

$$\frac{\partial M^T}{\partial \vec{X}_j} =$$

	$\dfrac{\partial M^T}{\partial V_j}$	$\dfrac{\partial M^T}{\partial y_{i,j}}$						$\dfrac{\partial M^T}{\partial T_j}$	$\dfrac{\partial M^T}{\partial x_{i,j}}$						$\dfrac{\partial M^T}{\partial L_j}$
		1	2	3	.	.	c		1	2	3	.	.	c	
M^T	0	0	0	0	.	.	0	$\left(\dfrac{Z_{Cj}}{\|v_k\|} \sum_{i=1}^{c} v_i \right) \dfrac{\partial r_j}{\partial x_{i,j}}$	$\left(\dfrac{Z_{Cj}}{\|v_k\|} \sum_{i=1}^{c} v_i \right) \dfrac{\partial r_j}{\partial x_{i,j}}$						0

$$(0.214)$$

These partial derivatives must be calculated for each stage where the reaction takes place. The other partial derivatives are represented as submatrices A_n and B_n. The partial derivatives for the previous stage *n-1* with respect of the other variables in the boiler are defined by Equation 3.78 when $j = n\text{-}1$:

The submatrices are:

$$\underline{A}_n = \frac{\partial \vec{F}_n}{\partial \vec{X}_{n-1}} \tag{0.215}$$

$$\underline{B}_n = \frac{\partial \vec{F}_n}{\partial \vec{X}_n} \tag{0.216}$$

The structure of $\underline{A}_n$ is given by:

$$\underline{A}_n = \frac{\partial \vec{F}_n}{\partial \vec{X}_{n-1}} =$$

		$\frac{\partial F_n}{\partial V_{n-1}}$	$\frac{\partial F_n}{\partial y_{i,n-1}}$						$\frac{\partial F_j}{\partial T_{j+1}}$	$\frac{\partial F_j}{\partial x_{i,j+1}}$						$\frac{\partial F_j}{\partial L_{j-1}}$
			1	2	3	.	.	c		1	2	3	.	.	c	
M_n		0	0	0	0	.	.	0	0	0	0	0	.	.	0	0
M_{in}	1	0	0	0	0	.	.	0	0	L_{n-1}	0	0	.	.	0	$x_{1,j+1}$
	2	0	0	0	0			0	0	0	L_{n-1}	0			.	$x_{2,j+1}$
	3	0	0	0	0			0	0	0	0	L_{n-1}			.	$x_{3,j+1}$
	.	.	.				.		.	.				.		.
	.	.	.				.		.	.				.		.
	c	0	0	.	.	.	.	0	0	0	.	.	.	.	L_{n-1}	$x_{c,j+1}$
M^T		0	0	0	0	.	.	0	$\left(\dfrac{Z_{Cn-1}}{\left|v_k\right|}\sum_{i=1}^{c}v_i\right)\dfrac{\partial r_{n-1}}{\partial x_{i,n-1}}$	$\left(\dfrac{Z_{Cn-1}}{\left|v_k\right|}\sum_{i=1}^{c}v_i\right)\dfrac{\partial r_{n-1}}{\partial x_{i,n-1}}$						0
$E_{i,n}$	1	0	0	0	0	.	.	0	0	0	0	0	.	.	0	0
	2	0	0	0	0		.	.	0	0	0	0			.	0
	3	0	0	0	0		.	.	0	0	0	0			.	0
	.	.	.				.		.	.				.		.
	.	.	.				.		.	.				.		.
	c	0	0	.	.	.	.	0	0	0					.	0
S_n^{L-V}		0	0	0	0	.	.	0	0	0	0	0	.	.	0	0

$$\tag{0.217}$$

The structure of $\underline{B}_n$ is given by:

$$\underline{B}_n = \frac{\partial \vec{F}_n}{\partial \vec{X}_n} =$$

			$\dfrac{\partial F_n}{\partial V_n}$	$\dfrac{\partial F_n}{\partial y_{i,n}}$ $i=$						$\dfrac{\partial F_n}{\partial T_n}$	$\dfrac{\partial F_n}{\partial x_{i,n}}$ $i=$						$\dfrac{\partial F_n}{\partial L_n}$
				1	2	3	.	.	c		1	2	3	.	.	c	
M_n			-1	0	0	0	.	.	0	$\left(\dfrac{Z_{Cn}}{\lvert v_k\rvert}\sum_{i=1}^{c}v_i\right)\dfrac{\partial r_n}{\partial T_n}$	$\left(\dfrac{Z_{Cn}}{\lvert v_k\rvert}\sum_{i=1}^{c}v_i\right)\dfrac{\partial r_n}{\partial x_{i,n}}$						-1
$M_{i,n}$	i^*	1	$-y_{1,n}$	$-V_n$	0	0	.	.	0								$-x_{1,n}$
		2	$-y_{2,n}$	.	$-V_n$	0			.	$\left(Z_{Cn}\dfrac{v_{i^*}}{\lvert v_k\rvert}\right)\dfrac{\partial r_n}{\partial T_n}$	$-L_n+\left(Z_{Cn}\dfrac{v_i}{\lvert v_k\rvert}\right)\dfrac{\partial r_n}{\partial x_{i,n}}$ $\Big/\ \left(Z_{Cn}\dfrac{v_{i^*}}{\lvert v_k\rvert}\right)\dfrac{\partial r_n}{\partial x_{i,n}}$						$-x_{2,n}$
		3	$-y_{3,n}$	.	0	$-V_n$			.		For $i=i^*$ $\big/$ For $i\neq i^*$						$-x_{3,n}$
		.	.	.	.				.								.
		.	.	.	.				.								.
		c	$-y_{c,n}$	0	.	.	.	.	$-V_n$								$-x_{c,n}$
M^T			0	0	0	0	.	.	0	$\left(\dfrac{Z_{Cn}}{\lvert v_k\rvert}\sum_{i=1}^{c}v_i\right)\dfrac{\partial r_n}{\partial T_n}$	$\left(\dfrac{Z_{Cn}}{\lvert v_k\rvert}\sum_{i=1}^{c}v_i\right)\dfrac{\partial r_n}{\partial T_n}$						-1
$E_{i,n}$	i^*	1	0														0
		2	0														0
		3	0	$x_{i,n}\dfrac{\partial K_{i,n}}{\partial y_{i,n}}-1$ $\Big/\ x_{i^*,n}\dfrac{\partial K_{i^*,n}}{\partial y_{i,n}}$						$x_{i^*,n}\dfrac{\partial K_{i^*,n}}{\partial T_{i,n}}$	$\dfrac{\partial\left(x_{i^*,n}K_{i^*,n}\right)}{\partial x_{i,n}}$						0
		.	.	For $i=i^*$ $\big/$ For $i\neq i^*$													.
		.	.														.
		c	0														0
S_n^{L-V}			0	-1	-1	-1	.	.	-1	0	1	1	1	.	.	1	0

(0.218)

Partial Derivatives: Calculation

To calculate the partial derivatives it is applied the numerical-perturbation method for nonlinear partial differential equations, which has the following form:

$$\frac{\partial F\left(x_1, x_2, \cdots x_n\right)}{\partial x_1} \approx \frac{\partial F\left(x_1 + h, x_2, \cdots x_n\right) - F\left(x_1, x_2, \cdots x_n\right)}{h} \tag{0.219}$$

Where the perturbation parameter is defined as:

$$\begin{aligned} h &= 10^{-7}\,|x1| &&\text{if}\quad |x1| > 1 \\ h &= 10^{-7} &&\text{if}\quad |x1| \leq 1 \end{aligned} \tag{0.220}$$

Calculation of the Euclidean norm and optimization of the Newton – Raphson method

The Newton – Raphson method is proposed for an iteration k:

$$J\left(\vec{X}^{k-1}\right) \cdot \Delta \vec{X}^k = -\vec{F}\left(\vec{X}^{k-1}\right) \tag{0.221}$$

Where:

$\vec{X}^{k-1}$ is a vector containing all the variables of the column, $k\text{-}1$ is related to the iteration at which the variables are contained in the vector.

$J\left(\vec{X}^{k-1}\right)$ is the Jacobian matrix of the system evaluated with the variables in the iteration $k\text{-}1$.

$\vec{F}\left(\vec{X}^{k-1}\right)$ is the vector of the functions evaluated with the variables in the iteration $k\text{-}1$.

$\Delta \vec{X}^k$ is a vector that indicates the change of the variables in the reactive distillation column. This vector can be expressed as:

$$\vec{X}^k = \vec{X}^{k-1} + \Delta \vec{X}^k \tag{0.222}$$

And isolating:

$$\vec{X}^k = \vec{X}^{k-1} + \Delta \vec{X}^k \tag{0.223}$$

To measure how close or far is the method to find a solution it is necessary to calculate the Euclidean norm of the discrepancy functions. The discrepancy functions are the same as the functions of the model but in their normalized form:

$$\frac{P\left(\vec{X}\right)}{Q\left(\vec{X}\right)} - 1 = 0 \qquad \rightarrow \quad \mathrm{H}\left(\vec{X}\right) - 1 = 0 \tag{0.224}$$

Some equations in the model are expressed in their normalized form such as the relations of equilibrium, the relations of sum and the bubble temperature. The rest of the equations must be normalized in order to be used as discrepancy functions.

– *Normalized total mass balance for the stage j*

From equation 9.6:

$$\bar{M}_j = \frac{L_{j-1} + V_{j+1} + F_j + Z_{Cj}\dfrac{v_i}{|v_k|}r_j}{\left(L_j + U_j\right) + \left(V_j - W_j\right)} - 1 = 0 \tag{0.225}$$

– *Normalized mass balance per component for the stage j*

From equation 9.1:

$$\bar{M}_{i,j} = \frac{L_{j-1}x_{i,j-1} + V_{j+1}y_{i,j+1} + F_j z_{i,j} + Z_{Cj}\dfrac{v_i}{|v_k|}r_j}{\left(L_j + U_j\right)x_{i,j} - \left(V_j - W_j\right)y_{i,j}} - 1 = 0 \tag{0.226}$$

– *Normalized energy balance for the stage j*

From equation 9.5:

$$\bar{H}_j = \frac{L_{j-1}\hat{H}_{L,j-1} + V_{j+1}\hat{H}_{V,j-1} + F_j\hat{H}_{F,j} + Q_j}{\left(L_j + U_j\right)\hat{H}_{L,j} - \left(V_j + W_j\right)\hat{H}_{V,j}} - 1 = 0 \tag{0.227}$$

– *Normalized mass balance in the column*

From equation 9.103:

$$\bar{M}^T = \frac{\displaystyle\sum_{p=2}^{j} F_p + \sum_{p=1}^{j}\left(\frac{Z_{Cp}}{|v_k|}r_p\sum_{i=1}^{c}v_i\right)}{L_n + V + \displaystyle\sum_{p=1}^{j}\left(U_p - W_p\right)} - 1 = 0 \tag{0.228}$$

The Euclidean norm of the vector of discrepancy functions is defined by:

$$\left\|\vec{F}\left(\vec{X}^k\right)\right\| = \sqrt{\sum_t \left(f_t\left(\vec{X}^k\right)\right)^2} \tag{0.229}$$

Where $\vec{X}^k$ is the vector of variables, $f_t\left(\vec{X}^k\right)$ is the component t of the vector of discrepancy functions.

The Newton – Raphson method is an iterative method, therefore, for each iteration there is a Euclidean norm for the vector of discrepancy functions. In ideal conditions the Euclidean norm should be diminish with every iteration. To solve or at least to reduce the impact of having a high Euclidean norm, it is used an optimization procedure, so it must be established a new recurrence function to update the value of the variables. This formula is defined by equation 9.119 as:

$$\vec{X}^k = \vec{X}^{k-1} + S_k \Delta\vec{X}^k \tag{0.230}$$

Where S_k is a scalar to define a step size.

Since $\vec{X}^{k}$ is a function of S_k, the optimization process is unidimensional with the following objective function:

$$G(S_k) = \sqrt{\sum_t \left(f_t\left(\vec{X}^{k}\right) \right)^2} = \sqrt{\sum_t \left(f_t(S_k) \right)^2} \qquad (0.231)$$

The main goal of the optimization process is to find a scalar Sk that minimizes the Euclidean norm of the vector of discrepancy vector.

Summary of the Newton – Raphson method for multiple variables applied to reactive distillation columns

The Newton – Raphson method can be summarized in the following steps:

1. To calculate the Jacobian matrix $\underline{J}\left(\vec{X}^{k-1}\right)$.

2. To calculate the vector of functions $-F\left(\vec{X}^{k-1}\right)$.

3. To solve the vector $\Delta\vec{X}^{k}$ by means of Gauss - Jordan elimination through partial pivoting of the system described by $J\left(\vec{X}^{k-1}\right) \cdot \Delta\vec{X}^{k} = -\vec{F}\left(\vec{X}^{k-1}\right)$.

4. To find the Euclidean vector of the discrepancy functions. If the Euclidean norm of the current iteration is higher than the Euclidian norm of the previous iterations, it is applied an optimization procedure.

5. To calculate the new value of the variables with $\vec{X}^{k} = \vec{X}^{k-1} + S_k\Delta\vec{X}^{k}$.

6. To calculate the Euclidean norm with the new values and then apply a tolerance criterion. If the criterion is not satisfied steps 1 to 6 must be repeated. The criteria is given by:

$$\sqrt{\sum_t \left(f_t\left(\vec{X}^{k}\right) \right)^2} \leq \lambda$$

Where λ is an established tolerance.

7. To calculate the heat duty for the condenser and boiler.

10.   Annex E - Detailed information for the production of methyl acetate by reactive distillation: Data tables and figures

Reactive distillation column with a single feed

Case 1: Column with a single feed, auto-catalyzed reaction and 10 separating stages
Table 10.1 shows the profiles obtained during the simulation of the reactive distillation column for Case 1.

Case 2: Column with a single feed, catalyzed reaction and 10 separating stages
Table 10.2 shows the profiles obtained during the simulation of the reactive distillation column for Case 2.

Case 3: Column with a single feed, catalyzed reaction and 25 separating stages
Table 10.3 shows the results obtained during the simulation of the reactive distillation column for Case 3. Figures 10.1, 10.2, 10.3 and 10.4 show the profiles.

Case 4: Column with a single feed, catalyzed reaction and 50 separating stages
Table 10.4 shows the results obtained during the simulation of the reactive distillation column for Case 4. Figures 10.5, 10.6, 10.7 and 10.8 show the profiles. Table 10.5 shows the behavior of the molar fraction in the distillate and the bottoms, and the conversion and recovery percentages as a function of the amount of catalyst for Cases 2, 3 and 4.

Reactive distillation column with two feed streams

Case 5: Column with two feed streams, auto-catalyzed reaction and 25 separating
Table 10.6 shows the results obtained during the simulation of the reactive distillation column for Case 5. Table 10.7 shows the behavior of the average temperature and reaction rate as a function of the residence time.

Case 6: Column with two feed streams, catalyzed reaction and 25 separating stages

Table 10.8 shows the results obtained during the simulation of the reactive distillation column for Case 6. Table 10.9 shows the behavior of the average temperature and reaction rate as a function of the residence time. Table 10.10 shows the behavior of the conversion and recovery percentages as a function of the reflux ratio. Table 10.11 shows the heat duty of the condenser and the boiler as a function of the reflux ratio.

Case 7: Column with two feed streams, catalyzed and auto-catalyzed reaction, 25 separating stages with enriching and reaction zones

Table 10.12 shows the results obtained during the simulation of the reactive distillation column for Case 7. Table 10.13 shows the behavior of the conversion and recovery percentages as a function of the amount of catalyst.

Case 8: Column with two feed streams, catalyzed and auto-catalyzed reaction, 25 separating stages with enriching, extraction, reaction and stripping zones

Table 10.14 shows the results obtained during the simulation of the reactive distillation column for Case 8. Table 10.15 shows the behavior of the conversion and recovery percentages as a function of the amount of catalyst.

Case 9: Column with two feed streams, catalyzed and auto-catalyzed reaction, 35 separating stages with enriching, extraction, reaction and stripping zones

Table 10.16 shows the results obtained during the simulation of the reactive distillation column for Case 8. Table 10.17 shows the behavior of the conversion and recovery percentages as a function of the amount of catalyst.

Table 10-1: Temperature, vapor and liquid phase composition, and liquid and vapor flow profiles in the distillation column for Case 1.

Stage	T [K]	Composition of liquid phase				Composition of vapor phase				Liquid [gmol/h]	Vapor [gmol/h]	Reaction rate[1] [kmol/m^3 -s]
		Methanol	Acetic acid	Methyl acetate	Water	Methanol	Acetic acid	Methyl acetate	Water			
1	312.31	0.9412	8.80E-06	0.0567	0.0021	0.8098	2.48E-07	0.1895	0.0007	42.24	0	-1.23E-14
2	314.83	0.9796	2.59E-04	0.0139	0.0062	0.9412	8.80E-06	0.0567	0.0021	42.23	84.48	1.33E-11
3	315.36	0.976	0.0037	0.0084	0.0119	0.9604	1.34E-04	0.0353	0.0041	42.18	84.47	3.58E-09
4	316.36	0.9316	0.0414	7.69E-03	0.0193	0.9586	1.87E-03	0.0325	0.007	42.38	84.42	5.19E-07
5	320.76	0.7555	0.2132	7.90E-03	0.0233	0.9364	0.0208	0.0321	0.0107	44.79	84.62	1.61E-05
6	329.29	0.4999	0.4745	7.70E-03	0.0179	0.8463	0.1104	0.0309	0.0123	176.65	87.03	9.38E-05
7	329.89	0.4779	0.4877	0.0096	0.0249	0.8253	0.1185	0.0386	0.0176	177.19	86.89	9.86E-05
8	332.18	0.4214	0.5337	0.0091	0.0358	0.7826	0.1516	0.0381	0.0277	180.19	87.43	1.21E-04
9	338.03	0.3037	0.6429	0.0072	0.0463	0.6647	0.2592	0.0315	0.0445	188.83	90.43	1.83E-04
10	347.60	0.1587	0.7928	0.0041	0.0445	0.4258	0.4978	0.0191	0.0572	87.76	99.07	2.53E-04

Heat duty [kJ/s]	
Condenser	-865.91
Boiler	837.67

---

[1] The volumetric retention per stage is 1 liter.

Table 10-2: Temperature, vapor and liquid phase composition, and liquid and vapor flow profiles in the distillation column for Case 2.

Stage	T [K]	Composition of liquid phase				Composition of vapor phase				Liquid [gmol/h]	Vapor [gmol/h]	Reaction rate[2] [kmol/g$_{cat}$ -s]
		Methanol	Acetic acid	Methyl acetate	Water	Methanol	Acetic acid	Methyl acetate	Water			
1	303.96	0.4522	4.66E-06	0.5408	0.0070	0.3552	7.32E-08	0.6420	0.0028	42.24	0.00	0
2	305.57	0.6439	2.79E-04	0.3340	0.0218	0.4522	4.66E-06	0.5408	0.0070	40.76	84.48	-5.50E-12
3	307.90	0.7551	0.0010	0.1946	0.0493	0.5462	2.02E-05	0.4394	0.0144	39.78	83.00	-4.83E-12
4	310.12	0.7647	0.0111	0.1280	0.0965	0.5988	2.71E-04	0.3731	0.0277	38.95	82.02	3.29E-11
5	314.29	0.6352	0.1193	0.0989	0.1466	0.6026	0.0058	0.3421	0.0495	38.82	81.19	5.57E-10
6	324.36	0.3821	0.4243	0.0901	0.1035	0.5527	0.0700	0.3163	0.0610	162.19	81.06	4.47E-09
7	323.49	0.3327	0.4054	0.1094	0.1525	0.4679	0.0616	0.3849	0.0855	156.57	72.43	2.95E-09
8	325.02	0.2956	0.4009	0.0941	0.2095	0.4837	0.0662	0.3757	0.1193	151.95	66.81	2.41E-09
9	330.42	0.2364	0.4287	0.0551	0.2798	0.4256	0.0997	0.2883	0.1864	149.14	62.19	2.73E-09
10	341.05	0.1470	0.5509	0.0191	0.2840	0.3658	0.2383	0.1168	0.2792	89.76	59.38	0

Heat duty [kJ/s]	
Condenser	-818.96
Boiler	586.99

---

[2] The amount of catalyst per stage is 25 g

Table 10-3: Temperature, vapor and liquid phase composition, and liquid and vapor flow profiles in the distillation column for Case 3.

Stage	T [K]	Composition of liquid phase				Composition of vapor phase				Liquid [gmol/h]	Vapor [gmol/h]	Reaction rate [kmol/g_{cat} -s]
		Methanol	Acetic acid	Methyl acetate	Water	Methanol	Acetic acid	Methyl acetate	Water			
1	303.69	0.4061	0.0000	0.5934	0.0005	0.3358	0.0000	0.6640	0.0002	42.24	0.00	0
2	304.48	0.5574	0.0000	0.4411	0.0015	0.4061	0.0000	0.5934	0.0005	41.19	84.48	-1.18E-11
3	305.76	0.6867	0.0001	0.3100	0.0033	0.4808	0.0000	0.5182	0.0010	40.37	83.43	-1.52E-11
4	307.03	0.7651	0.0001	0.2286	0.0062	0.5432	0.0000	0.4549	0.0019	39.93	82.61	-1.97E-11
5	307.88	0.8002	0.0002	0.1885	0.0111	0.5805	0.0000	0.4162	0.0033	39.71	82.17	-2.79E-11
6	308.37	0.8111	0.0003	0.1694	0.0192	0.5970	0.0000	0.3973	0.0057	39.56	81.95	-4.27E-11
7	308.73	0.8089	0.0005	0.1579	0.0327	0.6019	0.0000	0.3885	0.0097	39.40	81.80	-6.54E-11
8	309.15	0.7963	0.0011	0.1466	0.0560	0.6003	0.0000	0.3834	0.0163	39.13	81.64	-7E-11
9	309.97	0.7626	0.0101	0.1314	0.0959	0.5935	0.0002	0.3788	0.0275	38.55	81.37	5.61E-10
10	313.37	0.6310	0.1146	0.1161	0.1383	0.5766	0.0051	0.3726	0.0457	38.42	80.79	9.88E-09
11	323.37	0.3743	0.4235	0.1076	0.0946	0.5246	0.0660	0.3547	0.0548	162.47	80.66	8.98E-08
12	321.25	0.3164	0.4018	0.1530	0.1288	0.4154	0.0533	0.4614	0.0699	157.99	72.71	5.12E-08
13	320.03	0.2774	0.3867	0.1829	0.1530	0.3516	0.0465	0.5221	0.0798	155.00	68.23	3.47E-08
14	319.23	0.2487	0.3752	0.2046	0.1715	0.3084	0.0421	0.5623	0.0872	152.81	65.24	2.57E-08
15	318.65	0.2264	0.3661	0.2212	0.1863	0.2767	0.0391	0.5913	0.0929	151.10	63.05	2.02E-08
16	318.23	0.2083	0.3585	0.2346	0.1987	0.2521	0.0368	0.6134	0.0977	149.71	61.34	1.65E-08
17	317.89	0.1932	0.3521	0.2455	0.2091	0.2322	0.0350	0.6311	0.1017	148.55	59.95	1.38E-08
18	317.62	0.1805	0.3466	0.2546	0.2182	0.2158	0.0336	0.6454	0.1051	147.55	58.79	1.18E-08
19	317.41	0.1699	0.3418	0.2621	0.2262	0.2023	0.0325	0.6572	0.1081	146.68	57.79	1.03E-08
20	317.24	0.1612	0.3376	0.2678	0.2334	0.1914	0.0315	0.6664	0.1107	145.89	56.92	9.12E-09
21	317.15	0.1551	0.3340	0.2704	0.2405	0.1837	0.0308	0.6722	0.1133	145.12	56.13	8.29E-09
22	317.25	0.1531	0.3320	0.2653	0.2496	0.1815	0.0307	0.6713	0.1165	144.19	55.36	7.91E-09
23	318.18	0.1572	0.3367	0.2357	0.2704	0.1899	0.0333	0.6513	0.1256	142.68	54.43	8.53E-09
24	322.75	0.1555	0.3714	0.1505	0.3226	0.2165	0.0519	0.5680	0.1636	141.20	52.92	1.32E-08
25	335.98	0.1090	0.4913	0.0530	0.3467	0.2366	0.1621	0.3207	0.2807	89.76	51.44	0

Heat duty [kJ/s]	
Condenser	-818.96
Boiler	586.99
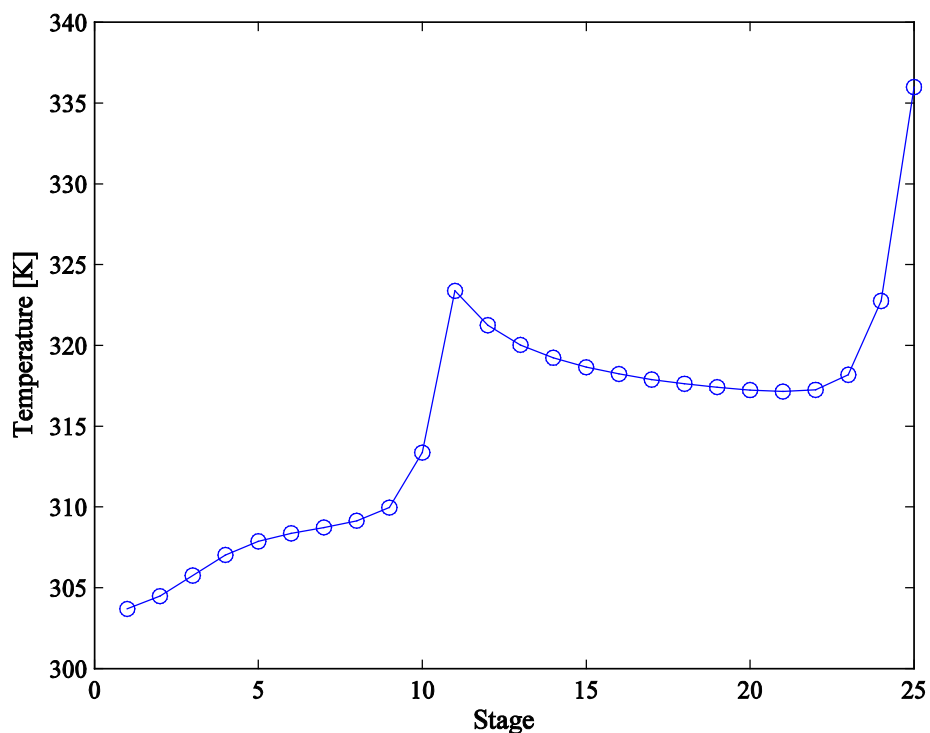
Figure 10-1: Temperature profile along the reactive distillation column for Case 3.
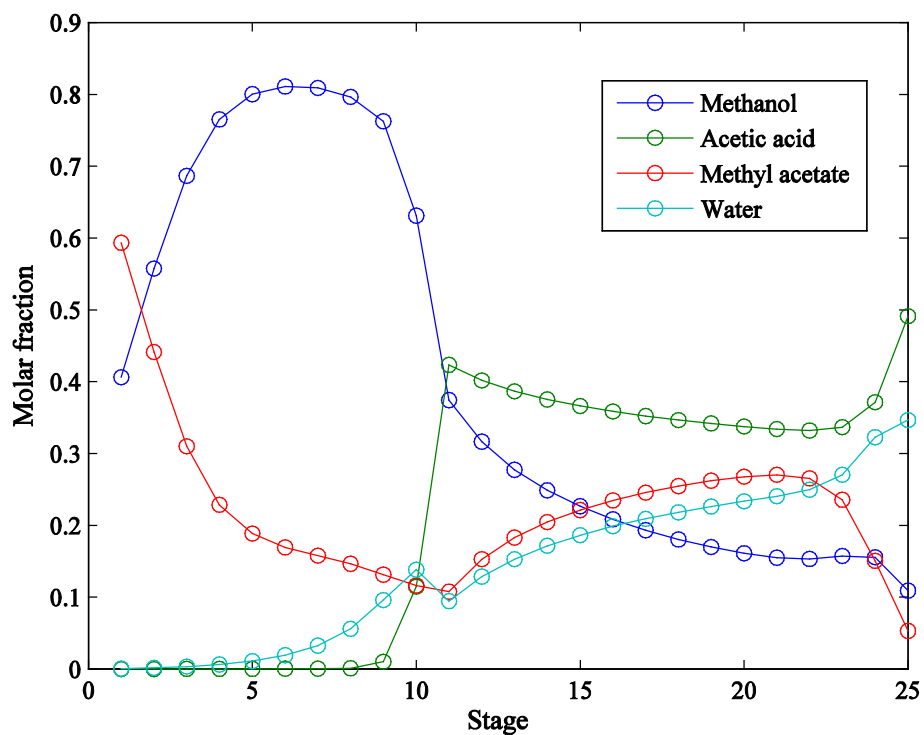
Figure 10-2: Liquid phase composition profiles along the column for Case 3.
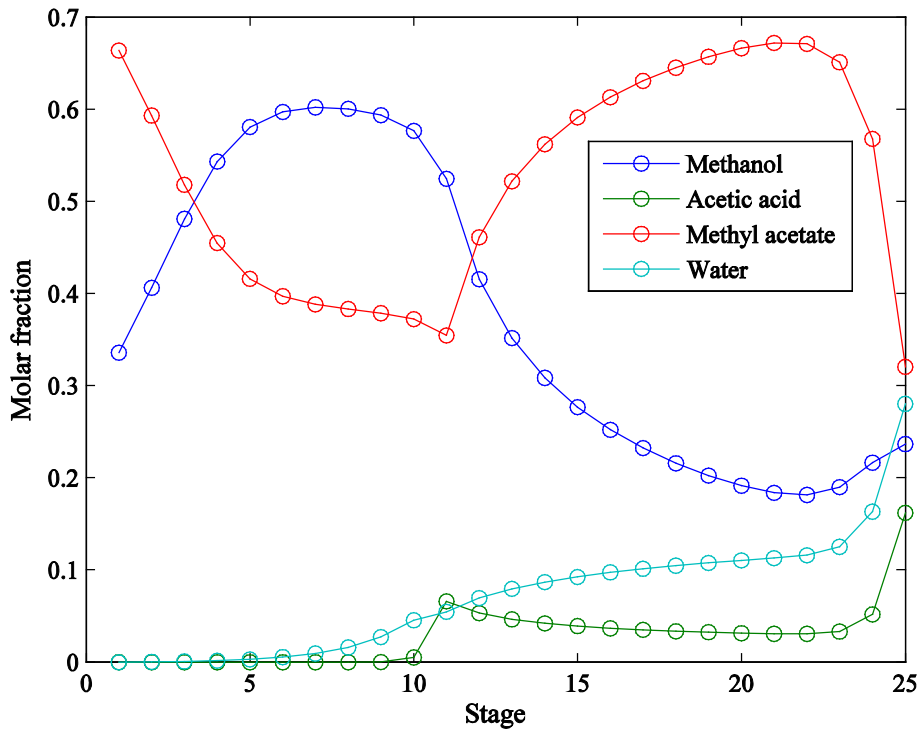
Figure 10-3: Vapor phase composition profiles along the column for Case 3.
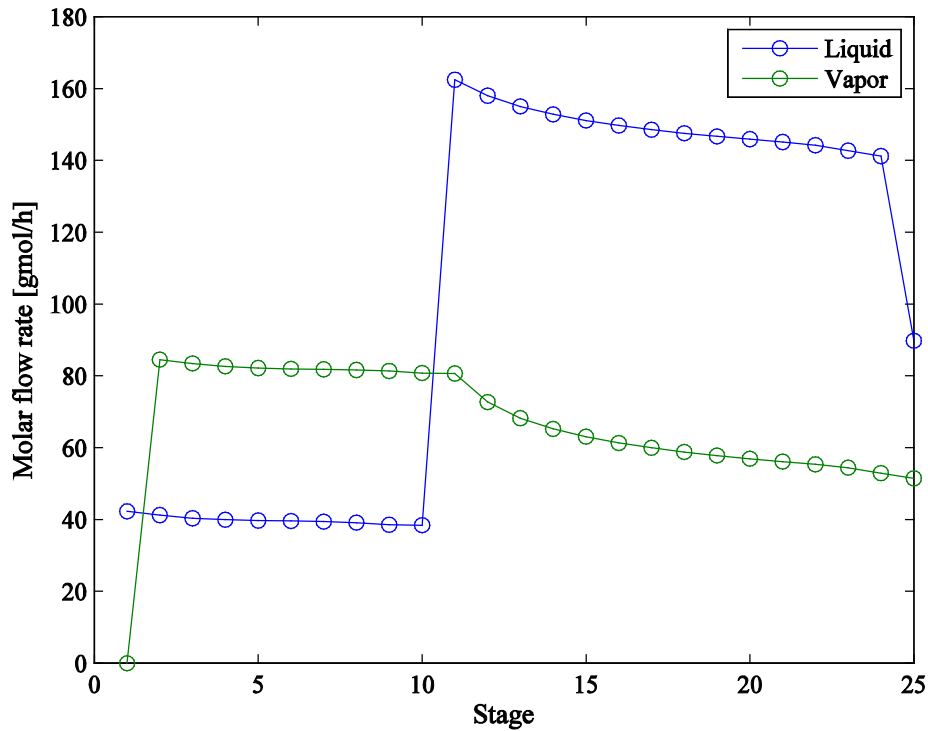
Figure 10-4: Liquid and vapor flow profiles along the column for Case 3.

Table 10-4: Temperature, vapor and liquid phase composition, and liquid and vapor flow profiles in the distillation column for Case 4.

Stage	T [K]	Composition of liquid phase				Composition of vapor phase				Liquid [gmol/h]	Vapor [gmol/h]	Reaction rate[4] [kmol/g_{cat} -s]
		Methanol	Acetic acid	Methyl acetate	Water	Methanol	Acetic acid	Methyl acetate	Water			
1	303.69	0.4066	5.26E-10	0.5934	6.53E-7	0.3361	8.38E-12	0.6639	2.73E-7	42.24	0.00	0
2	304.46	0.5578	3.33E-8	0.4422	1.82E-6	0.4066	5.26E-10	0.5934	6.53E-7	41.20	84.88	-1.43E-14
3	305.71	0.6874	7.74E-08	0.3126	3.86E-6	0.4812	1.31E-09	0.5188	1.25E-6	40.41	83.44	-1.84E-14
4	306.92	0.7673	1.36E-07	0.2327	7.30E-6	0.5439	2.53E-09	0.4561	2.26E-6	40.00	82.65	-2.41E-14
5	307.69	0.8056	2.21E-07	0.1944	1.29E-5	0.5820	4.36E-09	0.4180	3.95E-6	39.82	82.24	-3.46E-14
6	308.07	0.8217	3.53E-07	0.1783	2.21E-5	0.6002	7.18E-09	0.3998	6.72E-6	39.75	82.06	-5.41E-14
7	308.22	0.8281	5.67E-07	0.1719	3.68E-5	0.6078	1.17E-08	0.3922	1.12E-5	39.73	81.99	-8.77E-14
8	308.29	0.8305	9.16E-07	0.1694	6.06E-5	0.6109	1.90E-08	0.3891	1.84E-5	39.72	81.97	-1.43E-13
9	308.31	0.8315	1.48E-06	0.1684	9.91E-5	0.6120	3.08E-08	0.3879	3.01E-5	39.72	81.96	-2.33E-13
10	308.32	0.8118	2.41E-06	0.1680	1.61E-4	0.6125	5.00E-08	0.3875	4.90E-5	39.71	81.96	-3.79E-13
11	308.33	0.8319	3.91E-06	0.1679	2.62E-4	0.6126	8.11E-08	0.3873	7.96E-5	39.71	81.95	-6.15E-13
12	308.33	0.8318	6.33E-06	0.1677	4.24E-4	0.6127	1.31E-07	0.3872	1.29E-4	39.71	81.95	-9.95E-13
13	308.33	0.8317	1.02E-05	0.1676	6.87E-4	0.6126	2.13E-07	0.3872	2.09E-4	39.71	81.95	-1.61E-12
14	308.34	0.8315	1.66E-05	0.1674	1.11E-3	0.6126	3.45E-07	0.3871	3.38E-4	39.70	81.95	-2.60E-12
15	308.35	0.8310	2.68E-05	0.1671	1.80E-3	0.6124	5.57E-07	0.3870	5.47E-4	39.70	81.94	-4.19E-12
16	308.37	0.8304	4.32E-05	0.1667	2.92E-3	0.6122	9.00E-07	0.3869	8.85E-4	39.68	81.94	-6.75E-12
17	308.40	0.8293	6.97E-05	0.1659	4.73E-3	0.6118	1.45E-06	0.3867	1.43E-3	39.67	81.92	-1.08E-11
18	308.44	0.8276	1.12E-04	0.1646	7.69E-3	0.6113	2.35E-06	0.3864	2.32E-3	39.64	81.91	-1.74E-11
19	308.52	0.8247	1.80E-04	0.1626	0.0126	0.6103	3.78E-06	0.3859	3.78E-3	39.59	81.88	-2.77E-11
20	308.64	0.8198	2.88E-04	0.1593	0.0206	0.6087	6.09E-06	0.3851	0.0062	39.50	81.83	-4.37E-11
21	308.85	0.8115	4.71E-04	0.1539	0.0341	0.6061	1.01E-05	0.3938	0.0101	39.37	81.74	-6.69E-11
22	309.21	0.7967	1.09E-03	0.1449	0.0573	0.6017	2.40E-05	0.3816	0.0167	39.11	81.61	-7.10E-11
23	310.00	0.7622	1.01E-02	0.1306	0.0971	0.5938	2.44E-05	0.3781	0.0278	38.53	81.35	5.61E-10
24	313.40	0.6304	0.1147	0.1157	0.1391	0.5766	5.16E-05	0.3723	0.0460	38.41	80.77	9.87E-09
25	323.38	0.3742	0.4235	0.1075	0.0948	0.5245	0.0660	0.3546	0.0549	162.46	80.65	8.98E-08
26	321.26	0.3162	0.4019	0.1529	0.1290	0.4153	0.0534	0.4614	0.0700	157.98	72.70	5.12E-08
27	320.03	0.2773	0.3868	0.1828	0.1531	0.3515	0.0465	0.5221	0.0799	155.00	68.22	3.47E-08
28	319.23	0.2486	0.3753	0.2045	0.1716	0.3083	0.0422	0.5623	0.0872	152.81	65.24	2.57E-08
29	318.66	0.2262	0.3661	0.2212	0.1865	0.2766	0.0391	0.5913	0.0930	151.10	63.05	2.02E-08

30	318.23	0.2081	0.3586	0.2346	0.1988	0.2519	0.0368	0.6135	0.0978	149.71	61.34	1.65E-08
31	317.89	0.1930	0.3522	0.2456	0.2093	0.2320	0.0351	0.6313	0.1017	148.55	59.95	1.38E-08
32	317.62	0.1801	0.3467	0.2549	0.2183	0.2154	0.0336	0.6458	0.1052	147.56	58.79	1.18E-08
33	317.40	0.1690	0.3418	0.2629	0.2263	0.2013	0.0325	0.6581	0.1082	146.70	57.80	1.02E-08
34	317.21	0.1593	0.3376	0.2699	0.2333	0.1891	0.0315	0.6686	0.1108	145.95	56.94	8.98E-09
35	317.05	0.1507	0.3338	0.2760	0.2396	0.1785	0.0306	0.6777	0.1131	145.29	56.19	7.96E-09
36	316.92	0.1430	0.3304	0.2814	0.2452	0.1691	0.0299	0.6857	0.1153	144.69	55.53	7.11E-09
37	316.80	0.1361	0.3273	0.2863	0.2504	0.1608	0.0293	0.6928	0.1172	144.16	54.93	6.40E-09
38	316.69	0.1299	0.3245	0.2907	0.2550	0.1532	0.0287	0.6991	0.1189	143.68	54.40	5.79E-09
39	316.60	0.1242	0.3219	0.2946	0.2593	0.1464	0.0282	0.7048	0.1205	143.24	53.92	5.27E-09
40	316.52	0.1190	0.3195	0.2982	0.2632	0.1403	0.0278	0.7100	0.1220	142.84	53.48	4.81E-09
41	316.44	0.1143	0.3174	0.3015	0.2668	0.1347	0.0274	0.7147	0.1233	142.47	53.08	4.41E-09
42	316.38	0.1100	0.3154	0.3045	0.2701	0.1295	0.0270	0.7189	0.1246	142.13	52.71	4.06E-09
43	316.32	0.1060	0.3135	0.3072	0.2732	0.1248	0.0267	0.7228	0.1257	141.82	52.37	3.74E-09
44	316.27	0.1024	0.3118	0.3097	0.2761	0.1206	0.0264	0.7263	0.1268	141.53	52.06	3.47E-09
45	316.22	0.0993	0.3102	0.3117	0.2788	0.1169	0.0261	0.7292	0.1277	141.25	51.77	3.24E-09
46	316.19	0.0970	0.3088	0.3127	0.2814	0.1142	0.0259	0.7313	0.1286	140.97	51.49	3.05E-09
47	316.22	0.0963	0.3080	0.3105	0.2852	0.1133	0.0258	0.7311	0.1298	140.61	51.21	2.97E-09
48	316.64	0.0987	0.3113	0.2935	0.2964	0.1166	0.0269	0.7226	0.1338	139.81	50.85	3.17E-09
49	319.55	0.1020	0.3410	0.2178	0.3391	0.1294	0.0374	0.6761	0.1571	138.35	50.05	4.75E-09
50	332.19	0.0768	0.4593	0.0849	0.3789	0.1485	0.1224	0.4634	0.2657	89.76	48.59	0

Heat duty [kJ/s]	
Condenser	-810.486
Boiler	495.0368

---

[3] The amount of catalyst per stage is 25 g
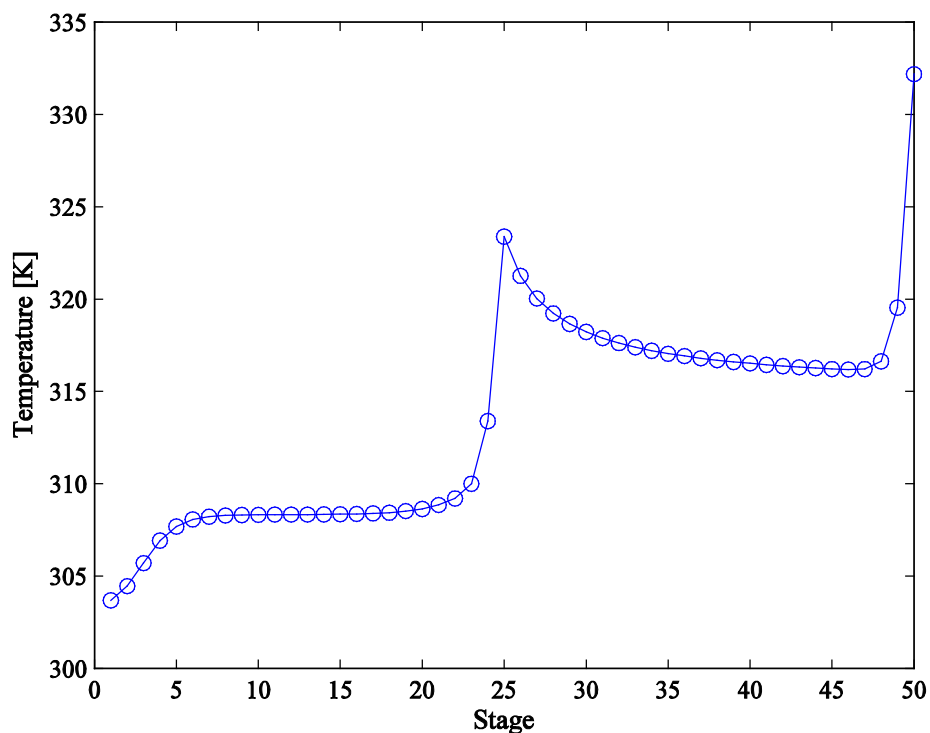
Figure 10-5: Temperature profile along the reactive distillation column for Case 4.
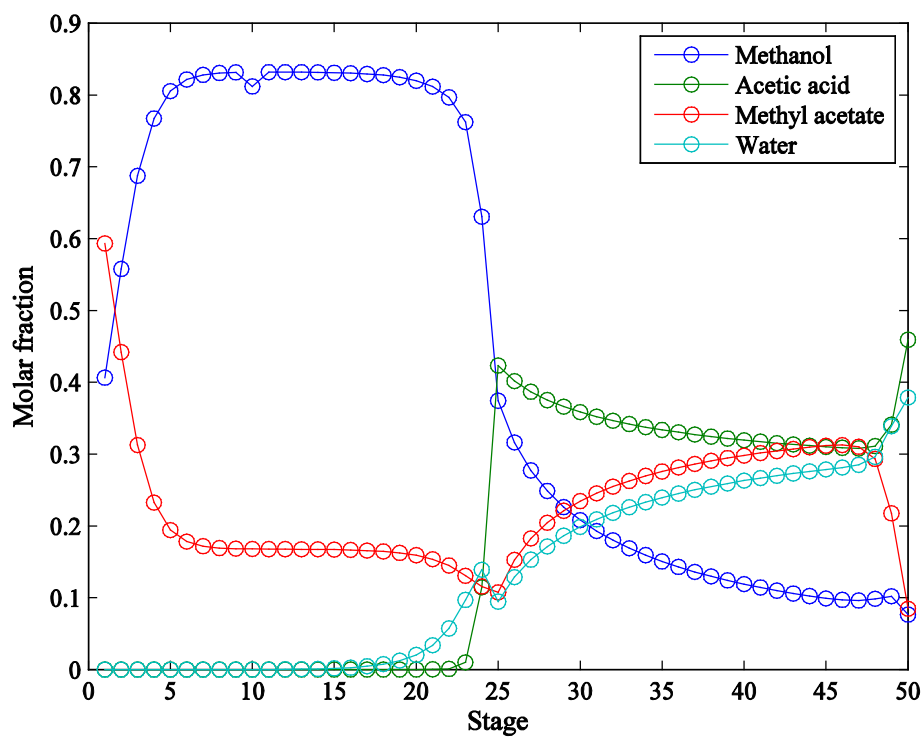
Figure 10-6: Liquid phase composition profiles along the column for Case 4.
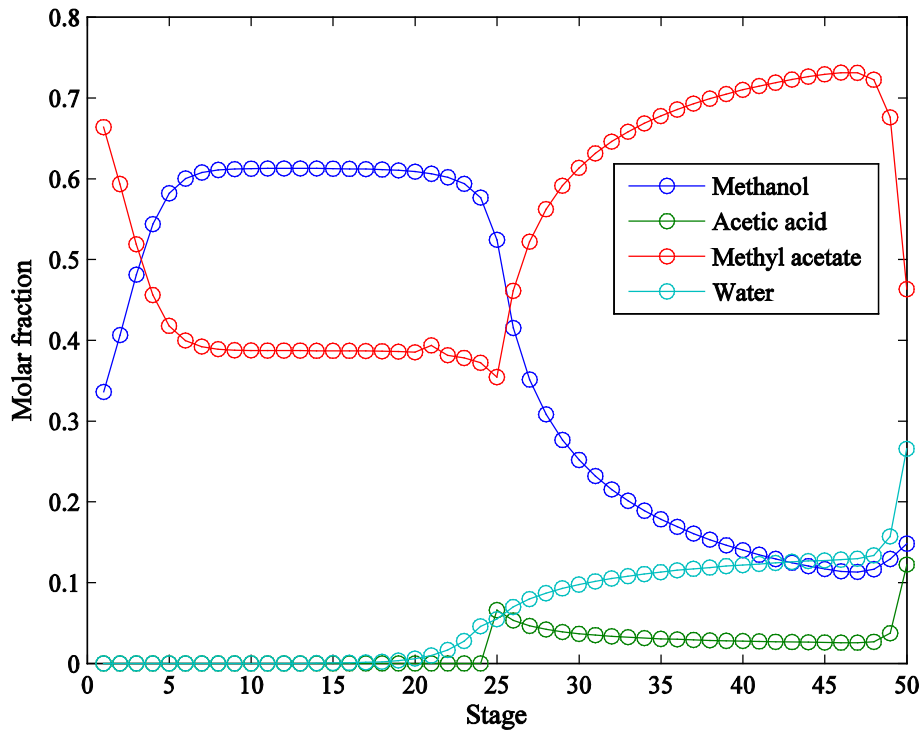
Figure 10-7: Vapor phase composition profiles along the column for Case 4.
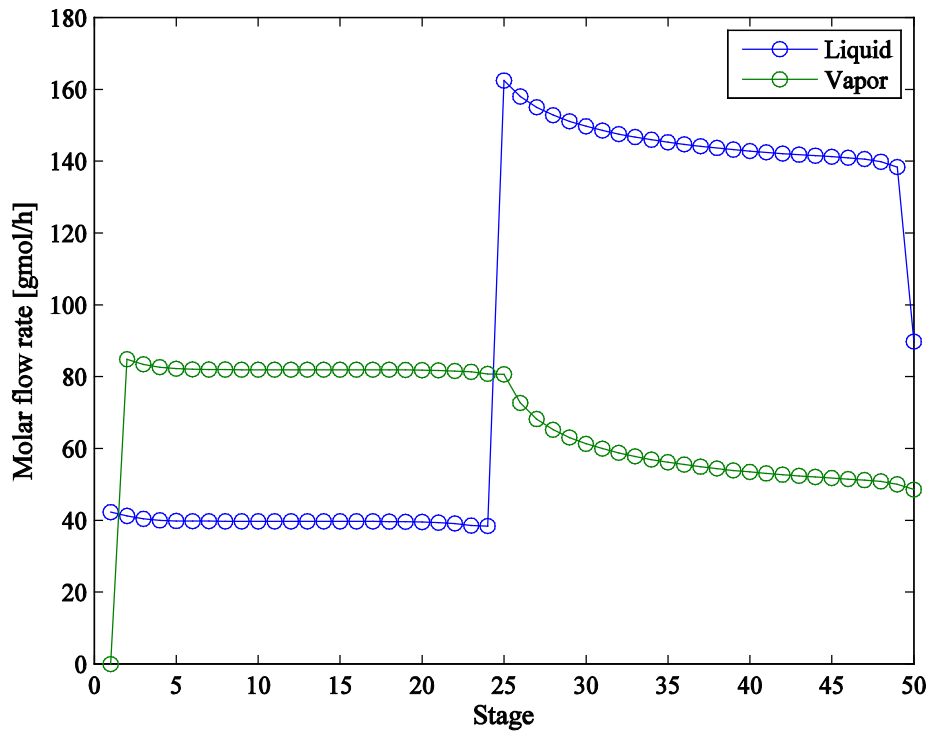
Figure 10-8: Liquid and vapor flow profiles along the column for Case 4.

Table 10-5: Behavior of the molar fraction in the distillate and the bottoms, and the conversion and recovery percentages as a function of the amount of catalyst for Cases 2, 3 and 4.

10 stages reactive distillation column					
Catalyst in the stage [g]	Total catalyst in the column [g]	Molar fraction of Methyl acetate		Conversion	Recovery
		Distillate	Bottoms		
0.5	4	0.0760	0.0045	6.4%	88.7%
2.5	20	0.2013	0.0073	16.1%	92.8%
5	40	0.2890	0.0092	23.0%	93.7%
25	200	0.5408	0.0181	43.1%	93.4%
50	400	0.6330	0.0275	51.5%	91.5%
250	2000	0.7233	0.0778	66.1%	81.4%
500	4000	0.7449	0.1007	71.4%	77.7%
2500	20000	0.7870	0.1219	77.8%	75.2%
5000	40000	0.8001	0.1224	78.9%	75.5%
25000	200000	0.8173	0.1217	80.1%	76.0%

25 stages reactive distillation column					
Catalyst in the stage [g]	Total catalyst in the column [g]	Molar fraction of Methyl acetate		Conversion	Recovery
		Distillate	Bottoms		
0.5	11.5	0.1481	0.0015	11.3%	97.9%
2.5	57.5	0.3628	0.0037	27.6%	97.9%
5	115	0.4381	0.0088	34.0%	95.9%
25	575	0.5934	0.0530	52.5%	84.0%
50	1150	0.6622	0.0780	61.6%	80.0%
250	5750	0.7345	0.1153	72.9%	75.0%
500	11500	0.7521	0.1174	74.5%	75.1%
2500	57500	0.7929	0.1170	77.5%	76.1%
5000	115000	0.8055	0.1165	78.4%	76.5%
25000	575000	0.8220	0.1157	79.5%	77.0%
500000	1150000	0.8249	0.1155	79.7%	77.1%

50 stages reactive distillation column					
Catalyst in the stage [g]	**Total catalyst in the column [g]**	**Molar fraction of Methyl acetate**		**Conversion**	**Recovery**
		Distillate	Bottoms		
0.05	2.4	0.0351	0.0003	2.7%	98.4%
0.25	12	0.1353	0.0008	10.2%	98.8%
0.5	24	0.2168	0.0011	16.3%	98.9%
2.5	120	0.3847	0.0067	29.7%	96.4%
5	240	0.4401	0.0244	36.6%	89.5%
25	1200	0.5934	0.0849	57.6%	76.7%
50	2400	0.6630	0.1036	65.7%	75.1%
250	12000	0.7365	0.1160	73.2%	74.9%
500	24000	0.7541	0.1160	74.5%	75.4%
2500	120000	0.7959	0.1151	77.4%	76.5%
5000	240000	0.8084	0.1148	78.3%	76.8%
25000	1200000	0.8243	0.1141	79.4%	77.3%
500000	2400000	0.8272	0.1140	79.6%	77.3%

Table 10-6: Temperature, vapor and liquid phase composition, and liquid and vapor flow profiles in the distillation column for Case 5.

Stage	T [K]	Composition of liquid phase				Composition of vapor phase				Liquid [gmol/h]	Vapor [gmol/h]	Reaction rate[4] [kmol/ m^3 -s]
		Methanol	Acetic acid	Methyl acetate	Water	Methanol	Acetic acid	Methyl acetate	Water			
1	329.52	0.7415	6.51E-08	0.2570	0.0015	0.5745	1.73E-09	0.4249	0.0006	62.31	0.00	-1.25E-15
2	332.84	0.8853	1.96E-06	0.1109	0.0038	0.7415	6.51E-08	0.2570	0.0015	62.30	93.31	-8.16E-14
3	334.87	0.9344	3.54E-05	0.0578	0.0078	0.8385	1.34E-06	0.1585	0.0031	62.10	92.40	-1.70E-12
4	335.68	0.9431	5.97E-04	0.0420	0.0143	0.8715	2.39E-05	0.1228	0.0057	61.98	92.20	2.11E-10
5	336.27	0.9284	0.0094	0.0371	0.0250	0.8772	4.02E-04	0.1122	0.0101	61.75	92.08	8.39E-08
6	339.00	0.8267	0.0990	0.0358	0.0384	0.8672	6.35E-03	0.1092	0.0173	62.62	91.85	1.15E-05
7	358.98	0.5477	0.3789	0.0348	0.0386	0.7993	0.0671	0.1074	0.0262	92.26	92.72	2.21E-04
8	349.16	0.5363	0.3770	0.0353	0.0514	0.7872	0.0670	0.1108	0.0350	92.71	96.56	2.18E-04
9	349.47	0.5271	0.3752	0.0334	0.0643	0.7811	0.0674	0.1076	0.0438	96.16	96.01	2.18E-04
10	349.81	0.5190	0.3733	0.0308	0.0769	0.7774	0.0679	0.1020	0.0526	95.62	95.46	2.20E-04
11	350.15	0.5117	0.3711	0.0281	0.0891	0.7748	0.0684	0.0957	0.0611	95.08	94.92	2.21E-04
12	350.46	0.5056	0.3685	0.0256	0.1003	0.7732	0.0686	0.0891	0.0690	94.55	94.38	2.22E-04
13	350.71	0.5011	0.3655	0.0231	0.1103	0.7727	0.0686	0.0826	0.0760	94.04	93.85	2.22E-04
14	350.89	0.4987	0.3618	0.0209	0.1185	0.7739	0.0682	0.0762	0.0817	93.55	93.34	2.21E-04
15	350.97	0.4993	0.3575	0.0189	0.1243	0.7773	0.0672	0.0700	0.0855	93.09	92.85	2.19E-04
16	350.92	0.5037	0.3520	0.0171	0.1272	0.7385	0.0656	0.0639	0.0869	92.66	92.39	2.15E-04
17	350.68	0.5134	0.3448	0.0155	0.1263	0.7934	0.0630	0.0581	0.0854	92.26	91.96	2.07E-04
18	350.15	0.5315	0.3334	0.0141	0.1210	0.8086	0.0585	0.0526	0.0803	91.85	91.56	1.94E-04
19	348.98	0.5666	0.3091	0.0129	0.1114	0.8320	0.0496	0.0475	0.0709	91.28	91.15	1.65E-04
20	345.59	0.6603	0.2241	0.0119	0.1038	0.8725	0.0265	0.0433	0.0577	127.48	90.58	8.13E-05
21	347.08	0.6030	0.2363	0.0109	0.1497	0.8398	0.0308	0.0434	0.0860	126.66	94.58	9.44E-05
22	350.91	0.4831	0.2795	0.0088	0.2286	0.7659	0.0474	0.0406	0.1461	126.42	93.76	1.46E-04
23	358.73	0.3047	0.3840	0.0065	0.3048	0.6070	0.1080	0.0350	0.2500	129.38	93.52	3.00E-04
24	368.86	0.1502	0.5385	0.0046	0.3067	0.3696	0.2591	0.0255	0.3458	137.10	96.48	4.86E-04
25	377.51	0.0626	0.6985	0.0026	0.2363	0.1698	0.4800	0.0132	0.3370	32.90	104.20	4.62E-04

---

[4] The volumetric retention per stage is 0.5 liters.

Heat duty [kJ/s]	
Condenser	-900.08
Boiler	914.33

Table 10-7: Behavior of the temperature and the average reaction rate as a function of the total residence time in the column for Case 5.

Residence time [h]	Average Temperature [K]	Maximum Temperature [K]	Minimum Temperature [K]	Reaction rate [kmol/ m^3- s]
0.81	349.43	382.87	334.14	2.50E-04
4.07	348.33	377.51	329.52	1.74E-04
8.14	347.92	374.07	327.79	1.38E-04
40.72	343.61	367.23	327.13	5.08E-05
81.43	341.70	364.92	327.79	2.83E-05
122.15	340.95	363.76	328.31	1.97E-05
162.87	340.51	363.11	328.67	1.52E-05
407.17	339.30	361.77	329.38	6.34E-06
814.34	338.58	360.48	329.52	3.21E-06
4071.71	337.92	356.94	329.50	6.49E-07
8143.42	337.86	356.33	329.44	3.25E-07

Table 10-8: Temperature, vapor and liquid phase composition, and liquid and vapor flow profiles in the distillation column for Case 6.

Stage	T [K]	Composition of liquid phase				Composition of vapor phase				Liquid [gmol/h]	Vapor [gmol/h]	Reaction rate [kmol/ g_{cat} -s]
		Methanol	Acetic acid	Methyl acetate	Water	Methanol	Acetic acid	Methyl acetate	Water			
1	329.03	0.0415	4.00E-05	0.9579	0.0006	0.0756	1.65E-06	0.9238	0.0005	63.21	0.00	
2	329.56	0.0213	9.05E-04	0.9772	0.0006	0.0415	4.00E-05	0.9579	0.0006	63.56	93.31	-2.62E-10
3	329.83	0.0137	2.71E-03	0.9825	0.0011	0.0273	1.24E-04	0.9715	0.0011	63.76	93.66	-5.19E-10
4	330.06	0.0105	7.42E-03	0.9796	0.0025	0.0211	3.53E-04	0.9761	0.0024	63.84	93.83	-1.21E-09
5	330.59	0.0084	0.0236	0.9622	0.0058	0.0166	1.23E-03	0.9764	0.0057	63.71	93.94	-2.25E-09
6	333.03	0.0060	0.1058	0.8755	0.0128	0.0109	7.87E-03	0.9690	0.0123	63.22	93.81	-1.79E-09
7	342.05	0.0035	0.3807	0.5949	0.0209	0.0058	0.0601	0.9137	0.0205	98.29	93.32	1.42E-09
8	342.07	0.0048	0.3807	0.5837	0.0308	0.0078	0.0593	0.9032	0.0297	97.78	97.59	5.29E-10
9	342.11	0.0062	0.3808	0.5719	0.0410	0.0101	0.0586	0.8925	0.0388	97.26	97.08	4.83E-10
10	342.16	0.0078	0.3809	0.5594	0.0519	0.0125	0.0579	0.8814	0.0482	96.72	96.56	5.38E-10
11	342.21	0.0095	0.3807	0.5456	0.0641	0.0151	0.0572	0.8695	0.0582	96.11	96.02	6.68E-10
12	342.26	0.0116	0.3800	0.5303	0.0781	0.0182	0.0562	0.8564	0.0693	95.39	95.41	9.47E-10
13	342.30	0.0144	0.3779	0.5129	0.0947	0.0221	0.0548	0.8415	0.0816	94.48	94.69	1.54E-09
14	342.27	0.0185	0.3734	0.4932	0.1149	0.0280	0.0525	0.8240	0.0955	92.28	93.78	2.73E-09
15	342.11	0.0255	0.3645	0.4705	0.1396	0.0376	0.0490	0.8029	0.1105	91.60	92.58	4.90E-09
16	341.73	0.0384	0.3490	0.4434	0.1692	0.0547	0.0438	0.7760	0.1255	89.24	90.90	8.38E-09
17	341.05	0.0631	0.3247	0.4085	0.2037	0.0855	0.0367	0.7398	0.1380	86.01	88.54	1.32E-08
18	340.02	0.1114	0.2888	0.3597	0.2402	0.1401	0.0281	0.6881	0.1437	81.82	85.31	1.90E-08
19	338.54	0.2070	0.2356	0.2912	0.2662	0.2348	0.0187	0.6111	0.1354	76.98	81.12	2.49E-08
20	335.29	0.4158	0.1296	0.2219	0.2326	0.3979	0.0067	0.4992	0.0962	108.98	76.28	2.17E-08
21	335.74	0.4310	0.1062	0.1789	0.2839	0.4133	0.0054	0.4723	0.1089	104.85	76.08	1.63E-08
22	338.33	0.4503	0.0832	0.0976	0.3690	0.4761	0.0049	0.3832	0.1358	100.14	71.95	1.56E-08
23	344.25	0.3865	0.0582	0.0305	0.5248	0.5497	0.0052	0.2348	0.2104	95.18	67.24	1.61E-08
24	353.84	0.2037	0.0392	0.0050	0.7521	0.5066	0.0073	0.0967	0.3894	90.59	62.28	1.71E-08
25	365.72	0.0642	0.0595	0.0002	0.8761	0.2825	0.0267	0.0086	0.6823	32.90	57.69	

Thermal load [kJ/s]	
Condenser	-802.34
Boiler	639.57

Table 10-9: Behavior of the average temperature and reaction rate as a function of the residence time for Case 6.

Total catalyst in the column [g]	Average Temperature [K]	Maximum Temperature [K]	Minimum Temperature [K]	Reaction rate[5] [kmol/ g_{cat}- s]
1.15	349.02	381.28	332.62	5.93E-07
5.75	348.66	377.36	329.42	3.46E-07
11.5	348.64	375.03	328.15	2.54E-07
57.5	348.97	368.40	327.11	9.95E-08
115	345.07	366.50	327.60	5.86E-08
172.5	343.83	365.84	328.06	4.19E-08
184	343.65	365.81	328.12	3.96E-08
230	343.01	365.83	328.30	3.25E-08
345	341.92	365.99	328.55	2.24E-08
460	341.27	365.99	328.71	1.70E-08
690	340.54	365.88	328.89	1.15E-08
920	340.13	365.79	328.98	8.67E-09
1150	339.85	365.72	329.03	6.95E-09
2300	339.21	365.39	329.11	3.49E-09
5750	338.80	364.84	329.17	1.40E-09
11500	338.65	364.50	329.19	7.02E-10
57500	338.53	364.09	329.21	1.41E-10
115000	338.51	364.02	329.21	7.03E-11

---

[5] The amount of catalyst per stage is 50g

Table 10-10: Behavior of the conversion and recovery percentages as a function of the reflux ratio for Case 6.

Reflux ratio	Reflux [gmol/h]	Molar fraction of Methyl acetate		Conversion	Recovery
		Distillate	Bottoms		
0.1	2.01	0.4590	0.0265	47.69%	94.067%
0.2	6.02	0.5019	0.0231	51.52%	95.210%
0.5	15.05	0.6355	0.0125	63.44%	97.894%
1	30.1	0.8573	2.8E-03	84.08%	99.643%
1.25	37.625	0.9205	1.2E-03	90.08%	99.863%
1.35	40.635	0.9383	6.0E-04	91.76%	99.930%
1.5	45.15	0.9558	3.5E-04	93.44%	99.960%
1.6	48.16	0.9589	3.1E-04	93.74%	99.965%
1.8	54.18	0.9602	2.6E-04	93.87%	99.970%
2	60.2	0.9590	2.4E-04	93.75%	99.973%
2.1	62.31	0.9579	2.3E-04	93.64%	99.973%
2.2	66.22	0.9566	2.3E-04	93.51%	99.974%
2.3	69.23	0.9550	2.3E-04	93.36%	99.974%
2.4	72.24	0.9533	2.3E-04	93.19%	99.974%
2.5	75.25	0.9515	2.3E-04	93.01%	99.974%
2.6	78.26	0.9495	2.3E-04	92.82%	99.974%
2.7	81.27	0.9475	2.3E-04	92.62%	99.974%
2.8	84.28	0.9453	2.3E-04	92.40%	99.973%
2.9	87.29	0.9430	2.3E-04	92.18%	99.973%
3	90.3	0.9406	2.4E-04	91.94%	99.972%
3.5	105.35	0.9272	2.7E-04	90.64%	99.968%
4	120.4	0.9118	3.2E-04	89.14%	99.962%
4.5	135.45	0.8947	3.9E-04	87.48%	99.952%
5	150.5	0.8761	4.9E-04	85.67%	99.939%
6	180.6	0.8356	8.2E-04	81.75%	99.893%
7	210.7	0.7936	1.4E-03	77.70%	99.813%
10	301	0.7089	3.3E-03	69.52%	99.496%

Table 10-11: Heat duty of the condenser and the boiler as a function of the reflux ratio for Case 6.

Reflux ratio	Reflux [gmol/h]	Thermal load Boiler [kJ/s]	Thermal load Condenser [kJ/s]
0.1	2.01	265.69	220.99
0.2	6.02	293.96	239.03
0.5	15.05	382.17	295.99
1	30.1	532.08	392.31
1.25	37.625	590.59	435.55
1.35	40.635	611.49	452.87
1.5	45.15	647.49	485.09
1.6	48.16	672.83	509.76
1.8	54.18	724.30	560.98
2	60.2	776.25	613.23
2.1	62.31	802.34	639.57
2.2	66.22	828.48	666.03
2.3	69.23	854.68	692.58
2.4	72.24	880.93	719.22
2.5	75.25	907.24	745.94
2.6	78.26	933.59	772.74
2.7	81.27	959.99	799.62
2.8	84.28	986.43	826.57
2.9	87.29	1012.93	853.59
3	90.3	1039.47	880.68
3.5	105.35	1172.86	1017.15
4	120.4	1307.41	1115.28
4.5	135.45	1443.12	1294.28
5	150.5	1579.95	1436.16
6	180.6	1856.82	1722.64
7	210.7	2137.28	2013.10
10	301	2978.87	2875.15

Table 10-12: Temperature, vapor and liquid phase composition, and liquid and vapor flow profiles in the distillation column for Case 7.

Stage	T [K]	Composition of liquid phase				Composition of vapor phase				Liquid [gmol/h]	Vapor [gmol/h]	Reaction rate [kmol/ g_{cat} -s]	Reaction rate [kmol/ g_{cat} -s]
		Methanol	Acetic acid	Methyl acetate	Water	Methanol	Acetic acid	Methyl acetate	Water				
1	329.78	0.0141	1.16E-07	0.9619	0.0240	0.0274	5.08E-09	0.9503	0.0023	63.21	0.00		-4.22E-10
2	329.98	0.0071	2.58E-06	0.9674	0.0255	0.0141	1.16E-07	0.9619	0.0240	63.29	93.31		-1.24E-08
3	330.05	0.0047	3.96E-05	0.9689	0.0264	0.0094	1.79E-06	0.9656	0.0250	63.31	93.39		-2.32E-07
4	330.09	0.0039	5.92E-04	0.9685	0.0270	0.0077	2.69E-05	0.9666	0.0256	63.26	93.41		-4.14E-06
5	330.33	0.0036	0.0084	0.9604	0.0275	0.0072	4.01E-04	0.9664	0.0261	62.85	93.36		-6.79E-05
6	332.48	0.0038	0.0841	0.8840	0.0281	0.0070	5.70E-03	0.9609	0.0264	62.12	92.95		-6.29E-04
7	341.69	0.0044	0.3712	0.5967	0.0277	0.0072	0.0566	0.9094	0.0267	97.42	92.22	5.98E-07	
8	341.72	0.0058	0.3713	0.5864	0.0366	0.0094	0.0560	0.8998	0.0348	96.97	96.72	8.31E-07	
9	341.75	0.0072	0.3713	0.5754	0.0461	0.0116	0.0554	0.8900	0.0430	96.50	96.27	9.25E-07	
10	341.79	0.0087	0.3712	0.5636	0.0564	0.0139	0.0547	0.8797	0.0517	95.98	95.80	1.08E-06	
11	341.83	0.0105	0.3709	0.5505	0.0681	0.0165	0.0540	0.8684	0.0612	95.39	95.28	1.38E-11	
12	341.87	0.0126	0.3700	0.5537	0.0817	0.0196	0.0530	0.8558	0.0717	94.69	94.69	2.00E-11	
13	341.89	0.0155	0.3676	0.5188	0.0980	0.0237	0.0515	0.8412	0.0835	93.79	93.99	3.27E-11	
14	341.83	0.0199	0.3628	0.4994	0.1179	0.0299	0.0493	0.8240	0.0968	92.58	93.09	5.75E-11	
15	341.65	0.0275	0.3536	0.4768	0.1421	0.0402	0.0458	0.8028	0.1111	90.90	91.88	1.01E-10	
16	341.25	0.0413	0.3379	0.4495	0.1713	0.0583	0.0407	0.7756	0.1253	88.55	90.20	1.70E-10	
17	340.57	0.0675	0.3138	0.4135	0.2051	0.0904	0.0340	0.7386	0.1369	85.34	87.85	2.62E-10	
18	339.58	0.1182	0.2786	0.3620	0.2412	0.1466	0.0260	0.6855	0.1418	81.20	84.64	3.72E-10	
19	338.22	0.2175	0.2268	0.2887	0.2670	0.2434	0.0173	0.6060	0.1334	76.41	80.50	4.86E-10	
20	335.24	0.4304	0.1236	0.2139	0.2321	0.4093	0.0063	0.4896	0.0948	108.44	75.71	4.26E-10	
21	335.85	0.4513	0.0997	0.1663	0.2827	0.4325	0.0050	0.4550	0.1074	104.31	75.54	3.72E-05	
22	338.49	0.4750	0.0758	0.0087	0.3604	0.5043	0.0044	0.3583	0.1329	99.50	71.41	3.10E-05	
23	343.76	0.4246	0.0515	0.0292	0.4947	0.5849	0.0043	0.2153	0.1973	95.48	67.00	3.01E-05	
24	352.00	0.2510	0.0346	0.0053	0.7092	0.5990	0.0054	0.0883	0.3474	91.04	62.58	3.00E-05	
25	363.76	0.0855	0.0559	0.0003	0.8583	0.3438	0.0217	0.0089	0.6255	32.90	58.14		4.96E-02

Heat duty [kJ/s]	
Condenser	-803.86
Boiler	639.99

Table 10-13: Behavior of the conversion and recovery percentages as a function of the amount of catalyst.

Catalyst in the stage [g]	Total catalyst in the column [g]	Molar fraction of Methyl acetate		Conversion	Recovery
		Distillate	Bottoms		
0.05	0.9	0.1173	3.4E-03	11.82%	96.96%
0.25	4.5	0.2625	2.3E-03	25.90%	99.07%
0.5	0	0.3676	1.7E-03	36.10%	99.50%
2.5	45	0.6953	6.7E-04	68.02%	99.89%
5	90	0.8164	3.8E-04	79.83%	99.95%
7.5	133	0.8751	2.6E-04	85.55%	99.97%
8	144	0.8827	2.5E-04	86.29%	99.97%
10	180	0.9055	2.1E-04	88.51%	99.98%
15	270	0.9335	1.7E-04	91.25%	99.98%
20	360	0.9455	1.6E-04	92.42%	99.98%
30	540	0.9555	1.8E-04	93.40%	99.98%
40	720	0.9597	2.2E-04	93.81%	99.98%
50	900	0.9613	2.7E-04	94.03%	99.97%
100	1800	0.9655	5.8E-04	94.42%	99.93%
250	4500	0.9675	1.2E-03	94.68%	99.86%
500	9000	0.9683	1.6E-03	94.80%	99.82%

Table 10-14: Temperature, vapor and liquid phase composition, and liquid and vapor flow profiles in the distillation column for Case 8.

Stage	T [K]	Composition of liquid phase				Composition of vapor phase				Liquid [gmol/h]	Vapor [gmol/h]	Reaction rate [kmol/ g_{cat} -s]	Reaction rate [kmol/ g_{cat} -s]
		Methanol	Acetic acid	Methyl acetate	Water	Methanol	Acetic acid	Methyl acetate	Water				
1	329.07	0.0430	9.43E-08	0.9353	0.0217	0.0760	3.79E-09	0.9051	0.0189	63.21	0.00		-1.30E-13
2	329.55	0.0229	2.21E-06	0.9533	0.0238	0.0430	9.43E-08	0.9353	0.0217	63.47	93.31		-4.47E-12
3	329.75	0.0152	3.51E.05	0.9597	0.0250	0.0294	1.53E-06	0.9475	0.0231	63.56	93.57		-9.08E-11
4	329.84	0.0124	5.40E-04	0.9613	0.0258	0.0242	2.38E-05	0.9519	0.0239	63.54	93.66		-1.69E-09
5	330.08	0.0115	0.0079	0.9543	0.0263	0.0223	3.66E-04	0.9529	0.0244	63.15	93.64		-2.79E-08
6	332.19	0.0121	0.0819	0.8792	0.0268	0.0217	5.36E-03	0.9482	0.0248	62.28	93.25		-1.61E-07
7	341.47	0.0127	0.3696	0.5904	0.0264	0.0221	0.0552	0.8975	0.0251	97.68	92.48		2.37E-06
8	341.50	0.0170	0.3706	0.5768	0.0356	0.0272	0.0547	0.8849	0.0332	97.24	96.98		2.76E-06
9	341.58	0.0194	0.3718	0.5624	0.0464	0.0307	0.0543	0.8725	0.0425	96.75	96.54		2.83E-06
10	341.71	0.0213	0.3733	0.5458	0.0596	0.0332	0.0540	0.8594	0.0534	96.19	96.05		2.65E-06
11	341.89	0.0229	0.3747	0.5260	0.0764	0.0352	0.0537	0.8445	0.0666	95.50	95.49		2.25E-06
12	342.09	0.0244	0.3744	0.5019	0.0993	0.0370	0.0528	0.8266	0.0836	94.60	94.80		1.58E-06
13	342.09	0.0261	0.3659	0.4743	0.1337	0.0387	0.0495	0.8052	.01067	92.43	93.90	6.27E-09	
14	342.09	0.0371	0.3554	0.4333	0.1742	0.0530	0.0456	0.7722	0.1292	89.74	91.73	7.89E-09	
15	342.25	0.0591	0.3404	0.3706	0.2299	0.0809	0.0412	0.7240	0.1540	85.93	89.04	1.20E-08	
16	343.10	0.0988	0.3169	0.2693	0.3150	0.1303	0.0373	0.6484	0.1840	80.44	85.23	1.84E-08	
17	345.49	0.1570	0.2648	0.1381	0.4401	0.2167	0.0342	0.5239	0.2252	73.21	79.74	2.89E-08	
18	348.43	0.2219	0.1724	0.0498	0.5559	0.3590	0.0253	0.3451	0.2706	66.27	72.51	3.80E-08	
19	348.47	0.3238	0.0859	0.0185	0.5717	0.5504	0.0108	0.1734	0.2654	62.25	65.57	3.06E-08	
20	344.49	0.5551	0.0303	0.0084	0.4062	0.7644	0.0023	0.0603	0.1730	96.52	61.35	1.36E-08	
21	345.74	0.5482	0.0304	0.0019	0.4195	0.7970	0.0035	0.0146	0.1859	96.43	63.62		1.99E-06
22	346.74	0.5130	0.0313	0.0006	0.4552	0.7870	0.0028	0.0046	0.2056	95.85	63.33		3.35E-06
23	348.10	0.4187	0.0353	0.0002	0.5457	0.7357	0.0038	0.0025	0.2579	94.43	62.95		3.84E-06
24	355.07	0.2419	0.0508	0.0001	0.7072	0.5862	0.0086	0.0020	0.3923	92.61	61.53		1.35E-05
25	364.77	0.0886	0.0804	0.0000	0.8339	0.3277	0.0332	0.0015	0.6376	32.90	59.71		4.37E-05

Heat duty [kJ/s]	
Condenser	-808.90
Boiler	651.27

Table 10-15: Behavior of the conversion and recovery percentages as a function of the amount of catalyst.

Catalyst in the stage [g]	Total catalyst in the column [g]	Molar fraction of Methyl acetate		Conversion	Recovery
		Distillate	Bottoms		
0.05	0.4	0.2070	3.2E-03	20.6	98.36
0.25	2	0.2655	2.5E-03	26.2	98.98
0.5	4	0.3198	2.0E-03	31.5	99.31
2.5	20	0.5442	8.4E.04	53.3	99.83
5	40	0.6712	4.9E-04	65.6	99.92
7.5	60	0.7440	3.5E-04	72.7	99.95
8	64	0.7555	3.3E-04	73.9	99.95
10	80	0.7930	2.6E-04	77.5	99.96
15	120	0.8482	1.6E-04	82.9	99.98
20	160	0.8775	1.2E-04	85.8	99.99
30	240	0.9097	7.8E-05	88.9	99.99
40	320	0.9260	5.9E-05	90.5	99.99
50	400	0.9353	5.0E-05	91.4	99.99
100	800	0.9506	3.5E-05	92.9	100.00
250	2000	0.9577	2.9E-03	93.6	100.00
500	4000	0.9600	2.8E-05	93.8	100.00
2500	20000	0.9624	2.7E-05	94.1	100.00
5000	40000	0.9627	2.7E-05	94.1	100.00

Table 10-16: Temperature, vapor and liquid phase composition, and liquid and vapor flow profiles in the distillation column for Case 9.

Stage	T [K]	Composition of liquid phase				Composition of vapor phase				Liquid [gmol/h]	Vapor [gmol/h]	Reaction rate [kmol/ g_{cat} -s]	Reaction rate [kmol/ g_{cat} -s]
		Methanol	Acetic acid	Methyl acetate	Water	Methanol	Acetic acid	Methyl acetate	Water				
1	329.78	0.0134	1.3E-07	0.9748	0.0118	0.0264	5.8E-09	0.9623	0.0112	63.21	0.00		-1.24E-13
2	329.98	0.0066	2.9E-06	0.9812	0.0122	0.0133	1.3E-07	0.8748	0.0118	63.22	93.31		-3.47E-12
3	330.05	0.0043	4.3E-05	0.9833	0.0124	0.0087	2.0E-06	0.9791	0.0120	63.35	93.42		-6.28E-11
4	330.09	0.0035	6.4E-04	0.9834	0.0125	0.0072	2.9E-05	0.9805	0.0121	63.31	93.45		-1.08E-09
5	330.33	0.0033	0.0088	0.9753	0.0125	0.0067	4.3E-04	0.9806	0.0122	62.90	93.41		-1.69E-08
6	332.52	0.0035	0.0859	0.8979	0.0127	0.0065	0.0060	0.9751	0.0123	62.21	93.00		-1.22E-07
7	341.68	0.0040	0.3722	0.6112	0.0125	0.0067	0.0579	0.9229	0.0124	97.79	92.31		4.34E-07
8	341.69	0.0050	0.3726	0.6059	0.0165	0.0082	0.0576	0.9178	0.0162	97.60	97.09		4.62E-07
9	341.71	0.0056	0.3730	0.6006	0.0208	0.0091	0.0574	0.9130	0.0202	97.41	96.90		3.77E-07
10	341.74	0.0060	0.3735	0.5951	0.0254	0.0098	0.0573	0.9083	0.0246	97.22	96.71		2.16E-07
11	341.78	0.0063	0.3739	0.5893	0.0305	0.0102	0.0571	0.9034	0.0293	97.01	96.52		-3.01E-09
12	341.82	0.0065	0.3742	0.5832	0.0361	0.0105	0.0569	0.8983	0.0344	96.77	96.31		-2.72E-07
13	341.84	0.0066	0.3739	0.5769	0.0426	0.0107	0.0564	0.8928	0.0401	96.43	96.07	5.66E-10	
14	341.86	0.0075	0.3739	0.5697	0.0489	0.0120	0.0560	0.8865	0.0455	96.12	95.73	3.30E-10	
15	341.90	0.0084	0.3740	0.5617	0.0558	0.0135	0.0556	0.8797	0.0513	95.78	95.42	3.29 E-10	
16	341.94	0.0095	0.3742	0.5528	0.0635	0.0151	0.0552	0.8721	0.0576	95.41	95.08	3.68 E-10	
17	342.00	0.0108	0.3744	0.5425	0.0724	0.0169	0.0548	0.8637	0.0647	94.98	94.72	4.28 E-10	
18	342.08	0.0122	0.3747	0.5302	0.0829	0.0190	0.0543	0.8539	0.0728	94.47	94.28	5.18 E-10	
19	342.20	0.0140	0.3752	0.5150	0.0959	0.0215	0.0539	0.8422	0.0824	93.85	93.77	6.57 E-10	
20	342.38	0.0162	0.3760	0.4953	0.1125	0.0246	0.0535	0.8276	0.0924	93.06	93.15	8.85 E-10	
21	342.68	0.0191	0.3776	0.4684	0.2349	0.0286	0.0534	0.8087	0.1093	92.00	92.36	1.303-09	
22	343.22	0.0233	0.3807	0.4295	0.1666	0.0343	0.0538	0.7827	0.1292	90.50	91.30	2.09E-09	
23	344.25	0.0295	0.3859	0.3708	0.2138	0.0429	0.0557	0.7446	0.1568	88.28	89.80	3.74E-09	
24	346.21	0.0392	0.3903	0.2847	0.2857	0.0574	0.0604	0.6857	0.1965	84.93	87.58	7.30E-09	
25	349.38	0.0542	0.3774	0.1801	0.3883	0.0839	0.0675	0.5958	0.2527	80.13	84.23	1.47E-08	
26	352.83	0.0769	0.3204	0.0915	0.5112	0.1351	0.0683	0.4757	0.3209	73.84	79.43	2.71E-08	
27	354.55	0.1138	0.2187	0.0397	0.6278	0.2316	0.0508	0.3452	0.3725	66.90	73.14	3.82E-08	
28	353.63	0.1768	0.1148	0.0166	0.6918	0.3888	0.0235	0.2156	0.3721	61.52	66.20	3.57E-08	
29	350.48	0.2959	0.0500	0.0078	0.6464	0.5826	0.0069	0.1021	0.3084	59.39	60.82	2.08E-08	
30	345.08	0.5467	0.0167	0.0041	0.4325	0.7817	0.0013	0.0324	0.1846	94.65	58.69	7.73E-09	

31	345.87	0.5378	0.0168	0.0008	0.4445	0.7974	0.0013	0.0070	0.1942	94.53	61.75	6.35E-07
32	346.71	0.5040	0.0173	0.0002	0.4785	0.7844	0.0015	0.0020	0.2121	93.96	61.63	7.41E-07
33	348.92	0.4121	0.0194	0.0001	0.5684	0.7347	0.0020	0.0010	0.2622	92.53	61.06	1.21E-06
34	354.72	0.2339	0.0280	1.1E-05	0.7380	0.6976	0.0051	0.0008	0.3965	90.43	59.63	4.66E-06
35	364.57	0.0746	0.0443	1.6E-05	0.8810	0.3245	0.0182	0.0006	0.6568	32.90	57.53	1.78E-05

Table 10-17: Behavior of the conversion and recovery percentages as a function of the amount of catalyst.

Catalyst in the stage [g]	Total catalyst in the column [g]	Molar fraction of Methyl acetate		Conversion	Recovery
		Distillate	Bottoms		
0.005	0.09	0.1928	0.0033	19.2	99.1405
0.025	0.45	0.2097	0.0031	20.8	98.3994
0.05	0.9	0.2287	2.9E-03	22.7	98.6366
0.25	4.5	0.3361	1.9E-03	33.0	99.3851
0.5	9	0.4328	1.5E-03	42.5	99.6327
7.5	45	07098	6.3E-04	69.4	99.9035
8	90	0.8178	2.9E-04	79.95	99.9607
10	135	0.8604	1.9E-04	84.1	99.9760
15	144	0.8657	1.8E-04	84.6	99.9776
10	180	0.8824	1.4E-04	86.2	99.9825
15	270	0.9091	9.2E-05	88.9	99.9889
20	360	0.9271	6.5E-05	90.6	99.9924
30	540	0.9487	3.7E-05	92.7	99.9957
40	720	0.9674	2.1E-05	94.5	99.9976
50	900	0.9748	1.6E-05	95.3	99.9982
100	1800	0.9779	1.4E-05	95.6	99.9984
150	2700	0.9788	1.43-05	95.7	99.9985
200	3600	0.9792	1.3E-05	95.7	99.9985
250	4500	0.9795	1.3E-05	95.7	99.9985
350	6300	0.9798	1.3E-05	95.8	99.9985
500	9000	0.9801	1.3E-05	95.8	99.9986
1000	18000	0.9805	1.3E-05	95.8	99.9986
2500	45000	0.9807	1.3E-05	95.8	99.9985
5000	90000	0.9808	1.3E-05	95.9	99.9985

11. Annex F - Graphical representations of the operating units and mass balances

This appendix contains the graphical representations of all operating units taken into account in composing the flow sheets. Each operating unit performs a given task by means of a single piece of processing equipment or unit operation, or a group of such processing equipment or unit operations.

As mentioned in the text, the mass balance around each operating unit is based on a plant capacity of 200 MM Lb butanol/yr, 325 days/yr. The purities of butanol, ethanol, and acetone are specified as 99.9% weight, 99.5% weight, and 99% weight, respectively.

Table 11-1: Operating units identified and their costs

	Operating units			Function	Basis for identification	Cost			
No.	No. Sub-unit	Designation	Type			Capital 10^3US\$/ 10^3US\$/year	Operating (10^3US\$/year)	Total (10^3US\$/year)	Method of estimation
1	-	H1	Hydrolysis reactor	Hydrolysis of corn starch (S) to produce glucose (G) with water (W)	Heuristics	-	-		-
2	-	F1	Fermenter	Production of acetone (A), butanol (B) and ethanol (E) from glucose with byproducts carbon dioxide (C) and hydrogen (H) and water (W)	Heuristics	-	-		-
3	-	G1	Gas stripper	Removal of large amount of W (and suspended solids) from the fermentation broth	Heuristics	2180/727	871	1598	Simulation
4	-	D1	Distillation column	Removal of acetone from the mixture of B, E, W and A	Simulation	2088/696	873	1569	Simulation
5	-	A1	Azeotropic distillation	Separation of E, B, and W from the mixture of E, B, W	Simulation	49653/16551	218800	235351	Heuristics / Simulation
6	-	D2	Distillation column	Separation of A and E from the mixture of A, E, B, and W	Simulation	2294/765	891	1656	Simulation
7	-	D3	Distillation column	Separation of A from the mixture of A and E	Simulation	1831/610	864	1474	Simulation
8	-	A2	Azeotropic distillation	Separation of B from the mixture of B and W	Simulation	19861/6620	87520	94140	Heuristics / Simulation
9	-	E1	Solvent Stripper	Extraction of A, E, and B from their aqueous solution	Heuristics	1189/396	5231	5627	Heuristics/ Time-value Scaling

Table 13-1 (cont.): Operating units identified and their costs

No.	No. Sub-unit	Designation	Type	Function	Basis for identification	Capital 10^3US$/ 10^3US$/year	Operating (10^3US$/year)	Total (10^3US$/year)	Method of estimation
10	-	S1	Distillation column	Removal and recovery of 2-ethyl-1-hexanol (X) from the mixture of A, E, B, and X	Simulation	1914/638	864	1502	Simulation
11	11-1	D5	Distillation column	Separation of A from the mixture of A, E, and B (simple-direct, part 1)	Simulation	2392/797	902	1699	Simulation
	11-2	D6	Distillation column	Separation of E from the mixture of E and (simple-direct, part 2)	Simulation	2058/686	873	1559	Simulation
12	12-1	D7	Distillation column	Separation of B from the mixture of A, E, and B (simple-indirect, part 1)	Simulation	1684/561	852	1413	Simulation
	12-2	D8	Distillation column	Separation of A from the mixture of A and E (simple-indirect, part 2)	Simulation	2275/758	892	1650	Simulation
13	13-1	DD9	Distillation column	Separation of A, B and the mixture of E and B from the mixture of A, E, and B (complex-sidestream-B-direct, part 1)	Simulation	6684/2228	2666	4894	Heuristics/ Factor scaling: factor =1.502
	13-2	D10	Distillation column	Separation of E from the mixture of E and B (complex-sidestream-B- direct, part 2)	Simulation				

Table 13-1 (cont.): Operating units identified and their costs

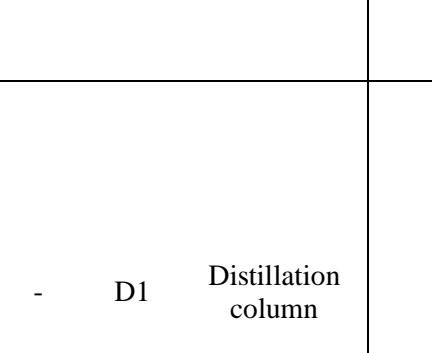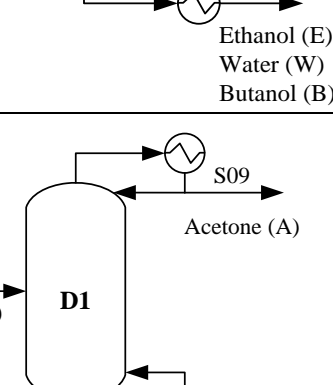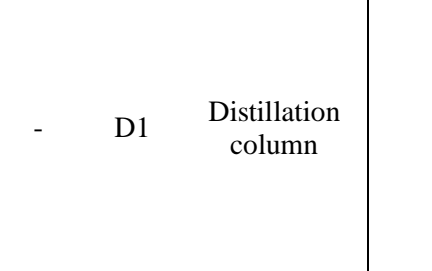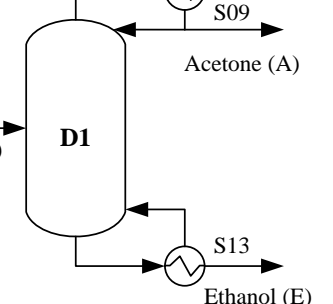| No.	No. Sub-unit	Designation	Type	Function	Basis for identification	Capital 10^3US$/ 10^3US$/year	Operating (10^3US$/year)	Total (10^3US$/year)	Method of estimation
14	14-1	D11	Distillation column	Separation of E from the mixture of E and B (complex sidestream-B- direct, part 2)	Simulation	6301/2100	2513	4613	Heuristics/ Factor scaling: factor =1.416
	14-2	D12	Distillation column	Separation of A from the mixture of A and E (complex sidestream-A- indirect, part 2)	Simulation				
15	-	D13	Distillation column	Separation of A, E, and B from the mixture of A, E, and B (complex- sidestream above)	Simulation	6079/2026	2425	4451	Heuristics/ Factor scaling: factor =1.366
16	-	D14	Distillation column	Separation of A, E, and B from the mixture of A, E, and B (complex- sidestream below)	Simulation	6412/2137	2558	4695	Heuristics/ Factor scaling: factor =1.441
17	17-1	D15	Distillation column	Separation of A, mixture of E and B, and B from the mixture of A, E, and B (complex-sidestream- rectifier, part 1)	Simulation	6862/2287	2737	5024	Heuristics/ Factor scaling: factor =1.542
	17-2	D16	Distillation column	Separation of E and B from the mixture of E and B (complex- sidestream- rectifier, part 2)	Simulation				
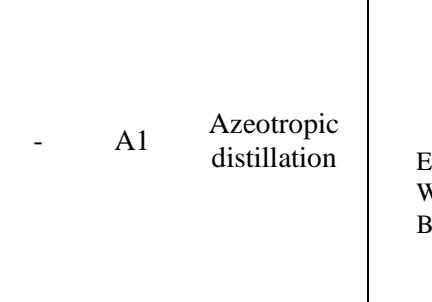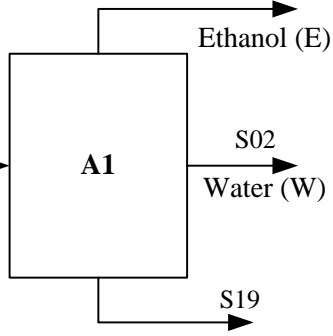
Table 13-1 (cont.): Operating units identified and their costs

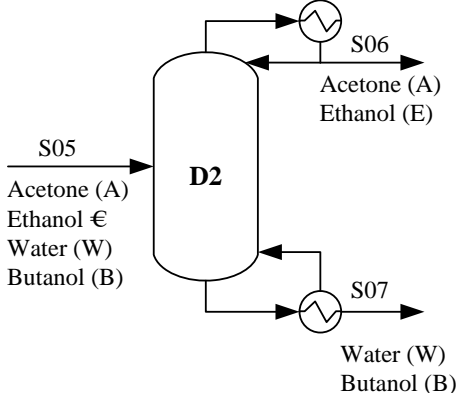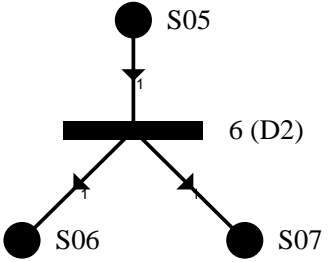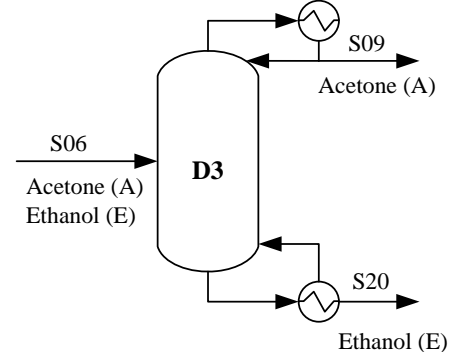|						Cost			
No.	**No. Sub-unit**	**Designation**	**Type**	**Function**	**Basis for identification**	**Capital** 10^3US$/ 10^3US$/year	**Operating** (10^3US$/year)	**Total** (10^3US$/year)	**Method of estimation**
18	18-1	D17	Distillation column	Separation of A, mixture of A and E, and B from the mixture of A, E, and B (complex-sidestream-stripper, part 1)	Simulation	6746/2249	2691	4940	Heuristics/ Factor scaling: factor =1.516
	18-2	D18	Distillation column	Separation of A and E from the mixture of A and E (complex-sidestream-stripper, part 2)					
19	19-1	D19	Distillation column	Separation of mixture of A and E, and B from the mixture of A, E, and B (complex-indirect, part 1)	Simulation	8068/2689	3218	5907	Heuristics/ Factor scaling: factor =1.813
	19-2	D20	Distillation column	Separation of A and E from the mixture of A and E (complex-indirect, part 2)					
20	20-1	D21	Distillation column	Separation of A, and mixture of E and B from the mixture of A, E, and B (complex-direct, part 1)	Simulation	3124/1041	1246	2287	Heuristics/ Factor scaling: factor =0.702
	20-2	D22	Distillation column	Separation of E and B from the mixture of E and B (complex-direct, part 2)					
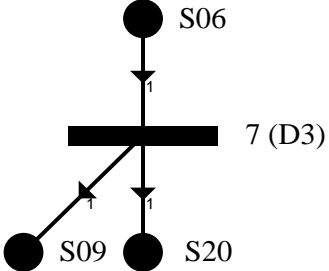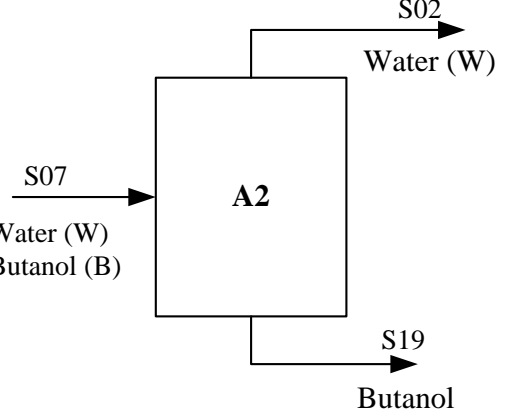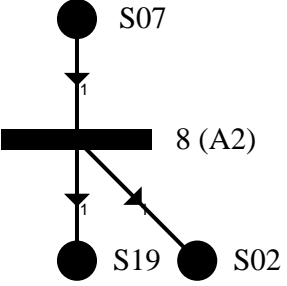
Table 13-1 (cont.): Operating units identified and their costs

	Operating units			Function	Basis for identification	Cost			
No.	No. Sub-unit	Designation	Type			Capital 10³US$/10³US$/year	Operating (10³US$/year)	Total (10³US$/year)	Method of estimation
21	21-1	D25	Distillation column	Separation of mixture of A and E, and mixture of E and B from the mixture of A, E, and B (complex- Petlyuk type IIIb, part 1)	Simulation	4210/1403	1679	3082	Heuristics/ Factor scaling: factor =0.946
	21-2	D26	Distillation column	Separation of A, E, and B from the mixture of A and E, and mixture of E and B (complex-Petlyuk type IIIb, part 2)					
22	22-1	D27	Distillation column	Separation of mixture of A and E, and mixture of E and B from the mixture of A, E, and B (complex- Petlyuk type II, part 1)	Simulation	4156/1385	1658	3043	Heuristics/ Factor scaling: factor =0.934
	22-2	D28	Distillation column	Separation of A and E from the mixture of A and E (complex-Petlyuk type II, part 2)					
	22-2	D29	Distillation column	Separation of E and B from mixture of E and B (complex-Petlyuk type II, part 3)					

Table 11-2: Diagrammatic Representations and Mass Balances of Operating Units Identified.

				Operating units		Streams	
					Diagram representations		
No.	No. Sub-unit	Designation	Separator type or distillation column configuration	Conventional (with component flow rate in 10^3lb/hr)	P-graph	Designation	Flow rate (10^3 lb/hr)
1	-	H1	Hydrolysis reactor				
2	-	F1	Fermenter				

3	-	G1	Gas Stripper			S00	1815
						S01	1740
						S05	75
4	-	D1	Distillation column			S05	75
						S09	11
						S13	64
5	-	A1	Azeotropic distillation			S13	64
						S02	35
						S19	26
						S20	3

6	-	D2	Distillation column			S05 75
						S06 14
						S07 61
7	-	D3	Distillation column			S06 14
						S09 11
						S20 3
8	-	A2	Azeotropic distillation			S07 61
						S02 35
						S19 26
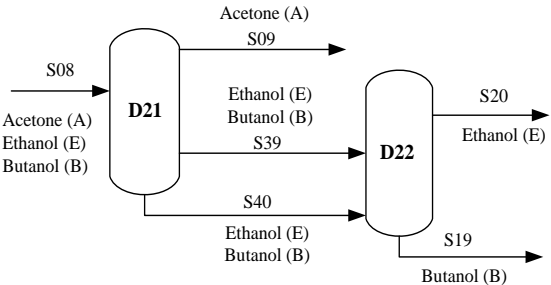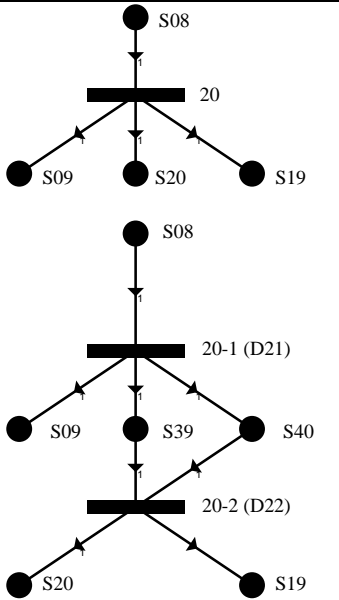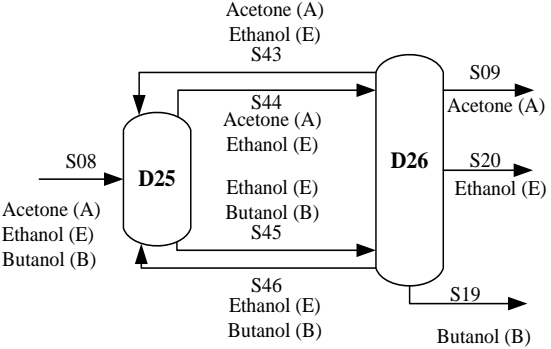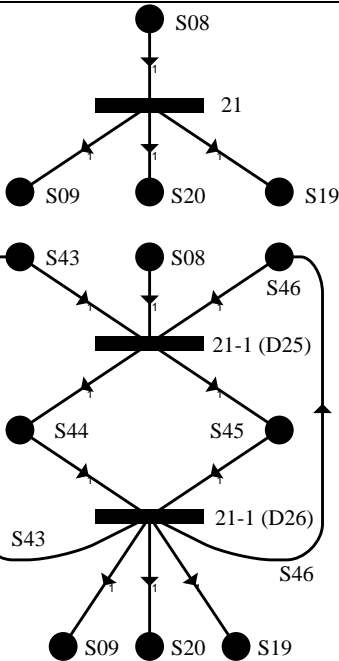
9	-	E1	Extractor			S00 1815
						S11 1952
						S03 1780
						S16 1987
10	-	S1	Solvent stripper			S16 1987
						S08 35
						S11 192
11	11-1	D5	Simple / Direct			S08 35
						S09 7
						S15 28

Cell 9 (E1) — Extractor process diagram:

S00: Acetone (A), Ethanol (E), Water (W), Butanol (B) → E1

S16: Acetone (A), Ethanol (E), Butanol (B), 2-ethyl-1-hexanol (EH)

S11: 2-ethyl-1-hexanol (EH)

S03: Acetone (A), Ethanol (E), Water (W), Butanol (B)

Superstructure: S00, S11 → 9 (E1) → S03, S16

Cell 10 (S1) — Solvent stripper process diagram:

S16: Acetone (A), Ethanol (E), Butanol (B), 2-ethyl-1-hexanol (EH) → S1

S08: Acetone (A), Ethanol (E), Butanol (B)

S11: 2-ethyl-1-hexanol (EH)

Superstructure: S16 → 10 (S1) → S08, S11

Cell 11-1 (D5) — Simple / Direct process diagram:

S08: Acetone (A), Ethanol (E), Butanol (B) → D5

S09: Acetone (A)

S15: Ethanol (E), Butanol (B)

Superstructure: S08 → 11-1 (D5) → S09, S15

	Process diagram	Network		
11-2 D6	**D6** — S15 → Ethanol (E), Butanol (B); S20 Acetone (A); S19 Butanol (B)	S15 → 11-2 (D6) → S20, S19	S15	28
			S19	26
			S20	2
12-1 D7	**D7** — S08 → Acetone (A), Ethanol (E), Butanol (B); S06 Acetone (A), Ethanol (E); S19 Butanol (B)	S08 → 12-1 (D7) → S06, S19	S08	35
			S06	9
			S19	26
12 ——— Simple /indirect				
12-2 D8	**D8** — S06 → Acetone (A), Ethanol (E); S09 Acetone (A); S20 Ethanol (E)	S06 → 12-2 (D8) → S09, S20	S06	9
			S09	7
			S20	2

13	13-1 DD9	Complex / sidestream – B direct	13-2 D10			S08 35 S09 7 S19 26 S20 2
14	14-1 D11	Complex / sidestream - A indirect	14-2 D12			S08 35 S09 7 S19 26 S20 2

15	-	D13	Complex / sidestream - above			S08	35
						S09	7
						S19	26
						S20	2
16	-	D14	Complex / sidestream - below			S08	35
						S09	7
						S19	26
						S20	2
17	17-1	D15	Complex / sidestream - rectifier			S08	35
						S09	7
	17-2	D16				S19	26
						S20	2

18-1	D17			S08	35
18		Complex / sidestream - stripper		S09	7
18-2	D18			S19	26
				S20	2
19-1	D19			S08	35
19		Complex / indirect		S09	7
19-2	D20			S19	26
				S20	2

20	20-1 D21 Complex / direct 20-2 D22			S08	35
				S09	7
				S19	26
				S20	2
21	21-1 D25 Complex / Petlyuk type IIB 21-2 D26			S08	35
				S09	7
				S19	26
				S20	2

Process diagram D21/D22 flowsheet:

S08 → D21
Acetone (A), Ethanol (E), Butanol (B)

D21:
- Acetone (A) — S09
- Ethanol (E), Butanol (B) — S39 → D22
- Ethanol (E), Butanol (B) — S40 → D22

D22:
- Ethanol (E) — S20
- Butanol (B) — S19

Process diagram D25/D26 flowsheet:

S08 → D25
Acetone (A), Ethanol (E), Butanol (B)

D25:
- Acetone (A), Ethanol (E) — S43
- Acetone (A), Ethanol (E) — S44 → D26
- Ethanol (E), Butanol (B) — S45 → D26
- Ethanol (E), Butanol (B) — S46

D26:
- Acetone (A) — S09
- Ethanol (E) — S20
- Butanol (B) — S19

22-1	D27				S08	35
22-2	D28	Complex / Petlyuk type II			S09	7
22					S19	26
22-2	D29				S20	2

Acetone (A)
Ethanol (E)
S47

D28

S09

Acetone (A)

S48
Acetone (A)
Ethanol (E)

S08

D27

S20   Ethanol (E)

Ethanol (E)
Butanol (B)
S49

D29

S50
Ethanol (E)
Butanol (B)

S19

Butanol (B)

S08

22

S09   S20   S19

S47   S08   S50

22-1 (D27)

S48   S49

22-2 (D28)   22-3 (D29)

S47   S50

S09   S20   S20   S19

12.   References

[1] Wakeham WA, Cholakov GS, Stateva RP. Consequences of property errors on the design of distillation columns. Fluid phase equilibria. 2001;185(1):1-12.

[2] Humphrey JL. Separation processes: playing a critical role. Chemical Engineering Progress. 1995;91(10):31-41.

[3] Mix T, Dweck J. Conserving energy in distillation. 1982.

[4] Soave G, Feliu JA. Saving energy in distillation towers by feed splitting. Applied Thermal Engineering. 2002;22(8):889-96.

[5] Hostrup M, Gani R, Kravanja Z, Sorsak A, Grossmann I. Integration of thermodynamic insights and MINLP optimization for the synthesis, design and analysis of process flowsheets. Computers & Chemical Engineering. 2001;25(1):73-83.

[6] Li X, Kraslawski A. Conceptual process synthesis: past and current trends. Chemical Engineering and Processing: Process Intensification. 2004;43(5):583-94.

[7] Carlson EC. Don't gamble with physical properties for simulations. Chemical Engineering Progress. 1996;92(10):35-46.

[8] Gmehling J, Möllmann C. Synthesis of distillation processes using thermodynamic models and the Dortmund data bank. Industrial & engineering chemistry research. 1998;37(8):3112-23.

[9] Rarey J, Gmehling J. Factual data banks and their application to the synthesis and design of chemical processes and the development and testing of thermophysical property estimation methods. Pure and Applied Chemistry. 2009;81(10):1745-68.

[10] Agar DW. Multifunctional reactors: old preconceptions and new dimensions. Chemical Engineering Science. 1999;54(10):1299-305.

[11] Agar DW, Ruppel W. Multifunktionale Reaktoren für die heterogene Katalyse. Chemie Ingenieur Technik. 1988;60(10):731-41.

[12] Sharma M. Separations through reactions. Journal of Separation Process Technology. 1985;6(9):16.

[13] !!! INVALID CITATION !!!

[14] FAH S. Dampfdrucke ternarer gemische. II. Theoretischer teil. Z Phys Chem. 1901;36:413-49.

[15] Storonkin A, Morachevskii A. O Ravnovesii Rastvor Par V Sisteme Benzol Tsiklogeksan Izopropilovyi Spirt. Zhurnal Fizicheskoi Khimii. 1956;30(6):1297-307.

[16] Brzostowski W, Malanowski S, Świętosławski W. Vapour-liquid equilibria in binary systems of pyridine bases1959.

[17] Prigogine I, Henin F. On the general theory of the approach to equilibrium. I. Interacting normal modes. Journal of mathematical physics. 1960;1(5):349-71.

[18] de Groot SR, Mazur P, King AL. Non-equilibrium thermodynamics. American Journal of Physics. 1963;31(7):558-9.

[19] Vogelpohl A. Rektifikation von Dreistoffgemischen. Teil 1: Rektifikation als Stoffaustauschvorgang und Rektifikationslinien idealer Gemische. Chemie Ingenieur Technik. 1964;36(9):907-15.

[20] Vogelpohl A. Rektifikation von Dreistoffgemischen. Teil 2: Rektifikationslinien realer Gemische und Berechnung der Dreistoffrektifikation. Chemie Ingenieur Technik. 1964;36(10):1033-45.

[21] Petlyuk F, Platonov V, Girsanov I. Calculation of Optimum Distillation Cascades. Khim Promst, 40 (6). 1964:445-53.

[22] Petlyuk F, Platonov V. Thermodynamically Reversible Multicomponent Distillation, Khim. Promst; 1964.

[23] Petlyuk F, Platonov V, Girsanov I. The design of optimal rectification cascades. Khim Prom. 1964;45:445-53.

[24] Espinosa J, Scenna N, Pérez G. Graphical procedure for reactive distillation systems. Chemical Engineering Communications. 1993;119(1):109-24.

[25] Espinosa J, Martinez E, Perez G. Dynamic behavior of reactive distillation columns. Equilibrium systems. Chemical Engineering Communications. 1994;128(1):19-42.

[26] Pisarenko YA, Serafimov L, Cardona C, Efremov D, Shuwalov A. Reactive distillation design: analysis of the process statics. Reviews in chemical engineering. 2001;17(4):253-327.

[27] Serafimov L, Pisarenko Y, Kulov N. Coupling chemical reaction with distillation: Thermodynamic analysis and practical applications. Chemical engineering science. 1999;54(10):1383-8.

[28] Agreda V, Partin L, Heise W. High-purity methyl acetate via reactive distillation. Chemical Engineering Progres. 1990:40-6.

[29] Cardona C, Matallana L, Gómez P, Cortés L, Pisarenko Y. Phase equilibrium and residue curve analysis in DIPE production by reactive distillation. Conference Phase equilibrium and residue curve analysis in DIPE production by reactive distillation.

[30] Cardona C, López L, López F. Separación de ácido láctico por destilación reactiva. Revista Universidad EAFIT. 2012;40(135):40-53.

[31] Noeres C, Kenig E, Gorak A. Modelling of reactive separation processes: reactive absorption and reactive distillation. Chemical Engineering and Processing: Process Intensification. 2003;42(3):157-78.

[32] Thery R, Meyer XM, Joulia X, Meyer M. Preliminary design of reactive distillation columns. Chemical Engineering Research and Design. 2005;83(4):379-400.

[33] Taylor R, Krishna R. Modelling reactive distillation. Chemical Engineering Science. 2000;55(22):5183-229.

[34] Harmsen J. Reactive distillation: the front-runner of industrial process intensification: a full review of commercial applications, research, scale-up, design and operation. Chemical Engineering and Processing: Process Intensification. 2007;46(9):774-80.

[35] Kiss AA, Bildea CS, Dimian AC. Design and control of recycle systems by non-linear analysis. Computers & chemical engineering. 2007;31(5):601-11.

[36] Schoenmakers HG, Bessling B. Reactive and catalytic distillation from an industrial perspective. Chemical Engineering and Processing: Process Intensification. 2003;42(3):145-55.

[37] Серафимов Л, Тимофеев В, Писаренко Ю, Солохин А. Технология основного органического синтеза. Совмещенные процессы. М: Химия. 1993.

[38] Kiva V, Hilmen E, Skogestad S. Azeotropic phase equilibrium diagrams: a survey. Chemical Engineering Science. 2003;58(10):1903-53.

[39] Giessler S, Danilov R, Pisarenko Y, Serafimov L, Hasebe S, Hashimoto I. Feasibility study of reactive distillation using the analysis of the statics. Industrial & engineering chemistry research. 1998;37(11):4375-82.

[40] Doherty M, Buzad G. Reactive distillation by design. Chemical engineering research & design. 1992;70(A5):448-58.

[41] Office of Industrial Technology: Energy Efficiency and Renewable Energy USDoE. Distillation column modeling tools. 2001.

[42] Türkay M, Grossmann IE. Logic-based MINLP algorithms for the optimal synthesis of process networks. Computers \& Chemical Engineering. 1996;20 %6(8):959-78 %&.

[43] Westerberg AW, Hutchinson HP, Motard RL, Winter P. Process flowsheeting: Cambridge University Press Cambridge, 1979.

[44] Friedler F, Tarjan K, Huang YW, Fan LT. Combinatorial algorithms for process synthesis. Computers \& Chemical Engineering. 1992;16 %6:S313-S20 %&.

[45] Friedler F, Tarjan K, Huang YW, Fan LT. Graph-theoretic approach to process synthesis: polynomial algorithm for maximal structure generation. Computers \& Chemical Engineering. 1993;17 %6(9):929-42 %&.

[46] Friedler F, Tarjan K, Huang YW, Fan LT. Graph-theoretic approach to process synthesis: axioms and theorems. Chemical Engineering Science. 1992;47 %6(8):1973-88 %&.

[47] Nagy AB, Adonyi R, Halasz L, Friedler F, Fan LT. Integrated synthesis of process and heat exchanger networks: algorithmic approach. Applied Thermal Engineering. 2001;21 %6(13):1407-27 %&.

[48] Anokhina E, Cardona C, Pisarenko YA, Ponomarev E. Basic design stages of combined processes by the example of the production of allyl alcohol by allyl acetate butanolysis. Part 2: separation of a reaction mixture removed from the reaction-rectification column for allyl alcohol synthesis. Chemical Industry in Russia. 1996;11:689.

[49] Pisarenko YA, Cardona C, Serafimov L. Reactive Distillation Processes. Advances in Research and Practical Application. Moscow Ed Lutich. 2000:268.

[50] Barbosa D, Doherty MF. The simple distillation of homogeneous reactive mixtures. Chemical Engineering Science. 1988;43(3):541-50.

[51] Barbosa D, Doherty MF. Design and minimum-reflux calculations for single-feed multicomponent reactive distillation columns. Chemical Engineering Science. 1988;43(7):1523-37.

[52] Suzuki I, Yagi H, Komatsu H, Hirata M. Calculation of multicomponent distillation accompanied by a chemical reaction. Journal of Chemical Engineering of Japan. 1971;4(1):26-33.

[53] Wang J, Henke G. Tridiagonal matrix for distillation. Hydrocarbon Processing. 1966;45(8):155-&.

[54] López JA, Trejos VM, Cardona CA. Objective functions analysis in the minimization of binary VLE data for asymmetric mixtures at high pressures. Fluid phase equilibria. 2006;248(2):147-57.

[55] Navarro-Espinosa I, Cardona C, López J. Experimental measurements of vapor–liquid equilibria at low pressure: Systems containing alcohols, esters and organic acids. Fluid Phase Equilibria. 2010;287(2):141-5.

[56] Gmehling J. Present status of group-contribution methods for the synthesis and design of chemical processes. Fluid Phase Equilibria. 1998;144(1):37-47.

[57] Bessling B, Löning JM, Ohligschläger A, Schembecker G, Sundmacher K. Investigations on the synthesis of methyl acetate in a heterogeneous reactive distillation process. Chemical engineering & technology. 1998;21(5):393-400.

[58] Pöpken T, Steinigeweg S, Gmehling J. Synthesis and hydrolysis of methyl acetate by reactive distillation using structured catalytic packings: experiments and simulation. Industrial & engineering chemistry research. 2001;40(6):1566-74.

[59] Peng D-Y, Robinson DB. A new two-constant equation of state. Industrial & Engineering Chemistry Fundam

entals. 1976;15(1):59-64.

[60] Wong DSH, Sandler SI. A theoretically correct mixing rule for cubic equations of state. AIChE Journal. 1992;38(5):671-80.

[61] Renon H, Prausnitz JM. Local compositions in thermodynamic excess functions for liquid mixtures. AIChE journal. 1968;14(1):135-44.